MicroRNA regulation in the inflammatory response

Athena Martin

BBSRC DTP

Gene Regulation and RNA Biology

School of Pharmacy

Supervisor: Catherine Jopling

Declaration

Except where acknowledged in the text, I declare that this dissertation is my own work and it is based on the research work that was undertaken by myself, Athena Martin, in the Gene Regulation & RNA Biology group, School of Pharmacy, Faculty of Science, University of Nottingham, UK.

Abstract

The interplay between poly(A) tail length and miRNA regulation has been previously studied. Moretti *et al.,* (2012) found that longer poly(A) tail lengths correlated with greater miRNA mediated repression, with miRISC association triggering the displacement of PABP from the poly(A) tail. This is in agreement with Rissland *et al.,* (2017) who found that miRISC has the ability to alter the composition of the mRNP, in particular the association of PABP and eIF4G while not impacting on poly(A) tail length. On the other hand, Eisen *et al.,* (2020), found that miRNAs only stimulated deadenylation of transcripts with very short poly(A) tails.

However, the interaction between poly(A) tail length and miRNA regulation has not been investigated within the context of a biological system with physiologically relevant poly(A) tail changes. As such, this project aimed to investigate how miRNA regulation is changing over the course of inflammation and how the changing poly(A) tail lengths of key inflammatory mediators may be affecting miRNA regulation.

Through the use of inhibition and overexpression studies as well as Ago2 immunoprecipitation, this study has established that TNF is regulated by miR-181a and that this regulation is changing over the course of the inflammatory response. However, the changing poly(A) tails of TNF mRNA are not affected by miR-181a regulation.

Interestingly, through the use of siRNA knockdown this study has made a novel discovery that the non-canonical polymerases TENT4A and TENT4B are required for maintenance of high TNF mRNA levels later in the inflammatory response, but more work is required to elucidate their mechanism of action.

Furthermore, a tetracycline inducible cell line was successfully generated, providing a useful tool for investigation of miR-181a regulation via the TNF 3'UTR with transcriptional induction outside of the numerous other processes that are occurring within inflammation.

Overall, the investigations within this study have provided a greater understanding of miRNA regulation of TNF mRNA and how this is changing over the course of inflammation.

Acknowledgements

First and foremost, I owe a tremendous thank you to my supervisor Catherine for all her support, understanding and guidance as well as all the opportunities she has given me throughout my PhD. I honestly could not have asked for a better supervisor.

I also owe a big thank you to Angie, the post doc in my lab for her seemingly endless knowledge, kindness and skill. Her bubbly attitude and willingness to help no matter what the question will forever be appreciated. Likewise, I need to thank Poppy for giving me the best start to my PhD and teaching me everything I needed to know to get started.

I would also like to thank the wider GRRB community and lab members for supporting me throughout my PhD, there was always someone that had a buffer someone was missing or clubbing together to work through whatever problem people were having.

A big thank you is also owed, to my partner, James for putting up with me through all the highs and lows of my PhD, managing to keep me sane through the process.

Equally I owe a thank you to the rest of my friends and family for always believing in me and encouraging me to do my best. Especially my parents, who wholeheartedly supported me despite not really understanding what I was doing.

I also need to thank the BBSRC for funding my project along with the BBSRC-DTP team for providing plentiful training opportunities and support. I particularly need to thank Sandra for her support, she was always able to provide a huge confidence boost when needed.

Contents

List of Tables

List of Figures

List of Abbreviations

3'UTR – 3' untranslated region

ADAR – Adenosine deaminase acting on RNA

Ago – Argonaute

APA – Alternative polyadenylation

ARE – AU-rich element

ATP – Adenosine tri-phosphate

CCR4 – Carbo catabolite repressor 4

cDNA - Complementary DNA

CircRNA – Circular RNA

CLRs – C-type Lecithin receptors

CPE – Cytoplasmic polyadenylation element

CPEB – CPE-binding protein

CPSF – Cleavage and polyadenylation specificity factor

COX2 - Cyclooxygenase 2

DAMP – Damage associated molecular pattern

DCP – mRNA decapping enzyme subunit

DDX6 – Dead-box ATPase

DGCR8 - DiGeorge critical region 8

DMEM - Dulbecco's Modified Eagle Medium

DMSO - Dimethyl sulfoxide

DNA - Deoxyribonucleic acid

dsRNA - Double-stranded RNA

DTT - Dithiothreitol

E.coli - Escherichia coli

ECL - Electrochemiluminescence

EDTA - Ethylenediaminetetraacetic acid

ELISA - enzyme linked immunosorbent assay

ER - Endoplasmic Reticulum

FBS - Fetal bovine serum

HeLa - Henrietta Lacks

HRP -Horseradish peroxidase

HuR – Human antigen R

IL- Interleukin

IP - Immunoprecipitation

IRAK1 - Interleukin 1 Receptor Associated Kinase 1

IRF – Interferon regulatory factors

LB - Luria-Bertani

LPS - lipopolysaccharide

lncRNA - long non-coding RNA

m7G 7-Methylguanosine

miRNA - microRNA

mRNA - Messenger RNA

NEB - New England Biolabs

Nf-κB – Nuclear factor κB

NLRs – Nod like receptors

NOT – Negative regulator of transcription

Nt - Nucleotides

PABP - Poly(A)-binding protein

PAMP – pathogen associated molecular pattern

PAN – poly(A) specific riobonuclease

PAP – poly(A) polymerase

PAT – poly(A) tail test

PBS - Phosphate buffered saline

PCR - Polymerase chain reaction

PI – Protease inhibitor

Pre-microRNA - Precursor microRNA

Pri-microRNA - Primary microRNA

PRR- Pattern recognition receptor

PTGS2 - Prostaglandin synthase II

qRT-PCR - Quantitative real-time polymerase chain reaction

RBP – RNA-binding protein

RISC - RNA-induced silencing complex

RLC - RISC-loading complex

RNA - ribonucleic acid

RLRs – RIG-I like receptors

RT – Room Temperature

SDS-PAGE - Sodium dodecyl sulfate - polyacrylamide gel electrophoresis

SHIP1 – SH-2 containing inositol 5’ polyphosphatase

siRNA - Short-interfering RNA

snRNA - Small nuclear RNA

SOCS1 – Suppressor of cytokine signalling 1

TENT – Terminal nucleotidyl transferases

TDMD – Target directed microRNA degradation

TLR – Toll-like receptors

TRBP - Trans-activation response RNA binding protein

tRNA - Transfer RNA

TNF – Tumour Necrosis factor

TNRC6 – trinucleotide repeat containing 6

TTP – Tristetraprolin

TUT – Terminal uridyl transferase

XRN1 – Exoribonuclease 1

Chapter 1 – Introduction

The inflammatory response is a complex network of signals that are activated in response to infection or injury. Mis-regulation of the inflammatory response can lead to chornic inflammation and inflammatory disease such as inflammatory bowel disease and Crohn's disease (Matricon *et al.,* 2010, Cuchet-Lourenco *et al.,* 2018) As such, it is important that the intricate network of regulatory that controls the inflammatory response is understood, so better treatments and therapeutics can be developed. One regulatory mechanism involved in regulating the inflammatory response are microRNAs. These small RNAs regulate the levels of mRNA during the response by translationally repressing the transcripts or by triggering their deadenylation and subsequent degradation. Furthermore, it has been recently found that certain key inflammatory mediators such as TNF, have poly(A) tails that change in length over the course of the inflammatory response (Crawford, 1997, Gandhi, 2016, Kwak *et al.,* 2022).

Therefore, one of the key questions this study aims to answer is how changing poly(A) tail length is interacting with microRNA regulation over the course of the inflammatory response and how this regulation is changing as inflammation progresses. The other key question this study aims to investigate is whether mRNA age is affecting miRNA regulation within inflammation.

1.1 The inflammatory response

The immune response is formed of two branches, the innate immune response and the adaptive immune response. The innate immune response is a more general response compared to the adaptive immune response which is more specific. The adaptive response is acquired after initial exposure to antigens forming a specific response to subsequent exposure to the same antigen (Janeway., 2001).

Inflammation is an innate immune response that is triggered by infection or tissue injury. The inflammatory response predominantly involves the delivery of innate immune cells to the site of infection or injury (Reviewed by Medzhitov., 2008) that is coordinated by specific molecular mediators.

Dysregulation of the inflammatory response can lead to chronic inflammatory disease such as inflammatory bowel disease and Crohn's disease (Matricon *et al.,* 2010, Cuchet-Lourenco *et al.,* 2018). Impairment of anti-inflammatory mechanisms or excessive inflammatory signals leads to chronic inflammation, often characterised by the persistent production of pro-inflammatory mediators such as cytokines and eicosanoids (reviewed by Chiurchiu *et al.,* 2018). Continued release of pro-inflammatory signals leads to the continuous recruitment of innate immune cells. The continuous inflammatory state can lead to irreversible damage and the production of disease symptoms (Leuti *et al.,* 2020). Therefore, the inflammatory response must be tightly regulated.

1.1.1 Initiation of inflammation

Canonically, the response is initiated by the recognition of non-self-molecules referred to as pathogen-associated molecular patterns (PAMPs) or endogenous molecules known as damage-associated molecular patterns (DAMPs) by pattern recognition receptors (PRRs) such as Toll-like receptors (TLRs) (O'Neill, Golenbock & Bowie, 2013), Nod-like receptors (NLRs) (Maekawa, Kufer & Schulze-Lefert, 2011), RIG-I like receptors (RLRs) (Loo & Gale, 2011) and C-type lectin receptors (CLRs) (Dambuza *et al.,* 2015). Ligation of these receptors activates the transcription factors NF-κB and interferon regulatory factors (IRFs), resulting in the production of pro-inflammatory cytokines, chemokines, tissue degrading enzymes, and type-1 interferons, respectively (Akira, Uematsu & Takeuchi, 2006).

1.1.2 PAMPs and DAMPs

PAMPs are defined as a set of conserved molecular patterns that are present on all microorganisms within a given class but are absent from the host (Medzhitov & Janeway, 1997, Janeway & Medzhitov, 2002). The major PAMPs are often surface molecules such as lipoproteins, surface glycoproteins and membrane components such as peptidoglycans and lipopolysaccharide. Other major PAMPs include microbial nucleic acids such as double stranded RNA as well as DNA (Reviewed by Tang *et al.,* 2012).

DAMPs are cell-derived, often produced through trauma, ischemia and tissue damage and can be present with or without pathogenic infection to initiate an inflammatory response (Rubartelli *et al.,* 2007, Lotze *et al.,* 2007). Some DAMPs are

proteins and examples include high mobility group box 1 (HMGB1) and heat shock proteins (HSPs). Other DAMPs include hyaluronic acid, extracellular matric (ECM) fragements generated upon tissue injury, upregulated ECM molecules and plasma components. DAMPs can also be other non-protein molecules such as uric acid, ATP, heparan sulfate, DNA and RNA (Scaffidi *et al.,* 2002, Tang *et al.,* 2012, Murao *et al.,* 2021). Both of these kinds of molecular patterns bind to PRRs to trigger the inflammatory response (Tang *et al.,* 2012, Li & Wu, 2021).

1.1.3 Pattern recognition receptors

PAMPs and DAMPs are sensed by PRRs and as such there are a wide range of different PRRs to specifically recognise the wide range of foreign molecular patterns (Li & Wu, 2021).

The most studied and best understood family of PRRs are the Toll-like receptors (TLRs). The TLRs are transmembrane receptors that often bind surface molecules found on the outside of microorganisms such as lipopolysaccharide (Akira *et al.,* 2006).

TLRs are comprised of an extracellular region, a transmembrane region and an intracellular region (Kawai & Akira, 2010). The extracellular region contains leucine rich repeats (LRRs) which facilitate the recognition of PAMPs and DAMPs by the TLR. The intracellular region contains a Toll/IL-1R homology (TIR) domain which is responsible for signal transduction (Brennan & Gilmore, 2018). Certain TLRs such as TLR3, 7, 8 and 9 are able to bind viral nucleic acids (Diebold *et al.,* 2004, Heil *et al.,* 2004, Hemmi *et al.,* 2000). TLRs homodimerize in response to ligand binding and is essential for their activation (Chuenchor *et al.,* 2014) but there are a couple of exceptions such as TLR1 and 2 as well as TLR2 and 6 which form heterodimers (Farhat *et al.,* 2008).

A particular TLR of interest is TLR4. TLR4 binds lipopolysaccharide (LPS), a major cell wall component of Gram-negative bacteria, predominantly activating the NF-kB signalling pathway, which results in the production of pro-inflammatory cytokines such as tumour necrosis factor α (TNF-α, referred to as TNF), interleukin (IL)-12, IL1β and IL-6 as well as chemokines and tissue degrading enzymes (Meng & Lowell, 1997).

LPS-binding protein (LBP) and CD14 enhance the binding of LPS by TLR4 (Fujihara *et al.,* 2003, Miyake ,2003). Due to LPS having both hydrophilic and hydrophobic regions, LPS molecules often accumulate within large aggregates. LBP is a plasma protein that binds to LPS aggregates and delivers them to CD14 (Fujihara *et al.,* 2003). CD14 then acts to monomerise the LPS molecules, due to the LPS binding pocket being one LPS molecule large. CD14 the transfers the LPS molecule to TLR4 (Miyake, 2003) (Figure 1).

Binding of LPS via TLR4 requires an adaptor molecule myeloid differentiation 2 (MD-2). MD-2 is bound to the extracellular region of TLR4 (Park *et al.,* 2009). LPS binding then triggers the dimerization of two TLR4-MD-2 complexes triggering the activity of the Toll/IL-1R homology (TIR) domain recruiting adaptor proteins MyD88 or TIR-domain-containing-adaptor-inducing interferon β (TRIF) (O'Neill *et al.,* 2007, Watters *et al.,* 2007) (Figure 1).

Signalling via the TLR4 receptor can be MyD88-dependent or MyD88-independent (O'Neill *et al.,* 2007). In the majority of TLR signalling induction pathways MyD88 acts as a linker molecule to facilitate the release of NF-κB from its inhibitor Iκ-Bα, allowing NF-κB to translocate to the nucleus triggering the transcription of inflammatory mediators such as cytokines (Brikos *et al.,* 2008). The MyD88-independent pathway acts through the TRIF linker protein activating the IFN-regulatory factor 3 (IRF3) to produce a type 1 interferon response (Yamamoto *et al.,* 2003). The release of cytokines facilitates the recruitment of immune cells to the site of infection (Medzhitov 2007).

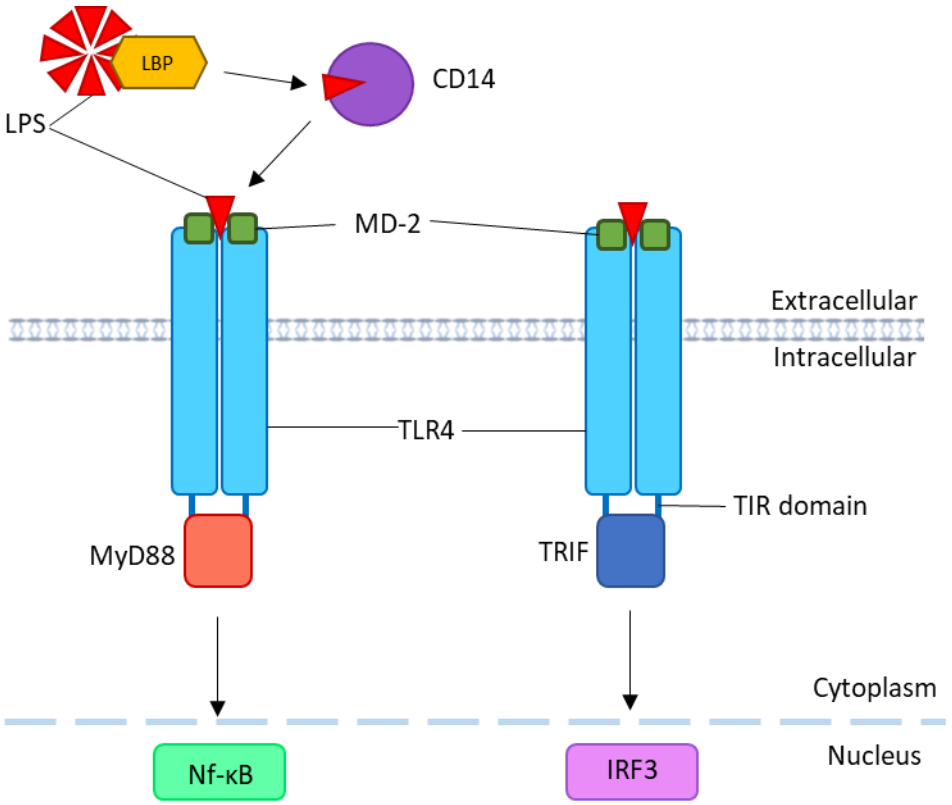

Figure 1. Simplified schematic of LPS binding to TLR4. MyD88- dependent signalling activates Nf-κB, MyD88 independent signalling via TRIF activates IRF3.

Another family of PRRs are the NOD-like receptors (NLRs), with NOD-1 and NOD-2 being the best studied. These receptors are intracellular receptors and recognise bacterial peptidoglycans that have invaded the cytoplasm, with NOD-1 preferentially recognising g-D-glutamyl-meso-diaminopimelic acid (iE-DAP) found in gram negative bacteria and NOD-2 preferentially recognising muramyl dipeptide (MDP) (Chamaillard *et al.,* 2003, Girardin *et al.,* 2003) (Figure 2). NOD-2 is also able to recognise single-stranded viral RNA (Girardin *et al.,* 2003). Activation of NLRs leads to the activation of the NF-κB signalling pathway. As such, TLRs and NLRs work synergistically to induce pro-inflammatory cytokine production (Takeuchi & Akira, 2010).

RIG-I-like receptors (RLRs) are also intracellular PRRs which are able to recognise viral nucleic acids (Yoneyama *et al.,* 2015, Rehwinkel *et al.,* 2020) (Figure 2). The three most characterised RLRs are RIG-I, MDA5 (melanoma differentiation-associated gene 5) and LGP2 (laboratory of genetics and physiology 2) (Barral *et al.,* 2009). RIG-I and MDA5 recognise double-stranded viral RNA to activate many downstream

inflammatory pathways, including the NF-κB and interferon signalling pathways (Chow *et al.,* 2018, Patel *et al.,* 2013) (Figure 2).

A final family of PRRs includes the C-type lectin receptors (CLRs), which are a phagocytic receptor. Instead of activating the cells via signal transduction, the CLRs bind to PAMPs and trigger phagocytosis to facilitate digestion of foreign molecules or bacteria to try and control infection (Freeman *et al.,* 2014) (Figure 2). CLRs are predominantly expressed on macrophages and dendritic cells, and preferentially recognise carbohydrates on the surfaces of pathogens (Ebner *et al.,* 2003).

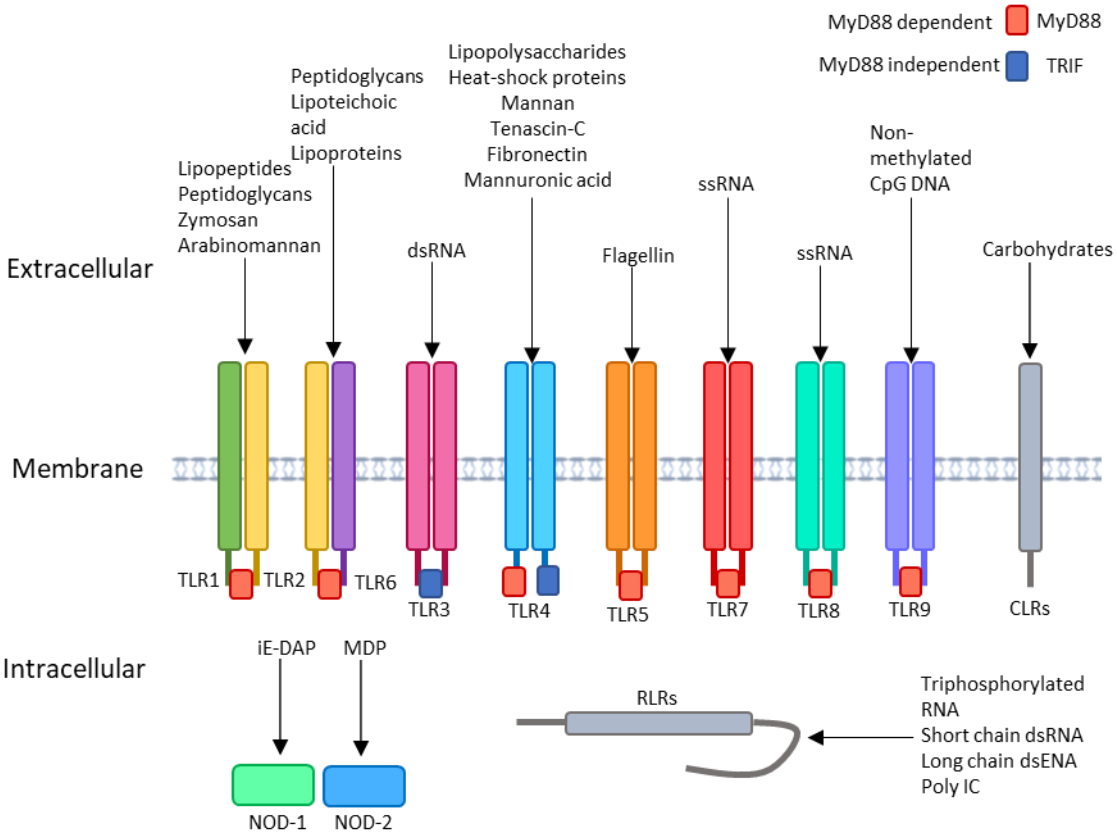

Figure 2. Schematic of main PRRs and their locations alongside their PAMPs/DAMPs ligands. TLR and CLR receptors are transmembrane receptors. NLRs and RLRs are intracellular receptors. TLRs induce inflammation via a MyD88-dependent or a MyD88-independent pathway.

1.1.4 Cells of the immune system

The immune response involves the actions of many different leukocytes. Leukocytes involved in the innate immune response are monocytes, neutrophils, eosinophils, basophils, mast cells and natural killer cells (Parker, 2017). Most of these cells are developed from a common myeloid progenitor with the exception of natural

killer cells that can also be derived from the lymphoid progenitor (Cichocki *et al.,* 2019).

On the other hand, the adaptive immune response involves the action of cells such as B and T cells, which are derived from common lymphoid progenitor cells (Janeway *et al.,* 2001). B cells mature in the bone marrow and are largely responsible for the production of immunoglobulins. T cells mature in the thymus and can differentiate into different effector cells, such as cytotoxic T cells and helper T-cells (Parker, 2017).

Monocytes and macrophages are sentinel cells that are often one of the first cells to detect infection or damage (Franken *et al.,* 2016). Macrophages can either be monocyte-derived or tissue-resident. Monocyte-derived macrophages are developed from migratory monocytes in response to micro-environmental cues (Reviewed by Jakubzick, Randolph & Henson, 2017). Conversely, tissue resident macrophages are not derived from monocytes and are actually developed from the foetal sack and yolk during embryogenesis (Hopkinson-Woolley *et al.,* 1994, Ginhox & Jung, 2014).

In response to infection or injury, macrophages are able to trigger the initiation of the innate immune response (Franken *et al.,* 2016). This is facilitated by the recognition of PAMPs and DAMPs by various PRRs present on the surface of the macrophages (Janeway *et al.,* 2001).

Furthermore, macrophages are able to engulf and digest cellular debris or foreign substances within the body in a process called phagocytosis. Phagocytosis can occur via opsonisation-dependent or opsonisation-independent pathways (Weiss & Schaible, 2015). Opsonised pathogens are those that have been covered by opsosins and are recognised by complement-specific receptors termed Fc-receptors on the macrophage surface. This facilitates the phagocytosis of pathogens by macrophages regardless of pathogen type (Ricklin *et al.,* 2010). Additionally, macrophages are equipped with various PRRs that allow the detection of specific PAMPs facilitating the phagocytosis of certain pathogens in an opsonisation-independent manner, particularly through the action of CLRs (Reviewed by Uribe-Querol & Rosales, 2020).

Furthermore, macrophages have very high plasticity and are able to polarise into many distinct activation states depending on the micro-environmental cues they encounter (Gordon & Taylor, 2005).

For example, there is a wide range of tissue-resident macrophages such as osteoclasts within the bone, Kupffer cells within the liver or alveolar macrophages within the lungs to name a few (Udagawa *et al.,* 1990, Naito *et al.,* 1997, Guilliams *et al.,* 2013). Furthermore, there are distinct subpopulations of macrophages within immune privileged sites such as the eyes and brain where they have functions in tissue remodelling and homeostasis (Murray & Wynn, 2011).

Originally, macrophages were thought to be polarised into two different states and were categorised as M1-like or classically activated and M2-like or alternatively activated (Mills *et al.,* 2000).

M1 is a pro-inflammatory state activated by interferons, microbial products or cytokines such as TNF (Mills *et al.,* 2000). The M1 state serves to mediate defence against pathogenic infections.

M2 is an reparative state stimulated by a range of factors such as IL-4, immune complexes, IL-10 or glucocorticoids (Mantovani *et al.,* 2004) and can help promote the cessation of the inflammatory response and also promote wound healing in the case of inflammation in response to injury (Ferrant *et al.,* 2012, Ferrer *et al.,* 2016).

However, while M1 and M2 has been used to categorise macrophages, there is a consensus that heterogeneity and functional plasticity of macrophages far exceeds the boundaries of these categories. Depending on their role within the wound healing process, macrophages have been categorised as pro-inflammatory, tissue repair or resolving macrophages (Wynn & Vannella, 2016).

1.2 Key inflammatory mediators

Both TNF and *cyclooxygenase-2* (COX-2, *PTGS2*) are induced in response to LPS and have roles in the inflammatory response. Furthermore, both TNF and COX-2 have been found to have poly(A) tails that change in length during inflammation (Gandhi, 2016).

1.2.1 Tumour necrosis factor (*TNF*)

TNF is a cytokine that is predominantly product by macrophages, T-lymphocytes and natural killer cells during acute inflammation. TNF functions as a trimer and exists in both a transmembrane and a soluble form (Horiuchi *et al.,* 2010). TNF is known to be a major regulator of inflammation that induces the release of other inflammatory molecules, including cytokines and chemokines. TNF has also been implicated in the pathogenesis of inflammatory and autoimmune diseases rheumatoid arthritis, inflammatory bowel disease and psoriasis (Bradley, 2008, Jang *et al.,* 2021).

Soluble TNF is produced via the processing of transmembrane TNF by TNF-alpha-converting enzyme (TACE), where soluble TNF then facilitates the majority of TNF's biological function through the binding of either TNF receptor 1 (TNF-R1) or 2 (TNF-R2) (Liu & Han, 2001). The major signalling pathway for TNF is through the binding of TNF-R1. TNF-R1 is expressed by all tissues whereas TNF-R2 is predominantly expressed by immune and endothelial cells (Faustman & Davis, 2010).

The binding of TNF-R1 by TNF triggers the formation of four different signalling complexes know as I, IIa, IIb and IIc which all have distinct functions (Brenner *et al.,* 2015). Complex I signalling is known to result in the induction of inflammation, cell survival and proliferation to defend against infection (Brenner *et al.,* 2015). On the other hand, the formation of complexes IIa and IIb triggers apoptosis via the activation of caspase-8. Instead of apoptosis, the formation of complex IIc triggers necroptosis (Holbrook *et al.,* 2019) (Figure 3).

Activation of TNF-R2 is proposed to be facilitated by the binding of transmembrane TNF to the receptor (Grell *et al.,* 1995). TNF-R2 signalling is predominantly associated with tissue regeneration, cell proliferation and survival, however this pathway is also

known to trigger inflammatory responses and aid in immune cell activation and migration (Probert, 2015).

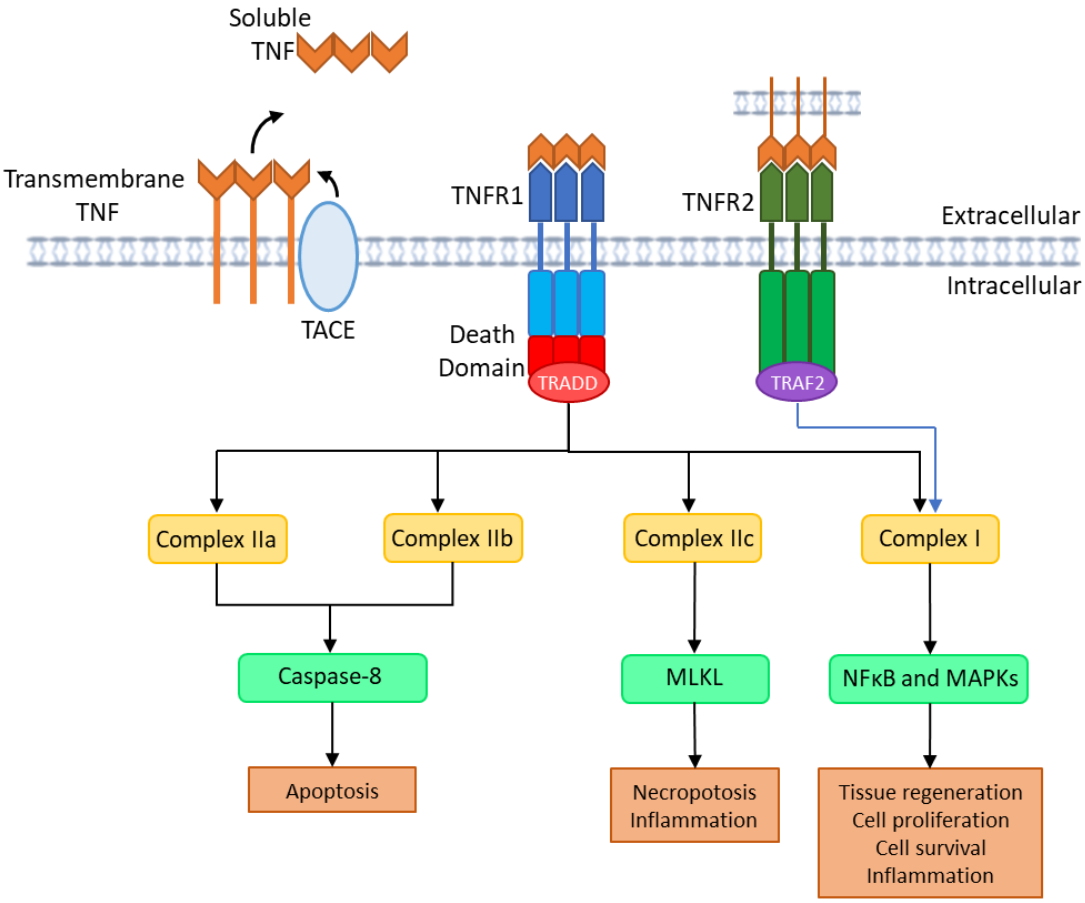

Figure 3. Simplified schematic of TNF-receptor signalling. Transmembrane TNF is converted to soluble TNF by TACE. TNFR1 is bound by soluble and transmembrane TNF. TNFR2 is predominantly bound by transmembrane TNF.

1.2.2 Prostaglandin synthase II (*PTGS2*)

PTGS2, also known as Cyclooxygenase (COX) 2, is responsible for the production of prostanoids like prostaglandin E2 (PGE2) from arachidonic acid (Dubois *et al.,* 1998), which have pro-inflammatory functions (Ahrenstedt *et al.,* 1994, Yao *et al.,* 2019). *PTGS2* is the main target for nonsteroidal anti-inflammatory drugs (NSAIDs) (Smith & Murphy, 2002, Kirkby *et al.,* 2015).

PTGS2 is an inducible early response gene that can be triggered via activation of various signalling pathways by various stimuli such as LPS, TNF, interleukin-1 (IL-1), epidermal growth factor (EGF), platelet activating factor (PAF), and arachidonic acid (Yucel-Lindberg *et al.,* 1999, Medeiros *et al.,* 2010, Fort-Nieves *et al.,* 2012).

Production of PGE2 by PTGS2 results in the up-regulation of pathways involved in inflammation, proliferation, transformation, survival, angiogenesis and metastasis (Satoh *et al.,* 2012). *PTGS2* up-regulation has been implicated in tumuorigenesis in cancers such as breast cancer, colon cancer and melanoma (reviewed by Gandhi *et al.,* 2017).

PGE2 acts through the activation of G-protein coupled receptors (GPCRs) EP1-4 (Trebino *et al.,* 2003) to trigger the classic signs of acute inflammation such as redness, swelling and pain (Funk, 2001). PGE2 binding to different E series of prostaglandin (EP) receptors can mediate the functions of different immune cell types such as macrophages, dendritic cells and T and B lymphocytes (Dey *et al.,* 2006).

The production of both inflammatory mediators TNF and PTGS2 are also regulated by the general control of gene expression.

1.3 Eukaryotic gene expression

Not only is the control of gene expression is important for maintaining homeostasis within the cell. Control of gene expression is also responsible for regulating the production of cytokines within the inflammatory response alongside other physiological processes such as cell differentiation and cellular stress responses.There are three major processes that occur for gene expression, transcription, translation and mRNA turnover and there are many mechanisms that contribute to the regulation of these three processes in order to control gene expression (Reviewed by Pope & Medzhitov, 2018, Buccitelli & Selbach, 2020).

1.3.1 Transcription

The production of mRNA involves the copying of one strand of the dsDNA in a process called transcription. DNA is stored within highly organised structures called chromatin. This is aided by histone proteins which the DNA wraps around to form structural units (Kornberg & Thomas, 1974). Transcription occurs at accessible regions within the chromatin structure, where RNA Polymerase II is responsible for the transcription of precursor mRNA (pre-mRNA). RNA Pol II binds to the promoter region of a protein-encoding gene aided by various transcription factors (Roeder, 1996, Grunberg & Hahn, 2013). The polymerase then moves down the template strand of DNA to the transcription start site (TSS) before beginning to read the template strand in a 3' to 5' direction. This produces a pre-mRNA transcript in the 5' to 3' direction. Transcription is terminated by the transcription of a poly(A) signal (PAS). The PAS is recognised by cleavage and polyadenylation specificity factor (CPSF) and cleavage stimulation factor (CstF) proteins which facilitate the binding of other effector proteins to cleave the pre-mRNA transcript, allowing RNA Pol II to be released from the DNA template accompanied by the addition of a poly(A) tail to the 3' end (Brown & Gilmartin, 2003, Mandel *et al.,* 2008). After 11-14nt have been added by PAP, nuclear poly(A) binding protein (PABPN1) is able to bind to the poly(A) tail (Meyer *et al.,* 2002). Initial polyadenylation of the mRNA within the nucleus by PAP is slow until PABPN1 is able to bind the first 10-11nt (Wahle,1991, Kerwitz *et al.,*2003). After which, PAP activity increases facilitating the rapid increase in poly(A) tail length up to 200-250nt (Kuhn *et al.,*2003). However, it has been discovered that the initial poly(A) tail length within the nucleus can vary and is not always 200-250nt

(Williams, 2021). Additionally, PABPN1 has been found to be required for the efficient export of mature mRNA transcripts from the nucleus (Fuke & Ohno, 2008, Apponi *et al.,* 2010) although the mechanism by which PABPN1 facilitates export is unclear.

While transcription is occurring a protective 7-methyguanosine (m^7G) cap s added to the 5' end of the mRNA transcript (Filipowicz *et al.,* 1976, Shatkin, 1976). The cap is bound by the cap binding complex (CBC) which has important roles in the protection of the mRNA transcript as well as aiding the mRNA transcript's export from the nucleus and later facilitating the pioneer round of translation of the mRNA transcript (Izaurralde *et al.,* 1992, Izaurralde *et al.,* 1994, Flaherty *et al.,* 1997).

Additionally, most mRNA transcripts in higher eukaryotes undergo processing co-transcriptionally by the spliceosome. The spliceosome removes introns from the pre-mRNA transcript to produce the mature mRNA sequence. (Herzel *et al.,* 2017). Alternative splicing of the pre-mRNA transcript by the spliceosome facilitates the production of different transcripts from the same gene (Nilsen & Graveley, 2010) (Figure 4).

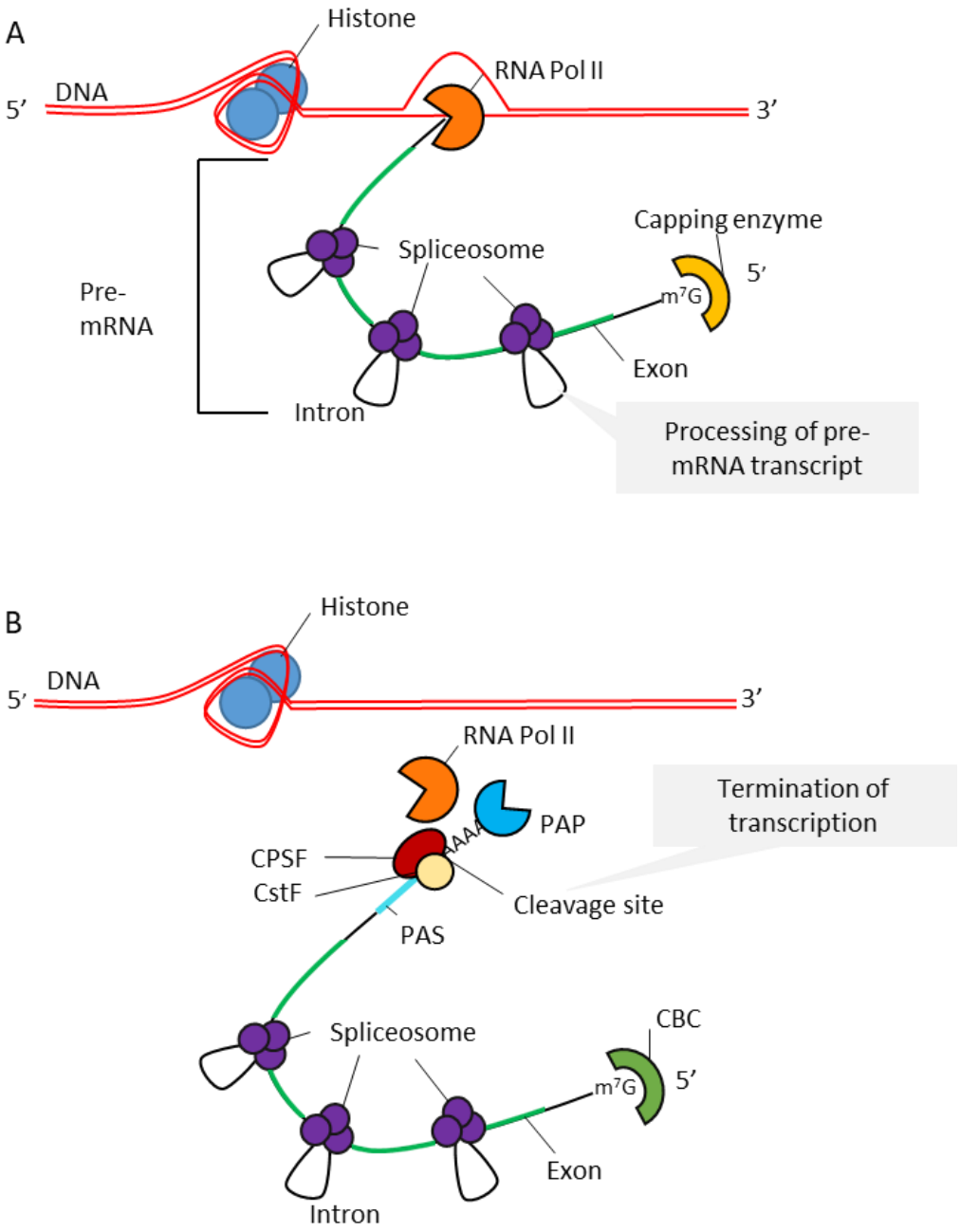

Figure 4. Simplified schematic of transcription and co transcriptional events. A) Extension of the mRNA transcripts by Pol II, alongside transcript processing by the spliceosome and addition of the m^7G cap. **B)** Termination of transcription and addition of the poly(A) tail.

1.3.2 Translation

Once the mature mRNA has been produced, it is then exported to the cytoplasm through the nuclear pore complex where it can then be translated into protein (Reviewed by Carmody & Wente, 2009). The mature mRNA sequence contains a coding region flanked by 5' and 3' untranslated regions (UTRs) which can influence translation and mRNA stability (Mignone *et al.,* 2002).

Translation is carried out by the ribosome which moves along the RNA transcript in a 5' to 3' direction to produce the protein. The ribosome is recruited by the translation initiation complex, which assembles around the m^7G cap on the 5' end of the mRNA. The translation initiation complex consists of eIF4E which binds to the cap itself (Sonenberg *et al.,* 1979, Liu *et al.,* 2011), eIF4A which unwinds the 5'UTR of the mRNA transcript, aided by either eIF4B or eIF4H (Altmann *et al.,* 1995) and a large scaffold protein eIF4G which binds both eIF4E and cytoplasmic poly(A) binding protein (PABPC), bringing the ends of the mRNA together forming a closed loop (Deo *et al.,* 1999, Marcotrigiano *et al.,* 2001) (Figure 5). The interaction of eIF4G with PABPC helps stabilise the interaction of eIF4E with the cap (Borman *et al.,* 2000). Furthermore, PABPC also enhances the ATPase and helicase activity of eIF4A (Bi *et al.,* 2000). The combined interactions of PABPC with the translation initiation factors helps facilitate the translation of the mRNA.

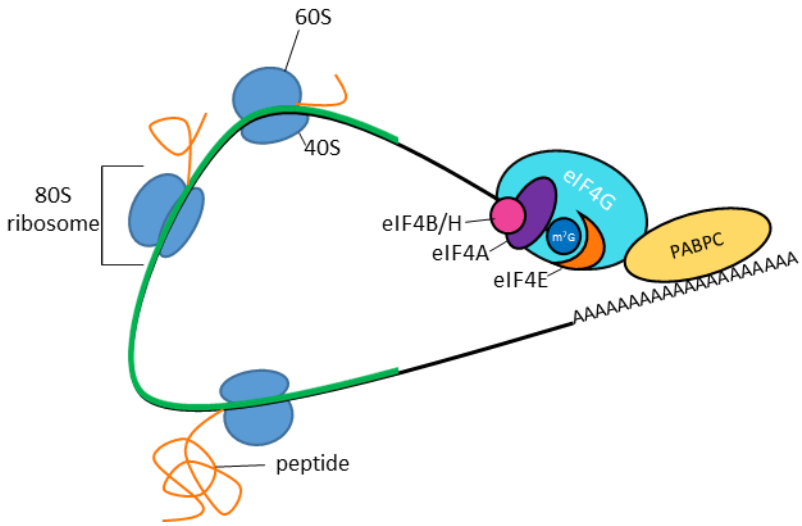

Figure 5. Simplified schematic of the closed loop model of translation.

Once the closed loop has been formed, the 40S subunit of the ribosome is then recruited to the mRNA transcript via the interaction of eIF3 with eIF4G, eIF5, and the eIF2-GTP-Met-tRNAi (Temary) complex (Merrick, 2004). The ribosome then scans along the mRNA from the 5'end until the initiator tRNA recognises the first AUG start codon in the correct context when the 60S subunit of the ribosome is then recruited via the hydrolysis of GTP bound to eIF2 (Huang *et al.,*1997, Schmitt *et al*., 2002).

The elongation stage of translation is facilitated by the release of eIF2-GDP. This allows the completed 80S ribosome to elongate the nascent peptide chain, moving along the mRNA transcript (Zuk *et al.,* 1998). Aminoacylated tRNAs with the complementary anticodon loop for each codon are recruited to the appropriate codon and are received by the A site of the ribosome facilitated by the elongation factor eEF1A. As the ribosome translocates along the mRNA, the tRNA is moved into the P site as the new tRNA enters the A site. This facilitates the addition of each new amino acid onto the nascent peptide chain within the P site. The tRNA then exits the ribosome through the E site (Schneider-Poetsch *et al.,* 2010).

Once the ribosome reaches and recognises a stop codon, the release factors eRF1 and eRF3 form a complex with GTP and bind to the ribosome A site. Hydrolysis of the GTP by eRF3 alongside hydrolysis of the peptidyl-tRNA by eRF1 releases the newly synthesised peptide (Dever *et al.,* 2012). The ribosome is then free to perform another round of translation.

1.3.2.1 RNA modifications and translational efficiency

There are a wide range of modifications to the RNA can also have an impact on translational efficiency. Methylation is one key modification that can have an impact on translational efficiency, for example the N^1-Methyladenosine (m^1A) modification within the 5'UTR of cytosolic mRNAs increases the translational efficiency of the transcript (Saffra *et al.,* 2017).

On the other hand, the 5-Methylcytosine (M^5C) modification has been found to be associated with translational repression. M^5C modification are often found on rRNAs and tRNAs, but have also been located on mRNAs as well (Squires *et al.,* 2012). With regards to mRNAs, M^5C modifications near the start codon of the has been

associated with reduced ribosome association, reducing the translational efficiency of that transcript (Schumman *et al.,* 2020).

Acetylation has also been shown to promote the translation of mRNAs. In HeLa cells N4-Acetylcytidine (ac^4C) modification at the wobble site of a Cysteine codon increased translation within a luciferase reporter assay (Arango *et al.,* 2018).

1.3.3 mRNA turnover and decay

Once transcripts have been translated into to protein, the mRNA is then often degraded. Canonical mRNA decay involves the deadenylation of the poly(A) tail to approximately 10-12nt where the 5' cap is then removed before the mRNA transcript is degraded in either a 5'3' direction by XRN1 or in a 3'-5' direction by the cytoplasmic exosome (Muhlrad *et al.,* 1994, Garneau *et al.,* 2007).

Deadenylation is considered to be the rate limiting step in the mRNA degradation process (Decker *et al.,* 1993). The majority of deadenylation is mediated by two protein complexes, the poly(A)-specific ribonuclease 2 (PAN2)-PAN3 complex and the carbon catabolite repressor 4 (CCR4)- negative regulator of transcription (NOT) complex.

The PAN2-PAN3 complex is comprised of the catalytic subunit (PAN2) supported by two copies of the adaptor protein (PAN3) which facilitates recruitment to the poly(A) tail of the target mRNA via interactions with PABPC (Wahle & Winkler, 2013). It is thought that the PAN2-PAN3 complexes initially deadenylates the first 200-110nt of the poly(A) tail where deadenylation of the final 110nt is then performed by the CCR4-NOT complex, although this is not always the case. Furthermore, it is not clear how the activity of PAN2-PAN3 is regulated (Yamashita *et al.,* 2005, Yi *et al.,* 2018, Passmore & Coller, 2022)

The CCR4-NOT complex is comprised of seven different subunits. One subunit of CCR4-NOT is CNOT1 which acts as a scaffold protein to facilitate the assembly of the whole CCR4-NOT complex. Two of the other subunits are exonucleases Caf1 and CCR4. CCR4 is able to deadenylate poly(A) tails that are bound by PABPC by triggering the release of PABPC from the poly(A) tail, whereas Caf1 is only able to remove adenosine residues not bound by PABPC (Webster *et al.,* 2018, Passmore & Coller, 2022). Subunits CNOT2 and CNOT3 are involved with decapping of mRNA

(Alhusaini *et al.,* 2016), while CNOT9 is required for the interaction with RNA and RNA binding proteins (Sgromo *et al.,* 2018, Raisch *et al.,* 2019). Lastly, CNOT4 is a ubiquitin ligase that can promote protein degradation and monoubiquitylates ribosomal proteins (Panasenko, 2014, Jiang *et al.,* 2019) (Figure 6).

Recruitment of the CCR4-NOT complex to transcripts can occur via several different mechanisms. One mechanism is through the action of RNA binding proteins (RBPs) binding to regulatory elements with the 3'UTR of the mRNA to recruit CCR4-NOT. One example is tristetraprolin (TTP), which binds to AU-rich regions (AREs) within the 3'UTR. Intrinsically disordered regions (IDRs) within TTP interact with CCR4-NOT to mediate its recruitment (Figure 6) (Brooks & Blackshear, 2013, Fabian *et al.,* 2013). The microRNA-induced silencing complex (miRISC) can also recruit the CCR4-NOT complex through direct interactions with GW182 as discussed further below (Jonas & Izaurralde, 2015) (Figures 6 and 10).

Additionally, PABPC also facilitates the deadenylation of transcripts by aiding in the recruitment of the PAN2-PAN3 and CCR4-NOT complex (Mangus *et al.,* 2004, Uchida *et al.,* 2004, Webster *et al.,* 2018).

The CCR4-NOT complex triggers the decapping of the mRNA transcript by recruiting the mRNA-decapping enzyme subunit 1 (DCP1)-DCP2 complex. This is achieved by the interaction of CNOT1 with DEAD-box ATPase DDX6 a known translational repressor and decapping activator (Chen *et al.,* 2014). The binding of the MIF4G domain of CNOT1 to DDX6 changes DDX6 to its active conformation at the same time as incorporating DDX6 into the CCR4-NOT complex (Mathys *et al.,* 2014). Subsequent removal of the 5' m^7G cap by the DCP1-DCP2 complex is crucial for destabilisation of the transcript, facilitating mRNA degradation by 5'-3' exoribonuclease 1 (XRN1) (Braun *et al.,* 2012, Mathys *et al.,* 2014, Izgur *et al.,* 2015).

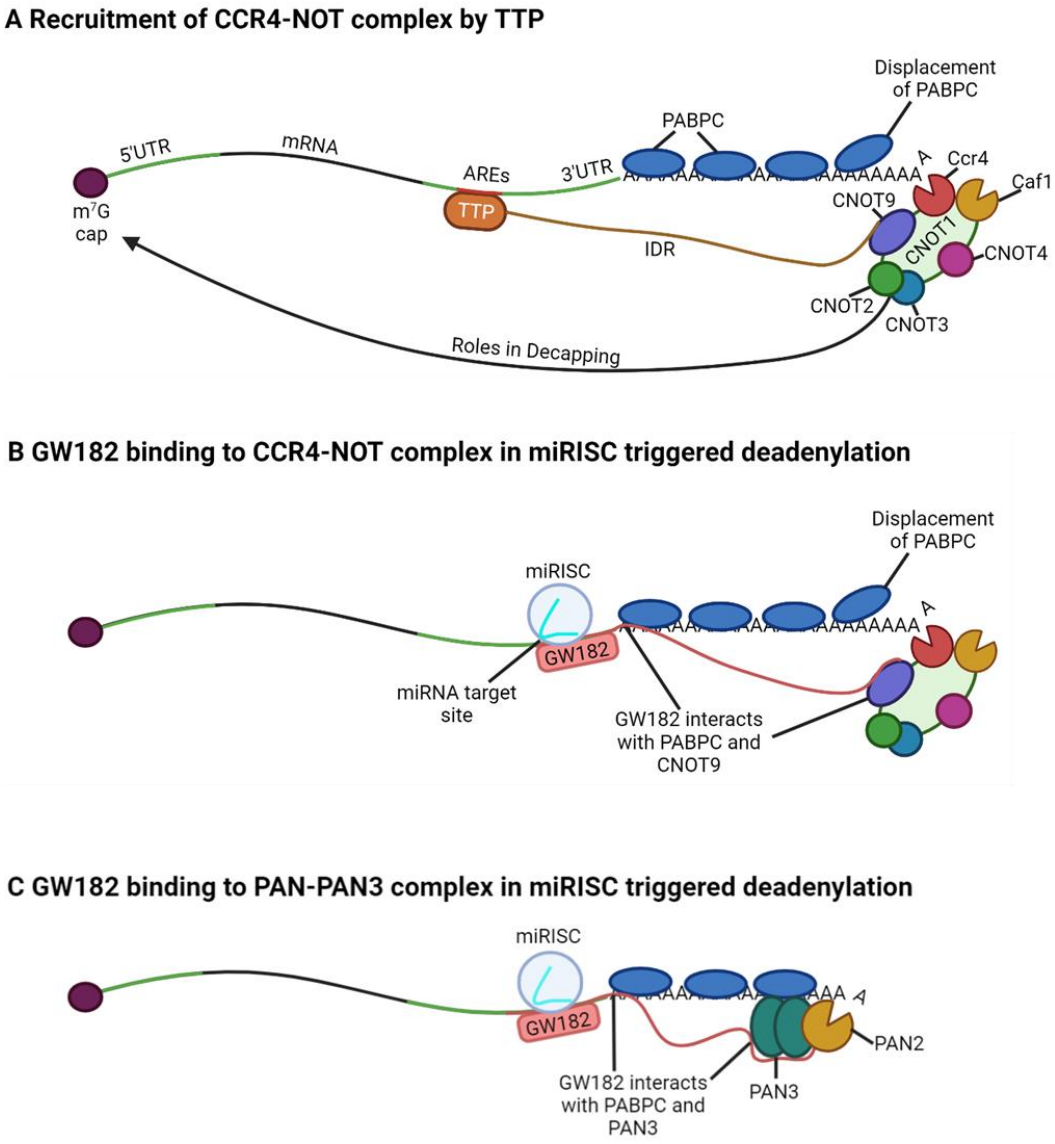

Figure 6. Schematic of mRNA deadenylation by the CCR4-NOT complex and the PAN2-PAN3 complex. **A)** Recruitment of CCR4-NOT complex to the mRNA by ARE binding protein TTP. **B)** Recruitment of CCR4-NOT complex to the mRNA by miRISC, facilitated by GW182 interactions with CNOT9 and PABPC. **C)** miRISC stimulation of deadenylation by PAN2-PAN3 via interactions of GW182 with PAN3 and PABPC.

1.4 Regulation of polyadenylation

As discussed above, poly(A) tails are added co-transcriptionally and are important in translation and mRNA turnover. As such, poly(A) tails are an important site for the regulation of gene expression. As mentioned above, a large portion of the roles of the poly(A) tails are mediated through the interaction of other proteins with poly(A) binding proteins (PABPs) that are associated with the poly(A) tail (Magnus *et al.,* 2003, Wigington *et al.,* 2014).

1.4.1 Poly(A) binding protein (PABP)

Humans have six PABPs in total, one nuclear PABP (PABPN1) and five cytoplasmic PABPs (PABPC1-5). PABPC1 (referred to as PABPC in text) is present in all major tissues whereas PABPC2-5 are all tissue-specific (Mangus *et al.,*2003, Gorgoni *et al.,* 2004).

All the PABPCs have similar structures consisting of four RNA-recognition motifs (RRMs) and a C-terminal region containing a peptide binding region denoted as a PABC domain (Kuhn & Wahle, 2004, Adam *et al.,* 1986, Sachs *et al.,* 1986). On the other hand, PABPN1 only contains a single RRM domain and an arginine rich C-terminal domain which facilitates the binding of adenosine residues (Magnus *et al.,* 2003).

PABPN1 binds to the first 10-11 adenosine residues via its RRM domain, stimulating PAP activity (Kuhn *et al.,* 2003, Kerwitz *et al.,*2003). PABN1 then coats the growing poly(A) tail, further stimulating PAP activity and facilitating mRNA export from the nucleus as discussed in section 1.3.1.

Once within the cytoplasm, PABPN is at some point exchanged for PABPC. However, the mechanism for the transition from PABPN to PABPC within the cytoplasm is unclear. It is speculated that the first round of translation may promote the switch between the two, with the ribosome dislodging PABPN (Sato & Maquat, 2009).

PABPC binds with high affinity to 12 adenosine residues, but physically spans about 30 nucleotides (Baer & Kornberg, 1983). Multiple PABPCs bind to the poly(A) tail, with longer tails able to bind more PABPC. However, the length of the poly(A) tail does not necessarily correlate with the number of PABPC molecules bound as PABPC

concentrations within the cell may limiting (Rissland *et al.,* 2017, Xiang & Bartel, 2021).

1.4.2 Poly(A) tail length

The average length of a poly(A) tail within mammals is 200nt (Edmonds *et al.,* 1971). However, poly(A) tail lengths can vary widely. Particularly, poly(A) tail lengths tend to correlate with serial binding of PABPC, so in multiples of 30, indicating that any exposed adenosine residues are quickly deadenylated (Lima *et al.,* 2017, Yi *et al.,* 2018). The discrete poly(A) tail lengths correlating to the PABPC footprint are only found for poly(A) tails of mRNA transcripts but not on other polyadenylated RNAs such as lncRNA (Lima *et al.,* 2017). This may suggest that the rapid removal of exposed adenosines on mRNA poly(A) tails may be linked to translation (Nicholson & Pasquinelli, 2019).

The length of the poly(A) tail can impact on translational efficiency particularly for translation initiation, with a longer tail traditionally thought to equate to more efficient translation (Eckmann, Rammelt & Wahle, 2010). However, a later study within *C.elegans* has found that longer poly(A) tails may instead be associated with transcripts of lower abundance that are poorly translated. Conversely, transcripts with shorter poly(A) tails are associated with highly expressed well translated genes (Lima *et al.,* 2017, Passmore & Coller, 2022).

1.4.3 Cytoplasmic polyadenylation

Polyadenylation can also occur within the cytoplasm in certain circumstances. Cytoplasmic polyadenylation usually mediates physiological processes such as germ-cell development, cellular division and cellular differentiation (Ivshina, Lasko & Richter, 2014). Widescale cytoplasmic polyadenylation of cytokines such as TNF has also been found to occur within the inflammatory response (Kwak *et al.,* 2022, Crawford, 1997).

Within oocytes and neurons, certain transcripts with short poly(A) tails are associated with transcripts that are translationally silent (Barkoff *et al.,* 1998, Richter, 1999, Subtelny *et al.,* 2014, Udagawa *et al.,* 2012). These transcripts then undergo cytoplasmic polyadenylation in order to translationally activate them (Barkoff *et al.,* 1998, Subtelny *et al.,* 2014, Udagawa *et al.,* 2012).

Within oocytes, during the early stages, PABPC is present in low concentrations, resulting in long tailed transcripts out competing short, tailed transcripts for PABPC binding. This allows for greater translation of the longer tailed transcripts (Xiang & Bartel, 2021).

It has also recently been discovered that upon LPS activation of macrophages, many transcripts important in immune function undergo tail elongation (Kwak *et al.,* 2022). Kwak *et al.,* (2022) suggest that changes in poly(A) tail length serve to increase the stability and therefore abundance of these transcripts during the inflammatory response. Although, the exact function of these tail changes in relation to translation is not clear.

The process of cytoplasmic polyadenylation usually requires the mRNA to contain a cytoplasmic polyadenylation element (CPE) within their 3'UTRs. In *Xenopus* oocyte development the CPE is bound by the CPE-binding protein (CPEB) (Hake & Richter, 1994). CPEBs are able to recruit machinery involved in either translational repression or cytoplasmic polyadenylation (Fernandez-Miranda & Mendez, 2014). Furthermore, CPEB protein family members are also involved in initiating polyadenylation-induced translation (Ivshina, Lakso & Richter, 2014).

Protein complexes involved in CPEB mediated polyadenylation or translational repression are assembled via Symplekin, a scaffold protein that allows for the assembly of larger protein complexes (Barnard *et al.,* 2004).

For both translational repression and cytoplasmic polyadenylation a deadenylating enzyme, poly(A) ribonuclease (PARN), and a polymerase interact with CPEB. Within the germline, the polymerase is usually germ-line development factor 2 (GLD2, TENT2) (Rouhana *et al.,* 2007). During translational repression, PARN is more active than GLD2, resulting in the poly(A) tail being removed as soon as it is added by GLD2. Following oocyte activation by progesterone, CPEB is phosphorylated (Sarkissian *et al.,* 2004) causing PARN to be removed from the RNA-protein complex, allowing GLD2 to extend the transcripts poly(A) tail (Kim & Richter, 2006).

Cytoplasmic polyadenylation is often mediated by non-canonical polymerases. One family of non-canonical polymerases are the terminal nucleotidyltransferases (TENTs), which also include the terminal uridylyltransferases (TUTs) (Warkocki *et al.,*

2018). However, the exact functions of each of the TENT proteins are not clear. There are eleven different TENT proteins which have been grouped into six sub-families TENT1-TENT6 (Yu & Kim, 2020) (Table 1).

The TENT proteins generally have specificity for adding adenosine residues onto the poly(A) tails, but TENT proteins that are specific for uridylyl residues are referred to as TUTs (Yu & Kim, 2020) (Table 1). However, the exact mechanism by which TENT proteins carry out cytoplasmic polyadenylation is not well understood. TENT2 interacts with CPEB and PARN to mediate polyadenylation within the germline (Radford *et al.,* 2008). On the other hand, while TENT4B is known to mediate nucleoside additions via CPEB (Burns *et al.,* 2011), how TENT4B interacts with CPEB to carry out its function is unknown. TENT5C also mediates cytoplasmic polyadenylation (Liudkovska *et al.,* 2022, Mroczek *et al.,* 2017), and while TENT5C is known to interact with PABPC, how TENT5C carries out its adenylating function is also unknown (Mroczek *et al.,* 2017).

An interesting novel role for specifically TENT4A and TENT4B is protecting from deadenylation by mixed tailing. TENT4A and TENT4B are able to incorporate any nucleotide into the poly(A) tail resulting in mixed tailing (Lim *et al.,* 2018). With a slightly greater preference for guanosine, the incorporation of other nucleosides into the poly(A) tail by TENT4A and TENT4B, helps protect the mRNA from rapid deadenylation. This mixed tailing has been found to be more prevalent for mRNA transcripts encoding secreted proteins that are processed at the ER (Lim *et al.,* 2018).

Table 1. Members of the TENT family. The alternative names for members of the TENT family as well as processes that they have been implicated in.

Subfamily name	Enzyme name	Alternative Names	Processes implicated in	Publications
TENT1	TUT1	Star-PAP, U6 TUTase, PAPD2	Uridylation of U6 snRNA promoting its maturation	Trippe *et al.,* 2006
TENT2	TENT2	GLD2, PAPD4, TUT2	Cytoplasmic polyadenylation within the germline	Rouhana *et al.,* 2007

TENT3	TUT4 TUT7	(TENTA, PAPD3, ZCCHC11) (TENT3B, PAPD6, ZCCHC6)	Uridylation of mRNAs to promote degradation	Chang *et al.,* 2018 Morgan *et al.,* 2017
			Uridylation of Histone mRNA to facilitate maturation	Mullen *et al.,* 2008 Schmidt *et al., 2011*
			Uridylation of pre-miRNAs to promote alternative processing or degradation	Kim *et al.,* 2015 Heo *et al.,* 2009
			Uridylation of miRNA to alleviate target repression or promote degradation	Gutierrez-Vazquez *et al.,* 2017
TENT4	TENT4A	POLS, PAPD7, TUT5, TRF4-1	Mixed tailing of mRNAs to enhance stability	Lim *et al.,* 2018
	TENT4B	PAPD5, TRF4-2, TUT3	Mixed tailing of mRNAs to enhance stability	Lim *et al.,* 2018
			Polyadenylation of miRNA	Boele *et al.,* 2014
			Polyadenylation of snoRNA to promote maturation	Berndt *et al.,* 2012
TENT5	TENT5A	FAM46A	Polyadenylation of mRNA to enhance stability and translation. (TENT5A and TENT5C have roles in inflammation)	Bliska *et al.,* 2019 Liudkovska *et al.,* 2022
	TENT5B	FAM46B		
	TENT5C	FAM46C		
	TENT5D	FAM46D		
TENT6	TENT6	MTPAP, PAPD1	Adenylation of mitochondrial mRNAs and tRNAs to promote translation and maturation	Nagaike *et al.,* 2005 Wilson *et al.,* 2014

1.4.4 Alternative polyadenylation

Approximately 50-80% of mammalian pre-mRNAs have alternative sites within the 3'-UTR where polyadenylation can occur, producing distinct mRNA isoforms. This is referred to as alternative polyadenylation (APA) (Hoque *et al.,* 2013, Detri *et al.,* 2012). APA causes the 3'UTR of these mRNA isoforms to vary due to the poly(A) tail being formed at different locations within the 3'UTR. This can result in the inclusion or exclusion of regulatory elements located within the 3'UTR such as AREs or miRNA target sites. As such, APA is able to contribute to the posttranslational regulation of mRNA transcripts (Ren *et al.,* 2020).

There are four different classes of APA. The most common are tandem 3'UTR APA and alternative terminal exon APA which both involve cleavage within the 3'UTR of the mRNA transcript. There is also intronic APA and internal exon APA which are far less common (Elkon, Ugalde & Agami, 2013). Changes to the 3'UTR by APA can have effects on the stability, translation efficiency, and localisation of mRNA transcripts (Andreassi & Riccio, 2009).

1.4.5 Changing poly(A) tail lengths in inflammation

Regulation of poly(A) tail lengths occurs during the inflammatory response. TNF is known to undergo readenylation during inflammation (Crawford *et al.,* 1997). Furthermore, Kwak *et al.,* (2022) have found that transcripts involved in immune function undergo widespread poly(A) tail changes during inflammation. In a separate study in a RAW 264.7 mouse macrophage model of inflammation, inhibition of polyadenylation or shortening of the poly(A) tail reduces the expression of inflammatory mRNAs, however, the expression of housekeeping mRNAs was unaffected (Kondrashov *et al.,* 2012). This suggests that poly(A) tail length is important in regulating the expression of inflammatory genes. Additionally, it has recently been discovered by the De Moor group that the initial poly(A) tail of inflammatory mRNAs changes in length over the course of the inflammatory response within LPS treated RAW 264.7 mouse macrophages. As transcription of inflammatory genes is induced, the length of the initial poly(A) tail increases, then shortens as transcriptional induction declines (Gandhi, 2016) (Figure 7). However,

the mechanism by which the change in poly(A) tail length is occurring is not yet known.

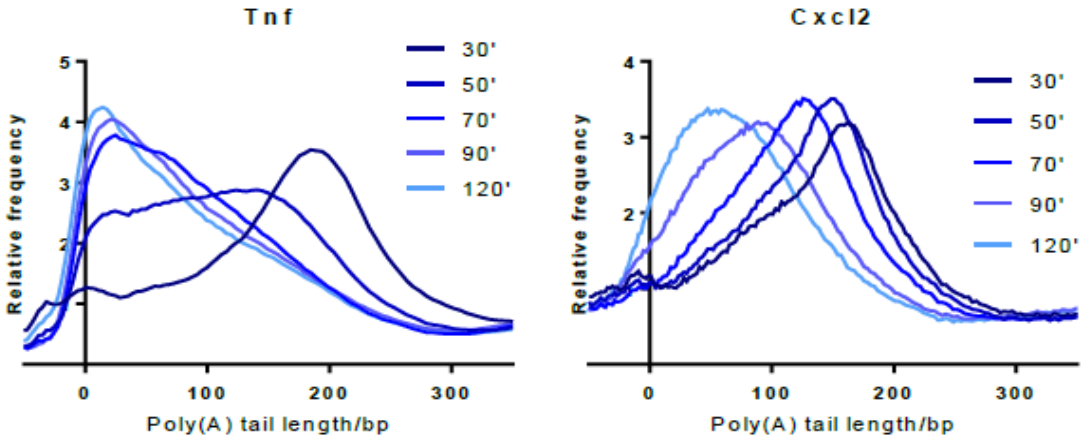

Figure 7. Poly(A) tail length of TNF and Cxcl2 after treatment with lipopolysaccharide (LPS). RAW 264.7 cells treated for 30, 50, 70, 90, and 120 minutes.(Gandhi, 2016).

A final factor that can influence the length of the poly(A) tail within the cell and therefore control gene expression are microRNAs, due to their ability to be able to trigger the deadenylation and subsequent degradation of mRNA transcripts.

1.5 Overview of microRNAs

MicroRNAs (miRNAs) are small 21-23 nucleotide (nt) RNAs that regulate mRNA transcripts via translational repression and mRNA decay. MiRNAs are critical for normal animal development and have wide roles in physiological processes such as cardiac function, ovulation, the immune system, and the progression of cancer. As such, miRNAs are associated with various diseases when their regulation is disrupted (Tian, An & Niu, 2017, Baley & Li, 2012, Mehta & Baltimore, 2016, Peng & Croce, 2016). The first miRNA to be discovered was *lin-4* within *Caenorhabditis elegans,* which when mutated results in an inability to properly develop adult features (Lee, Feinbaum & Ambros, 1993). The gene was found to encode a small RNA that facilitated post-transcriptional repression of the mRNA by binding to complementary regions within the 3'UTR (Lee, Feinbaum & Ambros, 1993, Lau *et al.,* 2001). It was then later found that many different miRNAs are present in many different species including humans (Lagos-Quintana *et al.,* 2001, Lee *et al.,* 2001). Not long after, it was also established that miRNAs were tissue specific with certain miRNAs only expressed in certain tissues (Lagos-Quintana *et al.,* 2002).

1.5.1 MicroRNA biogenesis- canonical

1.5.1.1 Primary microRNAs

The majority of miRNAs are found within longer Pol II transcripts, either long noncoding RNAs (lncRNAs) or within the intronic regions of protein coding genes with a few being found within exons (Slezak-Procazka *et al.,* 2013). MiRNAs are often located in clusters containing a small group of miRNAs. These are then all transcribed together by RNA Pol II as polycistronic transcripts which are then later processed into individual miRNAs (Treiber, Treiber & Meister, 2009). Conversely, miRNAs can also be monocistronic, located on their own and transcribed individually. The newly transcribed miRNA is referred to as the primary-miRNA (pri-miRNA). These pri-miRNAs contain the mature miRNA sequence within a hairpin structure (Lee *et al.,* 2004) (Figure 8).

These primary-miRNAs are firstly processed co-transcriptionally by the microprocessor to form a precursor-miRNA (pre-miRNA), consisting of a ~60nt bp stem loop with ~2nt overhang. This allows the pre-miRNA to be exported into the cytoplasm by Exportin 5 and RAN-GTP (Figure 8) (Yi *et al.,* 2003).

The microprocessor consists of two subunits, Drosha and DGCR8. Dimeric DGCR8 recognises a conserved UGU sequence within the apical loop region of the pri-miRNA hairpin in which it binds. DGCR8 thus acts as an anchor which then allows Drosha to cleave the pri-miRNA (Nguyen *et al.,* 2015). The microprocessor complex measures the 35bp stem from both ends and makes offset cuts at 13nt and 11nt from one end and 22nt and 24nt at the other end to produce the pre-miRNA (Fang & Bartel, 2015).

1.5.1.2 Dicer and Argonaute proteins

Once exported to the cytoplasm by Exportin 5 (Yi *et al.,* 2003) the pre-miRNA undergoes further processing by Dicer, removing the loop and leaving the mature miRNA duplex. The duplex has 2nt 3' overhangs at each end and contains the active miRNA, usually the 5p strand, paired to the passenger strand, usually the 3p strand. (Figure 8). The mature miRNA strand is loaded into the Argonaute (Ago) protein, forming a part of the RNA-induced silencing complex (RISC) that translationally represses mRNA transcripts (Figure 8).

Within mammals, there are four Ago proteins, 1-4, with Ago2 being the most highly expressed and having the best characterised roles (Liu *et al.,* 2004). The Ago proteins are comprised of four key domains, the amino (N) - terminal domain, the Piwi-Argonaute-Zwille (PAZ) domain, the MID domain, and the P-element inducted wimpy test (PIWI) domain (Jinek & Doudna, 2009). The PAZ domain is responsible for binding the 3' nucleotide of the miRNA while the MID and PIWI domains hold the miRNA 5' nucleotide (Sheu-Gruttadauria & MacRae, 2017).

Ago 1, 2 and 3 are expressed in many different cell lines and tissues whereas Ago4 is less well expressed (Petri *et al.,* 2011). It is thought that Ago4 may be more tissue specific and it has been found to be involved with spermatogenesis within mice (Hu *et al.,* 2012).

For loading to occur, the Ago protein uses ATP to assume a high-energy conformation, allowing the miRNA duplex to access the binding pocket (Sheu-Gruttadauria & MacRae, 2017). The determination of which strand becomes the active miRNA is due to which 5' end of the miRNA duplex is most suitable for binding within the pocket. There are two determinants of which 5' end is most suitable for binding. The preferentially loaded strand is usually the one with the less stably paired

5’end (Khvorova *et al.,* 2003, Schwarz *et al.,* 2003). Ago proteins also prefer binding an adenosine residue within the binding pocket (Kawamata, Yoda & Tomari, 2011).

In some cases, both strands are equally loaded onto the Ago protein. For example, miR-34b-5p and miR-34b-3p have been found within human cells to be expressed in equal concentrations and have distinct mRNA targets (Cordova-Rivas *et al.,* 2019). Once loaded, the Ago protein returns to its steady state conformation promoting the expulsion of the passenger miRNA strand, forming the mature RNA-induced silencing complex (Sheu-Gruttadauria & MacRae, 2017).

In the case of Ago2 loading, the passenger strand is nicked by Ago2 endonuclease activity and is removed from the RISC by CP30, an endonuclease. Removal of the passenger strand by CP30 activates the RISC complex facilitating its regulatory function (Liu *et al.,* 2009, Ye *et al.,* 2011) (Figure 8).

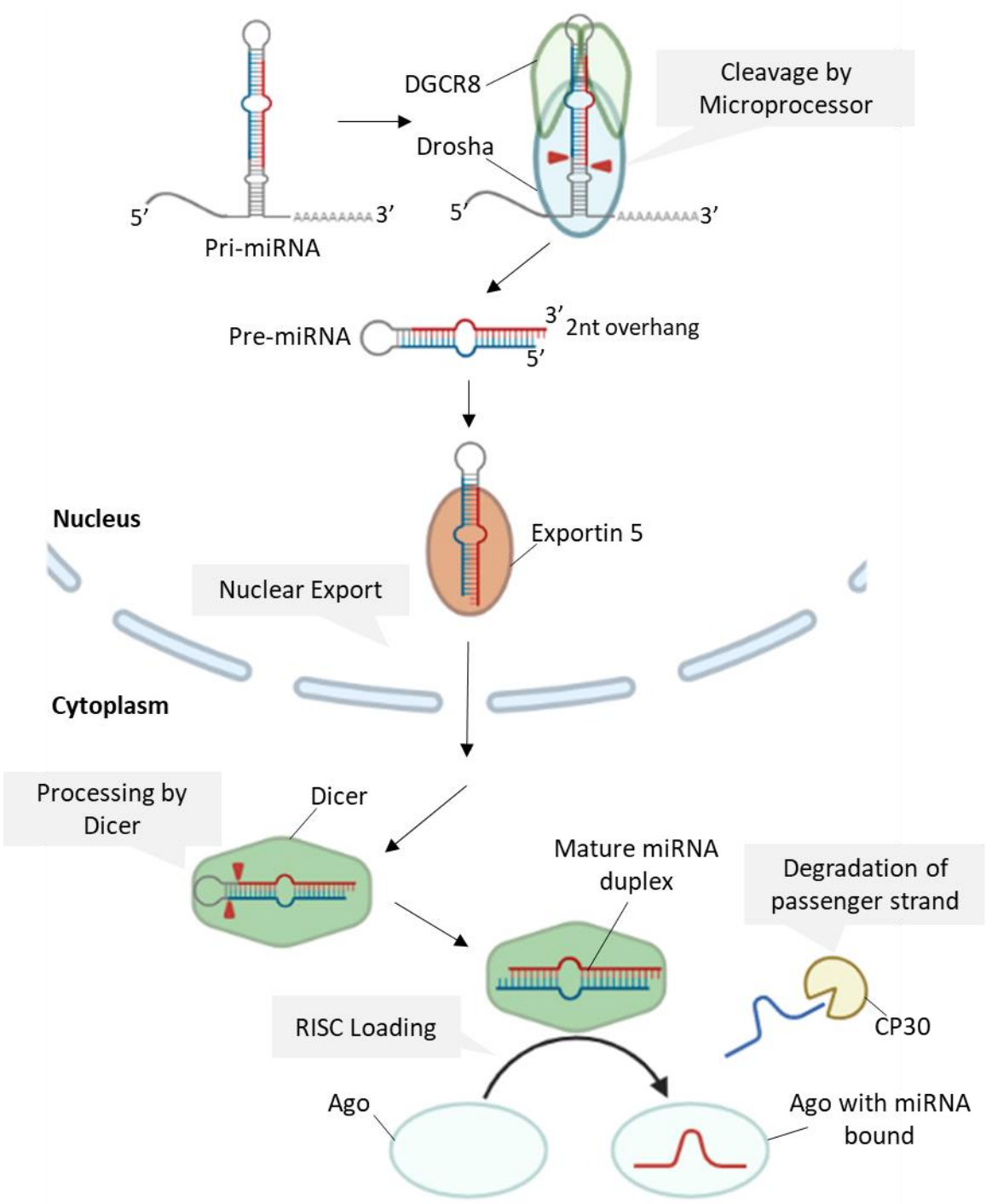

Figure 8. Canonical miRNA biogenesis. Pri-miRNA is processed by the microprocessor consisting of Drosha and DGCR8 within the nucleus to form the pre-miRNA. The pre-mRNA is exported to the cytoplasm by Exportin 5 where it then undergoes further processing by Dicer to form the mature miRNA duplex. One strand of the duplex is then loaded onto the Ago protein while the other strand is degraded by CP30.

1.5.2 MicroRNA biogenesis – non-canonical

There are pathways in which non-canonical miRNA biogenesis can occur. They are often grouped into Drosha/DGCR8 – independent and Dicer-independent methods. One example of a Drosha-independent miRNA pathway is the production of miRNAs due to the direct action of the spliceosome on specialised introns known as mirtons. The mirtons form hairpins like that of pre-miRNA structures, although they are generally longer and contain more bulges and internal loops. The mirtons skip processing by microprocessor but enter the canonical pathway to be cleaved by Dicer (Ruby, Jan & Bartel, 2007).

Another example of a microprocessor independent class of miRNA is the 7-methylguanosine (m^7G) capped pre-miRNA, generated by direct transcription of the pre-mRNA. These pre-miRNAs are shorter than normal and do not require processing by microprocessor and are exported straight to the cytoplasm by exportin 1. There is a strong 3p strand bias as the m^7G cap prevents the 5p strand from loading into the Ago protein (Xie *et al.,* 2013).

Finally, pre-miRNAs can also be processed to mature miRNAs in a Dicer-independent pathway. The Ago2 protein carries out the pre-miRNAs final processing as the substrates are too short to be processed by Dicer. MiR-451 in particular is known to be processed by Ago2. A short pre-miR-451 is generated by Drosha that is finally cleaved by Ago2 to form the mature miR-451 (Yang *et al.,* 2010).

1.5.3 Regulation of microRNA biogenesis

Regulation of miRNA production can occur in many different ways and at many different levels in the biogenesis pathway (Gebert & MacRae, 2019).

1.5.3.1 Transcription

As many pri-miRNAs are located within the intronic regions of protein coding genes, transcription of these pri-miRNA is often regulated by the gene specific promoter and any transcription factors that may bind to it (Krol *et al.,* 2010). However, it has been found that some promoters of intronic miRNAs are distinct from the promoters of the genes they are located within (Monteys *et al.,* 2010). MiRNA gene regulation can also be affected by epigenetic control such as DNA methylation and histone modification (Davis-Dusenbery *et al.,* 2010).

1.5.3.2 Drosha and Dicer

Post-translational modifications and cofactors are able to change the activity or specificity of the microprocessor, regulating miRNA production (Kim *et al.,* 2010, Auyeung *et al.,* 2013). Phosphorylation of Drosha by glycogen synthase kinase 3β (GSK3β) targets the microprocessor to the nucleus instigating the processing of newly synthesised pri-miRNAs (Kim *et al.,* 2010, Tang *et al.,* 2010). Deacetylation of Drosha by histone deacetylase 1 (HDAC1), increases the affinity of Drosha for pri-miRNA (Wada *et al.,* 2012). DCGR8 is also phosphorylated which helps increase microprocessor activity and miRNA levels (Herbert *et al.,* 2013). A cofactor involved in enhancing microprocessor activity is hemin. Hemin aids the DGCR8 subunits in recognising the UGU motif within the apical loop of the pri-miRNA, increasing cleavage specificity (Nguyen *et al*., 2018).

In humans, Dicer interacts with TAR RNA-binding protein (TRBP). TRBP acts to regulate the processing efficiency of some pre-miRNAs and helps tune the length of mature miRNAs (Fukunaga *et al.,* 2012, Lee *et al.,* 2012). *DICER1* mRNA in humans also contains a target site for let-7, which acts as a negative feedback loop between Dicer and its product let-7 (Tokumaru *et al.,* 2008, Forman *et al.,* 2008).

RNA-binding proteins binding to regions of the pre-miRNA can also positively or negatively regulate their processing by Dicer. LIN28 interferes with Dicer processing of pre-let-7 by binding to the terminal loop (Heo *et al.,* 2008). KH-type splicing regulatory protein (KSRP) also binds to the terminal loop of various pre-miRNAs, promoting Dicer mediated processing (Trabucchi *et al.,* 2009).

1.5.3.3 MicroRNA turnover

Although more stable that mRNA, miRNAs still have a rate of turnover. However, the rate of turnover varies widely and is specific for different tissues and miRNAs (Ruegger & Grosshans, 2012). For example, miRNAs within neuronal tissues exhibit a much faster rate of turnover compared to other tissues (Krol *et al.,* 2010). A direct mechanism of miRNA turnover is target RNA-directed miRNA degradation (TDMD). TDMD is where complete complementarity between the miRNA and its target mRNA promotes the miRNA's turnover (Ameres *et al.,* 2010).

Non-templated nucleotide addition (NTA) is miRNA specific across different tissues and usually involves adenylation or uridylation at the 3'end. NTA serves to regulate

the stability of various miRNAs, serving to either reduce or increase stability. For example, GLD2 (TENT2), stabilises miR-122 in the liver by the addition of a single adenosine residue (Katoh *et al.,* 2009). Conversely, adenylation of miR-21 by TENT4B (PAPD5) triggers the degradation of miR-21 (Boele *et al.,* 2014). Additionally, uridylation of miRNAs can also promote their degradation. For instance, uridylation by terminal uridylyltransferase 4 (TUT4) primes many miRNAs for degradation during T-cell activation (Gutierrez-Vazquez *et al.,* 2017).

1.5.4 MicroRNA target recognition and regulation

In most instances, miRNAs bind to regions complementary to their seed within the 3'UTR of target mRNA. The seed region is situated between nucleotides two and eight of the miRNA sequence (Bartel 2009, Huntzinger & Izaurralde 2011). MiRNA target binding is often enhanced by supplementary pairing of the region between nucleotides 13-16 (Grimson *et al.,* 2007) (Figure 9). A single target mRNA may have multiple miRNA target sites, likewise, each miRNA can target multiple mRNAs. The interaction of the seed region with the target mRNA allows the RNA-induced silencing complex (RISC) to mediate translational repression and decay of the mRNA target. Within plants and for siRNAs, Ago2 acts as an endonuclease to cleave target mRNA at fully complementary sites (Diederichs & Harbour, 2007). Complementarity to nucleotides 10 and 11 is required for cleavage to occur and most animal miRNAs have evolved sites that avoid this pairing (Liu *et al.,* 2004, Park & Shin, 2014).

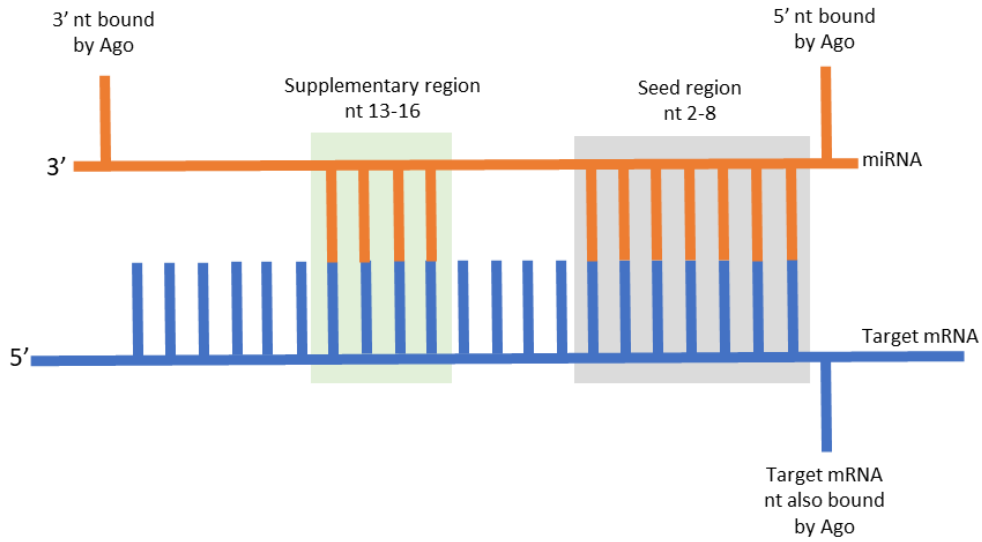

Figure 9. Binding of the miRNA seed region to its target mRNA. The seed region binds to a complementary site within the mRNA 3'UTR. This binding is essential for miRNA regulation to occur. There is also supplementary binding of the miRNA to the target mRNA between nt 13-16 of the miRNA.

1.5.4.1 Mechanism of microRNA mediated mRNA degradation

MiRNA binding to 3'UTR sites leads to decreased levels of the corresponding protein. However, the exact mechanism of miRNA regulation has been difficult to elucidate, but both translational repression and mRNA deadenylation and degradation have been implicated (Behm-Ansmant *et al.,* 2006, Braun *et al.,* 2011, Fabian *et al.,* 2011, Pillai *et al.,* 2005, Mathonnet *et al.,* 2007, Meijer *et al.,* 2013). The level of repression for miRNAs is generally lower than for siRNAs. However, it has been found that numerous different miRNAs can bind to the same target mRNA, acting cooperatively to increase the repression of protein production of the target mRNA (Hashimoto *et al.,* 2013).

1.5.4.2 TNRC6/ GW182 proteins

MicroRNA mediated regulation is assisted by members of the GW182 protein family also known as the TNRC6 family (Rehwinkel *et al.,* 2005, Jakymiw *et al.,* 2005). Within mammals, there are three TNRC6 proteins, A, B, and C (Meister *et al.,* 2005, Baillat & Shiekhattar 2009).

The GW family of proteins all have an N domain containing multiple glycine-tryptophan (GW) repeats. It is the N domain that interacts with the Ago proteins facilitating association with target mRNA via PABPC (Huntzinger & Izaurralde, 2011). A GW protein is able to bind up to three Ago proteins at once (Elkayam *et al.,* 2017). This allows for the possibility of cooperative action of multiple miRNAs on the same target.

The interaction of GW proteins with PABPC has been suggested to prevent the interaction of PABPC with the eIF4G, preventing mRNA circularisation and thus translation initiation. As PABPC facilitates RISC binding, it has been suggested that the length of the poly(A) tail correlates with increased silencing efficiency due to greater PABPC occupancy (Zekri *et al.,* 2009, Moretti *et al.,* 2012).

1.5.4.3 Deadenylation and degradation of miRNA target mRNAs

MiRNA binding of the target mRNA results in the recruitment of the deadenylases PAN2-PAN3 and CCR4-NOT, promoting deadenylation of the target mRNA as described in section 1.3.3. The TNRC6 proteins bind directly to the CNOT1 subunit of CCR4-NOT or directly to PAN3 in order to facilitate deadenylation of the mRNA target (Jonas & Izaurralde, 2015). TNRC6 can bind to two deadenylases at a

time and directly interacts with both the PAN2-PAN3 complex as well as the CCR4-NOT complex (Behm-Ansmant *et al.,* 2006, Braun *et al.,* 2011, Fabian *et al.,* 2011) (Figure 10).

Furthermore, TNRC6 interaction with PABPC disrupts the closed loop model by interrupting the binding of eIF4G with PABPC (Zekri *et al.,* 2009).

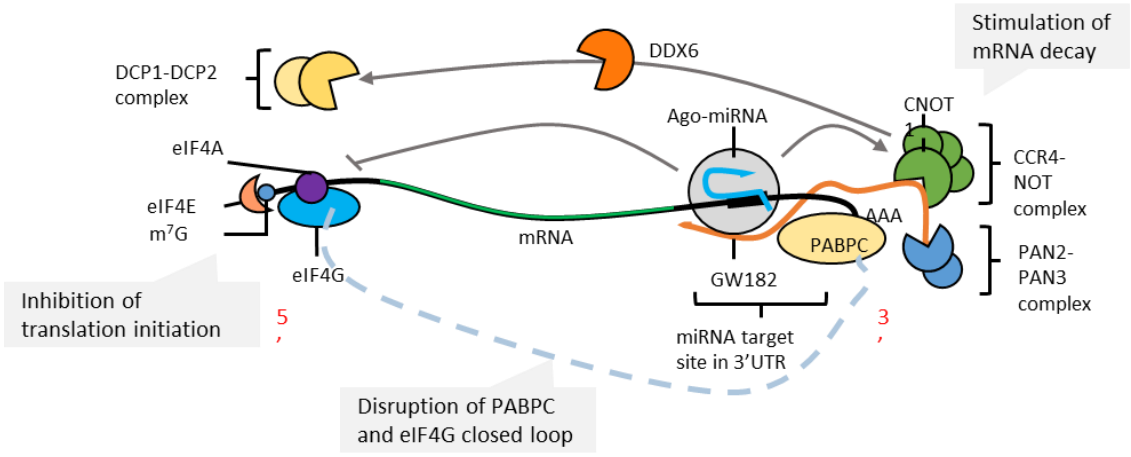

Figure 10. Mechanism of miRNA mediated decay and inhibition of translation initiation. GW182 recruits deadenylase complexes PAN2-PAN3 and the CCR4-NOT complex. Binding of the RISC complex to the mRNA also triggers the dislodging of translation initiators eIF4A1. CCR4-NOT complex also recruits the DCP1-DCP2 complex which removes the m^7G cap

1.5.4.4 MicroRNA mediated translational repression

MiRNAs can also regulate mRNA transcripts via translational repression, reducing protein production (Pillai *et al.,* 2005, Mathonnet *et al.,* 2007). The method by which miRNAs mediate translational repression is not fully understood.

Translation initiation is thought to be inhibited via the disruption of eukaryotic initiation factor 4 F (eIF4F) complex facilitated by the CCR4-NOT complex (Mathonnet *et al.,* 2007, Meijer *et al.,* 2013). The eIF4F complex assembles around the m^7G cap at the 5' end of the mRNA facilitating assembly of the ribosome and translation as described in section 1.3.2.

Furthermore, some studies suggest this process is aided by DDX6. It has been shown that binding of DDX6 to the eIF4E transporter (4E-T) competes with eIF4G for binding to eIF4E helping to promote RNA decay (Kamenska *et al.,* 2014, Nishimura *et al.,* 2015). DDX6 was shown to be recruited to mRNA transcripts via interaction with

CNOT1 promoting the decapping and therefore translational repression of mRNA targets (Chen *et al.,* 2014, Mathys *et al.,* 2014).

Conversely, other research suggests that translational repression is mediated by specifically the interaction of eIF4A-II with CCR4-NOT, without the involvement of DDX6 (Meijer *et al.,* 2013, Wilcyzynska *et al.,* 2019, Meijer *et al.,* 2019). It has been shown that the RISC complex causes eIF4A-II to dissociate from the target mRNA preventing scanning by the ribosome and formation of the eIF4F translation initiation complex (Meijer *et al.,* 2013). Meijer *et al.,* (2013) found that knockdown of eIF4-II but not eIF4-I resulted in the stabilisation of a reporter mRNA with let-7 target sites. Furthermore, Meijer *et al.* (2013) found that eIF4-II interacts directly with the CCR4-NOT complex via CNOT7. Additional data by Wilcyzynska *et al.,* (2019), confirm using RIP-seq that eIF4A-II is required for miRNA mediated translational repression and suggest that DDX6 is likely to have a broader role in mRNA regulation as opposed to being required for purely miRNA-mediated regulation.

1.5.5.5 Localisation of translationally repressed mRNAs

mRNAs that are translationally repressed or actively undergoing deadenylation and decay are located in cytoplasmic ribonucleoproteins granules called processing bodies (P-bodies). P-bodies are predominantly enriched for proteins related to translational repression and 5'-3' mRNA decay such as XRN1, DDX6 and CCR-4NOT as well as miRISC components such as Ago2 and GW182 (George *et al.,* 2018, Liu *et al.,* 2005).

On the other hand, mRNA that is actively being translated is located within polysomes. mRNAs that are translationally repressed can move out of P-bodies into the polysome pool under varying different growth or stress conditions (Brengues *et al.,* 2005, Bhattacharyya *et al.,* 2006). This indicates that the translational repression within P-bodies is reversible and the components of P-bodies, including miRNA and the RISC complex are able to act as regulatory houses to control gene expression.

1.5.5 Regulation of miRNA function

MicroRNA function can be regulated in several different ways. Editing of the miRNA sequence, changes to Ago function, or the interaction of other RBPs with the

miRNA can alter how miRNAs carry out their function (Reviewed by Gebert & MacRae, 2019).

1.5.5.1 MicroRNA arm switching

One way in which miRNA activity is regulated is via arm switching. Switching between whether the 5p or the 3p strand of the mature miRNA duplex is selected for loading onto the Ago protein. As the different strands will have opposing sequences, they are able to bind to different target mRNAs. However, the exact mechanism by which arm switching occurs is not fully understood. One mechanism found for miR-324 arm switching within mice is that alternative processing by Dicer triggered by uridylation of the pre-miRNA creates a miRNA-duplex with a different terminus that is then preferentially selected by Ago resulting in a switch from the 5p strand to the 3p strand (Kim *et al.,* 2020). It has also been suggested that strand selection is dependent on target availability, as binding of the miRNA to its target can facilitates its stabilisation (Chatterjee *et al.,* 2011, Tsai *et al.,* 2016). Furthermore, preferences for one strand or the other can be tissues specific. For example, miR-194-5p in mice is highly expressed within the brain with very limited expression of miR-194-3p. However, in other tissues such as the lungs and ovaries both miR-194-5p and miR-194-3p are expressed equally (Ro *et al.,* 2007).

One key arm switching event within inflammation is miR-155 during the inflammatory response. Although, how the strand switching occurs for miR-155 is not clear. The ratio of miR-155-5p to 3p changes throughout the stages of dendritic cell activation (Zhou *et al.,* 2010). Zhou *et al.,* (2010) found that miR-155-3p expression peaked at three hours after stimulation of TLR4 and was found to promote the expression of cytokines TNF and IL1-β. On the other hand, miR-155-5p expression was found to peak at 12 hours after TLR7 activation, targeting components of TLR signally, acting to reduce cytokine expression. Additionally, within macrophages, both miR-155-5p and miR-155-3p have been found to be expressed in differing levels in response to stimulation of various inflammatory pathways (Simmonds, 2019). Due to this disparity between miR-155-5p and miR-155-3p expression, it has been speculated that the control of miR-155-5p and miR-155-3p expression within macrophages is under the control of distinct immune regulatory pathways (Ruggiero *et al.,* 2009, Simmonds, 2019).

1.5.5.2 Editing of microRNA sequences

Formation of isomirs is one way in which miRNA activity is regulated. Isomirs are variants of mature miRNAs that can vary in sequence, length, or both (Tan *et al.,* 2014), and are formed via 3' editing after production. Alternative cleavage by both Drosha and Dicer can alter or shift the seed sequence producing 5' isomirs resulting in a change of mRNA target (Neilsen, Goodall & Bracken, 2012). Specifically, alternative cleavage by Dicer serves to modulate the seed sequence of 3p miRNA strands and can subsequently affect which guide strand is selected by Ago (Lee & Doudna, 2012).

Editing of the miRNA sequence is also a way in which miRNA function can be regulated. The most common type of miRNA precursor editing is deamination whereby adenosine is converted to inosine by adenosine deaminase acting on RNA (ADAR). This change alters the base pairing of the mature miRNA to the target mRNA. Moreover, editing of the pri-miRNA by ADAR can promote its degradation, further serving to regulate miRNA expression (Nishikura, 2016).

1.5.5.3 Sponging of microRNAs

MiRNAs can also be sequestered by sponges also referred to as competitive endogenous RNAs (ceRNAs) (Ebert *et al.,* 2007, Poliseno *et al.,* 2010). These sponges are often lncRNAs or circular RNAs (circRNAs) that have miRNA binding sites within their sequence (Kartha *et al.,* 2014). It is thought that these ceRNAs compete for binding of the miRNA with the target mRNA transcripts, sequestering away the miRNA and facilitating the upregulation of the miRNA target gene expression (Kartha *et al.,* 2014). Although how much of an impact miRNA sponges have on altering gene expression is controversial (Broderick & Zamore, 2014, Thomson & Dinger, 2016).

1.5.5.4 Modifications to microRNA target sites

MicroRNA activity can also be regulated through the modifications of miRNA target sites within the 3'UTRs of target mRNAs. Ago proteins are unable to recognise N^6-methlyadenosine modification in RNA, which could affect how miRNAs interact with their targets (Schirle *et al.,* 2015). In addition, the formation of different mRNA 3'UTR isoforms via APA can add or remove miRNA target sites. The different 3'UTR lengths generated by APA can impact on mRNA stability and translation by affecting

what miRNAs can bind, altering the post-transcriptional regulation of the mRNA (Akman & Erson-Bensan, 2014, Nam *et al.,* 2014).

1.5.5.5 Regulation of Ago function

Argonaute proteins can undergo post-translational modifications in order to regulate their function. One example is hydroxylation of Ago2 by prolyl-4-hydroxylase, which acts to stabilise Ago2 (Qi *et al.,* 2008).

It has also been found that Ago proteins can be phosphorylated at several different sites. The site at which Ago is phosphorylated determines the effect on Ago function. Phosphorylation of Ago has been shown to regulate the localisation of Ago proteins, binding of Ago to small RNAs, and the gene silencing ability of Ago (Zeng *et al.,* 2008, Rudel *et al.,* 2011, Golden *et al.,* 2017).

Phosphorylation in the linker region of Ago at Serine387 by MAP-kinase-activated protein kinase 2(MAPK-APK2) or RACγ serine/threonine-protein kinase (AKT3) results in increased miRNA mediated repression (Zeng *et al.,* 2008). Whereas phosphorylation at either tyrosine393 or tyrosine592 results in reduced levels of Ago2-associated miRNAs and miRNA loading (Shen *et al.,* 2013, Rudel *et al.,* 2011, Mazumder *et al.,* 2013).

Ago phosphorylation has also been found to occur in response to specific triggers. Phosphorylation of tyrosine393 is often in response to hypoxic stress (Shen *et al.,* 2013). Another example is Ago phosphorylation of tyrosine529 within macrophages during the inflammatory response. Upon stimulation of macrophages with LPS, Ago2 is phosphorylated causing currently bound miRNAs to dissociate. This dissociation is proposed to allow for the increase in expression of inflammatory genes facilitating the progression of the inflammatory response (Mazumder *et al.,* 2013).

1.5.5.6 Interaction of RBPs with microRNA regulation

RBPs can also modulate miRNA-target interactions via binding to regulatory elements within the 3'UTRs of target mRNAs.

AU-rich element binding factor 1 (AUF1), has been found to enhance miRNA loading onto Ago2 by binding mature miRNAs, facilitating their transfer to Ago2. As such, AUF1 promotes miRNA-mediated mRNA degradation (Yoon *et al.,* 2015, Min *et al.,* 2017).

Conversely, HuR has been found to reduce the activity of miRNAs. One such mechanism is that HuR aids the export of miRNA via exosomes. Within the liver, HuR facilitates the export of miR-122 via exosomes during cellular stress by unloading them from the miRISC and then binding the displaced miRNAs to facilitate their export (Mukherjee *et al.,* 2016). This process of HuR mediated miRNA export has also been found to occur within the inflammatory response as Goswami *et al.,* (2020) also observed HuR mediated decoupling of miRNAs with their target miRNAs followed by the export of miRNAs within LPS stimulated RAW 264.7 cells. As HuR binds AU-rich sequences it is possible that HuR could reversibly bind specific miRNA with AU/G sequences (Goswani *et al.,* 2020).

Additionally, HuR has also been found to act as a sponge for miRNAs (Kundu *et al.,* 2012, Poria *et al.,* 2016). Kundu *et al.,* 2012 found that the addition of HuR within HEK 293 cells reduced the association of target mRNAs with the miRISC. However, this action is not mediated by HuR interaction with miRISC proteins such as TNRC6 or Ago2. Furthermore, HuR disrupts miR-21 translational repression of PDCD4 mRNA with MCF-7 cells. Overexpression of HuR caused a shift in PDCD4 mRNA to the polysome fractions indicating a reversal of translational repression (Poria *et al.,* 2016). Poria *et al.,* 2016 suggest that HuR is dislodging the miRNA from its target mRNA either through direct interaction of HuR with the miRNA or via HuR binding of AREs that are in close proximity of the miRNA target site.

1.5.5.7 Poly(A) tail length and microRNA regulation

The poly(A) tail lengths of transcripts are variable and as such can impact miRNA regulation. One study by Moretti *et al* (2012), used a reporter system with mRNAs containing miR-2 binding sites and distinct poly(A) tail lengths of 0, 62 and 98 to investigate the link between poly(A) tail length, PABPC and miRNA regulation. Moretti *et al,* (2012) found that there was greater miRNA-mediated repression of the reporter mRNAs with longer poly(A) tail lengths. Furthermore, Moretti *et al.,* (2012) propose that as PABPC is required for the recruitment of the miRISC, and longer poly(A) tails are more likely to have more PABPC associated, there is greater recruitment of the miRISC to transcripts with longer poly(A) tail lengths during the early phases of miRNA regulation.

However, Rissland *et al.,* 2017 found that within human cells PABPC occupancy on steady-state poly(A) tails varied widely and longer poly(A) tails did not necessarily coincide with greater PABP occupancy. For example, mRNAs encoding ribosomal proteins had some of the highest PABP occupancies despite having shorter poly(A) tails.

A study by (Eisen *et al.,* 2020) found that miRNAs preferentially deadenylate mRNA transcripts with shorter poly(A) tails, with steady-state poly(A) tail lengths remaining largely unaffected by miRNA regulation. Eisen *et al.,* 2020 suggest that miRNAs serve to accelerate deadenylation and decay of an mRNA target once the tail has already been shortened, preventing the build-up of short-tailed isoforms, and propose this is due to accelerated decapping of the mRNA transcript.

However, the intricacies of how miRNA regulation and poly(A) tail length impact one another is still largely unknown. Moreover, the interplay between poly(A) tail length and miRNA regulation has yet to be examined within the context of a biological system in which there are physiological changes in poly(A) tail length. Furthermore, how this interaction fits into the larger regulatory system of other inflammatory miRNAs and other post-transcriptional regulatory mechanisms within the inflammatory response is unknown.

1.6 MicroRNA and post-transcriptional regulation during inflammation

The complex network of signals that coordinate the inflammatory response is under strict regulation at many different levels. One important form of regulation during inflammation is the post-transcriptional regulation of mRNA. The 3'UTR of mRNA is an important site for post-transcriptional regulation, as it contains many regulatory elements such as AREs and miRNA target sites (Section 1.3.3). As such, one important regulatory mechanism includes miRNA. MiRNAs regulate many aspects of the inflammatory response, from its initiation to its cessation (Forster, Tate & Hertzog, 2015). The section below focuses on miRNAs and mRNAs that were investigated within this project or are of particular importance during inflammation.

1.6.1 MicroRNAs in the inflammatory response

1.6.1.1 miR-155

MiR-155 is considered to be an important regulator during inflammation (Mahesh & Biswas, 2019). MiR-155 is encoded by the MIRHG155 gene within the B-Cell integration cluster (BIC) gene. The BIC gene contains several transcription factor binding sites, including an Nf-κB binding site alongside an interferon-sensitive response element (ISRE) and an interferon regulatory factors (IRF) binding site (Tam, 2001) allowing for the production of miR-155 via many different inflammatory pathways. MiR-155 expression is particularly responsive to several different cytokines such as TNF, Il-1β as well as various PAMPs and DAMPs (O'Connell *et al.,* 2007).

MiR-155 expression rapidly increases upon TLR4 activation, serving as a pro-inflammatory regulator ensuring the initiation of the response (O'Connell *et al.,* 2007). miR-155 regulates suppressor of cytokine signalling 1 (SOCS1) (Pathak *et al.,* 2015) and SH-2 containing inositol 5' polyphosphatase 1 (SHIP1) (Cekic *et al.,* 2011), reduction in expression of SOCS1 and SHIP1 facilitate NFκB signalling allowing TNF levels to rapidly rise facilitating the progression of the response (O'Connell *et al.,* 2009).

1.6.1.2 miR-181a

MiR-181a belongs to the miR-181 family of microRNAs containing miR-181a, miR-181b, miR-181c, and miR-181d. The miR-181 family is encoded by three

different transcripts located on three different chromosomes. MiR-181a and miR-181b are clustered together in two different locations. In humans, the miR-181a1 and miR-181b1 cluster is located on chromosome 1, and the miR-181a2 and miR181b2 cluster is located on chromosome 9. The miR-181c and miR-181d cluster is found on chromosome 19 (Figure 11A). All four family members contain identical seed sequences and very similar sequences overall, so are likely to bind largely overlapping mRNA targets (Indreiri *et al.,* 2020) (Figure 11B).

The whole miR-181 family has been found to have an essential role in inflammation by regulating many signalling pathways including those downstream of Nf-κB (Sun *et al.,* 2014). In particular, the miR-181 family has been implicated in regulating the stability of TNF mRNA (Dan *et al.,* 2015, Corsetti *et al.,* 2018). MiR-181a has also been found to directly target IL1α and also inhibits the production of other proinflammatory cytokines such as IL-6, IL-8, and IL-1β, helping to control excessive inflammation within THP-1 cells (Xie *et al.,* 2013). Overexpression of miR-181a also results in increased production of IL-10 which has anti-inflammatory effects (Hutchinson *et al.,* 2013).

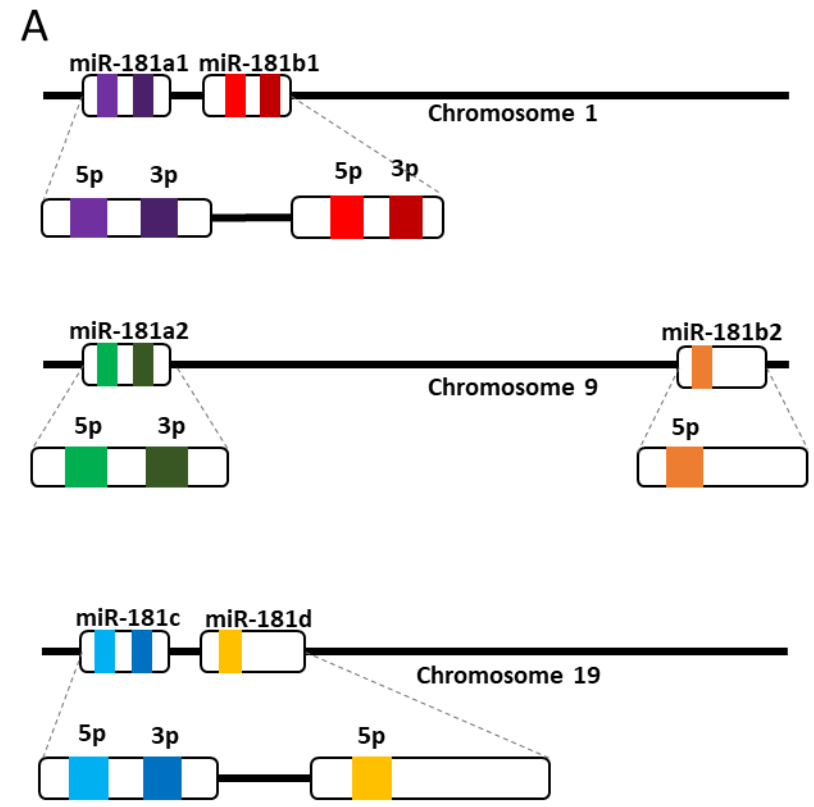

B

Mmu-miR-181a-5p	A A C A U U C A A C G C U G U C G G U G A G U
Mmu-miR-181b-5p	A A C A U U C A U U G C U G U C G G U G G G U
Mmu-miR-181c-5p	A A C A U U C A A C – C U G U C G G U G A G U
Mmu-miR-181d-5p	A A C A U U C A U U G U U G U C G G U G G G U

Figure 11. Genomic locations of miR-181 family members. A) Genomic location of miR-181 family members. **B)** Mature sequences that are generated from the 5p arm of miR-181 family members. Sequences from miRBase. Blue nucleotides indicate seed sequence which is conserved between members. Green nucleotides are conserved between members. Adapted from Sun et al., 2015

1.6.1.3 miR-26b

MiR-26b is a member of the miR-26 family of miRNAs and is located on chromosome 2 in both humans and mice. The miR-26 family also has two other members, miR-26a-1 found on chromosome 3 and miR-26a-2 located on chromosome 12 for both humans and mice. Both miR-26a-1 and miR-26a-2 have the same sequence while the seed sequence of miR-26b differs by two nucleotides (Icli *et al.,* 2014).

MiR-26b has been found to be important in regulating the inflammatory response within microglia particularly in response to hypoxic conditions (Kang *et al.,* 2018).

MiR-26b has also been implicated in regulating PTGS2, helping to regulate allergic inflammation, and inflammation within macrophages (Liu *et al.,* 2015, Kwon *et al.,* 2015).

1.6.1.4 Other microRNAs with roles in inflammation

MiR-21 expression serves to subdue the inflammatory response and drive the transition to the wound healing stage of the innate immune response. Overexpression of miR-21 after lipopolysaccharide (LPS) stimulation results in increased IL10 production and a reduction in TNF and IL6 (Barnett et al., 2016). MiR-21 largely facilitates this transition by modulating the effects of miR-155. Like miR-155, miR-21 is induced by Nf-κB in response to TLR4 activation by LPS (O'Neill et al, 2011) however, miR-21 reduces inflammation by increasing levels of IL10. MiR-21 achieves this increase in IL10 by targeting programmed cell death protein 4 (PDCD4). PDCD4 is required for NF-kB activation and is a negative regulator of IL10 (Sheedy et al., 2010). Increased levels of IL10 are then able to directly suppress the effects of miR-155 reducing inflammation (O'Neill et al., 2011, Lui & Abraham, 2013) (Figure 12).

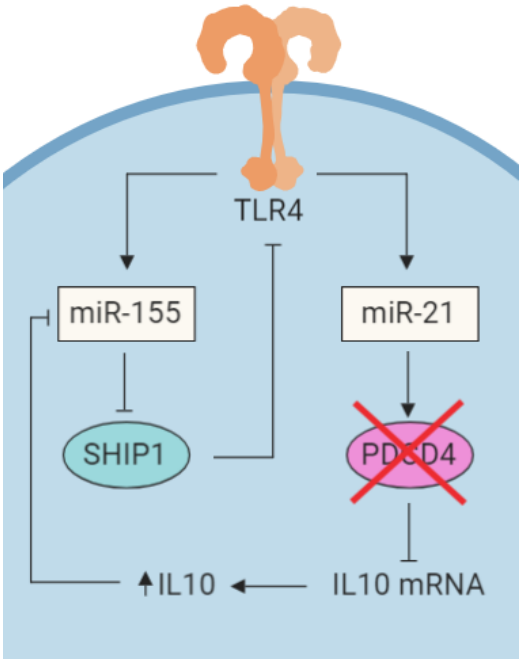

Figure 12. miR-21 regulation of miR-155 induced by TLR4 signalling.

Alongside miR-21, miR-146a also aids in the cessation of inflammation by targeting tumour necrosis factor 6 (TRAF6) and interleukin 1 receptor associated kinase 1 (IRAK1). TRAF6 and IRAK1 are positive regulators of TLR4 signalling, so miR-146a targeting serves to reduce TLR4 signalling, helping to reduce the inflammatory response (Nahid *et al.,* 2009). Studies performed in mice that were deficient in miR-146a showed excess production of pro-inflammatory cytokines and hyperresponsiveness to bacterial infection. This implies that miR-146a is acting as a negative regulator of TLR signalling helping to control the duration of the inflammatory response (Boldin et al., 2011). In addition, miR-146a has also been implicated in regulating IL-6 production via targeting Notch 1. Notch1 is known to induce IL6 as such, the downregulation of Notch1 by miR-146a reduces IL6 production also contributing to the reduction in the pro-inflammatory response (He et al., 2014). Moreover, miR-146b is induced by IL10 and has been found to target TLR4 serving to downregulate TLR4 expression and thus pro-inflammatory signalling. This results in the reduction of pro-inflammatory cytokines and chemokines helping to bring the inflammatory response to an end (Curtale et al., 2013).

However, the extent to which miRNAs play a role in regulating the inflammatory response is extensive, ranging from aiding phagocytosis to the polarisation of cells (Curtale, Rubino & Locati, 2019).

1.6.2 Regulation of TNF and PTGS2 mRNA

1.6.2.1 Regulation of TNF

TNF mRNA has many sites within the 3'UTR with roles in post-transcriptional regulation. Some of these include target sites for miRNAs such as miR-125b, miR-130, and miR-181a, although only miR-181a has been experimentally confirmed (Corsetti *et al.,* 2018, Zhu *et al.,* 2017). There is also a string of AU-rich elements (AREs) within the 3'UTR of TNF that contribute to its posttranscriptional regulation. The ARE is defined as an AUUUA motif and the TNF 3'UTR contains five overlapping repetitions of this motif (Barreau *et al.,* 2005). AREs within the TNF 3'UTR recruit tristetraprolin (TTP, *ZFP36*) which induces rapid deadenylation and mRNA decay via recruitment of the CCR4-NOT complex when cells are at rest (Carballo *et al.,* 1998, Kwak *et al.,* 2022). Inflammation triggers the phosphorylation of Human antigen- R (HuR), an RNA binding protein, causing it to relocate to the cytoplasm (Srikantan & Gorospe,

2012). HuR then binds to the AREs within the TNF 3'UTR, overriding the action of TTP, stabilising the TNF mRNA (Katsanou *et al.,* 2005). Both trans-acting factors work as a regulatory loop to control TNF expression within macrophages during inflammatory and resting cell states (Khalaj *et al.,* 2017).

Furthermore, TTP and HuR are known to either enhance (Jing *et al.,* 2005) or prevent (Bhattacharyya *et al.,* 2006) repression of specific mRNAs by miRNAs. HuR has been shown to compete with miR-181 for binding of the TNF 3'UTR (Dan *et al.,* 2015).

1.6.2.2 Regulation of PTGS2

PTGS2 mRNA also undergoes posttranscriptional regulation via the 3'UTR. PTGS2 mRNA has AU-Rich Elements (AREs) within its 3'UTR which are bound by many trans and cis-acting elements. One example is HuR which serves to stabilise mRNA transcripts, facilitating their translation (Dixon *et al.,* 2001). TTP is another trans-acting factor that binds to the AREs of PTGS2 and serves to destabilise the PTGS2 transcript by recruiting the CCR4-NOT complex triggering transcript decay (Young *et al.,* 2009).

The 3'UTR of PTGS2 also contains miRNA target sites. In particular, PTGS2 has two target sites for miR-26b both of which have been shown to regulate PTGS2 mRNA levels (Kwon *et al.,* 2015). PTGS2 has also been shown to be regulated by miR-101b in inflammation (Liu *et al.,* 2015) and miR146a in lung cancer (Cornett *et al.,* 2014).

The PTGS2 transcript also undergoes alternative polyadenylation, which generates two different 3'UTR isoforms. These different isoforms alter the number of regulatory elements within the 3'UTR affecting the posttranscriptional regulation of the PTGS2 transcript (Ren *et al.,* 2020). The shorter PTGS2 isoform is lacking some of the AREs present within the longer isoform. Furthermore, the longer isoform was shown to be less stable than the shorter PTGS2 isoform (Hall-Pogar *et al.,* 2005).

The shorter PTGS2 isoform also only contains one miR-26b target site as opposed to the two found within the longer PTGS2 isoform which may impact on miRNA regulation (An *et al.,* 2013).

1.7 Aims and Objectives

Key inflammatory genes have mRNAs with poly(A) tails that change in length over the course of the inflammatory response. Using the inflammatory response as a model, this project aimed to investigate whether changing poly(A) tail length affects miRNA regulation. This provides a unique system for giving us insight into the role of poly(A) tail length in miRNA-mediated repression, within a biological context in which it is subject to change, while also facilitating a deeper understanding of the role of miRNAs in the inflammatory response. Furthermore, how miRNA regulation changes over the course of transcriptional induction, outside of the context of inflammation will also be investigated. As such the objectives of the project are as follows:

1. Determine whether miRNA binding and regulation of mRNAs changes over the course of the inflammatory response.
2. Establish whether differences in poly(A) tail length and mRNA age influence miRNA binding and regulation.

Prospective miRNA-mRNA pairings will be validated using inhibition and overexpression experiments within the mouse macrophage cell line RAW 264.7 cells. This will be accompanied by the generation of luciferase reporters to assess direct binding. The poly(A) tail lengths will initially be assessed by PAT assay and initial effects of poly(A) tail length on miRNA regulation assessed PAT assays in combination with miRNA inhibition and overexpression.

Additionally, synthetic luciferase reporter RNAs with miRNA targets in the 3'UTR and differing lengths of poly(A) tail could be generated, also facilitating the assessment of how poly(A) tail length affects the binding and regulation by miRNAs.

Global analysis of miRNA effects on inflammatory mRNAs by next-generation sequencing in combination with TAIL-seq could also be performed to gain a wider view on how poly(A) tail lengths are interacting with miRNA regulation over the course of inflammation.

Assessing how miRNA binding and regulation changes over the response will be done via Ago2 immunoprecipitation, looking at how miRNA and target mRNA association with Ago2 changes over time.

The effects of mRNA age on miRNA regulation and binding could be assessed by 4-thio-U labelling of nascent RNA. The labelled RNA can be isolated by biotinylation and streptavidin pulldown and then characterised by qPCR and PAT assays. This method can be used to label nascent inflammatory RNAs and in combination with analysis of the unlabelled RNA will allowing the precise characterisation of changes in RNA synthesis/decay that occur following LPS stimulation of RAW 264.7 cells. This technique can also be combined with Ago2 immunoprecipitation to establish whether miRNAs are binding to newly synthesised RNA versus older transcripts.

The luciferase approach can also be used to generate a tetracycline inducible model to mimic the transcription that occurs during inflammation and determine how it is responding to miRNA regulation. Alternatively, results could be followed up in other inflammatory cells lines, or primary macrophages.

Chapter 2 – Materials and Methods

2.1 Materials

2.1.1 General cell culture reagents

Table 2. Cell culture reagents.

Reagent	Supplier
Dulbecco's modified eagle medium (DMEM)	Sigma-Aldrich
Feotal bovine serum (FBS)	Gibco
Optimem	Gibco
Lipofectamine RNA iMax/2000	Invitrogen
Trypsin-EDTA (Trypsin)	Invitrogen
Fugene	Promega
Phosphate buffered saline (PBS)	4.3 mM Na_2HPO_4, 1.5 mM KH_2PO_4, 137mM NaCl, 2/7mM KCl, pH 7.4

2.1.2 miRNA inhibitors, mimics and siRNAs

Table 3. miRNA inhibitors, mimics, and siRNAs used in transfections

Reagent	Sequence	Specificity	Supplier
TENT4A (PAPD7) siRNA	On-TargetPlus SMARTpool	Mouse	Horizon Discovery
TENT4B (PAPD5) siRNA	OnTargetPlus SMARTpool	Mouse	Horizon Discovery
HuR (Elavl1) siRNA	OnTargetPlus CAGUUUCAAUGGUCAUAAA	Mouse	Horizon Discovery
Negative control siRNA	OnTargetPlus Non-targeting Pool	Mouse	Horizon discovery
miR-181a-5p inhibitor	miRCURY LNA miRNA inhibitor 5'AACAUUCAACGCUGUCGGUGAGU	Mouse, Human	Qiagen
miR-26b-5p inhibitor	miRCURY LNA miRNA inhibitor 5'UUCAAGUAAUUCAGGAUAGGU	Mouse, Human	Qiagen
Inhibitor negative control A	miRCURY LNA miRNA inhibitor TAACACGTCTATACGCCCA	Mouse, Human	Qiagen
miR-181a mimic	miRCURY LNA miRNA mimic 5'AACAUUCAACGCUGUCGGUGAGU	Mouse, Human	Qiagen
Mimic Negative Control	miRCURY LNA miRNA mimic UCACCGGGUGUAAAUCAGCUUG	Mouse, Human	Qiagen

2.1.2 Plasmids

Table 4. Plasmids used and generated. The backbone and modification/insert for each plasmid used. Primers used to generate inserts and modifications for each plasmid. Green text indicates restriction site. All plasmids have Ampicillin resistance. CLJ lab – Catherine Jopling Lab, AM- generated by Athena Martin. Plasmid maps in Supplementary Figures (13-16)

Plasmid Name	Backbone	Source of backbone	Insert/ modification	Primers used	Primer sequence 5'-3'
WT Luc TNF 3'UTR	pGL3-MCS Firefly luciferase reporter	CLJ lab	TNF 3'UTR – cDNA	TNF_ Forward_Spe1	GGACTAGTGACAGTGACCTGGACTGTCC
				TNF_Reverse_Pst1	AACTGCAGAGCTCAGCTCAGCTCCGTTTTCACA
				TNF_Forward Amplify	AGGGGATTATGGCTCAGGGT
				TNF_Reverse_Amplify	CCCGTAGGGCGATTACAGTC
Mut Luc TNF 3'UTR	WT Luc TNF 3'UTR Firefly luciferase reporter	AM	Single nt mutation in miR-181a binding site - plasmid	WT_Spe1_Forward	CTAGGATGAAGCTTACTAGTGACAG
				miR-181a_mutant_Reverse	CAAATAAATACAATCATAAGC
				WT_Pst1_Reverse	GAATTCTGCAGAGCTCAGCTCC
				miR-181a_mutant_forward	GCTTATGATTGTATTTATTTG
Renilla Luciferase	Renilla Luciferase	CLJ Lab	N/A	N/A	N/A
Luc PTGS2 3'UTR	pGL3-MCS Firefly luciferase reporter	CLJ Lab	PTGS2 3'UTR - cDNA	PTGS2_Forward_Spe1	GGACTAGTAGCCAGTGAGAAGGGAAATGAA
				PTGS2_Reverse_EcoRI	CCCGGAATTCATTTCTAGCATCTTGGTAGGGC
				PTGS2_Forward_HpaI	GCGTTAACAGCCAGTGAGAAGGGAAATGAA
				PTGS2_Reverse_SalI	ACGCGTCGACATTTCTAGCATCTTGGTAGGGC
WT Luc TNF 3'UTR -AREs	WT Luc TNF 3'UTR	AM	Removal of AREs - plasmid	ARE removal primer forward_Spe1	ACTAGTGCTTATGAATGTATTTATTTGGAAGG
				ARE removal primer reverse_Pst1	GAATTCTGCAGAGCTCAGC
pcDNA Luc TNF 3'UTR	pcDNA5-FRT-TetO-fSNAPc	Addgene	Luc TNF 3'UTR, removal of SNAP tag - plasmid	Afl II luciferase TNF 3'UTR forward	GGCATTCCGGTACTTAAGGTAAAGCCAC
				Luciferase TNF 3'UTR reverse	GTATCTTATCATGTCTGCTCGAAG
Flp-recombinase	pCAG-FLpo	Addgene	N/A	N/A	N/A

2.1 Cloning

2.1.1 Transformations

Table 5. Buffer compositions for growth of bacteria

Buffer	Composition
Luria-Bertani (LB) medium	1% w/v tryptone, 0.5% w/v yeast extract and 1% w/v NaCl in diH2O, pH 7.0. For solid medium, 2% w/v bacteriological agar was added. Medium was autoclaved and stored at room temperature until required.
SOC medium	2% tryptone, 0.5% yeast extract, 10 mM NaCl, 2.5 mM KCl, 10 mM MgCl2, 10 mM MgSO4, and 20 mM glucose. Purchased from NEB and stored at 4°C
Ampicillin	1000 X stock solution made as 100 mg/mL in sterile 50% sterile diH_2O and 50% EtOH to prevent freezing and stored at -20°C.
Selective LB plates	Ampicillin was added to melted LB agar medium to make a final concentration of 1X and poured onto Petri dishes in a laminar flow hood. Plates were stored at 4ºC for up to 1 month.

Plasmids were transformed via heat shock into 50µl of competent DH5α cells (Sigma). Competent cells were defrosted on ice before 5µl of ligation mixture was added. Cells were then left for a further 30 minutes on ice before undergoing heat shock at 42°C for 90 seconds then ice for 2 minutes. 200µl of SOC recovery media (Table 5) was added and the cells were left to recover for one hour at 37°C in a shaking incubator. Transformation mixture was then spread onto Ampicillin LB agar plates (Table 5) and left to grow overnight at 37°C.

2.1.2 Minipreps

For minipreps, 10ml of LB (Table 5) with 10µl of Ampicillin stock (Table 5) was inoculated with selected colonies and grown overnight at 37°C within a shaking incubator. Cultures were spun down in 15ml falcon tubes for 10 minutes at 4000g at 4°C (Eppendorf 5810 R) and the supernatant was discarded. Plasmid DNA was isolated from the bacterial pellet by miniprep using the Wizard plus SV DNA

purification system by Promega. The protocol was followed according to the manufacturer's instructions except for eluting in 50µl of nuclease free water as opposed to 100µl. DNA concentration was measured using the nanodrop.

Minipreps were assessed via restriction digests (section 2.1.5) and minipreps that appeared to contain the correct insert were selected for sequencing (Source bioscience).

2.1.3 Maxiprep

A single colony was selected and transformed as per section 2.1.1 then grown overnight at 37°C, shaking, in 10ml LB media supplemented with 0.1% Ampicillin (1mg/ml). 500µl of this subculture was then added to a further 300ml of LB broth and Ampicillin (1mg/ml) topped up to a concentration of 0.1% and grown for a further 24 hours at 37°C in a shaking incubator. After 24 hours the culture was divided into six 50ml falcons and spun down at 4000g for 10 minutes at 4°C. The supernatant was discarded, and the plasmid was isolated using the Qiagen Plasmid Plus Maxi kit. The pellets were recombined at the resuspension step. The manufacturer's protocol was followed, and plasmids were eluted in 400µl then aliquoted and stored at -80°C.

2.1.4 PCR

Inserts were generated by PCR amplification of cDNA generated in section 2.3.3 or from plasmid DNA with specific primers (Table 4 and 6). Amplification of 1ng plasmid or 500ng of cDNA was performed using a master mix containing 0.25µl Phusion High-Fidelity DNA Polymerase (NEB) and 10µl high fidelity (HF) Buffer (concentration of 1x), 10µl Betaine solution (Sigma Aldrich), 2.5µl DMSO (NEB), 1µl 10uM dNTPs and 0.5µl of each primer in a final volume of 50µl with nuclease free water per reaction. PCR cycling was performed as below.

Step	*Cycles*	*Temperature*	*Time*
Enzyme Activation	1	95°C	5 mins
Denaturation		95°C	1 min
Annealing	40	(Table 6)	1 min
Extension		72°C	2 mins
Final Extension	1	72°C	10 mins

Table 6. Primer pairs with their annealing temperatures.

Primer pair	Annealing Temp
TNF_ Forward_Spe1 **TNF_Reverse_Pst1**	60°C
TNF_Forward Amplify **TNF_Reverse_Amplify**	65°C
WT_Spe1_Forward **miR-181a_mutant_Reverse**	55°C
WT_Pst1_Reverse **miR-181a_mutant_forward**	55°C
WT_Spe1_Forward **WT_Pst1_Reverse**	63°C
PTGS2_Forward_Spe1 **PTGS2_Reverse_EcoRI**	70°C
PTGS2_Forward_HpaI **PTGS2_Reverse_SalI**	70°C
ARE removal primer forward_Spe1 **ARE removal primer reverse_Pst1**	60°C
Afl II luciferase TNF 3'UTR forward **Luciferase TNF 3'UTR reverse**	60°C
Luc 3' Forward **CMV_Forward**	61°C

2.1.5 Pjet cloning

For increased restriction digest efficiency all PCR products were inserted into a PJET plasmid following manufacturer's instructions. A restriction digest (section 2.1.6) was then carried out to generate the insert. The pJET plasmid is a blunt cloning vector used as part of the Invitrogen CloneJET kit.

2.1.6 Restriction Digests

All restriction digests were carried out on plasmids, either the pJET plasmid to produce an insert or the plasmid backbone. Restriction digests were performed in a reaction volume of 20µl containing 1µg DNA, 5µl 1X Cutsmart buffer, 1µl appropriate restriction enzymes (Table 7) and nuclease free water up to 50µl total volume. Digests were incubated at 37°C for 2.5 hours, then heat inactivated at 70°C for 15 mins.

Table 7. Restriction enzymes used to digest inserts shown in Table 4 alongside the plasmid that the insert was ligated into.

Plasmid name	Gene	Plasmid	Enzymes
WT/Mut Luc TNF 3'UTR	TNF insert	pGL3-MCS (Jopling,2008)	Spe1-HF (NEB) Pst1-HF (NEB)
Luc PTGS2 3'UTR	PTGS2 insert	pGL3-MCS (Jopling,2008)	Sal1 (NEB) Hpa1 (NEB)
pcDNA Luc TNF 3'UTR	Luciferase TNF 3'UTR insert	pcDNA5-FRT-TetO-fSNAPc	AflII (NEB) ApaI (NEB)

2.1.6 Agarose gel Electrophoresis

PCR products, plasmids, and restriction digests were analysed via gel electrophoresis. 20µl of sample with 4µl of 6x SDS free loading dye (NEB) and 3µl of ladder (either 100bp or 1kb, Thermofischer) were run on a 1% agarose gel in 1x ttis-borate-EDTA (TBE) (0.13M Tris, pH 7.6, 45mM boric acid, 2.5mM EDTA) at 120V for 1 hour. Gel images were visualised using the Quantity One software.

For band extraction, bands were visualised using blue light, and the desired bands were excised using a clean scalpel and forceps. Excess agarose was trimmed away, and the DNA was extracted using the NEB Monarch gel extraction kit followed as per manufacturer's instructions. Eluted in 50µl of nuclease free water and quantified using the nanodrop.

2.1.7 Ligations

The TNF, PTGS2, or Luciferase TNF 3'UTR inserts were ligated into the relevant plasmid (Table 4) using the NEB T4 ligase. A 3:1 ratio of insert to vector was used for ligations. Reactions were performed in a final volume of 20ul containing 1µl T4 DNA ligase (NEB), 2µl 10xT4 ligase buffer, 50 ng digested plasmid, 37.5ng digested insert and nuclease free water. The 10 xT4 ligase buffer was stored in aliquots at -20°C to prevent ATP degradation. Ligations were left either overnight at 4°C or for one hour at room temperature. 5µl of ligation mixtures were then transformed as per section 2.1.1.

2.1.8 Sequencing of Plasmids.

Table 8. Primers used for sequencing plasmids. Which plasmids primers were used on are indicated.

Primer	Sequence	Plasmid
Luc 3'_Forward	GCGTATCTCTTCATAGCCTT	WT Luc TNF 3'UTR
		Mut Luc TNF 3'UTR
		Luc PTGS2 3'UTR
CMV_forward	CGCAAATGGGCGGTAGGCGTG	pcDNA Luc TNF 3'UTR

Plasmids isolated via miniprep or maxiprep were sent to Source bioscience for Sanger sequencing alongside their appropriate sequencing primer (Table 8). 5µl of plasmid at a concentration of 100µg/ml and 5µl of sequencing primer at 3.2ng/ml.

2.4.9 Generation of luciferase-TNF 3'UTR plasmid containing mutant miR-181a target site via three-step PCR

Using the WT Luc TNF 3'UTR as a template (Table 4), two initial PCR reactions were performed using Phusion HF enzyme (Thermofischer) to insert a single nucleotide mutation at the fourth nucleotide within the miR-181a binding site.

PCR1: WT Spe1 Forward + miR-181a mutant reverse (Tables 4 and 6)

PCR2: WT Pst1 Reverse + miR-181a mutant forward (Tables 4 and 6)

Both PCR products were then run on a 1% agarose gel (Section 2.1.6). Both PCR product bands were cut out from the gel and placed in the same tube. The two gel fragments were then frozen overnight at -20°C. Liquid release from freezing the gel fragments was then used as template for the third PCR.

PCR3: WT Spe1 Forward + WT Pst1 Reverse (Tables 4 and 6)

The mutant insert band generated was then ligated as per 2.1.7 into the cut firefly luciferase vector to generate the Mut Luc TNF 3'UTR plasmid.

2.2 Cell culture

RAW264.7 cells obtained from ATCC (TIB-71) were cultured in Dulbecco's modified eagle media (DMEM) (Sigma) with 10% foetal bovine serum (FBS) (Gibco). FBS was batch tested and LPS induction of inflammatory response confirmed. Cells were maintained within T75 flasks. Cells were passaged into a new flask via mechanical scraping when confluence reached 80%, cells were spun down at 200g for 5 mins at room temp within 15ml falcons, medium removed, and suspended in new media before the split was added to a new flask. Cells were normally split 1:12 three times a week to maintain. Experiments were performed on cells between passage 10 and 30. Not growing RAW 264.7 cells past passage 30 is crucial as RAW 264.7 cells start to phenotypically change, affecting data reliability (Figure 13) (Taciak *et al.,* 2018).

Serum starvation was performed using DMEM supplemented with 0.5% FBS for 24 hours before LPS treatment.

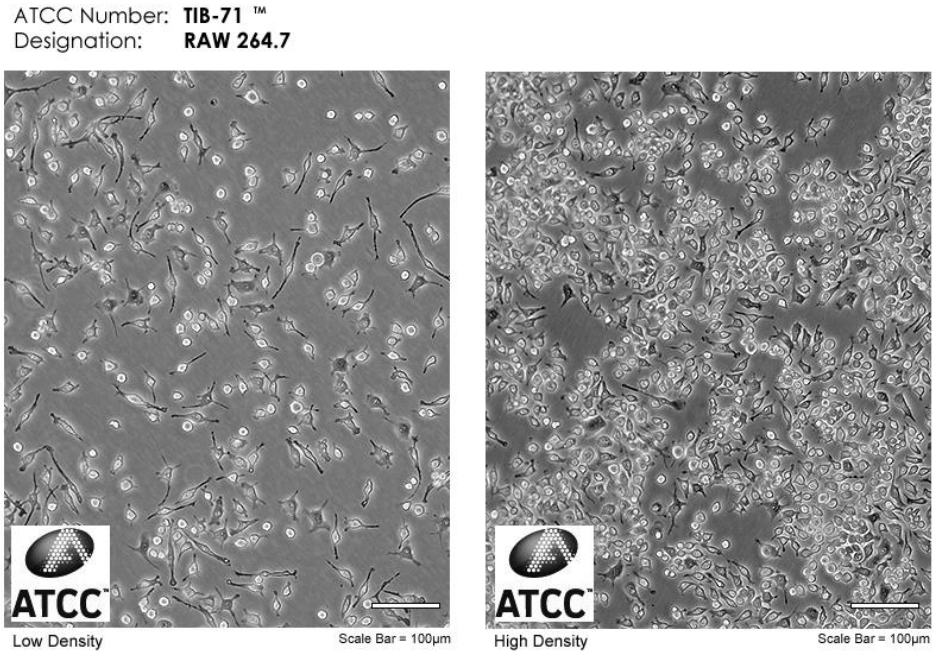

Figure 13. Morphology of RAW 264.7 cells at different densities when cells are unstimulated. Image taken from ATTC website (ATCC, 2023).

HEK 293 (CRL-1573) cells from the Winkler lab, Hela (CCL-2) cells from the Proudfoot lab and Flp-in T-Rex HEK 293 cells (Invitrogen, R780-07) were cultured in Dulbecco's modified eagle media (DMEM) (Sigma) with 10% FBS (Gibco) in T75 flasks to maintain.

Cells were passaged into a new flask via the addition of 2ml trypsin (Thermofischer) when confluence reached 80%. Cells were normally split 1:10 three times a week for routine maintenance. Experiments were performed on cells between passage 10 and 40.

Mycoplasma testing was routinely performed using the ATCC universal mycoplasma detection kit as per manufacturer's instructions.

2.2.1 Freezing cells

For storage, cells were cryopreserved in liquid nitrogen. Cells were grown to approximately 80% confluency within 10 cm dishes 24 hours before cryopreservation. Each 10cm dish equated to one vial of cells. Following either mechanical scraping with a cell scraper for the RAW 264.7 cells or trypsinisation for the HEK 293, HeLa, Flip-in T-rex HEK 293, or Tet Luc TNF 3'UTR HEK 293, the cells were pelleted by centrifugation at 200g for 5 mins at 4°C within 15ml falcon tubes. The supernatant was then discarded, and cells were resuspended in freezing mixture comprised of 1ml FBS with 10% DMSO. Cells were then stored at -80°C in an isopropanol freezing container to control cooling at a rate of -1°C a minute before transfer to liquid nitrogen.

2.2.2 Thawing cells

Upon removal from liquid nitrogen, cells were immediately placed in a 37°C water bath to thaw. The cell aliquot was then added to DMEM medium supplemented with 10% FBS. The resuspended cells were then pelleted by centrifugation at 200g for 5 mins at room temperature. The supernatant was then discarded and cells resuspended in further 10% FBS DMEM for routine maintenance in a T75 flask as detailed above. Cells were left to recover for a week before any experiments were performed.

2.2.3 Stimulation with Lipopolysaccharide (LPS)

RAW264.7 cells were grown to approximately 80% confluency within 6-well plates. The medium was then aspirated, cells were washed two times in the same volume of Phosphate buffer saline (PBS) solution before being replaced with 0.5% FBS serum starvation media. The RAW264.7 cells were cultured for a further

24 hours before being directly pipetting LPS into the existing 0.5% DMEM within the well. Once the LPS was added the plate was swirled to mix.

Initially the LPS used was from Sigma and was resuspended in DMEM at a stock concentration of 1mg/ml and stored as aliquots at -20°C. The Sigma LPS was used for the initial LPS time course experiments, miR-26b inhibition experiments and the first miR-181a inhibition experiments. A switch was then made to the TLR4 specific Enzo LPS as it undergoes a more stringent purification process ensuring only one inflammatory pathway is activated. The Enzo LPS came ready to use and was stored in the original container at 4°C. The majority of experiments were performed with the Enzo LPS, including the miRNA time courses.

100ng/ml and 1µg/ml concentrations of LPS were trailed but all experiments were performed with 1µg/ml LPS for the required time with both different LPS (Supplementary Figure 1). In general, multiple wells were seeded and several different time points analysed. Time courses were performed by adding LPS at different time points and harvesting all at the same time.

2.2.4 Transfection of miRNA inhibitors and mimics

For a 6-well plate RAW264.7 cells were seeded 24 hours before transfection and grown to approximately 60-70% confluent. Cells were transfected with a final concentration of 10nM miRNA inhibitor or mimic in lipofectamine RNA iMAX (invitrogen) in Optimem media (Gibco) as per manufacturer's protocol (Supplementary Figure 21). Inhibitors and mimics used are listed in Table 3. The Lipofectamine was incubated in Optimem for five mins at room temperature before the inhibitor/mimic and Optimem mixture was added to the Lipofectamine and Optimem mixture. Once combined the Lipofectamine and inhibitor/mimic transfection mixture was incubated for 20 mins at room temperature. A control mixture containing a non-targeting negative control oligo instead of inhibitor/mimic was made in parallel. Before transfection mixture was added to the cells the media was removed, cells were washed twice with PBS and replaced with 700µl serum starvation media, 300µl of transfection mixture containing either the inhibitor/mimic or negative control oligo was then added in droplets into appropriate wells. The plate was then swirled to mix.

Transfection mixture was left on the cells for 6 hours before the medium was replaced with fresh serum starvation media. LPS treatment was performed 24 hours after inhibitor or mimic transfection. The negative control used for the inhibition experiments was Negative control A (Qiagen). The negative control used for mimic experiments was Negative Control miRCURY LNA miRNA Mimic (Qiagen) (Supplementary Figures 2 and 4)

2.2.5 Co-transfection of plasmid, miRNA inhibitors, and mimics

Inhibitor and mimic transfections performed in HEK 293 cells were for luciferase assays and were performed in 24-well plates. The inhibitors and mimics were transfected alongside reporter plasmids (Table 4 and 9) using Lipofectamine 2000 as per manufacturer's instructions. Cells were seeded 24 hours before transfection and grown to an approximate confluency of 70%. HEK 293 cells were transfected with a final concentration of 5nM miRNA inhibitor or mimic in Optimem media. Different concentrations of inhibitors and mimics were trailed in a 24-well plate and 5nM was selected. Plasmids were transfected at a final concentration of 0.2µg/ml TNF 3'UTR luciferase reporter plasmid and 0.1µg/ml renilla reporter plasmid per well of a 24-well plate. Before transfection mixture was added to the cells the media was removed, cells were washed twice with PBS and replaced with 400µl DMEM with 10% FBS. 100µl of transfection media was added in droplets and left on the cells for 6 hours before the media was changed. Luciferase assay was then performed 24hrs later. The negative control used for both the inhibition and overexpression experiments was Negative control A (Qiagen). The negative control used for mimic experiments was Negative Control miRCURY LNA miRNA Mimic (Qiagen).

2.2.6 Transfecting siRNAs

For a 6-well plate RAW 264.7 cells were transfected with a final concentration of 10nM siRNA in Lipofectamine RNA iMAX (Invitrogen) in Optimem media (Gibco). SiRNAs used were TENT4A, TENT4b, HuR, and a non-targeting negative control (Table 3).

A double knockdown was performed for both siRNAs. Cells were seeded 24 hours before the first round of transfection and grown to a confluency of approximately

40%. Cells were transfected using Lipofectamine RNA iMax with two hits of 10nM siRNA 24 hours apart. For the first hit, the transfection mixture was assembled as described in section 2.1.2, with siRNA oligos in place of the inhibitors and mimics. In total three different transfection mixtures were generated in parallel. The first mixture contained the TENT4A and TENT4B siRNAs. The second mixture contains the HuR siRNA. The third mixture contains the non-targeting negative control siRNA. Cells were washed twice with PBS and the media replaced with 1.7ml DMEM with 10% FBS. 300µl of appropriate transfection mixture was then added by droplets into each well. The media was then changed 24hrs later.

After the media change at 24 hours, the cells were then transfected with the second hit of siRNA knockdown. The transfection mixtures were assembled in the exact same way as the day before. Cells were washed twice with PBS before 1.7ml of serum starvation media (DMEM with 0.5% FBS) was added. The second round of transfection mixture was then applied in droplets and the media changes after a further 24 hours. LPS treatment was performed 48hrs after the initial transfection.

2.2.7 Fugene transfection to establish a stable cell line

Flp-in T-rex HEK 293 cells were transfected using Fugene (Promega) transfection to insert a firefly luciferase gene alongside the TNF 3'UTR into a locus under the control of a tetracycline inducible promoter. In order to insert the luciferase gene and TNF 3'UTR into the inducible cell line, two plasmids were used. A pcDNA expression vector containing the luciferase gene and TNF 3'UTR which was generated in the lab. The other plasmid encodes the Flp-in recombinase and was bought in from addgene (Table 4).

The Flp-in-Trex HEK293 cells were seeded into 6cm plates and grown to a confluency of approximately 80% before transfection. The plasmids were transfected in a ratio of 1:9 with 1µg of the pcDNA expression vector and 9µg of the flp-in recombinase vector resulting in a final concentration of 10µg/ml of plasmid (Table 9). To make the transfection mixture, per well 470µl of Optimem was combined with 20µl of Fugene and 10µl of plasmids, the tube was inverted to mix and incubated for 5 mins at room temperature. The cells in the 6cm dishes were then washed twice with PBS and 2.5ml

of 10% FBS DMEM media was added. 500µl of transfection mixture was then added in droplets into the well. The media was then changed 24 hours later.

Cells were then treated with Hygromycin 48 hours after initial transfection to select for successfully transfected cells.

In order to determine the concentration of Hygromycin to use for selection, a kill curve was performed. Flp-in T-Rex HEK293 cells were seeded into a 6-well plate 24 hours before drug treatment and grown to an approximate confluency of 50%. Each well was treated with a different concentration of Hygromycin: 1000µg/ml, 750µg/ml, 500µg/ml, 250µg/ml, 100µg/ml, and 0µg/ml. The Hygromycin was kept at a stock solution of 50mg/ml and the appropriate volume was pipetted directly into the well containing 2ml of 10% FBS DMEM. Once the Hygromycin was pipetted into the well, the plate was swirled to mix. The cells were grown for 10 days and the media was replaced with fresh Hygromycin containing media every 2-3 days.

The drug concentration that killed all the cells within 7 days was 250µg/ml and was chosen for selection of successfully transfected cells.

Cells were then treated with 250µg/ml Hydromycin to select for successfully transfected cells. Three mixed cell populations were generated and maintained in parallel. Successfully transfected cells were then cultured in medium containing 250µg/ml Hygromycin and referred to as Tet Luc TNF 3'UTR HEK 293s.

Table 9. Plasmids used in transfections. Plasmid maps in the appendices

Plasmid	Transfection Reagent	Cells transfected
WT Luc TNF 3'UTR	Lipofectamine 2000	HEK 293
Mut Luc TNF 3'UTR	Lipofectamine 2000	HEK 293
Renilla Luciferase	Lipofectamine 2000	HEK 293
pcDNA Luc TNF 3'UTR	Fugene	Flp-in TRex HEK 293
Flp-in recombinase	Fugene	Flp-in TRex HEK 293

2.2.8 Genotyping stable cell lines

Table 10. Primers used for genotyping Tet Luc TNF 3'UTR HEK 293 transgenic cell line

Genotyping primer	Sequence	Region amplified
CMV_f	CGCAAATGGGCGGTAGGCGTG	Luciferase TNF 3'UTR
Bhg_R	TAGAAGGCACAGTCGAGG	Luciferase TNF 3'UTR

The three transgenic mixed cell populations A, B, and C were characterised. Firstly, A, B and C were plated into separate wells within a 6-well plate and grown to approximately 80% confluency before genomic DNA was extracted using the GenElute™ Mammalian Genomic DNA Miniprep Kit (Sigma Aldrich) as per manufacturer's instructions. Genomic DNA was eluted in 50µl of nuclease free water and quantified using the nanodrop. Mixed populations A, B, and C were then genotyped via PCR (section 2.1.4) using primers (Table 10) that bound to the CMV promoter upstream of the firefly luciferase gene and the Bhg poly(A) signal downstream of the TNF 3'UTR. PCR products were run on an agarose gel and visualised as per section 2.1.6.

The PCR product generated from genomic DNA was also set for sequencing and sequenced using the CMV_F primer (Table 10). 10µg/ml of PCR product and 3.2ng/ml of primer in volumes of 5µl were sent to Source Bioscience.

2.2.9 Stimulation with tetracycline/doxycycline

Tet Luc TNF 3'UTR Hek 293 cells were seeded into 6-well plates 24 hours before stimulation and grown to an approximate confluency of 80%. The cells were then treated with 2µg/ml of doxycycline as recommended by the manufacturer directly into the well (Supplementary Figure 17). Once the doxycycline was added, the well was swirled to mix. Doxycycline was added over a series of time points and the cells were harvested all at once.

2.3 RNA Techniques

2.3.1 RNA isolation using Reliaprep kits

RNA>200nt for mRNA analysis via qPCR was extracted from RAW 264.7, HEK293, HeLa, Flp-in T-Rex HEK293, or Tet Luc TNF 3'UTR HEK 293 cells grown in 6-well plates using the Promega Reliaprep RNA miniprep kit. Medium was removed from the wells. The cells were then washed twice with the same volume of PBS and subsequently lysed in BLTG buffer provided with the kit. The manufacturer's protocol was followed exactly, and RNA was eluted in 15µl of nuclease free water.

2.3.2 RNA isolation using TRI reagent

Total RNA for miRNA analysis by qPCR was extracted using TRI-reagent (Sigma). RNA was extracted from RAW264.7, HEK293, Hela and Tet Luc TNF 3'UTR HEK293 cells grown in 6-well plates. When ready to harvest, the medium was removed from the wells and each well was washed twice with PBS. 1ml of TRI-reagent was then added directly to each well at room temp. The Tri-reagent was pipetted up and down within the well to ensure all the cells had been lysed. The TRI-reagent containing the lysed cells was then moved to microfuge tubes and 200µl of Chloroform was added to each tube. The tubes were then shaken vigorously for 30 seconds and left to incubate for 10 minutes at room temperature. The samples were then centrifuged at 17,000g for 15 mins at 4°C. The aqueous layer for each isolation was then transferred to a new microfuge tube and 500µl of filtered isopropanol (Sigma) was added to each tube alongside 1µl of co-precipitant glycoblue (Invitrogen). Each tube was inverted to mix. The isolates were then left to precipitate overnight at -20°C.

The following day the isolates were then centrifuged at 17,000g for 10 mins at 4°C. The supernatant was then removed, and the pellet was washed in 500µl of 75% ethanol. Further centrifugation at 17,000g for 10 mins at 4°C was performed. The supernatant was again discarded and the pellet was left to air dry for 5 mins before the pellet was resuspended in 15-40µl nuclease free water.

Immunoprecipitation samples were also extracted using TRI-reagent. RNA was extracted by directly adding 1 ml of TRI-reagent onto magnetic beads containing

the immunoprecipitants. The RNA isolation was then performed as described above.

All RNA was quantified using the nanodrop and stored short term at -20°C and long term at -80°C.

2.3.3 Reverse Transcription- quantitative PCR (RT-qPCR)

Reverse transcription was performed using GoScript reverse transcription mix, and random primers (Promega). 100ng of RNA was used for each reaction in a total volume of 20µl, with the exception of RNA extracted from the immunoprecipitation where equal volumes were used. Incubations were done within a PCR thermocycler in accordance with the manufacturer's protocol. The cDNA was then used as template for qPCR.

qPCR was performed on a Qiagen Rotor-Gene Q qPCR machine. GoTaq qPCR System from Promega was used for qPCR in a volume of 10ul with 0.5µl of cDNA and a final primer concentration of 0.25µM (Table 11), 1x GoTaq master mix. Each reaction was performed in triplicate. PCR programme as follows:

Step	Cycles	Temperature	Time
Enzyme Activation	1	95°C	2 mins
Denaturation	40	95°C	15 secs
Annealing and Extension		60°C	1 min

Gain optimisation at 60°C was performed at the beginning of the run before melt. Fold change was calculated using the 2-ΔΔCt method relative to a housekeeping control. Primers were checked by serially diluting cDNA and plotting the Ct values against logged concentration, checking for a linear fit.

Table 11. RT-qPCR primers used to quantify mRNA levels. HPRT and GAPDH are housekeeping genes. F – Forward primer. R – Reverse primer.

Primer Name	Organism	Direction	Sequence 5'-3'
HPRT	Mouse	F	GGTGTTCTAGTCCTGTGGCC
		R	AGTGCAAATCAAAAGTCTGGGG
GAPDH	Mouse	F	AAGAAGGTGGTGAAGCAGGC
		R	ATCGGAAGGTGGAAGAGTGGG
TNF	Mouse	F	CTATGGCCCAGACCCTCACA
		R	CCACTTGGTGGTTTGCTACGA
PTGS2 long	Mouse	F	CAGCCAGGCAGCAAATGGTT
		R	AGTCCGGGTACAGTCACAT
IL1b	Mouse	F	AGATGAAGGGCTGCTTCCAAA
		R	GGAAGGTCCACGGGAAAGAC
TLR4	Mouse	F	TCCCTGCATAGAGGTAGTTCC
		R	TCAAGGGGTTGAAGCTCAGA
TNF un	Mouse	F	ACACTGACTCAATCCTCCCC
		R	AGCCTTGTCCCTTGAAGAGA
Tent4A	Mouse	F	ACAACAAACAACCAGACCAGG
		R	ATGGCTGGGGAAGTTAACACTG
Tent4B	Mouse	F	GTGAGAGCAGCAGACCTCATT
		R	TCCCTGGGATGTAACTGAAGGA
HuR	Mouse	F	ATCAGACCACAGGTTTGTCC
		R	GTTGGGATTGGCTGCAAACT
Tnrc6A	Mouse	F	TCCATGGAGCGAATCCTTAC
		R	ATGAAACTGGAACCTGAGGGG
Tnrc6B	Mouse	F	TCCTGGTATGGTTCTGGCTT
		R	GCATGGTGGCTTTCTTGTGTG
RPL28	Mouse	F	TACAGCACGGAGCCAAATAA
		R	ACGGTCTTGCGGTGAATTAG
GAPDH	Human	F	CGTTCTCAGCCTTGACGGTG
		R	CATCGCTCAGACACACACCATGGG
TNF 3'UTR	Human	F	AGGTTGCCTCTGTCTCAGAATC

Luciferase	Human	R	CTCTGTGAGGAAGGCTGTGCAT
		F	CTAAGGAAGTCGGGGAAGCG
		R	ATCCCCCTCGGGTGTAATCA

2.3.4 MicroRNA RT-qPCR

MiRNA cDNA synthesis utilised the Taqman miRNA assays (Thermofisher) and TaqMan microRNA Reverse Transcription kit. A mastermix was created without RNA. Per 14.5µl reaction, 0.15µl 10µM dNTPs, 0.1µl RNasin, 1.5µl 10x RT buffer, 1µl multiscribe, 3µl U6 snRNA Taqman primer, 3µl miR-181a-5p Taqman primer, 3µl miR-26b-5p Taqman primer and 2.75µl nuclease free water. 1000ng/µl of RNA was added to each sample.

The cDNA was then placed in a thermocycler and the following programme run:

Temperature	**Time**
16°C	30 minutes
42°C	30 minutes
85°C	5 minutes

MiRNA qPCR with the Taqman miRNA probe (Thermofischer) was performed on the Qiagen Rotor-gene Q qPCR machine using the supplied PCR mixture. Reaction volume was 10µl with 1.6µl cDNA to 9.3µl of reaction mixture containing the Taqman miRNA probe of interest with enzyme included alongside nuclease free water. Each reaction was performed in triplicate.

Step	Cycles	Temperature	Time
Enzyme Activation	1	95°C	10 mins
Denaturation	40	95°C	15 secs
Annealing and Extension		60°C	1 min

MiRNA cDNA synthesis for Argonaute immunoprecipitation (Ago IP) utilised the miRCURY LNA RT kit from Qiagen as a smaller RNA input concentration was required. Protocol was followed exactly as per manufacturer's instructions. Equal volumes of 20% input, Ago2 IP and IgG IP RNA was used for cDNA synthesis.

MiRNA qPCR for Ago IP was also performed on Qiagen Rotor-gene Q qPCR machine, using miRCURY LNA miRNA PCR reaction mixture from Qiagen. The reaction volume was 10µl with 1µ of cDNA to 9µl of reaction mixture containing the enzyme master mix, miRNA assay of interest (Qiagen miRCURY LNA miRNA Custom PCR Assay), and nuclease free water. Each reaction was performed in triplicate.

The PCR programme was as follows:

Step	Cycles	Temperature	Time
Enzyme Activation	1	95°C	2 min
Denaturation	40	95°C	10 secs
Annealing and Extension		56°C	1 min

2.3.6 Poly(A) tail measurements.

Poly(A) tails were measured via a PAT assay (Gandhi, 2016). An anchor sequence was ligated onto the end of poly(A) tails within an RNA sample (Figure 14). The anchor sequence contains a dideoxycytosine to prevent its 3' end from being ligated onto the poly(A) tail. Additionally, the anchor sequence is also preadenylated at the 5' end to facilitate the use of a T4 RNA ligase 2 truncated KQ enzyme (NEB) (Table 12).

Ligation was performed in a 20µl reaction containing 500ng of RNA alongside 1µmol of PAT anchor (20µM stock), of PEG8000, 1x T4 RNA ligase buffer without ATP (NEB), 200 units of T4 RNA ligase 2, truncated KQ and nuclease free water. The reaction mixture was incubated at 16°C overnight.

The ligated RNA was then converted to cDNA using Superscript III (Invitrogen). Initially, the RNA samples are incubated at 65°C for 5 minutes with 5µl PATR1 oligo (20µM) which binds to the PAT anchor, alongside 2µl of dNTP mix (10mM) in30µl.

Finally, 1µl cDNA was added to a PCR mixture containing 33.75µl nuclease free water, 10µl 5x Gotaq flexi buffer (Promega), 3µl $MgCl_2$ (25mM), 1µl dNTP mix (10mM), 1µl PAT-R1 oligo (20µM), 1µl 2nd forward gene specific primer (20µM) and 0.25µl of GoTaq, Flexi (Promega) (Figure 14A).

For nested PAT, the nested anchor (20µM) was ligated onto the RNA and two rounds of PCR were performed. The first round of PCR utilised the DachR1 Oligo in place of the PATR1 Oligo and the 1st forward gene specific primer. The second round of interest then utilised the PATR1 Oligo and the 2nd forward gene specific primer (Figure 14B).

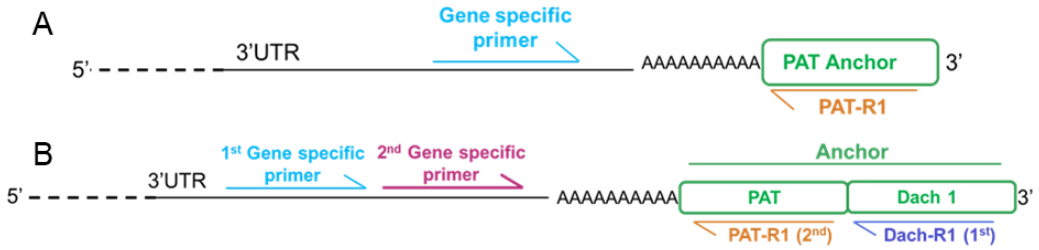

Figure 14. PAT assay infographic. A) Anchor and primer placement used for standard PAT PCR. **B)** Anchor and primer placement used for Nested PAT PCR

Table 12. Oligos used for PAT assays

PAT Primer	Sequence
PAT Anchor	5' rApp GGT CAC CTT GAT CTG AAG ddC 3'
Nested (Dach) Anchor	5' rApp GGT CAC CTT GAT CTG AAG CCA GCT GTA GCT ATG C ddC 3'
PATR1 Oligo	GCTTCAGATCAAGGTGACCTTTTT
DachR1 Oligo	GGCATAGCTACAGCTGGC
TNF PAT 1	CTCTACCTTGTTGCCTCCTC
RPL28 PAT 1	GCCACTTCTTATGTGAGGAC
TNF PAT 2	TTTCTGTGAAAACGGAGCT
RPL28 PAT 2	CGTGGTAGTTATGAAACGCA

PCR Protocol:

Step	Cycles	Temperature	Time
Enzyme Activation	1	95°C	5 mins
Denaturation	40	95°C	1 min
Annealing		58°C	1 min
Extension		72°C	2 mins
Final Extension	1	72°C	10 mins

PCR products were then run on a 1.2% Agarose gel at 78V for 1.5-3 hours.

2.4 Protein Techniques

2.4.1 Antibodies

Table 13. Antibodies used for Immunoprecipitations and western blotting. IP- Immunoprecipitation. WB – western Blotting

Antibody	Dilution	Use	Species of Origin	Species recognised	Supplier
Recombinant IgG isotype control	1:2000	IP	Rabbit	Mouse, Human	Abcam ab172730
Anti-Ago2 antibody	1:500	IP	Rabbit	Mouse, Human	Abcam ab186733
Anti-COX2 antibody	1:1000	WB	Rabbit	Mouse	Abcam ab15191
Anti-tubulin antibody	1:2500	WB	Rabbit	Mouse	Abcam Ab6046
polyclonal goat anti-mouse secondary antibody	1:5000	WB	Goat	Rabbit	Sigma A6154

2.4.2 Buffer compositions for western blotting

Table 14. Buffers used in western Blotting and their compositions.

Buffer	Composition
RIPA Buffer	150mM NaCl, Tris-HCl 50mM, pH 8.0, 1% NP-40, 0.5% sodium deoxycholate, 0.1% SDS in ddH_2O
SDS Loading Dye	40% Glycerol, 240 mM Tris-HCl pH 6.8, 8% SDS, 0.04% bromophenol blue, 5% beta-mercaptoethanol
TGS Buffer	25mM Tris-HCl, pH 8.3, 192 mM glycine, 0.1% SDS
Transfer Buffer	50 mM Tris-HCl, pH 8.3, 192 mM glycine, 20% methanol
1x TBST	50mM Tris-HCL, 150mM NaCl, 0.05% Tween
5% Milk blocking solution	5% Marvel 0% fat milk powder in 1XTBST

2.4.3 Protein Extraction

RAW 264.7 cells were seeded in 6 well plates and grown to approximately 80% confluency before an LPS time course was performed to generate protein extracts for western blotting. Media was removed from the wells and the cells were washed with PBS twice on ice. After washing, 200µl of RIPA Buffer (Table 14) with protease inhibitor (PI) (Sigma Aldrich) was added directly to the plate. RIPA was left

on the cells for five minutes while on ice. The cells were scraped using a cell lifter, and the lysates were transferred to Eppendorf tubes on ice. The lysates were then sonicated in ice for five minutes at 30 second intervals, then left on ice for 5 mins. Following this, the lysates were spun down at 16,000xg for five minutes at 4C and the supernatant was kept.

Protein was quantified via Bradford assay (Bio-rad) standardised to bovine serum albumin (BSA, Alpha Diagnostic). Protein samples were stored at -80°C.

2.4.4 SDS-PAGE gel electrophoresis

Table 15. Quantity of components used to make stacking and resolving sections of SDS-PAGE gel

Component	Stacking gel (4%)	Resolving gel (12.5%)
30% Acrylamide	340µl	2.08ml
1.5M Tris pH 8.8	250µl	1.25ml
10% SDS solution	20µl	50µl
10% APS solution	20µl	50µl
TEMED	2µl	5µl
diH_2O	1.36ml	1.57ml

A set concentration of 40µg/ml of each protein sample was used for western blotting with 4x SDS loading buffer (Table 14) added to a concentration of 1X. The protein samples were then boiled at 95°C for 5 mins before being put on ice for 5 mins then loaded into a 12.5% SDS-PAGE minigel (Table 14) along with 5µl broad molecular weight range protein ladder (Pageruler, Thermofischer). Gels were run in 1x TGS buffer (Table 14), for 90 minutes at a constant 120V.

2.4.5 Western Blotting

Once the gel had run, the protein was transferred in transfer buffer (Table 14) via wet transfer at 80V for 1.5 hours onto PVDF membrane (Thermofischer). The membranes were pre-cut to size and pre-treated with methanol before use. The membrane and gel were sandwiched between a piece of gauze pre-soacked in transfer buffer on each side along with three sheets of filter paper pre-soaked also in transfer buffer on either side of the gel and membrane.

Once the proteins had transferred to the membrane, the membrane was blocked for 1h at RT with 5% milk in 1xTBST (Table 14) while rocking. The membrane was then washed three times in 10ml TBST for 5mins each. Following blocking, the membrane was incubated with primary antibody in milk overnight within a falcon tube, rolling. Primary antibodies used were anti-PTGS2 (COX-2) (Table 13) and anti-Tubulin (Table 13). The next morning the membranes were washed three times in 1x TBST at RT with rocking for 5 mins each before being incubated with polyclonal rabbit anti-mouse secondary antibody (Table 13) in 5% milk for 1 hour at RT with rocking. Subsequently, the membrane was washed another three times in 1xTBST at RT with rocking before 1ml ECL Prime western blotting detection reagent (Amersham) was prepared and enough applied to cover the membrane which was then placed within a small clear plastic pouch. After approximately 2 minutes the membrane was then imaged using the Fujifilm LAS-4000 imager.

2.4.6 Enzyme linked immunosorbent assay (ELISA)

An ELISA was used instead of a Western blot to detect TNF protein as TNF is secreted. Total medium was taken directly from each well of a six-well plate after a LPS time course. Media was stored at -20°C. Samples were diluted 1:16 with reagent diluent (1% BSA in PBS) before use.

ELISAs were performed in 96 well plates that were prepared the day before using the R&D Systems Mouse TNF-alpha Duoset ELISA and Duoset ancillary reagent kit. Wells were coated with 100µl of Capture Antibody for mouse TNF α at a concentration of 800ng/ml, sealed and left to incubate overnight at room temperature. Wells were washed three times in 1x wash buffer solution. Plates were then blocked-in reagent diluent (1% BSA in PBS) for one hour. Wells were washed and 100µl of each standard and 100µl of each sample added to the appropriate wells and incubated for a further two hours. Standard was diluted 1in 10 and then prepared as in Figure 15. Samples were added in triplicate (one replicate per well). Wells were again washed and then coated in 100µl per well of detection antibody at a working concentration of 75ng/ml and incubated for 2 hours. Washes were performed again, and 100µl Streptavidin-HRP diluted 1:40 was added to each well and left to incubate in the dark for 20 minutes. After a final wash step, 100µl of substrate solution comprised of equal volumes colour reagent A and colour reagent B was applied to each well and

incubated in the dark for 8-10 minutes. Then 50µl of Stop solution (2N H_2SO_4) was applied to the wells and the optical density of each well was determined immediately at 450 nm on a plate reader (BioTek Synergy HT). Each reaction was performed in triplicate.

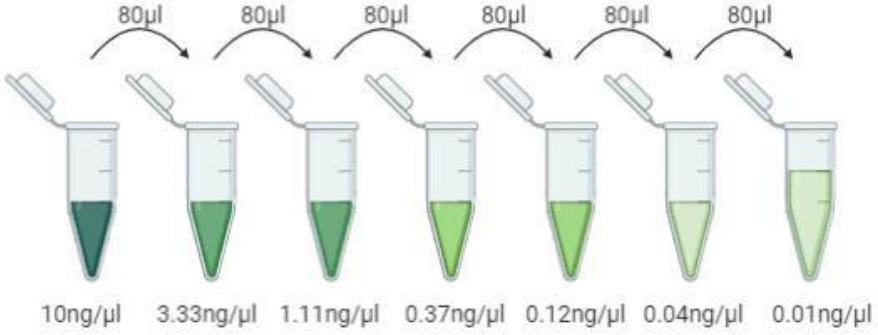

Figure 15. Serial dilution of the TNF protein standard used for the TNF ELISA. Used for quantification of protein within inhibition and overexpression of miR-181a sample.

2.4.6 RNA Immunoprecipitation (RIP)

RNA immunoprecipitation was used to isolate Ago2 and associated RNA from RAW 264.7 cells and Tet Luc TNF 3'UTR HEK 293 cells.

The Ago2 protein was immunoprecipitated and potential microRNA and mRNA targets were assessed via qPCR (Figure 16). RAW 264.7 or Tet-Luc TNF 3'UTR HEK 293 cells were grown in 6-well plates for 24 hours before either a combination of LPS, Doxycycline, or transfection and LPS time course treatments were performed.

20µl of magnetic protein A/G beads (Fischer Scientific) were suspended in 500µl of NET-2 Buffer (50mM Tris-HCL, 150mM NaCl, 0.05% NP-40) and blocked for 30 minutes (firstly just Bovine Serum Albumin (BSA)) 1mg/ml, subsequently with added glycogen 100ug/ml). The beads were then washed with NET-2 buffer via rotation for mins at 4˚C. Fresh NET-2 buffer containing antibody was added to the beads. The beads were then conjugated for two hours at 4°C with 1ug/ml of Recombinant Anti -Argonaute-2 antibody (Abcam cat no ab186733)) or with the Recombinant IgG isotype control antibody (Abcam, Rabbit monoclonal cat no ab172730) (Table 13).

Cytoplasmic lysates were prepared by adding 500µl NET-2 buffer directly to the cells after the media had been removed and the cells were washed twice with

PBS. The cells were scraped into NET-2 buffer and then underwent three rounds of sonication at 20 second intervals on ice. Lysates were left on ice for five minutes before being centrifuged at 16,000xg for 10 minutes at 4°C to remove debris. 20µl (20%) of lysate was used as an input control, 1ml of Tri reagent was added and then frozen at -20°C. This was done to allow the extraction of input and IP samples in parallel.

For the IP, NET-2 buffer was removed from the bead and 200µl of lysate was added to antibody-conjugated Ago2 beads and IgG beads then incubated overnight at 4°C while rotating. After incubation, the beads were washed four times at 4°C for 5 mins with rotation in 500µl high salt wash buffer (20mM Tris-HCL, 0.5M NaCl, 1mM EDTA, 10% NP-40) before Tri reagent was added directly to the beads for RNA extraction (Section 2.3.2). A higher salt wash buffer was used for washing instead of NET-2 buffer to try to increase the stringency of the IP (Figure 16).

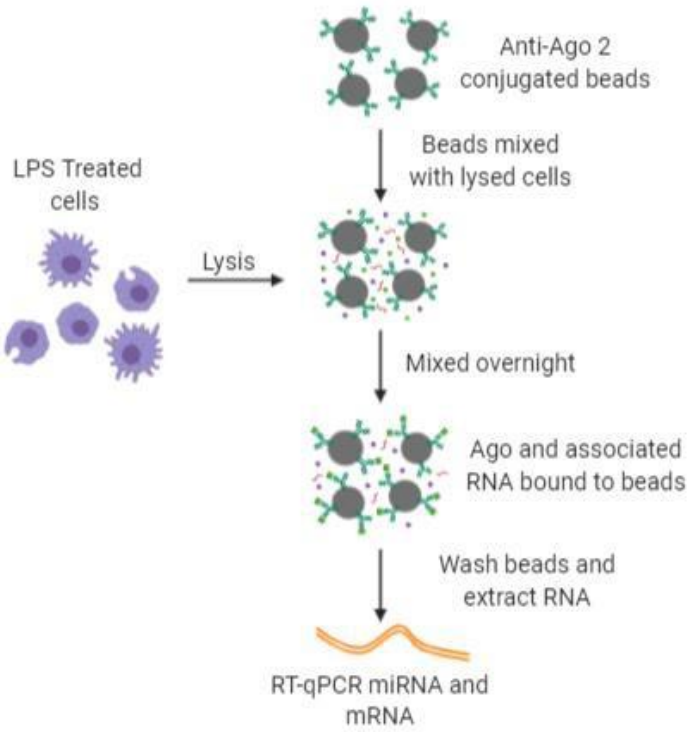

Figure 16. Schematic of the Ago Immunoprecipitation process

2.4.7 Luciferase assays

Luciferase assays were performed on HEK 293 lysate using the Promega Dual-Luciferase® Reporter Assay System. After 24hrs of transfection (Section 2.2.4), media is removed and cells are washed gently in PBS twice before 50µl 1x Passive lysis buffer was added to each well. Cells were rocked on ice for 15 minutes before being scraped with a 200µl pipette tip. Once lysed, 5µl of lysate was transferred to a white round bottom 96-well plate. Luminometer used was the Promega Glomax. Utilising the injectors 25µl of LARII was injected with a 10 second integration time and a 0.4 second delay between injection and measurement of the firefly output. Subsequently, 25µl of Stop and Glo was injected also with a 10 second integration time and a 0.4 second delay between injection and measurement of the renilla output. Luciferase data was normalised by dividing the firefly reading by the renilla reading, then the inhibitor/mimic output was divided by the negative control output for each plasmid. Statistically significant differences between treatment and control for the WT Luc TNF 3'UTR and Mut Luc TNF 3'UTR plasmids were determined using t-tests.

2.5 Data analysis and experimental design

2.5.1 Experimental design

For all experiments biological repeats are classified as the same experiments that has been performed on cells of different passage seeded on a different week and are distinct from the previous experiment and are classified as N=X. For example, N=1 for a miR-181a inhibition experiment ending in qPCR analysis would be passage 12 RAW 264.7 cells seeded and harvested one week and the experimental work flow followed through. The second biological repeat, N=2 would be passage 15 RAW 264.7 cells seeded and harvest on a different week to the N=1 experiment and the experimental workflow followed through.

On the other hand, technical repeats are classified as the same samples run at the same time within an experiment or instrument which are then averaged to give the overall result for the sample. For qPCR experiments, technical repeats were each cDNA and qPCR primer master mix were run in triplicate, these triplicate values were then averaged to give the Ct value for the sample. For ELISAs, the technical repeats, involved running each sample in triplicate. Each triplicate was classified as the same sample run in a separate well of a 96 well plate. These triplicate values were then averaged to give the overall value for the sample. Technical repeats for luciferase assays were the same treatment condition performed in parallel on three separate wells of a 24 well plate containing cells. For example, wells A1-3 in a 24 well plate would be transfected with the Renilla Plasmid, WT TNF 3'UTR plasmid and the miR-181a inhibitor. Then wells B1-3 would be transfected with Renilla Plasmid, WT TNF 3'UTR plasmid and the negative control oligo. Reading from these three wells would then be averaged after normalisation to give the overall reading for the sample.

2.5.2 Statistical analysis

Before any statistical tests were performed on a data set, the data was checked for normality on GraphPad Prism. If the data was confirmed to be normally distributed, a parametric test was performed. If the data is not normally distributed then a non-parametric test was performed.

Specific statistical analysis is detailed for each type of experiment below.

2.5.2 Analysis of qPCR data

All qPCR data was analysed using the $2^{-\Delta\Delta Ct}$ method. Housekeeping normalisation controls for RAW 264.7 cells were selected for over an eight hour LPS (1µg/ml) time course. Housekeeping genes tested were GAPDH, ACTB, HPRT and RPL28. GAPDH, HPRT and RPL28 were selected as normlalisation controls as their Ct values remained consistent with LPS treatment (Supplementary Table 1) For time courses plotted as XY graphs, the area under the curve was calculated for each repeat, and t-tests or Wilcoxon -t-test were performed to determine if there were any statistically significant differences.

All other qPCR data was checked for statistical significance by performing a one-way ANOVA with multiple comparisons and Bonferroni correction for normally distributed data or by multiple non-parametric t-tests with Bonferroni correction. For example, comparing between multiple treatments and controls at individual time points.

2.5.3 Analysis of ELISA data.

To calculate the protein concentrations for the ELISA, the absorbance values and the standards were fitted to a four-parameter logistic curve. The exact protein concentrations were then calculated.

The protein concentrations were then plotted over time as an XY graph. For comparisons between treatments the area under the curve was calculated for each repeat and t-tests or non-parametric t-tests based on normality of the data were performed to determine if there were any statistically significant differences.

Proteins concentrations were also plotted as relative expression (Treatment/Control) for each time point. Statistical difference between time points was analysed by performing a one-way ANOVA with multiple comparisons and Bonferroni correction or multiple non-parametric t-tests with Bonferroni correction dependent on normality.

2.5.4 Quantification of Western blots

Quantification of Western blots was performed using the ImageJ software. Each band was selected, and a histogram was created for both the protein of interest and the tubulin loading control. The value for the peaks corresponding to each band within the histogram were selected and a table of area and percentage for each band was generated. This table was exported to Excel where the relative density was

calculated. Each treatment percentage was divided by the control for both the protein of interest and the tubulin loading control. Each sample for the proteins of interest was then divided by the corresponding sample for the tubulin loading control to give the corrected relative density. These values were then plotted as a bar graph. After testing for normality any statistical differences between samples were calculated using a t-test.

Chapter 3

Analysis of miR-181a regulation of TNF mRNA over the course of Inflammation

3.1 Introduction

Inflammation is a complex process induced as a first response to infection or injury. Misregulation of the inflammatory response can result in chronic disease (Medzhitov, 2008). As such, inflammation is under strict regulation at many different levels. One key regulator is miRNAs. MicroRNAs are involved in regulating many different aspects of inflammation such as its initiation and cessation and processes such as phagocytosis and macrophage polarisation (Forster, Tate & Hertzog, 2015, Curtale, Rubino & Locati, 2019). The regulation of activation or inhibition of inflammation is usually through altered expression or regulation of specific miRNAs in stimulated immune cells. One key example is miRNA involvement in macrophage polarisation to either a pro or an anti-inflammatory state (Liu & Abraham, 2013).

MiRNAs often change in expression during inflammation to aid in the regulation of the response (Nejad *et al.,* 2018, Mann *et al.,* 2018). One very well known miRNA that expression changes during inflammation is miR-155 (Mann *et al.,* 2018, Mahesh & Biswas, 2019). MiR-155 is a pro-inflammatory miRNA whose increase in expression helps to drive the induction of the inflammatory response by downregulating anti-inflammatory genes (Mahesh & Biswas, 2019).

Changes in miRNA action during inflammation is regulated in a variety of different ways (Contreas & Rao, 2011). Mechanisms implicated in inflammation are upregulation of miRNA transcription by Akt1 (Androulidaki *et al.,* 2009) and increased microprocessor cleavage via TGF-β (Davis *et al.,* 2009).

Additionally, changes in polyadenylation may also serve as a regulatory mechanism for miRNA activity. Certain mRNAs such as TNF and CXCL2, that are induced during inflammation, have been found to have initial poly(A) tails that vary in length over the course of the inflammatory response within RAW 264.7 cells (Gandhi., 2016). Additionally, PTGS2 has also been found to display these changing poly(A) tail lengths

within the serum response in NIH3T3 cells (Singhania *et al.,* 2019) but PTGS2 also has a role in inflammation (Simon, 1999).

TNF and CXCL2 are both pro-inflammatory cytokines that help orchestrate key inflammatory processes (Bradley, 2007). PTGS2 catalyses the production of prostaglandins also involved in elevating inflammation (Simon, 1999, Ricciotti & Fitzgerald., 2011).

For TNF and CXCL2 the poly(A) tails are initially long before becoming shorter as the inflammatory response proceeds (Gandhi, 2016). Additionally, PTGS2 also shows a similar poly(A) tail change within the serum response with the initial tail lengths starting long before shortening over the duration of the serum response (Singhania *et al.,* 2019). As such, these changing poly(A) tails may be affecting the miRNA regulation of these mRNAs over the course of the inflammatory response.

An aim of this project was to determine, for specific mRNAs that were previously shown to experience changes in poly(A) tail length during the course of inflammation, how these changes affect miRNA regulation of the respective mRNA. Before this question can be answered, miRNAs targeting these transcripts with changing poly(A) tails needed to be identified and the prospective pairings validated.

The approach was taken to look for known miRNA targeting of TNF, CXCL2, and PTGS2, then carried out experiments to establish whether this miRNA regulation was observed within our system and how the miRNA regulation changes over the course of the inflammatory response.

3.2 Identification of miRNA-mRNA pairings

The approach taken sought to identify miRNAs known to target inflammatory mRNAs that display poly(A) tail changes. In particular, the focus was placed on identifying miRNAs that pair with mRNAs such as TNF, PTGS2, and CXCL12 that are shown to vary in poly(A) tail length and be induced by LPS driven TLR4 signaling. All three mRNAs display poly(A) tails that shorten in length as the response progresses (Gandhi, 2016).

Candidate miRNA-mRNA pairings were initially identified using database searching. The databases used were Target Scan, miRBase, and miRTarBase. MiRNAs had to be present within all three databases to be considered for selection (Figure 17). Initial searches were performed using Target scan to identify potential miRNAs and their binding sites. TargetScan also gives information on the type of binding site as well as how well the miRNA and its binding site is conserved. Three miRNAs were chosen to move forward with for each mRNA, selecting those that were highly conserved and had preferential binding sites. All identified miRNAs were then checked on miRbase, which provides annotation scores and confidence that the miRNA is genuine and not a fragment picked up in next generation sequencing. For the miRNAs identified, were checked for high annotation confidence indicating the miRNAs are real, making sure the miRNAs are expressed at high enough levels to physiologically function and are not degradation products that have been detected in NGS studies. The identified miRNAs were then checked whether they were present within miRTarBase. miRTarBase documents experimentally validated miRNA-target interactions. As such miRTarBase was used to check whether the potential miRNA pairings have had any experimental validation. These pairings were then cross-referenced against current literature to check whether the potential pairings have been suggested to act within the inflammatory response. Pairings selected were miR-26b-5p as a regulator for Prostaglandin- endoperoxide synthase 2 (PTGS2) and miR-181a-5p as a regulator for tumour necrosis factor-alpha (TNF-α) (Figure 17, 18). These miRNAs were identified as having 8mer binding sites as well as being identified by miRTarBase to have been experimentally validated to target their respective mRNAs via reporter assay, western blot, and qPCR. These miRNA-mRNA pairings had the greatest number of studies supporting the regulatory pairs within the inflammatory response (Li *et al.,* 2013, Zhu *et al.,* 2017, Corsetti *et al.,* 2018, Zhang *et al.,* 2019, Kwon *et al.,* 2015, Li *et al.,* 2015, Ge *et al.,* 2019).

mRNA	Potential miRNA	TargetScan		miRBase		miRTarBase			Publications
		Present	Binding site	Present	Annotation score	Present	Strong evidence	Less strong evidence	
TNF	miR-181a-5p	Yes	8mer	Yes	High	Yes	RA, WB, qPCR		4
	miR-125b-5p	Yes	7mer-m8	Yes	High	Yes	RA	Other	1
	miR-130a-3p	Yes	7mer-m8	Yes	High	Yes	RA, WB, qPCR		2
PTGS2	miR-26b-5p	Yes	8mer	Yes	High	Yes	RA, WB, qPCR	Other	3
	miR-103-3p	Yes	8mer	Yes	High	No			0
	miR-101b-3p	Yes	7mer-m8	Yes	High	Yes	RA, WB, qPCR	Other	1
CXCL2	miR-7-5p	Yes	7mer-m8	Yes	High	No			0
	miR-141-5p	Yes	7mer-m8	Yes	High	Yes		Clip-seq	0
	miR-129-5p	Yes	7mer-A1	Yes	High	No			1

8mer	an exact match to positions 2-8 of the mature miRNA (the seed + position 8) followed by an 'A'
7mer-m8	an exact match to positions 2-8 of the mature miRNA (the seed + position 8)
7mer-A1	an exact match to positions 2-7 of the mature miRNA (the seed) followed by an 'A'

RA	Reporter Assay
WB	Western Blot

Figure 17. The selection process for choosing miRNA-mRNA pairings for validation. MicroRNAs were identified using TargetScan, miRBase and miRTarBase for three mRNA targets, TNF, PTGS2, CXCL2, shown to have changing poly(A) tails by Gandhi (2016). Prospective miRNA-mRNA pairings were then cross-referenced against literature to check for ties to inflammation and any previous experimentally suggested association.

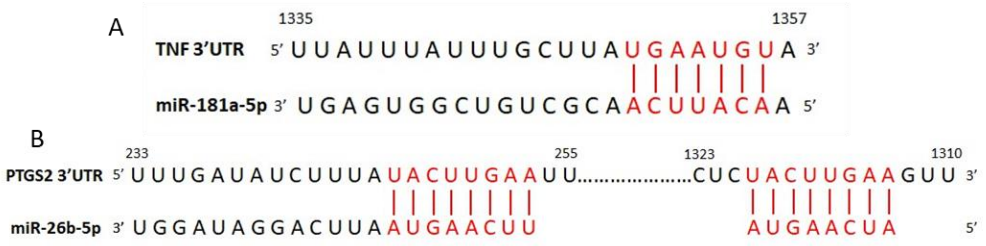

Figure 18. MicroRNA binding sites within 3'UTR of selected candidate inflammatory mRNAs. A) Binding site for miR-181a-5p seed region within the 3'UTR of TNF mRNA. **B)** Binding sites for miR-26b-5p seed region within the 3'UTR of PTGS2 mRNA.

3.3 PTGS2 and TNF are induced in response to lipopolysaccharide (LPS) within RAW 264.7 cells

Having identified miRNA-inflammatory mRNA pairings, a model of inflammation first needed to be established. Mouse macrophage, RAW 264.7 cells were selected as inflammation is easily induced within this cell line. Furthermore, RAW 264.7 cells were the cells used by Gandhi (2016) when discovering the changing poly(A) tail lengths within inflammation. In keeping with being consistent with Gandhi (2016), 1ug/ml LPS (Sigma) was used to stimulate inflammation within the RAW 264.7 cells.

Induction of TNF and PTGS2 was measured via qPCR to check that they were being induced within the model of inflammation. As an additional check for whether

inflammation was being stimulated within the RAW 264.7 cells, the levels of IL-1b mRNA were also measured (Figure 19). The expression of these three mRNAs was checked after an hour of inflammation as an initial time point. One hour was selected as the initial time point as Gandhi (2016) saw clear induction of TNF, PTGS2, and IL1-b by one hour.

All three mRNAs were induced in response to LPS, confirming that the inflammatory response is being stimulated within the RAW 264.7 cells. The induction for IL-1b was the greatest, but both TNF and PTGS2 mRNA levels are increased with one hour of LPS stimulation. The induction for TNF is slightly larger than PTGS2 when normalising to both GAPDH and HPRT (Figure 19 A and B). Relative to the induction seen by Gandhi (2016), the induction of TNF mRNA at one hour is much smaller, with a fold change of around 50 compared to a fold change of around 200 when normalised to HPRT (Figure 19). The relative increase in IL1-b however, is similar between this system and Gandhi (2016). GAPDH and HPRT were chosen as housekeeping genes for normalisation as their expression does not change over inflammation.

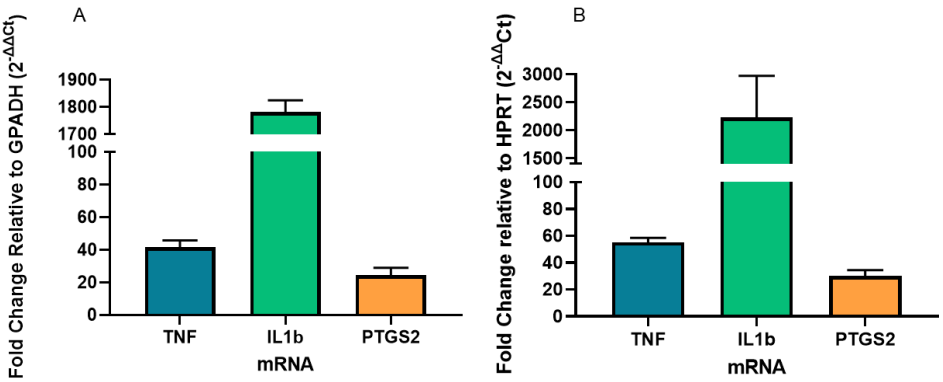

Figure 19. Induction of inflammation by Sigma LPS. A) Induction of inflammatory mRNA in response to 1µg/ml LPS treatment of RAW246.7 cells for one hour. mRNA levels were measured via RT-qPCR and the data was analysed by $2^{-\Delta\Delta Ct}$ normalised to GAPDH, relative to unstimulated cells. N=3. Error bars represent the SD. B) Same as A but data normalised to HPRT.

3.4 miR-181a and miR-26b expression levels do not change significantly during inflammation

We wanted to establish whether miR-181a and miR-26b change in expression over the course of inflammation. RAW 264.7 cells were treated with LPS over a series of time points, then the expression levels of miR-181a and miR-26b

were measured via RT-qPCR. MiR-155 was used as a positive control for inflammation as its induction during inflammation is well established (Quinn *et al.,* 2014).

MiR-155 expression increased over the course of inflammation as expected (Figure 20A). Conversely, the expression patterns for both miR-181a and miR-26b show very little change over the inflammatory response (Figure 20). These experiments were performed with a TLR4 specific LPS as described in section 3.6.

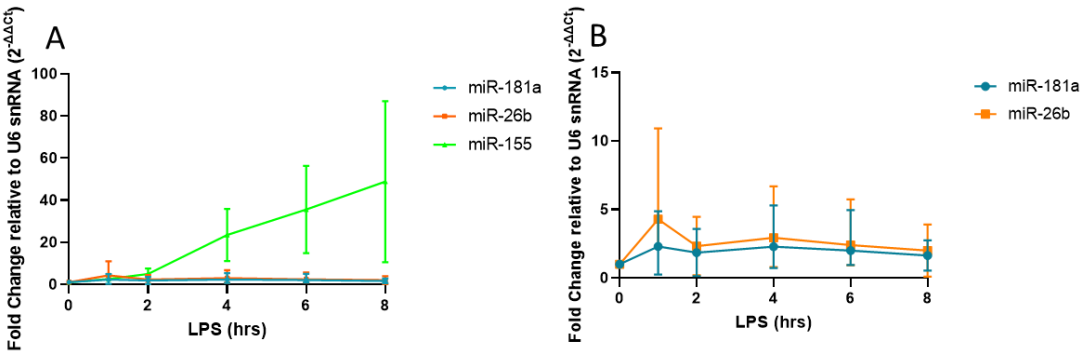

Figure 20. MicroRNA expression during inflammation. A) Expression of miR-181a, miR-26b and miR-155 over an eight-hour LPS (1µg/ml, Enzo) time course. miRNA levels were analysed by RT-qPCR and normalised to U6 snRNA and plotted relative to the zero hour time point N=4. Error represents SD **B)** Same as A except the miR-155 data has been removed.

3.5 Inhibition of miR-26b has no impact on PTGS2 mRNA or protein levels during inflammation

To verify whether the selected miRNAs were indeed regulating their previously identified mRNA target, miRNA inhibition experiments were performed. Inhibitions were carried out utilising the Qiagen miRCURY LNA inhibitors. These were selected due to their locked nucleic acid (LNA) technology which increases the potency of the inhibitor as it overcomes the problems with lower GC content reducing inhibitor potency as a result of weaker binding. The inhibitors were transfected using Lipofectamine RNA iMAX using the same conditions that have been established for siRNA knockdown within RAW 264.7.

Starting with miR-26b and PTGS2, miR-26b was inhibited and the mRNA levels for PTGS2 were measured over a two-hour time course of inflammation following LPS treatment. There is the expected induction of PTGS2 mRNA with LPS treatment over time. However, there was no difference in PTGS2 mRNA levels between the miR-26b

inhibition and negative control treatments over the inflammatory time course (Figure 21A). Additionally, the no transfection control has a greater induction of PTGS2 mRNA at 120 minutes than either the inhibitor or control transfected samples, this is likely to be due to the transfection reagent partially inducing an inflammatory response and affecting the no LPS baseline in these conditions. When looking at the effect of miR-26b inhibition on PTGS2 mRNA at each individual time point there is also no significant increase in PTGS2 mRNA (Figure 21B).

Furthermore, when looking at the protein level, there is a clear induction of PTGS2 with LPS treatment at 120 minutes for all three conditions. However, when looking at whether miR-26b inhibition affected PTGS2 protein levels by western blot, there was also no distinct change to be seen (Figures 21C and 21D, Supplementary Figure 3).

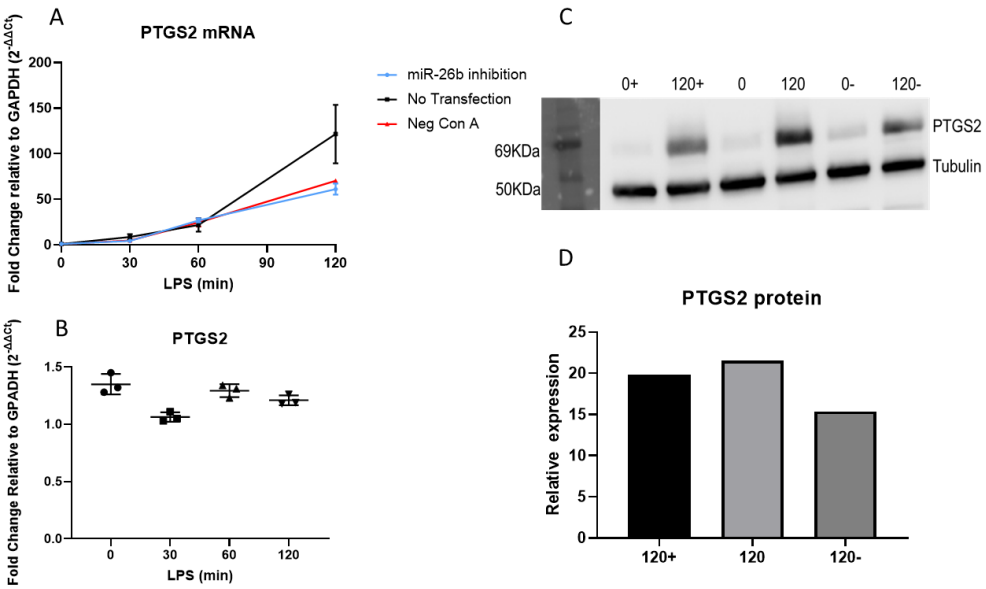

Figure 21. **Effect of miR-26b inhibition on PTGS2 levels. A)** PTGS2 mRNA levels with miR-26b inhibition over a 120-minute LPS (1ug/ml, Sigma) time course in RAW 264.7. miR-26b inhibitor (10nmol) or negative control oligo (10nmol) were transfected over 24 hours. Data measured by RT-qPCR and analysed by $2^{-\Delta\Delta Ct}$ normalised to GAPDH and plotted relative to the zero hour time point. N=3. Error indicates SD. **B)** Same as A but data is plotted relative to the negative control at each time point. **C)** Western blot showing effect of miR-26b-5p inhibition on PTGS2 protein levels with no LPS (0) and 120 minutes after LPS treatment (1ug/ml). miR-26b inhibitor (10nmol) or negative control oligo (10nmol) were transfected over 24 hours. 0+, 120+ denotes miR-26b-5p inhibition, 0 120 denotes no transfection control, 0-, 120-, denotes Negative Control A. Tubulin used as a loading control. N=2. Error bars represent SD **D)** Quantification of C relative to each treatments no LPS control (0-time point) normalised to the loading control. Relative expression is in arbitrary units.

3.6 Inhibition of miR-181a increases TNF mRNA and protein levels during inflammation

Having seen no evidence that miR-26b is regulating PTGS2 within this system, the effect of inhibiting miR-181a on TNF levels were investigated as an alternative model of a miRNA regulating an mRNA that shows changes in poly(A) tail length during inflammation. Initially, TNF mRNA levels following LNA miR-181a inhibition with a Qiagen miRCURY LNA inhibitor were measured over a four hour LPS time course. There is an increase in TNF mRNA with miR-181a inhibition compared to the negative and no transfection controls when looking at inflammation over time with the greatest difference being seen at four hours (Figure 22A). This suggests there is some inhibitory effect of miR-181a on TNF. Additionally, when looking purely at the effect of miR-181a inhibition on TNF mRNA relative to the negative control, there is also an increase in TNF. The largest impact of miR-181a inhibition on TNF mRNA when looking at individual time points was at the zero LPS time point (Figure 22B).

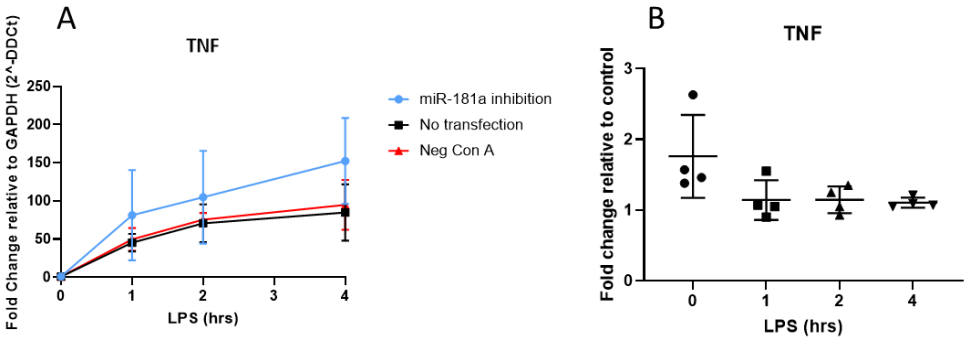

Figure 22. Effect of miR-181a inhibition on TNF mRNA levels. A) TNF mRNA levels with miR-181a inhibition over a four-hour LPS (1ug/ml, Sigma) time course in RAW 264.7. miR-181a inhibitor (10nmol) or negative control oligo (10nmol) were transfected over 24 hours. Data measured by RT-qPCR and analysed by $2^{-\Delta\Delta Ct}$ normalised to GAPDH and plotted relative to the zero hour time point. N=4. Error bars indicate SD. **B)** Same as A but data is plotted relative to the negative control at each time point. N=4. Error represents SD.

Following these initial experiments, there was some concern about the specificity of the LPS (Sigma). The Sigma LPS undergoes a less stringent purification process than other TLR4-specific LPS, as such the Sigma LPS is likely to activate TLRs such as TLR1, 2, and 6 which recognise other bacterial peptides such as lipoproteins, peptidoglycans, and porin or TLR5 which recognises flagellin (Akira *et al.,* 2006). On

the other hand, TLR4 is specific for detecting LPS (Akira, 2006). It was decided that a purely TLR4-specific LPS (Enzo) would be used for future experiments. Using a TLR4 specific LPS means that the inflammatory response is only being stimulated by one inflammatory pathway instead of many. This reduces confounding variables and should reduce some variability.

The induction of inflammatory markers, TNF, PTGS2 and IL-1b were tested with the TLR4-specific LPS to ensure the inflammatory response was still being stimulated within the RAW 264.7 cells. With the TLR4-specific LPS, the induction of PTGS2 was greater than TNF. This single experiment confirmed that the inflammatory response is being stimulated effectively, but as it is not repeated it is not possible to draw conclusions on the magnitude of inflammatory mRNA induction (Figure 23).

From this point, all inflammatory inductions were performed with the TLR4-specific LPS.

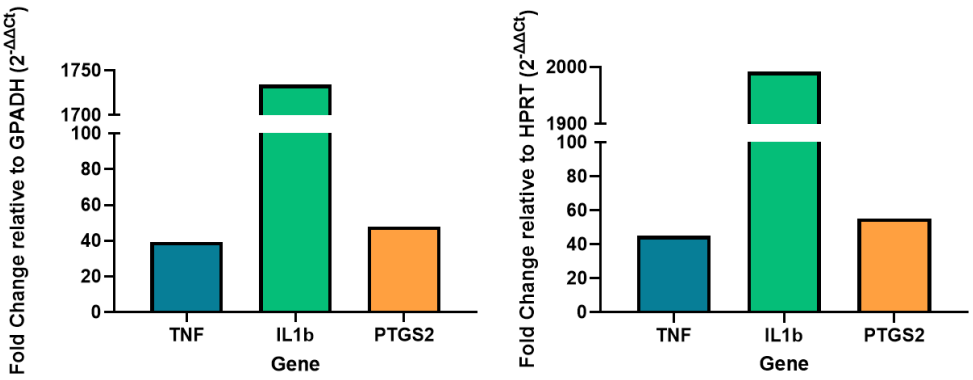

Figure 23. **Induction of inflammation by Enzo LPS. A)** Induction of inflammatory mRNA in response to 1µg/ml LPS for one hour. Data was measured via RT-qPCR and the data were normalised to GAPDH. N=1 **B)** Same as A but data was normalised to HPRT. N=1.

Inhibition experiments for miR-181a were repeated with the new Enzo LPS, this time over an eight-hour inflammatory time course. When looking at the effect of miR-181a inhibition over time, there is a two-threefold increase in TNF mRNA compared to the no transfection and negative controls when data is normalised to either GAPDH or HPRT (Figure 24A, 24B). Furthermore, the difference between miR-181 inhibition and the negative control is significant in both Figures 24A ($p<0.05$, AUC) and 24B ($p<0.05$, AUC). There is also no significant difference between the no

transfection and negative control treatments. This increase in TNF mRNA confirms that miR-181a is negatively regulating TNF.

Additionally, when looking at the impact of miR-181a inhibition at the individual time points, there is a one-twofold increase in TNF mRNA following inhibition compared to the control. Plotting the data relative to the negative control at each time point looks at the direct effect of miR-181a inhibition on TNF mRNA. (Figures 24C and 24D). However, this increase in TNF mRNA with miR-181a inhibition compared to the negative control is greatest at the zero hour time-point with a fold change of two. This does still suggest that TNF mRNA is de-repressed with miR-181a inhibition, with more effect apparent when TNF mRNA levels are low.

Finally, the effect of miR-181a inhibition on TNF protein levels was measured via ELISA as TNF is secreted. The time course of induction for TNF protein is much slower due to the requirement for translation and export. The effect of miR-181a inhibition on TNF protein levels is much clearer than on mRNA with a two-threefold increase in TNF protein levels at eight hours between inhibition and control treatment. There is a significant increase in TNF protein level ($p<0.01$, AUC) over the course of the inflammatory time course (Figure 24E). Furthermore, when looking at the relative increase in TNF at each time point, there is a two-three fold increase in TNF with miR-181a inhibition compared to control at each time point bar the zero-hour time point (Figure 24F). As such this may indicate that miR-181a is having a greater effect on the translation of TNF mRNA into protein.

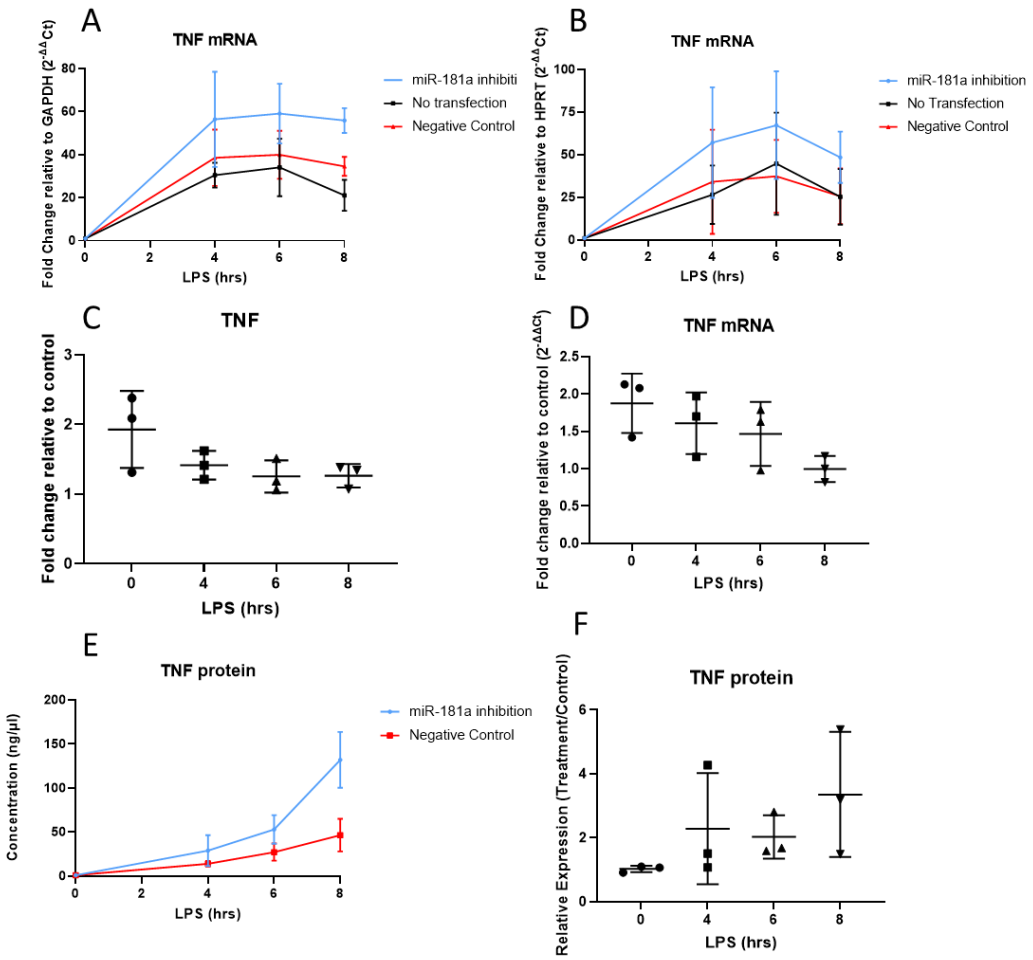

Figure 24. Effect of inhibiting miR-181a on TNF mRNA over 8 hours of inflammation. A) TNF mRNA levels with miR-181a inhibition over and eight-hour LPS (1ug/ml) time course in RAW 264.7. miR-181a inhibitor (10nmol) or negative control oligo (10nmol) were transfected over 24 hours. Data measured by RT-qPCR and analysed by $2^{-\Delta\Delta Ct}$ normalised to GAPDH and plotted relative to the zero hour time point. N=3. Significant increase in TNF mRNA with miR-181a inhibition ($p<0.05$, AUC). N=4. Error indicates SD. **B)** Same as A but data is normalised to HPRT. Significant increase in TNF mRNA with miR-181a inhibition ($p<0.05$, AUC). N=4. Error represents SD. **C)** Same as A but data is plotted relative to the negative control at each time point. **D)** Same as B but data is plotted relative to the negative control at each time point. **E)** Effect of miR-181a-5p inhibition on TNF protein levels over an eight-hour LPS (1ug/ml) LPS time course measured by ELISA. N=3. Significant decrease in TNF protein with miR-181a inhibition ($p<0.01$, AUC). Error bars indicates SD. **F)** Same as E except each time point has been plotted relative to the control. N=3. Error represents SD.

3.7 Overexpression of miR-181a decreases TNF mRNA and protein levels during inflammation

Following on from the inhibition experiments, miR-181a overexpression experiments were performed to see if an increase in miR-181a resulted in increased repression of TNF mRNA. In contrast to the inhibition experiments, overexpressing miR-181a resulted in a two-threefold decrease in TNF mRNA levels over the course of inflammation compared to the no transfection and negative controls (Figures 25A, 25B). This decrease in TNF mRNA levels was significant when the data were normalised to both GAPDH ($p<0.05$, AUC) and HPRT ($p<0.05$, AUC). This decrease in TNF mRNA over the course of inflammation with miR-181a overexpression confirms that miR-181a is negatively regulating TNF mRNA levels.

Furthermore, there is also a one-twofold decrease in TNF mRNA levels with miR-181a overexpression when looking at each individual time point relative to the negative control (25C and 25D). The reduction in TNF mRNA is significantly stronger at later time points, particularly the six and eight hour time points.

The decrease in TNF mRNA is greatest at the eight hour time point, with this decrease being significant when the data is normalised to both GAPDH ($p<0.05$, t-test) and HPRT ($p<0.05$, t-test) (Figures 25C and 25D). This determines that miR-181a is having the greatest impact later on in the inflammatory response. This contrasts with the miR-181a inhibition experiments where there is more impact of inhibition earlier in the response.

Finally, when looking at the impact of miR-181a overexpression on TNF protein levels over the course of the response, there is a significant decrease in TNF protein quantity (Figure 25E, $p<0.001$, AUC). Moreover, when looking at the effect of miR-181a overexpression on protein levels at individual time points, there is a strong repression of TNF later into the response with the six and eight-hour time points displaying a significant decrease (Figure 25F). There is a much stronger effect of overexpression on TNF protein levels suggesting that most of the effect of miR-181a is translation as opposed to affecting mRNA stability.

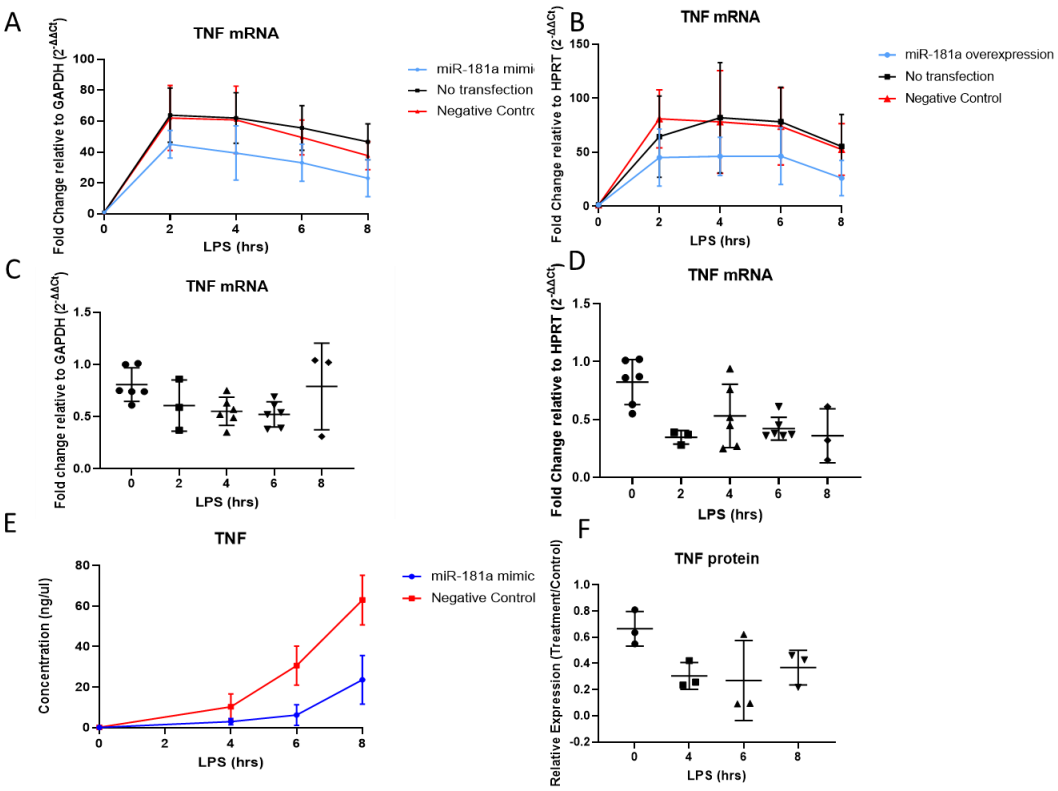

Figure 25. Effect of overexpressing miR-181a on TNF mRNA over 8 hours of inflammation. A) TNF mRNA levels with miR-181a overexpression over and eight-hour LPS (1ug/ml) time course in RAW 264.7. miR-181a mimic (10nmol) or negative control oligo (10nmol) were transfected over 24 hours. Data measured by RT-qPCR and analysed by $2^{-\Delta\Delta Ct}$ normalised to GAPDH and plotted relative to the zero hour time point. N=6 (0, 4, 6 hrs) N=3 (2, 8 hrs). Significant decrease in TNF mRNA with miR-181a overexpression ($p<0.05$, AUC). Error indicates SD. **B)** Same as A but data is normalised to HPRT. Significant decrease in TNF mRNA with miR-181a overexpression ($p<0.05$, AUC). N=6 (0, 4, 6 hrs) N=3 (2, 8 hrs). Error represents SD **C)** Same as A but data is plotted relative to the negative control at each time point. Significant decrease in TNF mRNA relative to the negative control (four: $p<0.001$ six: $p<0.0001$, t-test with Bonferroni correction) N=6 (0, 4, 6 hrs) N=3 (2, 8 hrs). Error represents SD **D)** Same as B but data is plotted relative to the negative control at each time point. Significant decrease in TNF mRNA relative to the negative control at (two: $p<0.001$, four: $p<0.001$, six: $p<0.001$, eight: $p<0.001$, t-test with Bonferroni correction) N=6 (0, 4, 6 hrs) N=3 (2, 8 hrs). Error represents SD **E)** Effect of miR-181a-5p overexpression on TNF protein levels over an eight-hour LPS (1ug/ml) LPS time course measured by ELISA. Significant decrease in TNF protein with miR-181a overexpression ($p<0.001$, AUC). N=3. Error bars indicate SD. **F)** Same as E except each time point has been plotted relative to the control. Significant decrease in TNF proteins levels with miR-181a inhibition (six: $p<0.0001$, eight, $p<0.0001$, t-tests with Bonferroni correction). N=3. Error represents SD.

3.8 MiR-181a regulation of TLR4 during inflammation

TLR4 is also identified by computational algorithms to be a target of miR-181a and is upstream of TNF within the inflammatory induction pathway. To check whether changes in TNF mRNA expression were due to the effects of miR-181a regulation on TLR4 mRNA the effects of miR-181a inhibition and overexpression levels on TLR4 mRNA were investigated.

Initially, TLR4 mRNA expression over the course of inflammation was measured by RT-qPCR. While TLR4 mRNA expression initially decreases at two hours post LPS treatment before slowly rising again at eight hours, this difference was not significant (Figure 26). This is consistent with previous findings for TLR4 (Maris *et al.,* 2006)

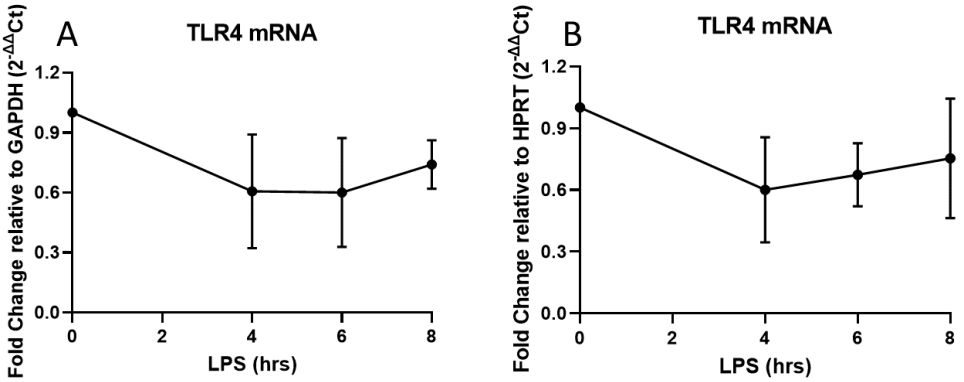

Figure 26. TLR4 mRNA expression over eight hours of inflammation. A) TLR4 mRNA levels over an eight-hour LPS (1ug/ml) time course. Measured by RT-PCR, analysed by $2^{-\Delta\Delta Ct}$. Data normalised to GAPDH and plotted relative to the zero-hour time point. N=3. Error indicates SD **B)** Same as A but normalised to HPRT. N=3. Error indicates SD.

When cells were treated with a miR-181a inhibitor, there was an increase in TLR4 mRNA compared to the no transfection and negative controls over the course of inflammation (Figures 27A and 27B). However, the increase seen in TLR4 mRNA within miR-181a inhibition over time is not significant. When looking at the effect of miR-181a inhibition on TLR4 mRNA at each individual time point, there is also no significant change (Figures 27D and 27C). This small effect of inhibition at the TLR4 mRNA level may be due to miR-181a mainly acting at the level of translation, but a

western blot to look at the effect of miR-181a inhibition on TLR4 protein level has not been performed. The alternative is that inhibitor transfection is inefficient.

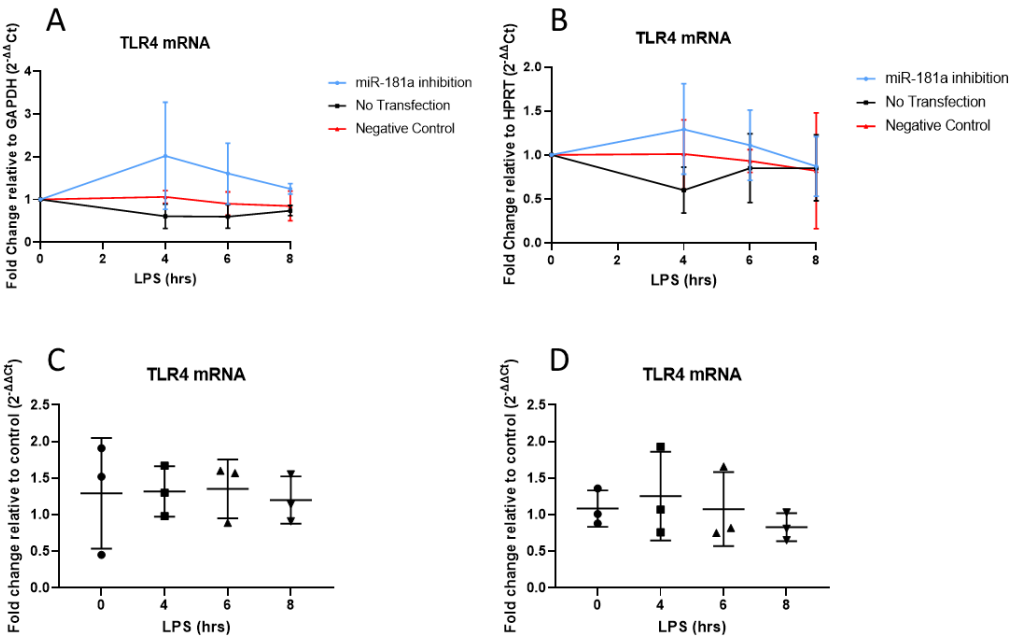

Figure 27. Effect of inhibiting miR-181a on TLR4 mRNA over 8 hours of inflammation. A) TLR4 mRNA levels with miR-181a inhibition over and eight-hour LPS (1ug/ml) time course in RAW 264.7. miR-181a inhibitor (10nmol) or negative control oligo (10nmol) were transfected over 24 hours. Data measured by RT-qPCR and analysed by $2^{-\Delta\Delta Ct}$ normalised to GAPDH and plotted relative to the zero hour time point. N=3. Error indicates SD. **B)** Same as A but data is normalised to HPRT. N=3. Error indicates SD **C)** Same as A but data is plotted relative to the negative control at each time point. N=3 Error represents SD **D)** Same as B but data is plotted relative to the negative control at each time point. N=3. Error represents SD.

Conversely, when miR-181a is overexpressed, there is a slight decrease in TLR4 mRNA over the course of inflammation compared to the no transfection and negative control when normalised to both GAPDH and HPRT, however, this change is not significant (Figures 28A and 28B). There is a clear decrease in TLR4 mRNA when looking at the individual time points relative to the control (Figures 28C and 28D). Additionally, regulation at the protein level for TLR4 cannot be ruled out as it has not been investigated. While miR-181a may be regulating TLR4, there is not substantial evidence to say that changes in TNF mRNA and protein levels are due to regulation of TLR4 by miR-181a instead of direct regulation of TNF by miR-181a.

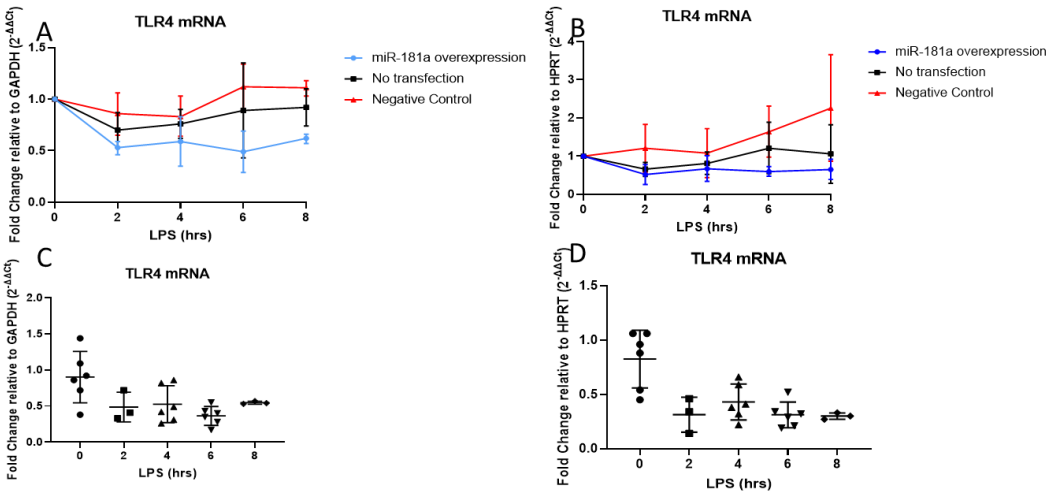

Figure 28. Effect of overexpressing miR-181a on TLR4 mRNA over 8 hours of inflammation. A) TLR4 mRNA levels with miR-181a overexpression over and eight-hour LPS (1ug/ml) time course in RAW 264.7. miR-181a mimic (10nmol) or negative control oligo (10nmol) were transfected over 24 hours. Data measured by RT-qPCR and analysed by $2^{-\Delta\Delta Ct}$ normalised to GAPDH and plotted relative to the zero hour time point. N=6 (0, 4, 6 hrs) N=3 (2, 8 hrs). Error indicates SD. **B)** Same as A but data is normalised to HPRT. **C)** Same as A but data is plotted relative to the negative control at each time point. N=6 (0, 4, 6 hrs) N=3 (2, 8 hrs). Error indicates SD **D)** Same as B but data is plotted relative to the negative control at each time point. N=6 (0, 4, 6 hrs) N=3 (2, 8 hrs). Error indicates SD.

3.9 MiR-181a regulation of TNF pre-mRNA levels during inflammation

To further investigate whether miR-181a regulation of TLR4 may be impacting TNF levels, the effect of miR-181a regulation on TNF pre-mRNA levels were investigated. RAW 264.7 cells were transfected with either a miR-181a Qiagen miRCURY LNA inhibitor or mimic then treated with LPS over an eight hour time course before the RNA was extracted and TNF pre-mRNA levels were measured using RT-qPCR. The pattern of TNF induction is very similar to that seen with the mature mRNA, especially when the data is normalised to HPRT (Figure 29A and 29B).

Additionally, when then looking at the effect of miR-181a inhibition on TNF pre-mRNA at each individual time point relative to the negative control there is also an increase in relative TNF pre-mRNA but the data is quite variable between time points and there is not significant difference (Figure 29C and 29D). This small increase may be due to miR-181a regulation of TLR4 as opposed to any regulation of TNF at the pre-mRNA level. Although, while there was an overall trend towards higher TNF pre-mRNA levels following miR-181a inhibition, this was not significant, so there is little evidence that TNF was indirectly regulated at the level of transcription by miR-181a.

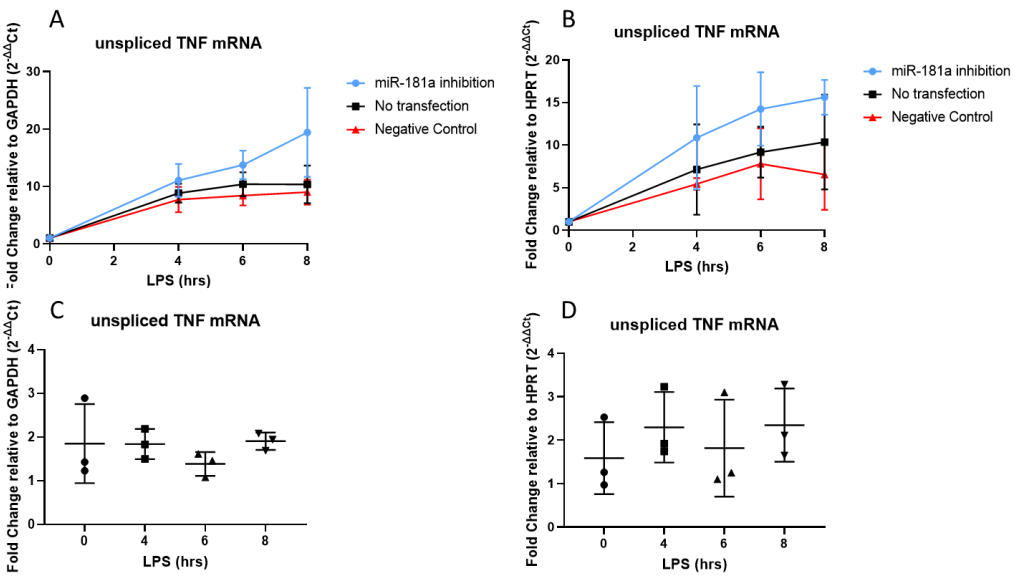

Figure 29. Effect of inhibiting miR-181a on TNF pre-mRNA over 8 hours of inflammation. A) Pre-TNF mRNA levels with miR-181a inhibition over and eight-hour LPS (1ug/ml) time course in RAW 264.7. miR-181a inhibitor (10nmol) or negative control oligo (10nmol) were transfected over 24 hours. Data measured by RT-qPCR and analysed by $2^{-\Delta\Delta Ct}$ normalised to GAPDH and plotted relative to the zero hour time point. N=3. Error bars indicate SD. **B)** Same as A but data is normalised to HPRT. N=3. Error bars indicate SD **C)** Same as A but data is plotted relative to the negative control at each time point. N=3. Error bars indicate SD **D)** Same as B but data is plotted relative to the negative control at each time point. N=3. Error bars indicate SD.

MiR-181a overexpression also resulted in a slight decrease at the pre-mRNA level for TNF, but this difference is much less clear than what is seen with miR-181a inhibition. Furthermore, the LPS time course in control conditions with miR-181a overexpression differs from the control conditions seen with miR-181a inhibition. This may be due to the large variation in the data. When looking at the effect of miR-181a overexpression levels on TNF pre-mRNA levels over time we see a slight decrease when the data is normalised to both GAPDH and HPRT (Figures 30A and 29B). Moreover, this slight decrease in TNF pre-mRNA is also seen when looking at the impact of miR-181a overexpression at each individual time point. However, the data is highly variable, especially at the zero hour time point (Figures 30C and 30D). Although these differences are not significant, there is a clear trend.

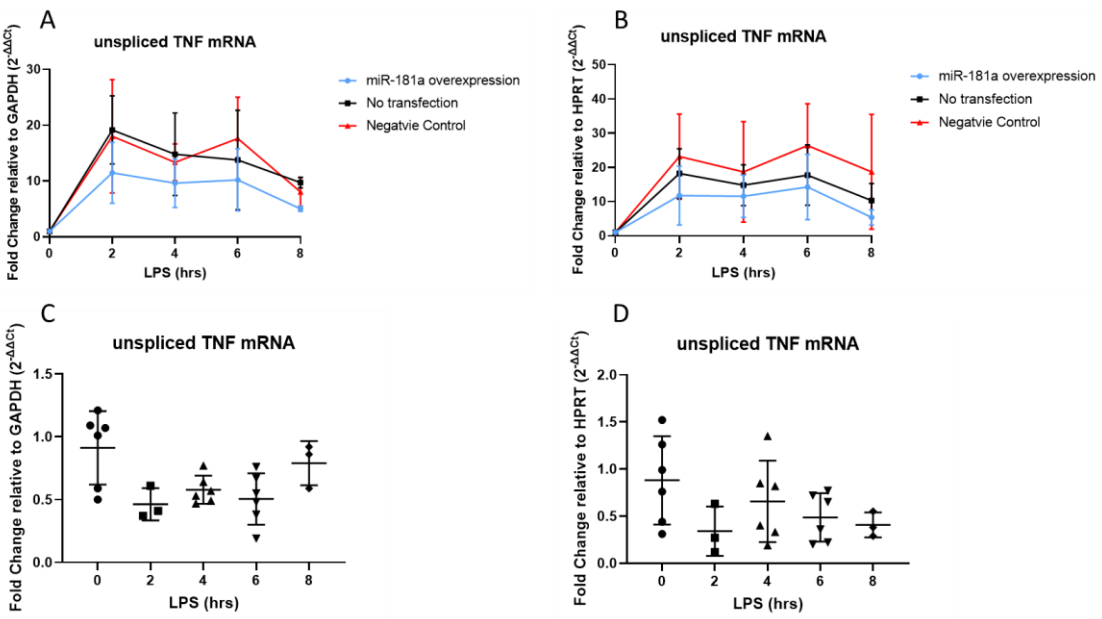

Figure 30. Effect of overexpressing miR-181a on TNF pre-mRNA over 8 hours of inflammation. A) Pre-TNF mRNA levels with miR-181a overexpression over and eight-hour LPS (1ug/ml) time course in RAW 264.7. miR-181a mimic (10nmol) or negative control oligo (10nmol) were transfected over 24 hours. Data measured by RT-qPCR and analysed by $2^{-\Delta\Delta Ct}$ normalised to GAPDH and plotted relative to the zero hour time point. N=6 (0, 4, 6 hrs) N=3 (2, 8 hrs). Error indicates SD. **B)** Same as A but data is normalised to HPRT. N=6 (0, 4, 6 hrs) N=3 (2, 8 hrs). Error indicates SD **C)** Same as A but data is plotted relative to the negative control at each time point. N=6 (0, 4, 6 hrs) N=3 (2, 8 hrs). Error indicates SD **D)** Same as B but data is plotted relative to the negative control at each time point. N=6 (0, 4, 6 hrs) N=3 (2, 8 hrs). Error indicates SD.

3.10 Discussion

Changes in TNF mRNA and protein levels when subjected to miR-181a inhibition or overexpression suggest that miR-181a is directly regulating TNF transcripts during the inflammatory response in RAW 264.7 cells. Furthermore, reporter assays that are shown later in the thesis have confirmed that miR-181a directly targets the TNF 3'UTR (Figure 43).

When looking at the effect of miR-181a inhibition at the mRNA level, there is a difference between the Sigma LPS (Figure 22A) time course and the Enzo LPS (Figure 24A) time course. The TNF induction appears to be larger when cells are treated with the Sigma LPS; however, the trends are similar between two different LPS over slightly different time courses. The reduced induction of TNF mRNA with the Enzo LPS could be due to having a greater specificity, designed to only activate the TLR4 pathway of inflammatory induction as opposed to the Sigma LPS which will induce additional pathways alongside the TLR4 pathway, resulting in greater induction of TNF. However, only one repeat was performed and no direct comparison between the two LPS were performed, so no clear conclusions can be drawn. It was decided that experiments would proceed with the TLR4-specific LPS as this allows us to look specifically at the TLR4 pathway and reduces any confounding effects that could occur from triggering additional inflammatory pathways.

MiR-181a is a modulator of macrophage polarisation (Bi *et al.,* 2016, Jiang *et al.,* 2021). Overexpression of miR-181a promotes the transition of macrophages to an M2 (alternatively activated) state, which is associated with an anti-inflammatory phenotype; conversely, inhibition of miR-181a promotes an M1 macrophage state. (Bi *et al.,* 2016). This supports our findings as overexpression of miR-181a is reducing TNF expression, consistent with the macrophages being polarised to an anti-inflammatory M2 phenotype, although the mechanism by which miR-181a promotes M2 polarisation is unknown. Furthermore, the increase in TNF expression seen when miR-181a is inhibited is in line with M1 polarisation of the macrophages.

While regulation of TNF by miR-181a has previously been investigated, it has not been established within this model of inflammation. Corsetti *et al.,* (2018) investigated miR-181a regulation of TNF within bone-marrow derived macrophages (BMDM) infected with *Brucella abortus.* In contrast to this study, miR-181a inhibition and overexpression experiments performed by Corsetti et al., (2018) show a larger

effect on TNF mRNA levels than within this study. However, they did not look at TNF protein levels or perform any direct reporter assays. While both models use macrophages, direct comparisons between different macrophage cell lines cannot always be drawn due to differing characteristics (Barbour *et al.,* 1998). Furthermore, while both systems look at inflammatory responses stimulated by bacteria, *B.abortus* infected cells trigger many more inflammatory pathways compared to cells stimulated with just LPS. Additionally, Corsetti *et al.,* (2018) looked at a single time point for both miR-181a inhibition and overexpression as opposed to over a series of time points. As such, our investigation differs substantially from what has previously been discovered by Corsetti *et al.,* (2018).

Direct regulation of TNF by miR-181a has been confirmed via reporter assay by Zhu *et al.,* (2017) however, they were looking at dendritic cells that had been induced by damage-associated molecular patterns (DAMPs) such as high mobility group box-1 protein (HMGB-1). While Zhu *et al.,* (2017) have shown that miR-181a is directly regulating TNF; their model was more focused on dendritic cell maturation as opposed to inflammation. As such, our model of inflammation is very different to Zhu *et al.,* (2017).Our results show that regulation of TNF by miR-181a does occur within our system and also displays how this regulation changes over the inflammatory response.

The changes seen at the TNF protein level with miR-181a inhibition and overexpression are much larger than the changes seen at the mRNA level. This suggests that miR-181a is aiding in prevention of translation initiation instead of facilitating destabilisation and degradation of TNF mRNA transcripts. There are many potential mechanisms of miRNA-mediated inhibition of translation initiation, but the exact mechanism remains unknown. Studies looking into translational repression by miRNAs have highlighted the eIF4F complex as having a critical role (Meijer *et al.,* 2013, Fukaya *et al.,* 2014, Fukao *et al.,* 2014) alongside the CCR4-NOT complex (Kuzuoğlu-Öztürk., *et al.,* 2016, Wilczynska *et al.,* 2019).

The significant trends seen at the TNF mRNA and protein levels over the course of inflammation, alongside the opposing effects seen with miR-181a inhibition and overexpression, strongly indicate that miR-181a negatively regulates TNF within RAW 264.7 cells.

However, miR-181a may affect inflammatory factors upstream of TNF that are causing a knock-on effect, producing the changes seen in TNF mRNA levels. For example, miR-181a may be regulating TLR4 expression. When any effects of miR-181a inhibition or overexpression on TLR4 mRNA were investigated, very little change in TLR4 mRNA was seen. Downregulation of the TLR4 pathway would cause downstream regulation of factors such as TNF, potentially resulting in the increase in TNF pre-mRNA seen with miR-181a inhibition or the decrease seen with miR-181a overexpression. The small change seen at the TLR4 mRNA level may be due to miR-181a having a greater regulatory effect at the translational level. If this were the case, then the changes we see for TNF pre-mRNA expression with miR-181a inhibition may be due to changes in TLR4 protein expression as opposed to any direct regulation of miR-181a at the pre-mRNA level.

Jiang *et al.,* 2018 performed a direct reporter assay within HEK293 cells that indicates that miR-181a is directly binding to the 3'UTR of TLR4. Furthermore, Jiang *et al.,* 2018 found that overexpression of miR-181a resulted in a decrease in TLR4 protein levels in RAW 264.7 cells treated with LPS, which we have not investigated. This confirms that the changes we are seeing at the TNF pre-mRNA level are a result of miR-181a regulation of TLR4. However, as there is such a strong effect of miR-181a inhibition and overexpression on TNF protein levels, the changes seen for TNF are not solely due to any effect of miR-181a on TLR4. Although, miR-181a may be regulating both TLR4 and TNF simultaneously to control the inflammatory response.

Inhibition experiments for miR-26b do not provide evidence that miR-26b is regulating PTGS2. There is no significant difference between the miR-26b inhibitor treatment and the negative control. Furthermore, when looking at whether miR-26b inhibition influenced PTGS2 protein level, there is also no observable difference (Figure 21). However, as there is also no change to PTGS2 at the protein level with miR-26b inhibition, other mechanisms may be occurring. PTGS2 has two binding sites for miR-26b as well as having two splice variants, one containing two miR-26b target sites and the other containing one miR-26b binding site. Additionally, the 3'UTR of PTGS2 contains numerous alternative polyadenylation sites (Hall-Pogar *et al.,* 2005) which may be affecting miRNA regulation. Due to the complex nature of PTGS2 mRNA transcripts, and the lack of change seen with miR-26b inhibition, it was

decided not to pursue this miRNA-mRNA pairing any further. With the numerous possible polyadenylation sites for PTGS2, investigating how this affects miRNA regulation would be challenging.

Finally, miR-181a and miR-26b expression do not appear to change significantly over the course of the inflammatory response. Jiang *et al.,* (2018) have previously shown that miR-181a decreases in expression in response to LPS stimulation before rising again. This fits with a reduction in miR-181a being associated with an inflammatory M1 phenotype (Bi *et al.,* 2016). However, the timeframe in which Jiang *et al.,* (2018) investigated miR-181a expression was over a 36 hours time course, focusing on later in the response when inflammation has ended. In contrast, this study focused on the initial induction of inflammation. Although, Jiang *et al.,* (2018) saw very little change in miR-181a expression between their zero and six-hour time points which correspond with findings within this study. Additionally, Jiang *et al.,* (2018) utilised 2µg/ml of LPS as opposed to 1µg/ml LPS, resulting in their initial inflammatory response being much stronger than in this model which would also influence their time course. As such, miR-181a may be changing in expression over a longer time scale but, miR-181a expression appears not to change during the first six-eight hours of inflammation.

In terms of studying the effects of poly(A) tail length on miRNA regulation, the lack of change in expression of miR-181a means there is one less variable to be concerned about.

Within this system, miR-181a is regulating TNF at both the mRNA and the protein levels. However, inhibition and overexpression experiments show that there is a much larger effect of miR-181a regulation at the TNF protein level. This suggests that instead of facilitating destabilisation and degradation of TNF mRNA transcripts, miR-181a is playing a larger role in translational repression fo TNF mRAN. Furthermore, miR-181a appears to have the greatest regulatory effect later in the inflammatory response. Moving forward, miR-181a and TNF are confirmed as regulatory pairing which we can use to study how changing poly(A) tail length affects miRNA regulation.

Chapter 4

Investigation of TNF mRNA poly(A) tail changes and miRNA binding over the course of inflammatory induction

4.1 Introduction

Poly(A) tails act to stabilise mRNA transcripts as well as facilitate their translation into protein (Fuke & Ohno., 2008, Kahvejian *et al.,* 2005, Subtelny *et al.,* 2014, Chorghade *et al.,* 2017). The poly(A) tail is added onto the 3'end of mRNA transcripts within the nucleus where it is bound by multiple copies of nuclear poly(A) binding proteins (PABPN). Once the mRNA has been exported to the cytoplasm, PABPN is replaced by the PABPC family of proteins, which occupies spans of 30 nucleotides (Reviewed by Wigington *et al.,* 2014). All PABPs serve to stablise mRNA transcripts, and PABPC has been implicated in translational efficiency via facilitating circularisation of the mRNA with eIF4G (Deo *et al.,* 1999, Marcotrigiano *et al.,* 2001). Furthermore, PABPC is required for TNRC6 binding, a component of the RISC complex (Braun *et al.,* 2013). As such, poly(A) tail length can act as a key regulator of gene expression (Lim *et al.,* 2016, Park *et al.,* 2016, Slobodin *et al.,* 2020).

MicroRNAs mediate deadenylation and decay of target mRNAs via the recruitment of the PAN2-PAN3 and CCR4-NOT deadenylase complexes (Wahle & Winkler, 2013). Deadenylated mRNAs are then decapped by DCP2 (Behm-Ansmant *et al.,* 2006) before the mRNA is degraded by XRN1 (Braun *et al.,* 2012)

Previous research has also found that miRNAs are able to alter the composition of the mRNP, particularly by reducing the association of PABP and eIF4G, disrupting the closed loop model of translation initiation, reducing translational efficiency (Moretti *et al.,* 2012, Rissland *et al.,* 2017). Furthermore, it has also been shown that longer poly(A) tails are more effective at recruiting miRISC due to the likelihood of their being increased PABP occupancy on longer poly(A) tails (Moretti *et al.,* 2012). However, it has also been discovered that while miRNAs are affecting mRNP composition they may not be impacting on steady-state poly(A) tail lengths (Rissland *et al.,* 2017). Instead, miRNAs may be preferentially deadenylating mRNA transcripts

with short poly(A) tails, while preventing translation initiation on longer mRNA transcripts (Eisen *et al.,* 2020). While longer poly(A) tail lengths increase the magnitude of miRNA mediated translational repression, the poly(A) tail and deadenylation are not a pre-requisite for miRNA mediated translational repression to occur (Meijer *et al.,* 2013).

Induction with LPS has been found to trigger cytoplasmic polyadenylation of TNF mRNA transcripts (Crawford *et al.,* 1997). Furthermore, Gandhi (2016) found that the poly(A) tail of TNF mRNA changes in length over the course of the inflammatory response.

LPS induced changes in the poly(A) tail length of TNF is a useful system to investigate how changing poly(A) tail length affects miRNA regulation in an endogenous context.

Furthermore, as LPS also leads to transcriptional induction of TNF, it enables the investigation of how miR-181a regulation changes over the inflammatory response in response to either transcriptional induction or changes in poly(A) tail length.

4.1.1 Poly(A) tail test

In order to determine whether the inflammatory response and miRNA regulation affect the poly(A) tail length of TNF, it was first necessary to develop a robust assay. The poly (A) tail test (PAT) is a PCR based assay that is used for mRNA specific poly(A) tail analysis. The PAT test involves ligating an anchor sequence onto the 3' end of the mRNA. cDNA is then generated from the mRNA and used as a template for PCR. The PCR utilises a gene specific primer for the gene of interest combined with a primer that binds to the anchor sequence to amplify the poly(A) tails (Figure 31). These products are then run on an agarose gel to visualise the poly(A) tails (Section 2.1.6).

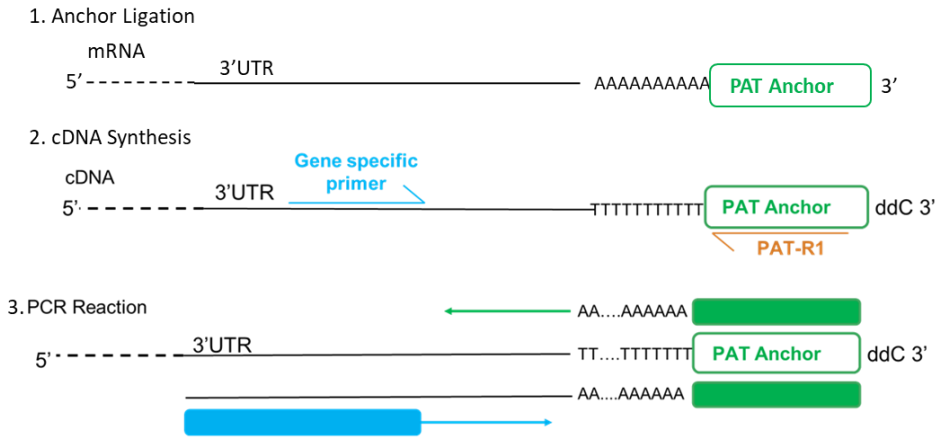

Figure 31. The poly(A) tail test. Schematic of the poly(A) tail test showing the cDNA template with the ligated PAT anchor and primer binding sites for the PCR reaction. The gene specific primer is located within the 3'UTR of the gene.

4.2 TNF poly(A) tail length changes during the initial inflammatory response

To establish whether TNF poly (A) tail length changed over the course of the inflammatory response, as previously observed by Gandhi (2016), total RNA was extracted from RAW 256.7 cells over a time course of LPS treatment and PAT was carried out on TNF mRNA. An initial PAT test over a 120 minute LPS time course was performed to assess whether TNF poly(A) tails were changing as expected within the selected model of inflammation (Figure 32, Supplementary Figures 5 and 6). The poly(A) tail of RPL28 was also measured as a control as Gandhi (2016) found that the poly(A) tail of RPL28 does not change over the course of inflammation.

Figure 32 shows that the poly(A) tail length of TNF changes in response to LPS stimulation over a two hour time course. At the zero hour time point, there is not enough TNF mRNA to observe the poly(A) tails by PAT assay, only the excess primer band is visible. However, the PCR product specific to TNF mRNA with a poly(A) tail is just detectable at 15 mins post LPS stimulation. The PCR product is approximately 300nt, resulting in an approximate modal poly(A) tail length of 85nt once the 215nt of 3'UTR amplified is deducted. The poly(A) tail of TNF then appears to increase to an approximate modal tail length of 135nt excluding the 3'UTR at 30 mins post LPS treatment. At 30 minutes, a multimer band is also present, denoted by an asterisk. The multimer bands are formed by loops of As and Ts annealing together during the PCR step.

At 60 minutes post LPS stimulation the poly(A) tail length appears to undergo deadenylation, leaving the almost completely deadenylated product at a modal poly(A) tail length of 0nt. The poly(A) tail length then appears to have a more diffuse distribution, but still with a modal poly(A) tail length of 0nt at 120 minutes post LPS treatment. In contrast, the PCR product for RPL28 remains constant at approximately 300nt, leaving a modal poly(A) tail length of approximately 41nt after the 259nt of 3'UTR is deducted. As such RPL28 was used as a control for subsequent PAT assays.

The exact length of the TNF poly(A) tail is hard to define due to the formation of multimer bands, denoted by an asterisk. While the poly(A) tails are clearly visible, the multimer bands may potentially obscure any longer poly(A) tails.

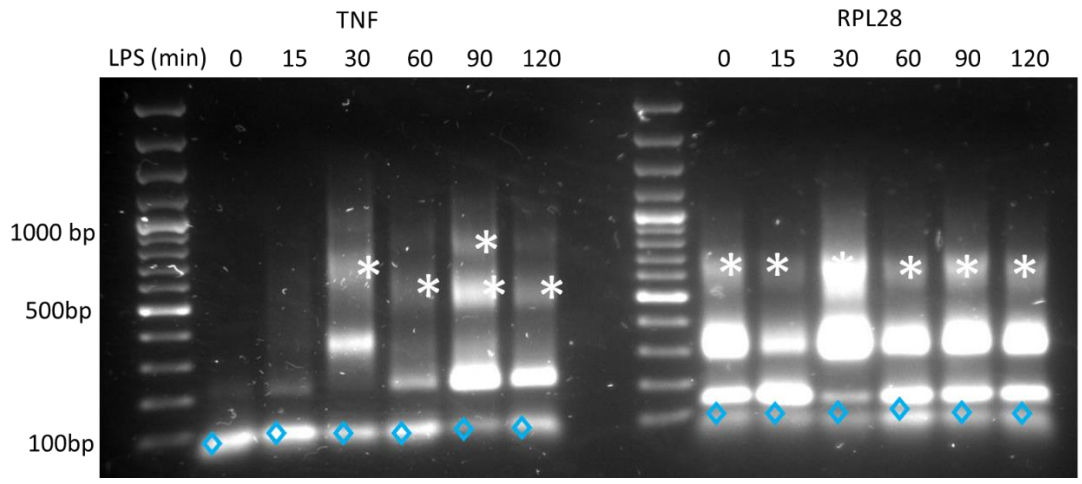

Figure 32. Poly(A) tail lengths of TNF and RPL28 over a 120 minute LPS (1µg/ml) time course. Agarose gel electrophoresis following PAT assay on total RNA from RAW 264.7 cells treated with LPS. Primers used were specific to TNF or RPL28. * denotes probable multimer bands. N=3.◇ Denotes excess primer bands.

4.3 Inhibition of miR-181a has no effect on TNF poly(A) tail length during the inflammatory response

After establishing that the poly (A) tail of TNF changes over the initial inflammatory response in RAW 264.7 cells, it was then determined whether miR-181a regulation affects TNF poly(A) tail over the course of the inflammatory response. To investigate this, miR-181a was inhibited in RAW 264.7 cells by transfection of a Qiagen LNA inhibitor, cells were treated with LPS 24 hours later and the PAT assay was used to determine if the TNF poly(A) tail lengths differed with miR-181a inhibition versus a control at different time points.

Initially, inhibition experiments were performed over a two-hour LPS time course as this is where the changes in TNF poly(A) tail were shown to occur (Figure 33A, Supplementary Figures 7 and 8).

Cells transfected with a non-target antisense negative control oligo display similar changes to poly(A) tail length of TNF mRNA as seen in Figure 33. The poly(A) tail lengths for TNF mRNA are initially longer at 30 minutes with an approximate length of 135nt (Figure 33A). The poly(A) tail lengths for TNF mRNA then begin to shorten at 60 minutes to approximately just the deadenylated product at around 0nt before becoming the poly(A) tail lengths develop a more diffuse poly(A) tail length distribution at 120 minutes after LPS treatment with the deadenylated product band the most prominent.

Poly(A) tail lengths of TNF within cells that had been transfected with miR-181a inhibitor show almost the exact same changes over the course of LPS treatment as cells transfected with the negative control oligo (Figure 33A). The PCR product for TNF mRNA with miR-181a inhibition at 30 minutes into inflammation are harder to observe on the gel than the PCR products with negative control transfection, but the tail length is similar at approximately 85nt. Furthermore, the TNF poly(A) tail length with miR-181a inhibition then shortens at 60 minutes to just the deadenylated product before again becoming more diffuse at 120 minutes into inflammation consistent with the poly(A) tail length observed with the negative control oligo. While there is no observable difference in poly(A) tail length of TNF mRNA with miR-181a inhibition or negative control treatment, RT-qPCRs run in parallel show that TNF mRNA levels increase with miR-181a inhibition at 60 and 120 minutes into inflammation (Figure 33B). This indicates miR-181a is impacting on TNF mRNA expression however, miR-181a regulation is not affecting the poly(A) tail length of TNF during the first 120 minutes of inflammation.

As there was no effect of miR-181a inhibition on TNF poly (A) tail length over 120 minute LPS treatment, PAT assays were then performed on 8-hour LPS time courses with miR-181a inhibition, as 6-8 hours is when there is the greatest effect of miR-181a regulation on TNF mRNA (Figure 23 (chapter 3), Figure 33D). The poly(A) tail length for TNF mRNA with negative control treatment, remains very consistent at four, six and eight hours following LPS treatment with a diffuse distribution of poly(A) tails spanning a range of 0-285nt with a modal tail length of 0nt (Figure 32C, Supplementary Figure 9). This is similar to what was observed at the 120 minute time point in Figure 33A, suggesting that the poly(A) tail length for TNF does not change after 120 minutes into the inflammatory response.

When looking at whether miR-181a inhibition had any effect on TNF poly(A) tail length at four, six and eight hours into inflammation, no difference was observed between the miR-181a inhibition and negative control (Figure 33C). The distribution of poly(A) tail lengths observed at four, six and eight hours is a diffuse distribution with an approximate range of 0-285nt and a modal poly(A) tail length of 0nt with miR-181a inhibition, the same as what was observed with the negative control oligo. This further indicates that miR-181a regulation is having no impact on the poly(A) tail length of TNF mRNA.

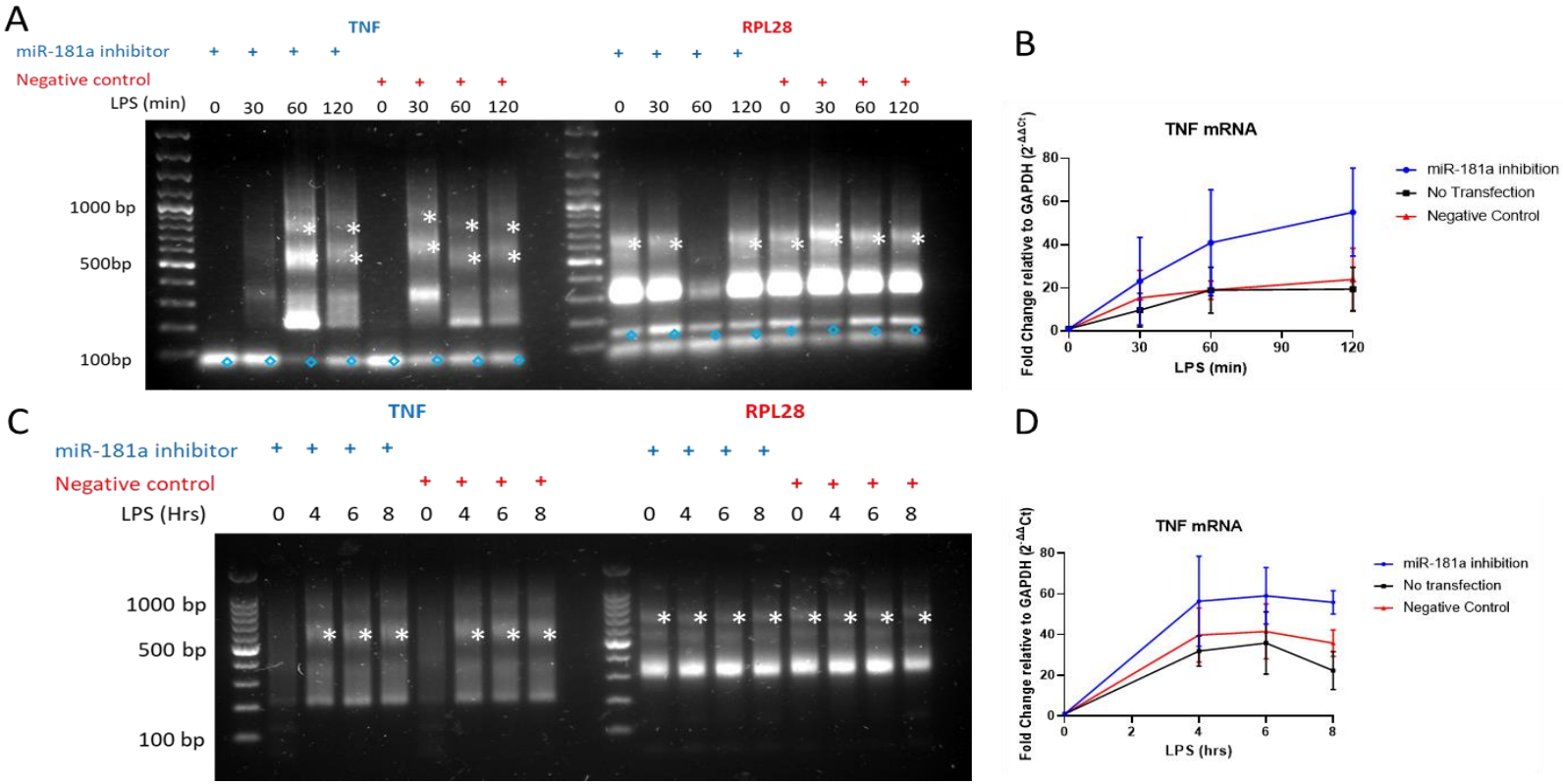

Figure 33. **TNF poly(A) tail length does not change with miR-181a inhibition. A)** Poly(A) tail lengths of TNF and RPL28 over a 120-minute LPS (1µg/ml) time course showing, miR-181a inhibitor or negative control (10nm final concentration) conditions. Poly(A) tail lengths were analysed by PAT assay and agarose gel electrophoresis. N=3. * denotes probable multimer bands. 💠 denotes excess primer bands **B)** TNF mRNA levels for the same samples as in A, analysed by RT-qPCR and normalised to 0 time point. N=3. Error represents SD. **C)** Same as A but over an 8-hour LPS time course. N=2 Error bars denote SD. **D)** Same as B but over an 8 hour LPS time course. N=3 Error bars denote SD.

4.4 Overexpression of miR-181a has no effect on TNF poly(A) tail length during the inflammatory response

As there was no impact of miR-181a inhibition on TNF poly(A) tail lengths despite the known role of miRNAs in mediating deadenylation of mRNA targets, it was decided to see if overexpression of miR-181a caused increased deadenylation of TNF mRNA resulting in shorter poly(A) tail lengths.

As with the miR-181a inhibition experiments, the effect of miR-181a overexpression on TNF poly(A) tail length was examined over the first 120 minutes following LPS treatment of RAW 264.7 cells when the TNF poly(A) tail undergoes changes (Figure 34A, Supplementary Figures 10 and 11).

Cells were transfected with either a Qiagen LNA miR-181a mimic or an antisense no targeting negative control oligo for 24 hours before treatment with LPS.

Cells transfected with the antisense negative control oligo display a similar pattern of TNF poly(A) tail length increase over the first 120 mins of inflammation as the negative control transfection in Figure 33B.

When looking at the poly(A) tail lengths for cells transfected with the miR-181a mimic there is no difference in the pattern of poly(A) tail length changes compared to the negative control transfection (Figure 34A). Similar to the negative control the approximate modal poly(A) tail length at 30 mins is 135nt, then decreasing to predominantly the deadenylated product at 60 before developing a more diffuse distribution at 120min. However, there is more PCR product at 30 and 60 minutes within the overexpression conditions, which could be due to greater ligation or amplification efficiency.

The effect of miR-181a overexpression on TNF mRNA levels at eight hours was then investigated, as this is when there is the greatest impact of miR-181a overexpression on TNF mRNA levels (Figure 34D). Cells transfected with an antisense negative control oligo (Figure 34C, Supplementary Figure 12) display a consistent poly(A) tail length for TNF as observed in Figure 33C. At four, six and eight hours into inflammation, the TNF poly(A) tail length has a consistent diffuse distribution of approximately 0-285nt with a modal poly(A) tail length of 0nt. Furthermore, when looking at whether miR-181a overexpression resulted in any changes in TNF poly(A) tail length, there is no difference between cells transfected with miR-181a mimic and

the negative control oligo with poly(A) tail lengths displaying a similar diffuse distribution with a modal poly(A) tail length of 0nt in overexpression conditions.

The lack of effect of miR-181a inhibition and overexpression on TNF poly(A) tail lengths despite changes in TNF mRNA levels suggest that miR-181a regulation is not leading to deadenylation of TNF mRNA transcripts. However, it could be that the PAT assay is not sensitive enough to detect and changes induced by miR-181a regulation. It could be that any deadenylation of TNF mRNA transcripts is followed by very rapid degradation so the deadenylated intermediate is not detectable by the PAT assay.

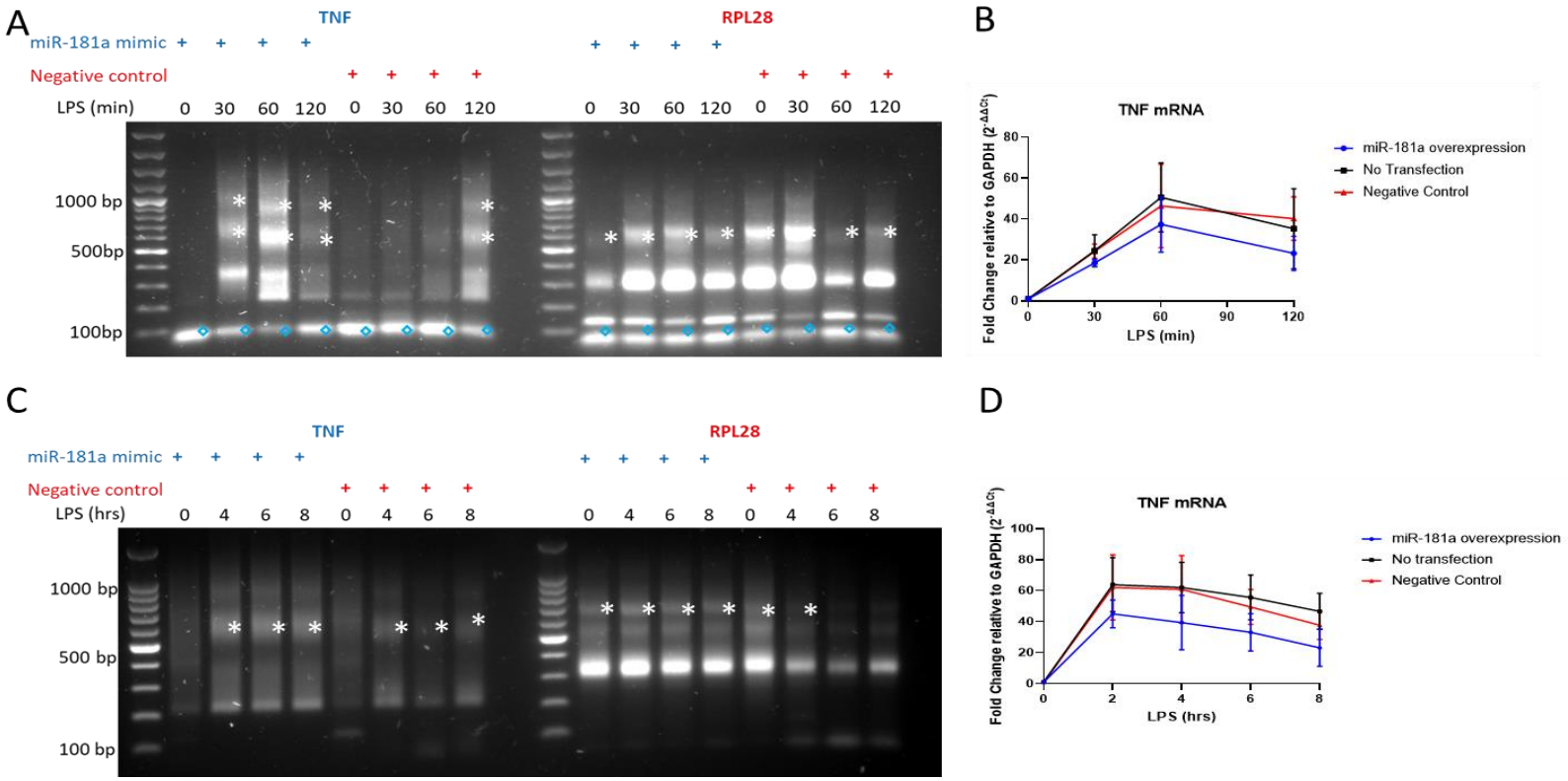

Figure 34. TNF poly(A) tail length changes with miR-181a overexpression. A) Poly(A) tail lengths of TNF and RPL28 over a 120-minute LPS (1µg/ml) time course showing no transfection control, miR-181a mimic (+) or negative control (-) (10nm final concentration) conditions. Poly(A) tail lengths were analysed by PAT assay and agarose gel electrophoresis. N=3. * denotes probable multimer bands. ◇ Denotes excess primer bands **B)** TNF mRNA levels for the same samples as in A, analysed by RT-qPCR and normalised to 0 time point. N=3. Error represents SD **C)** Same as A but over an 8-hour LPS time course. N=2. Error bars denote SD **D)** Same as B but over an 8-hour LPS time course. N=3 Error bars denote SD.

4.5 MiR-181a regulation of TNF increases over the course of inflammation

Previously, it had been established that miR-181a expression levels remain consistent over the course of the inflammatory response (Figure 20 (chapter 3)). As such, Ago2 Immunoprecipitation (IP) was used to establish whether miR-181a incorporation into RISC and binding to TNF mRNA changes over inflammation. Ago2 was selected as it is the most abundant Ago protein within RAW 264.7 cells (Mazumder *et al.,* 2013).

An antibody specific to Ago2 was used to immunoprecipitate RISC-bound RNA. The RNA was extracted, and RT-qPCR was used to separately investigate miRNA and mRNA association with the RISC at different time points following LPS treatment.

Ago2 IPs were performed over a one-hour LPS time course to see if there is any change in miR-181a association with Ago2 during the first hour of LPS treatment when the poly(A) tail changes for TNF are observed (Figure 35A).

Ago2 IPs were also performed over a six-hour LPS time course in order to look at changes in miR-181a association with Ago2 when the greatest changes in TNF mRNA levels with miR-181a inhibition and overexpression are observed (Figure 35B).

Across both time courses, miR-181a is significantly enriched within the Ago2 IP relative to input compared to the isotype control, indicating that the IP is specific (Figures 35A, 35B). Furthermore, miR-181a enrichment within Ago2 immunoprecipitants increases over the course of inflammation with the greatest enrichment seen at 6 hours post LPS stimulation ($p<0.01$ t-test). The increase in miR-181a is more pronounced between 0 and 60 minutes, with a twofold increase from 15-30 minutes and an overall three-fourfold increase in miR-181a enrichment between 0 and 60 minutes within Ago2 immunoprecipitants (Figure 35A). Comparatively, the miR-181a enrichment within Ago2 immunoprecipitants between two and six hours of LPS stimulation only increases slightly with a one-twofold increase in miR-181a enrichment (Figure 35B). This suggests that miR-181a may be having a larger regulatory effect as the inflammatory response progresses and that miR-181a association with RISC has the greatest increase within the first hour of inflammation.

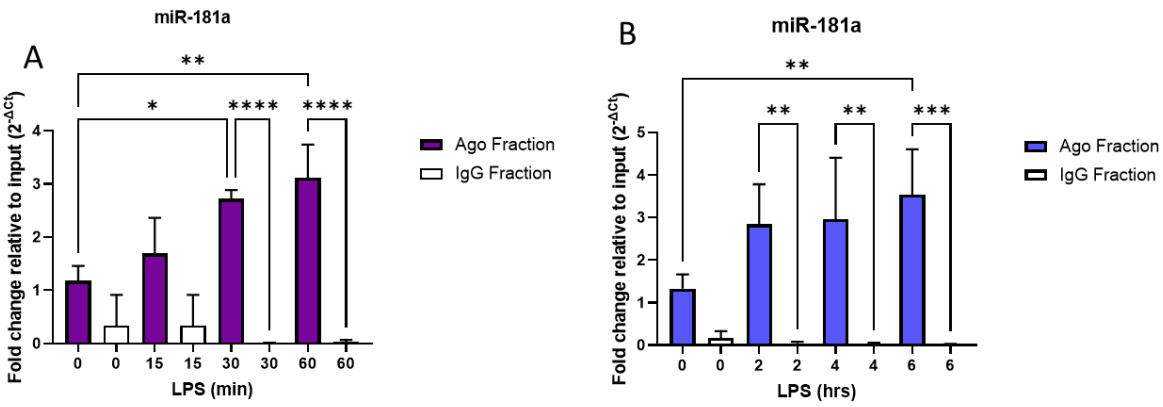

Figure 35. miR-181a association with Ago2 changes over the course of the inflammatory response. A) miR-181a isolated within Ago2 and IgG immunoprecipitants over a 60-minute LPS (1µg/ml) time course in RAW 264.7 cells. Data analysed by RT-qPCR. Data normalised relative to 20% input. N=3. Error Bars denote SD **B)** Same as A, but over a six-hour LPS time course. N=3. Error Bars denote SD.

When looking at TNF mRNA enrichment within Ago2 immunoprecipitants, there is also a significant enrichment of TNF mRNA within the Ago2 immunoprecipitants relative to input compared to the isotype control, also confirming the IP is specific (Figures 36A, 36B). This indicates that TNF mRNA is bound by miRNAs during inflammation, which may include other miRNAs as well as miR-181a. Similar to miR-181a there is an increase in TNF mRNA enrichment within the Ago2 immunoprecipitants over the course of inflammation. There is a steady increase in enrichment of TNF mRNA within the Ago2 immunoprecipitants over the first 60 min of inflammation with a fourfold increase (Figure 36A). Furthermore, there is also significant increase in TNF mRNA enrichment at six hours post LPS stimulation with a fourfold increase compared to the zero hour time point (Figure 36B) ($p<0.05$ t-test). TNF mRNA enrichment within the Ago2 immunoprecipitants indicates that TNF mRNA is being bound by miRNAs during the inflammatory response and that this binding is increasing as inflammation progresses over time. As such this suggests that TNF mRNA is undergoing greater miRNA regulation later in the inflammatory response.

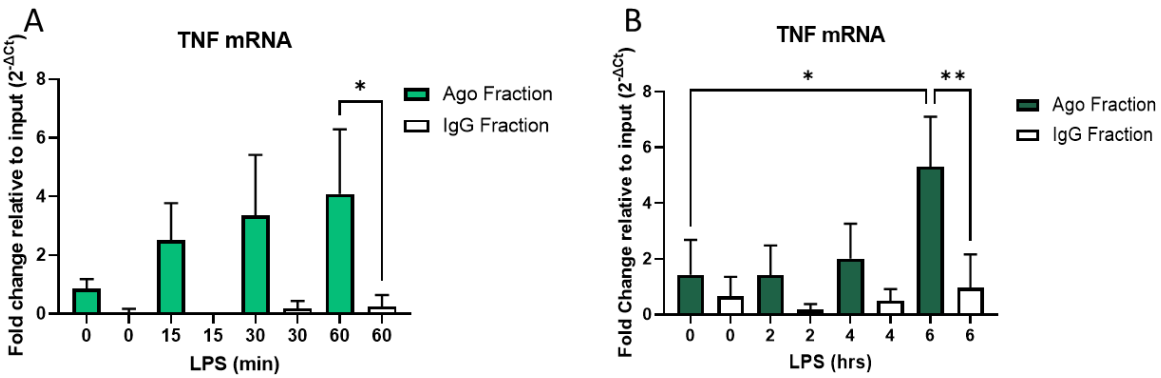

Figure 36. TNF mRNA association with Ago2 change over the course of the inflammatory response. A) TNF mRNA isolated within Ago2 and IgG immunoprecipitants over a 60-minute LPS (1µg/ml) time course in RAW 264.7 cells. Data analysed by RT-qPCR. Data normalised relative to 20% input. N=3. Error bars denote SD **B)** Same as A, but over a six-hour LPS time course. N=3. Error bars denote SD.

Ago2 association with TNF may be mediated by other miRNAs than miR-181a. To determine whether TNF mRNA is being recruited by miR-181a specifically Ago2 IPs were performed with and without miR-181a inhibition.

RAW 264.7 cells were transfected with either miR-181a inhibitor or a negative control oligo 24 hours before LPS stimulation for six hours. Lysates were extracted and the Ago2 IP was performed alongside an isotype control. RNA was extracted and RT-PCR was used to detect miR-181a or TNF mRNA within Ago2 immunoprecipitants.

miR-181a qPCR on Ago2 immunoprecipitants of cells transfected with the negative control oligo show a slight increase in miR-181a enrichment, with a 0.2 fold increase between zero and six hours relative to input (Figure 37A). In comparison, enrichment of miR-181a within the Ago2 immunoprecipitants of cells treated with miR-181a inhibitor still shows a slight increase from zero to six hours, but the overall fold changes are smaller. The fold change at zero hours relative to input with miR-181a inhibitor within the Ago2 isolate is 0.3, increasing to 1.2 at six hours. This suggests that miR-181a inhibition is reducing miR-181a association with Ago2. However, there are only two repeats of this experiment, so further investigation is needed before any firm conclusions can be drawn.

It was then examined whether miR-181a inhibition affected the enrichment of TNF mRNA within Ago2 immunoprecipitants. When looking at TNF mRNA enrichment within Ago2 immunoprecipitants for cells transfected with the negative control oligo, there appears to be a decrease in TNF mRNA enrichment from zero to six hours

(Figure 37B). There is a one-two fold decrease from zero hours to six hours relative to input. However, there is large variability in the data, particularly at the zero-hour time point. While, this variation is not due to low RNA quantity (Supplementary Figure 20), the confidence in the trends seen is low and more investigation is needed to be confident.

When comparing the enrichment of TNF mRNA within Ago2 immunoprecipitants of cells transfected with the miR-181a inhibitor as opposed to the negative control, there is an overall decrease in the amount of TNF mRNA detected within the Ago2 immunoprecipitants. There is a fivefold decrease in TNF mRNA within Ago2 immunoprecipitants between the negative control zero-hour time point and the miR-181a inhibition zero-hour time point. Additionally, there is a twofold decrease in TNF mRNA within Ago2 immunoprecipitants between the negative control and miR-181a inhibitor treatments at the six-hour time point This indicates that miR-181a mediates Ago2 interaction with TNF mRNA but does not exclude a possible role for other miRNAs. However, the enrichment of TNF mRNA within the Ago2 immunoprecipitants when miR-181a is inhibited is only slightly higher than that of the IgG immunoprecipitants suggesting that any contribution of other miRNAs may be minor. Due to experimental variability, this requires further investigation before any clear conclusions can be drawn.

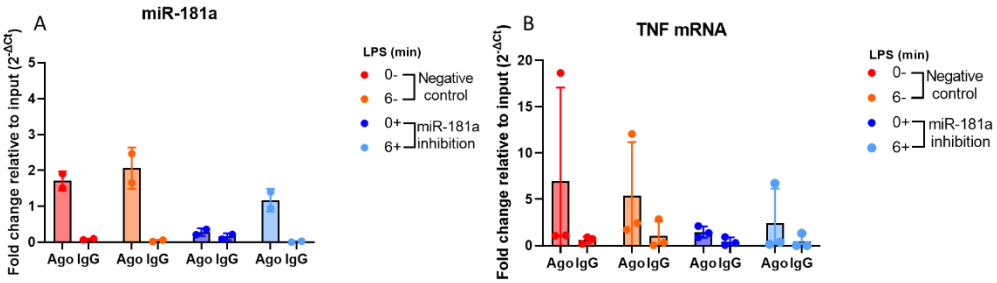

Figure 37. Ago2 Immunoprecipitation with miR-181a inhibition. A) miR-181a isolated within Ago2 and IgG immunoprecipitants with miR-181a inhibitor or Negative Control oligo (10nm final concentration) over a six-hour LPS (1µg/ml) time course. Data analysed via RT-qPCR. Data normalised relative to 20% input. N=2. Error bars indicate SD. **B)** Same as A, but displaying TNF mRNA levels. N=3. Error bars indicate SD.

4.6 Investigating poly(A) tail lengths of miRNA bound TNF mRNA by Nested PAT

It was investigated whether during inflammation the lengths of poly(A) tail for TNF mRNA associated with Ago2 were different to the general population of TNF

mRNA, that were not originally discernible by PAT assay. To do this, the Ago2 Ip approach was used to specifically isolate any RISC-bound TNF mRNA, and PAT assays performed on these samples in order to visualise the poly(A) tail lengths.

The standard PAT assays are not sensitive enough to accurately detect the poly(A) tails within the very small amounts of RNA isolated from an IP. Instead, the nested PAT technique was employed (Figure 38). Nested PAT utilises an additional amplification step enabling the detection of poly(A) tails in very small amounts of input RNA. Due to using two sets of gene specific primers, the nested PAT also allows for greater specificity.

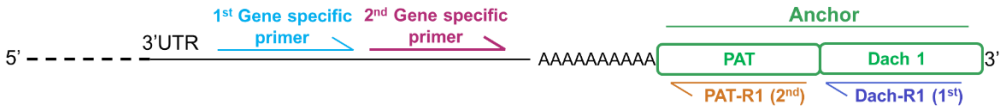

Figure 38. Schematic of Nested PAT primer locations. Gene specific primer 1 and Dach-R1 used in the first round of PCR. Gene specific primer 2 and PAT-R1 used in second round of PCR.

4.7 Poly (A) tail lengths of TNF mRNA bound by miRNAs is indistinguishable from the general pool of TNF mRNA

Nested PAT on the Ago2 IP input from the 60 min LPS time point for RPL28 shows the same pattern of poly(A) tail length as previous experiments (Figure 32) with an approximate modal poly(A) tail length of 41nt. When looking at the poly(A) tail lengths for RPL28 within the Ago2 immunoprecipitants, only the excess primer bands were visible indicating there are very low RPL28 mRNA levels within the sample. This indicates that the IP was specific and does not pull-down significant amounts of RPL28 mRNA (Figure 39A).

Moreover, nested PAT on the input samples from the 60 min Ago2 IP for TNF show only the excess primer band and a band denoting the 215nt section of TNF 3'UTR that the primers amplify. This is also the case when looking at poly(A) tail lengths for TNF mRNA within the Ago2 immunoprecipitants (Figure 39A).

The amount of mRNA is very small within both the input and Ago isolates, as such, highly abundant mRNAs such as RPL28 are detectable, but less abundant mRNAs are harder to detect with the nested PAT. As only the deadenylated form of TNF mRNA is observable within both the input and Ago2 isolates, it is hard to elucidate whether there is a clear difference in poly(A) tail length for TNF between the Ago2 samples and the input samples.

When looking at the nested PAT performed on the six hour Ago IP (Figure 39B) there is a consistent band for RPL28 within both the input samples and the Ago2 immunoprecipitants suggesting that this The presence of RPL28 within the Ago2 Ip for these samples could indicate that the pulldown was not as specific as the Ago2 IP performed over 60 minutes or that Ago2 does interact with RPL28 mRNA.

For TNF mRNA, within the input samples, the excess primer bands are observable as is the band denoting the TNF 3'UTR, the deadenylated TNF mRNA. Poly(A) tails are also observable within the input samples with just the deadenylated product visible with a modal length of 0nt similar to what was observed in Figures (33C Inhibition and 34C overexpression). Furthermore, TNF mRNA within the Ago2 isolates also only displays the deadenylated product with an approximate modal poly(A) tail length of 0nt. While there does not appear to be any difference in poly(A) tail length for TNF mRNA that is currently associated with miRNAs compared to the input sample, the Nested PAT technique is end-point PCR, so any TNF mRNA transcripts isolated within the Ago2 immunoprecipitants that are not associated with miRNAs are also amplified, so it is hard to draw any conclusions.

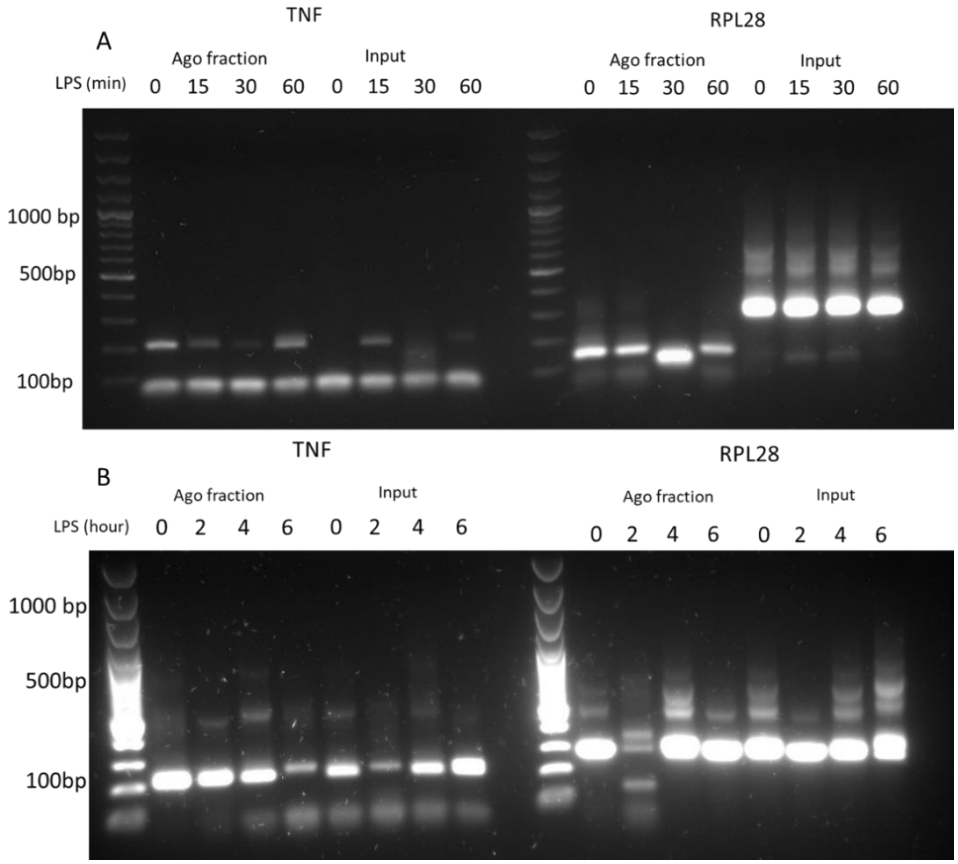

Figure 39. Poly(A) tail lengths of TNF pulled down within Ago2 Immunoprecipitation. A) Poly(A) tail lengths of TNF and RPL28 mRNA isolated within Ago2 and input samples over a 60-minute LPS (1µg/ml) time course. Data analysed by PAT assay and gel electrophoresis. N=1. **B)** Same as A, but over a six-hour LPS time course. N=1.

4.8 Discussion

4.8.1 miR-181a regulation of TNF appears to be translational

It has been previously shown that over the course of the inflammatory response TNF mRNA has short poly(A) tails that initially increase in length (Gandhi 2016). Moreover, it has also been shown that TNF mRNA undergoes cytoplasmic polyadenylation to rapidly increase poly(A) tail length (Crawford *et al.,* 1997), this increase in poly(A) tail length has been proposed to increase translational efficiency due to increased likelihood of PABPC association (Ivanov *et al.,* 2016). PAT assays (Figure 312 performed over LPS time courses confirm that TNF is undergoing a rapid increase in poly(A) tail length when the inflammatory response is triggered.

Crawford (1997) saw an increase in whole TNF mRNA transcript length by approximately 200nt after 30 min of LPS stimulation within RAW 264.7 cells when using northern blots to look at TNF mRNA transcripts. While they do not comment on length changes otherwise, their Northern Blots show that TNF mRNA transcripts decrease slightly in length after 30 min treatment of LPS in Actinomycin D conditions, when further transcription of new TNF mRNA transcripts was blocked. The approximate 200nt increase at 30 min is consistent with the PAT assays (Figure 32) over a 120 min LPS time course.

The changes observed in poly(A) tail length are similar to what was observed by Gandhi (2016). The poly(A) tail lengths for TNF were first visible at 15 minutes post LPS stimulation in Gandhi's study. Gandhi (2016) then observed an increase in length of the TNF poly(A) tail at 30 minute post LPS stimulation. The poly(A) tail length for TNF also did not change in length between 70 and 120 minutes in Gandhi's study. The poly(A) tail lengths observed by Ghandi (2016) is consistent with PAT assays over a 120-minute LPS time course in Figure 32.

There are a number of different factors that could explain why TNF poly(A) tail length is longer at 30 min before shortening slightly until 120 min where the poly(A) tail length then remains consistent. Other regulatory elements within the 3'UTR of TNF could be influencing the poly(A) tail length such as the AREs and any trans-acting factors that are binding (Dean *et al.,* 2001)(Figure 6).

Tris-tetraprolin (TTP) a trans-acting factor, is known to destabilise TNF mRNA transcripts by recruiting the CCR4-NOT complex to the mRNA transcript mediating

their deadenylation and decay (Fabian *et al.,* 2013). TTP mRNA has also recently been found to undergo readenylation with LPS stimulation, increasing its translation as inflammation progresses (Kwak *et al.,* 2022) (Figure 6a). As such TTP may be contributing to the decrease in TNF mRNA poly(A) tail length seen between 30 and 120 min, but this does not explain the whole picture as there is no further detectable increase in deadenylation between two and eight hours into inflammation. In the future, it could be interesting to look at the effects of knocking down TTP on the poly(A) tail length and expression of TNF mRNA during inflammation. Additionally, investigating how miR-181a and TTP regulation of TNF mRNA interacts via siRNA knockdown of TTP combined with miR-181a inhibition and overexpression experiments would also be interesting.

As there is no change in poly(A) tail length with miR-181a inhibition or overexpression, it does not look like miR-181a is triggering deadenylation of the TNF transcripts. However, previous research by Rissland *et al.,* (2017) found that posttranscriptional regulators such as miRNAs may alter the association of PABP and other eIF4G without necessarily affecting poly(A) tail length. Disruption of PABP and eIF4G binding with the mRNA prevents the formation of the closed-loop, reducing translational efficiency. Therefore, the lack of impact on poly(A) tail length with miR-181a inhibition or overexpression may not be unexpected. To investigate whether PABP binding of TNF mRNA transcripts is being disrupted by miR-181a, and whether this disruption changes over the course of inflammation, RNA immunoprecipitations (RIPs) for PABP looking at TNF mRNA association with and without miR-181a inhibition or overexpression could be performed. If miR-181a is disrupting PABP binding to facilitate translational repression of TNF mRNA, when miR-181a is inhibited, it would be expected to see an increase in TNF mRNA enrichment within the PABP isolates compared to negative control treatments. Conversely, with miR-181a overexpression, there would be a reduction in TNF mRNA enrichment within PABP isolates compared to negative control treatments. Similar experiments could also be performed to look at eIF4G disruption.

Furthermore, Eisen *et al.,* (2020) discovered that miRNA preferentially direct the deadenylating of shorter poly(A) tails. Using metabolic labelling with 5-ethynyl uridine (5EU) a uridine analog, and isolating cytoplasmic RNA that contained 5EU, Eisen *et al* (2020) found that when miR-1 was induced, miRNA mediated tail shortening of target mRNAs preferentially occurred on target mRNAs in the pre-

steady-state time period. When looking at TNF mRNA after LPS induction, the steady state poly(A) tail lengths are not reached until between 60 and 120 minutes. It may be that miRNA-mediated deadenylation is occurring at the zero hour time point before transcriptional induction of TNF in order to ensure TNF levels remain low. Upon transcriptional induction of TNF mRNA by LPS, poly(A) tail length of TNF rapidly increases and may trigger a switch in preference of miRNAs to mediate translational repression instead. On the other hand, the increase in poly(A) tail length at 30 minutes could also act increase the recruitment of miRISC via PABP to the TNF mRNA due to greater potential of increased PABP occupancy on the longer poly(A) tails (Moretti *et al.,* 2012), leading to increased deadenylation resulting in the shorter poly(A) tails observed at 60 minutes. Then as more TNF mRNA transcripts reach the shorter steady state poly(A) tail length at 120 minutes the wider distribution of poly(A) tail lengths could be due to the readenylation of newly synthesised TNF transcripts alongside continual deadenylation and translation.

However, the lack of change seen in the poly(A) tail length with miR-181a inhibition or overexpression could also be attributed to limitations of the PAT assay. Any small changes in TNF mRNA poly(A) tail length that are occurring due to miRNA mediated deadenylation may be unable to be detected. This could be due to a combination of an abundance of TNF mRNA transcripts at later time points with the end point PCR nature of the PAT assay means that any changes in TNF poly(A) tail length that are miRNA mediated may be masked by the majority of TNF transcripts that are not affected by miRNA mediated deadenylation.

Of note, a consistent issue with PAT gels is the formation of much larger products that look to track the changes of the lower bands or smears. These artefacts have been previously demonstrated to be due to the misalignment of poly(A):poly(T) stretches within the PCR product. During the repeated melting and annealing steps, loops of unpaired A or T nucleotides are formed which are free to pair with other unpaired loops of A or T bases within other fragments creating multimers (Figure 40). These multimers have a greater chance of forming with longer poly(A) tails and as such may slightly obscure any longer poly(A) tail lengths visualised on a gel. However, these multimer bands do track the general changes in poly(A) tail length, as such the approximate poly(A) tail lengths and how they are changing can still be determined.

An alternative to the PAT assay could be to use Oxford Nanopore sequencing to directly sequence the poly(A) tails of TNF at different time points during inflammation. As the rate at which nucleotides translocate through the pore is consistent (Krause *et al.,* 2019), the time spent within the pore could be used as a measure for how many adenosine residues are within a particular TNF mRNA transcript. This would allow the identification of any longer TNF mRNA transcripts that are being obscured by the multimer bands. Furthermore, it would facilitate the identification of any effect of miRNA mediated deadenylation at different time points during inflammation as it would be possib;e to look at individual transcripts giving you a more precise range of poly(A) tail lengths at each time point.

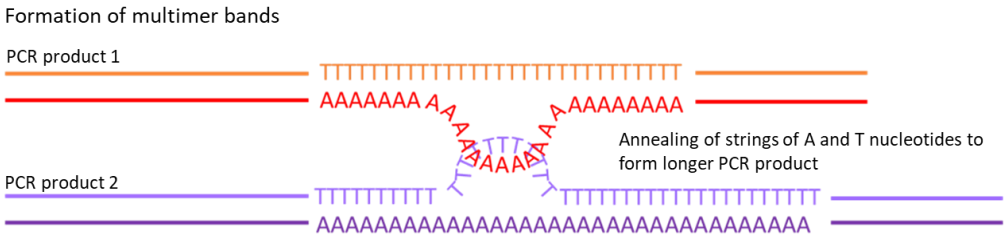

Figure 40. Schematic of the misalignment of stretches of poly(A) and poly(T) stretches within the PCR product generated by PAT PCR.

4.8.2 miR-181a regulation of TNF increases over the course of the inflammatory response

Ago2 IPs shows that microRNA regulation of TNF mRNA is increasing over the inflammatory response (Figures 35).

The increase in microRNA regulation of TNF over the first two hours of inflammation may be facilitated by the poly(A) tail length of TNF mRNA transcripts. Previous research has found that PABP aids in the recruitment of miRISC to target mRNA transcripts (Moretti *et al.,* 2012). Longer poly(A) tails generally have higher amounts of PABP bound to them, as such are likely to facilitate greater miRISC recruitment and thus the target mRNA transcripts are subjected to greater regulation by miRNAs (Moretti *et al.,* 2012). Therefore, the increased association of TNF mRNA transcripts within the Ago2 IPs over the first hour may be a result of increased miRISC recruitment due to the longer poly(A) tails after LPS stimulation.

However, the poly(A) tail lengths decrease at 60 minutes before reaching steady state levels, without a reduction in TNF mRNA enrichment within Ago2

immunoprecipitants at 60 minutes compared to 30 minutes when the longer tails are present. Furthermore, after two hours of LPS stimulation, the poly(A) tails of TNF reach a steady state length, TNF mRNA enrichment within Ago2 immunoprecipitants continues to increase up to eight hours post LPS treatment. Therefore, there may be other factors that are facilitating the increased enrichment of TNF mRNA within the Ago2 immunoprecipitants.

Additionally, miR-181a enrichment within Ago2 immunoprecipitants is also increasing as inflammation progresses (Figure 36). This increase in miR-181a association with Ago2 does not appear to be driven by an overall increase in miR-181a expression as it remains constant over the inflammatory response (Figure 20, Chapter 3). As such, it may be that there are other factors that are influencing the increased recruitment of miR-181a to Ago2 over the course of inflammation.

One factor could be that Ago2 expression levels are increasing over the course of inflammation allowing greater miRNA regulation to occur later in the response. However, qPCRs and Western Blots looking at Ago2 levels over an LPS time course would need to be performed to determine whether this is the case.

It has been found that miR-181a is sponged by the lncRNA MEG8 in macrophage polarisation to allow for an M1 inflammatory phenotype to be produced (Jiang *et al.,* 2021). Therefore, it is possible that miR-181a is being sponged in unstimulated cells and that miR-181a is slowly released from the sponge as inflammation progresses allowing greater miR-181a association with Ago2.

Another factor that could be influencing miR-181a association, is phosphorylation of Ago2. A study by Mazumder *et al.,* (2013) observed that within RAW 264.7 cells, Ago2 undergoes phosphorylation at Tyr-529 after LPS stimulation dislodging miRNA association with Ago2. Mazumder *et al.,* (2013) suggest that the increase in pro-inflammatory cytokine expression is a result of miRNA dissociation from Ago2 followed by a restoration of miRNA mediated repression to control hyperresponsiveness. However, the Ago2 Ips performed within this study do not show any reduction in miR-181a association within the Ago2 isolates after stimulation with LPS. Unless this initial loss for miR-181a is very rapid and occurs before 15-mins of LPS stimulation. If the phosphorylation and dephosphorylation of Ago2 is occurring very early on, the increase in miR-181a observed within the Ago2

immunoprecipitants could be the gradual reassociation of miR-181a with Ago2 as inflammation progresses.

A final factor which could be attributed to the increase in miR-181a association with Ago2 is arm switching. MiRNAs have been known to undergo arm switching, swapping the active strand between the 5p and the 3p forms (Giffiths-Jones *et al.,* 2011, Kim *et al.,* 2020). While it is not known whether miR-181a undergoes strand switching, it could be possible that the increase in miR-181a-5p within the Ago isolates could be a result of switching from the 3p strand. More of the miR-181a-3p strand may be associating with Ago2 early in the response, with miR-181a-5p being preferentially selected for as inflammation progresses. Arm switching could be checked for using primers for miR-181a-3p within the Ago2 IP samples to see if there is greater enrichment of the miR-181a-3p strand over the 5p strand early in inflammation.

It must be noted that there are four different Argonaute proteins, and while Ago2 may be the most well characterised (Liu *et al.,* 2004, Müller *et al.,* 2020) and most abundant within RAW 264.7 cells (Mazumder *et al.,* 2013), it cannot be ruled out that miR-181a association may behave differently for the other three Argonaute proteins. It could also be that miR-181a is preferentially associating with other Ago proteins at different points during the inflammatory response.

Furthermore, attempts to look at the poly(A) tail lengths of TNF mRNA that is associated with Ago2 immunoprecipitants compared to the general pool of TNF transcripts were unsuccessful due to limitations within the Ago2 IP and the PAT assay. As there is no cross-linking step within the Ago2 IP, the washes were performed using a high salt wash buffer in an attempt to remove non-specific binding, but contaminating mRNAs may still be present. As such, TNF transcripts that are not actively being regulated by miRNAs may also be present at low level within the immunoprecipitant. Cross-linking of Ago2 immunoprecipitants was initially trailed in the development of this technique, however due to difficulties with reversing the cross-linking introducing further experimental variability, this step was ultimately dropped. With the PAT assay being end point PCR, these low-level unbound TNF transcripts could also be amplified within the PCR, preventing the distinction between regulated and non-regulated TNF mRNA poly(A) tail lengths. However, the Ago2 IP is specific as there is very little non-specific binding within the

IgG isolates, but this does not mean that there are not any contaminating mRNAs present that are being amplified with the PAT assay.

Moretti *et al.,* (2012) found that within Ago1 Ips there was a greater enrichment of synthetic mRNAs with a poly(A) tail length of 62nt within their Ago isolates compared to synthetic mRNAs with a poly(A) tail length of 0. This could predict that TNF poly(A) tail lengths within the Ago isolates are likely to be longer that the general pool. Eisen *et al.,* (2020) suggest that miRNAs preferentially trigger the deadenylation of target mRNAs with shorter poly(A) tails so it could be at earlier time points poly(A) tails of TNF mRNA associated with Ago2 are shorter and then progressively get longer as translational repression becomes the preferred method of regulation.

In the future, different techniques could be employed to look at the poly(A) tail lengths of TNF mRNA that are associated with Ago2. One option would be to use nanopore sequencing to individually sequence the poly(A) tails of each TNF mRNA transcript over an LPS timepoint. This would allow much greater specificity in determining different pools of TNF mRNA transcripts and defining the exact lengths of TNF poly(A) tails.

To conclude, while the poly(A) tail lengths are changing over the course of inflammation, they do not appear to have an effect on miR-181a regulation of TNF. However, miRNA regulation of TNF mRNA transcripts is increasing during inflammation as there is a greater enrichment of TNF mRNA within Ago2 immunoprecipitants at later LPS time points. Furthermore, while miR-181a expression levels do not change during inflammation, miR-181a association with Ago2 increases during the inflammatory response although, the mechanism by which this is occurring is unknown.

Chapter 5

Investigation of the factors that influence miR-181a regulation of TNF during transcriptional induction in the inflammatory response.

5.1 Introduction

The inflammatory response has many different effects, including Ago2 phosphorylation (Mazumder *et al.,* 2013). As such, previous observations may be related to other effects occurring within inflammation as opposed to transcriptional induction or changes in poly(A) tail length. The 3'UTR of many cytokines, including TNF, aid in the regulation of the mRNA and are known interact with RNA binding proteins or regulatory RNAs (Mayr, 2019)

Through these interactions, the 3'UTR of mRNA transcripts can aid in localisation (Martin *et al.,* 2009), mRNA stability and translation of the mRNA transcript (Barreau *et al.,* 2006*,* Bartel, 2009, Chen *et al.,* 1995). Most protein interactions with the 3'UTR are mediated via regulatory elements located within the 3'UTR sequence (Mayr, 2017).

One regulatory element that many 3'UTRs contain are AU-Rich elements (AREs). AREs are often involved in regulating the stability of the mRNA. AREs are defined by a AUUUA motif and were first discovered within mRNA transcript encoding inflammatory cytokines (Caput *et al.,* 1986). This motif mediates the binding of various trans-acting factors that are involved in regulating the stability of the mRNA transcript (Barreau *et al.,* 2006). Certain trans-factors can act to destabilise the mRNA via the AREs (Barreau *et al.,* 2006). One important example is the binding of Tris-tetraprolin (TTP) to the AREs within TNF mRNA transcripts (Carballo *et al.,* 1998, Lai *et al.,* 1999). TTP binding to the AREs triggers the recruitment of the CCR4-NOT complex, mediating the deadenylation of the TNF mRNA transcript (Fabian *et al.,* 2013). On the other hand, AREs can also act to stabilise mRNA transcripts (Barreau *et al.,* 2006), and in the case of TNF, HuR is known to bind to the AREs to mediate TNF

mRNA stabilisation upon the activation of the inflammatory response within macrophages (Dean *et al.,* 2001, McMullen *et al.,* 2003).

TTP and HuR binding to the AREs of TNF mRNA act as a regulatory loop for TNF expression. HuR has a higher binding affinity than TTP for the AREs within the TNF 3'UTR (Min-Ju *et al.,* 2009). The activation of the inflammatory response triggers the translocation of HuR from the nucleus where it can then outcompete TTP binding of TNF mRNA transcripts, facilitating the production of TNF protein and the progression of the inflammatory response (Min-Ju *et al.,* 2009, Khalaj *et al.,* 2017). Furthermore, HuR has been implicated in interacting with miRNA regulation via facilitating the dissociation of specific miRNAs from their target mRNAs and then promoting the export of the miRNAs in exosomes (Kundu *et al.,* 2012, Poria *et al.,* 2016, Mukherjee *et al.,* 2016, Goswami *et al.,* 2020).

Furthermore, it has been shown that there are widespread changes in poly(A) tail length during inflammation (Kwak *et al.,* 2022), which could potentially be attributed to the action of non-canonical polymerases. TENT4A and TENT4B have been shown to have mixed tailing functions that protect mRNA transcripts from rapid deadenylation by the CCR4-NOT complex and preferentially act on transcripts that are processed at the ER (Lim *et al.,* 2018). Additionally, TENT5A and TENT5C have been suggested to be involved in regulating poly(A) tail lengths for small, secreted proteins such as lysozymes and cathepsins during innate immunity (Liudkovska *et al,* 2022)

This chapter aims to address whether miR-181a regulation of TNF changes in response to transcriptional induction outside of the context of inflammation. To investigate this, an inducible luciferase reporter system in a heterologous cell line was developed.

This chapter also looks to investigate how miR-181a interacts with other factors that bind and regulate the TNF 3'UTR or poly(A) tail length. This was done using siRNA knockdowns in combination with miR-181a inhibition in RAW 264.7 cells stimulated with LPS.

5.2 Selection of HEK293 as a suitable cell line for investigation of TNF 3'UTR reporters

First, a luciferase reporter approach was used to determine whether miR-181a regulates TNF by direct binding to the previously identified target site within the 3'UTR. The development of a luciferase reporter system facilitates detailed investigation of the different regulatory mechanisms that operate on the TNF 3'UTR in an orthogonal system, outside of the context of inflammation.

Before the assays could be carried out, an alternative cell line was selected to look outside of the context of inflammation and allow the development of an inducible stable cell line via the TRex system. Ideally, the alternative cell line would need to express miR-181a endogenously, as inhibition of the endogenous miRNA is more physiologically relevant than overexpression. HeLa and Hek 293 cell lines were selected as potential alternative cell lines due to high transfection efficiencies. The expression of miR-181a was then measured in the HeLa and Hek 293 cell lines and compared to miR-181a expression levels in RAW 264.7 cells. Looking at raw Ct values from RT-qPCR as a measure of expression with any Ct above 35 considered background, miR-181a had the greatest expression in the RAW 264.7 cells with a Ct value of 22 (Figure 41A). There is less miR-181a expression within the HeLa and Hek 293 cells, but the Hek 293 cells had a slightly greater expression with miR-181a detected at Ct 29 compared to Ct 32 within the HeLa cells (Figure 41A).

Furthermore, the induction of miR-181a by LPS was also examined within the HeLa and HEK293 cells. While these cell lines do not produce an inflammatory response, LPS is toxic, and the cells may still respond to its presence (Figure 41B). This is particularly relevant for HEK 293 which do express some LPS detecting receptors at low level and where low levels of LPS have been found to enhance protein production when using cells for recombinant protein productions (Faust 2021). RAW 264.7, HeLa, and HEK 293 cells were treated with LPS for one hour, miR-181a levels were assayed for using RT-qPCR and any change with LPS was plotted relative to the zero-time point for each cell line. While the HeLa cells showed no change in miR-181a expression in response to LPS, both the RAW 264.7 cell and the HEK 293 cells show an increase in miR-181a expression with LPS treatment (Figure 41B). HEK 293 cells did appear to give a response to LPS, displaying an increase in miR-181a expression on the basis of one independent experiment, but this was not

investigated further. Additionally, all further experiments within HEK 293 cells were carried out without LPS treatment. The small increase in miR-181a observed within the RAW 264.7 cells is not inconsistent with previous data, particularly given experimental variability and this data is only representative of one independent experiment.

Overall, as there is a generally higher level of miR-181a expression within the HEK 293 cells compared to the HeLa cells alongside a potential to induce miR-181a, the HEK 293 cell line was selected for transfection experiments including luciferase assays.

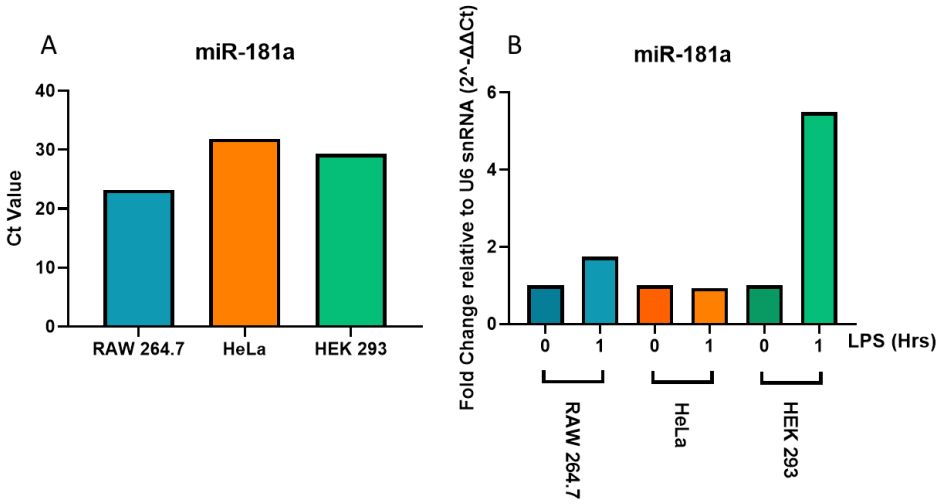

Figure 41. miR-181a is expressed in HEK293 cells. A) miR-181a expression in RAW 264.7, HeLa, and Hek 293 cells. Data was measured in triplicate by RT-qPCR and the raw Ct values were displayed. N=1. **B)** Induction of miR-181a expression with one-hour LPS (1µg/ml) treatment in RAW 264.7, HeLa, and Hek 293 cells. Data was measured by RT qPCR and analysed by $2^{-\Delta\Delta Ct}$ relative to U6 snRNA. N=1.

5.3 miR-181a directly regulates the 3'UTR of TNF mRNA

Once a suitable cell line had been selected, luciferase assays could be performed. Firstly, two luciferase reporters were generated (Figure 42) containing the firefly luciferase coding region followed by the TNF 3'UTR. The wild-type (WT) reporter contained the full TNF 3'UTR. Conversely the mutant (Mut) reporter has a mutated position within the miR-181a seed match within the TNF 3'UTR where the fourth nucleotide of miR-181a binding position was swapped from an adenine to a thymine residue. This would be expected to disrupt the miRNA binding due to the requirement for perfect complementarity between nucleotide 2-7 of a miRNA and its target site (Bartel, 2018). The mutant reporter was used as a control for miR-181a

binding. A Renilla luciferase reporter was also included in transfections, to allow for the normalisation of the firefly luciferase values and control for differences in transfection efficiency.

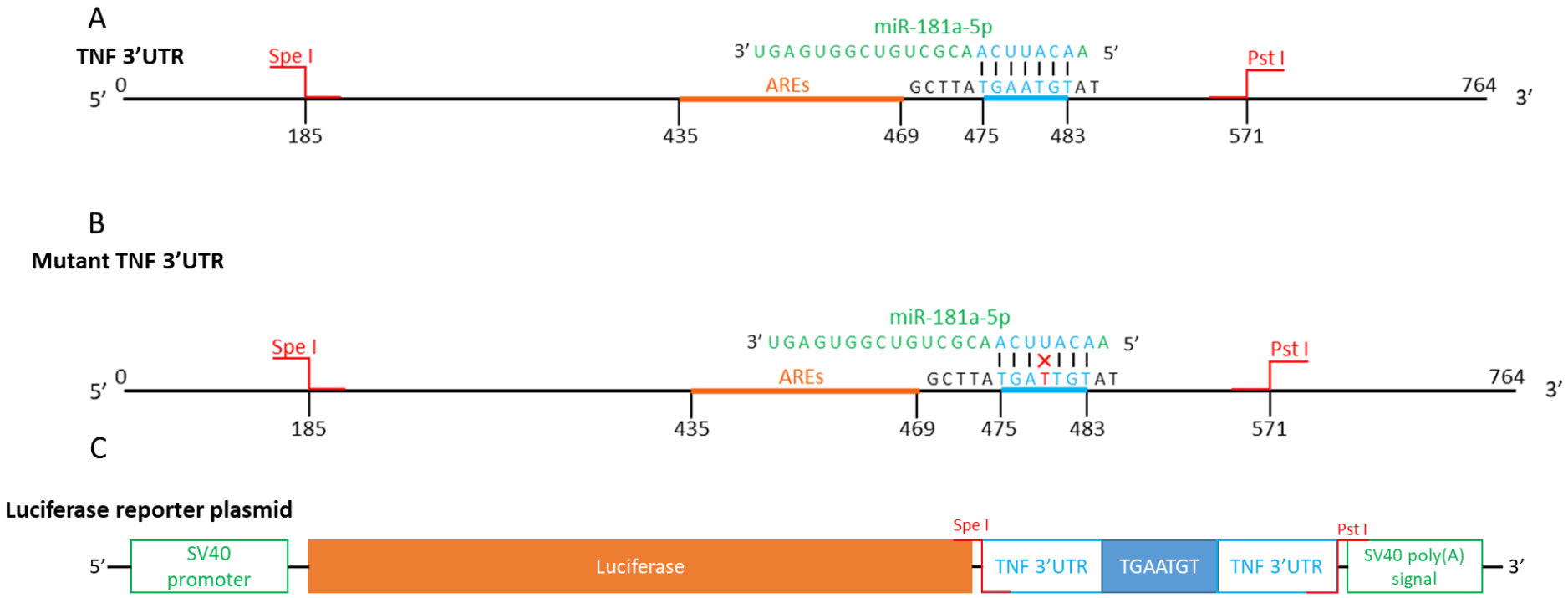

Figure 42. Schematic of the TNF 3'UTR luciferase reporter construction. A) TNF 3'UTR depicting the location and binding of miR-181a to the target site via the seed. Also indicates the location of the AREs and restriction sites used for cloning **B)** TNF 3'UTR with the mutated miR-1818a binding site disrupting miR-181a binding, including restriction sites for cloning. **C)** The firefly luciferase reporter showing the location and restriction sites where either the TNF 3'UTR or the mutant TNF 3'UTR were inserted.

HEK 293 cells were all transfected with the Renilla plasmid and either the WT or the mutant reporter alongside either a miR-181a inhibitor or the negative control oligo.

Cells were transfected for 24 hours before lysates were harvested and assayed for luminescence. Firefly luciferase output was normalised to Renilla output, then for each reporter the miR-181a inhibition or overexpression treatment was plotted relative to its negative control oligo (Figure 43).

miR-181a inhibition resulted in a 0ne-twofold increase in luciferase activity for the WT reporter compared to its negative control ($p<0.0001$, t-test) (Figure 44A). On the other hand, there was no difference in relative fluorescence with inhibition for the mutant reporter vs its negative control in which a single nucleotide within the miR-181a binding site was mutated. Therefore, miR-181a directly inhibits protein production from the luciferase reporter via this specific miR-181a target site in the TNF 3'UTR. Conversely, when miR-181a mimics were transfected instead of the inhibitors, miR-181a overexpression resulted in a twofold decrease in luciferase activity with the WT reporter compared to the negative control ($p<0.0001$, t-test) with no significant change with miR-181a overexpression for the mutant reporter vs its negative control (Figure 44B). This further confirms that miR-181a is directly binding to the 3'UTR of TNF mRNA and as such is having a direct effect on the regulation of TNF.

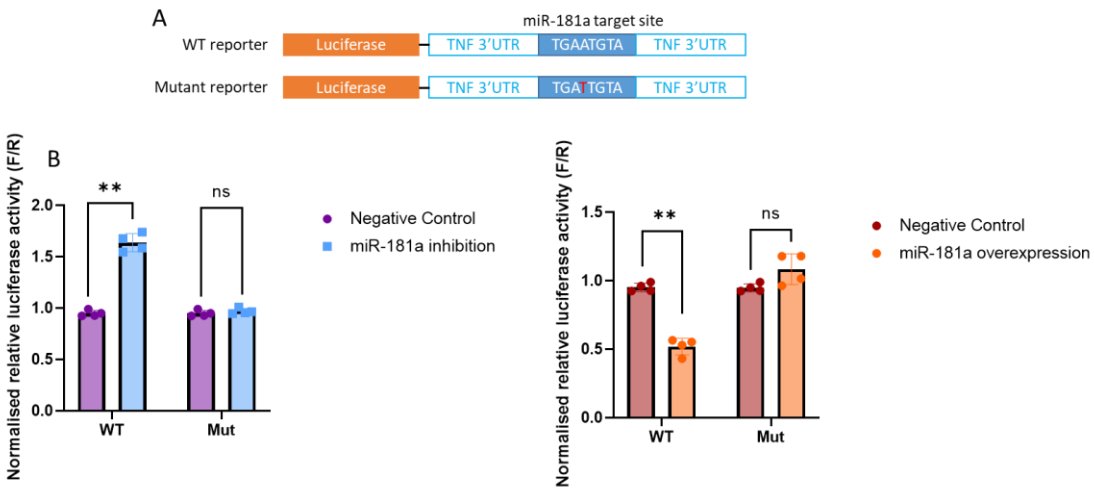

Figure 43. miR-181a regulates luciferase production via the 3'UTR of TNF mRNA transcripts. A) Schematic of the luciferase reporters. **B)** Firefly/Renilla (F/R) luciferase activity is increased with miR-181a inhibition with WT reporter. WT- wild-type luciferase reporter containing the TNF 3'UTR. Mut – Luciferase reporter with a mutated miR-181a binding site within the TNF 3'UTR. Hek 293 cells transfected with WT or Mut reporters alongside either the miR-181a inhibitor (5nmol) or negative

control oligo (5nmol), Data measured by luciferase assay, normalised to a Renilla plasmid, and plotted relative to the respective negative control. Significant increase in relative luciferase activity with the WT reporter compared to its negative control ($p<0.0001$, t-test). N=4. Error represents SD. **C)** Same as B except a miR-181a mimic (5nmol) and mimic negative control (5nmol) were transfected alongside the reporters. Significant decrease in relative luciferase activity with the WT reporter compared to its negative control ($p<0.0001$, t-test). N=4. Error represents SD.

5.4 Establishing an orthogonal inducible system to examine miR-181a regulation via the TNF 3'UTR

To look at miR-181a regulation of TNF outside the context of inflammation, an orthogonal inducible system was generated. One of the difficulties of interpreting the changes in miR-181a regulation of TNF seen in chapters 3 and 4 is that although TNF mRNA is induced and the poly(A) tail length changes during LPS stimulation of RAW 264.7 cells, there will also be other changes occurring within the cells during the inflammatory response. Having established that miR-181a represses protein production from a luciferase reporter containing the TNF 3'UTR in HEK 293 cells, this approach can be used to directly investigate how miR-181a regulation of TNF via the 3'UTR changes with transcriptional induction without the confounding effects of the full inflammatory response.

The TNF 3'UTR fused downstream of the stop codon of the firefly luciferase coding region was put under the control of an inducible promoter using the Flp-in T-rex system. The Flp-in T-rex system within a cell line contains a flip-in recombinase target site under the control of a tetracycline inducible promoter (Figure 44). This target site allows for the insertion of a gene of interest into the cell line via transfection of two plasmids, one encoding the flp-in recombinase and the other containing the gene of interest alongside a Hygromycin resistance gene to allow for the selection of cells with a successful integration event. Cells can then be treated with either tetracycline or doxycycline to induce transcription of the gene of interest.

As it has previously been established that endogenous miR-181a effectively targets the TNF 3'UTR within HEK 293 cells, the Flp-in T-rex HEK 293 cell line was selected for the Flp-in approach.

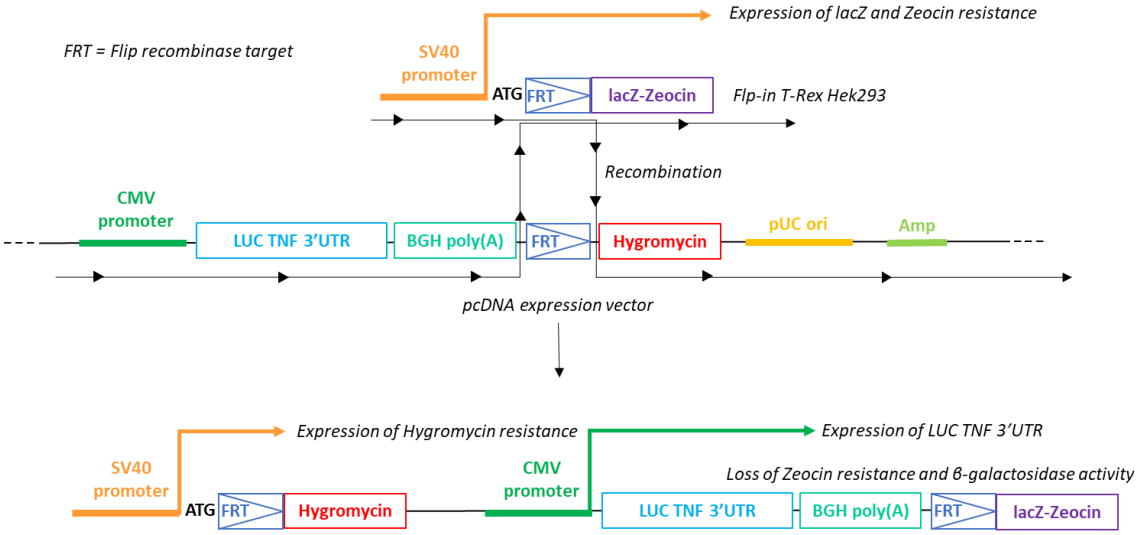

Figure 44. Schematic of the Flp-in T-rex system showing integration of the gene of interest via the flip-in recombinase.

Three mixed cell populations of transgenic Flp-in T-rex HEK 293s were successfully selected for with Hygromycin treatment, and named Tet Luc TNF 3'UTR HEK 293 A, B and C. Successful integration of the luciferase TNF 3'UTR gene of interest was checked for by extraction the genomic DNA from all three mixed populations (A, B and C) alongside the WT genomic DNA. Presence of the Luc TNF 3'UTR gene was then determined via PCR amplification using primers for the promoter region and the poly(A) tail signal either side of the Luc TNF 3'UTR gene (Figure 45A). A PCR product of the expected size was detected within all three cell lines but not the WT. Furthermore, sequencing of the PCR product further confirmed the insert is correct (Figure 45B).

Population A was selected for further study and all further experiments were performed using population A.

Once successful integration was confirmed, induction of the transgene by doxycycline (dox) was tested. Tet Luc TNF 3'UTR transgenic cells alongside the wild-type Flp-in T-rex HEK 293 cells were treated with dox over a 24-hour time course. RNA was then harvested and induction of Luc TNF 3'UTR was assayed for using RT-qPCR. Two sets of primers were used to look at Luc TNF 3'UTR mRNA expression, one set specific for the TNF 3'UTR and the other specific for the luciferase (Luc) coding region. Both sets of primers show that there is significant induction of Luc TNF 3'UTR mRNA with dox treatment within the transgenic cell compared to the Flp-in T-rex Hek 293s (TNF 3'UTR: $p<0.05$, AUC, Luc: $p<0.01$, AUC) (Figures 45C and 45D). Both

sets of primers show an initial three-fold increase in Luc TNF 3'UTR mRNA after one-hour of dox treatment that rises slightly at two hours dox treatment before dropping slightly for the remainder of the time course. This decrease is unexpected as dox has a half-life of 24 hours but was not significant.

Furthermore, luciferase assays were performed to determine whether luciferase enzyme was being produced. However, when assaying for luciferase activity, no signal greater than background could be detected, despite being able to observe induction of the Luc TNF 3'UTR mRNA and having sequenced the full coding region of Luc from the genomic DNA and confirmed it is correct.

Lastly, expression of miR-181a with dox induction was also investigated to see if dox was having any impact on miR-181a levels. Over a 24-hour dox time course, miR-181a levels remained constant (Figure 45E), indicating that any changes in miR-181a regulation over a dox time course are not due to changes in miR-181a expression.

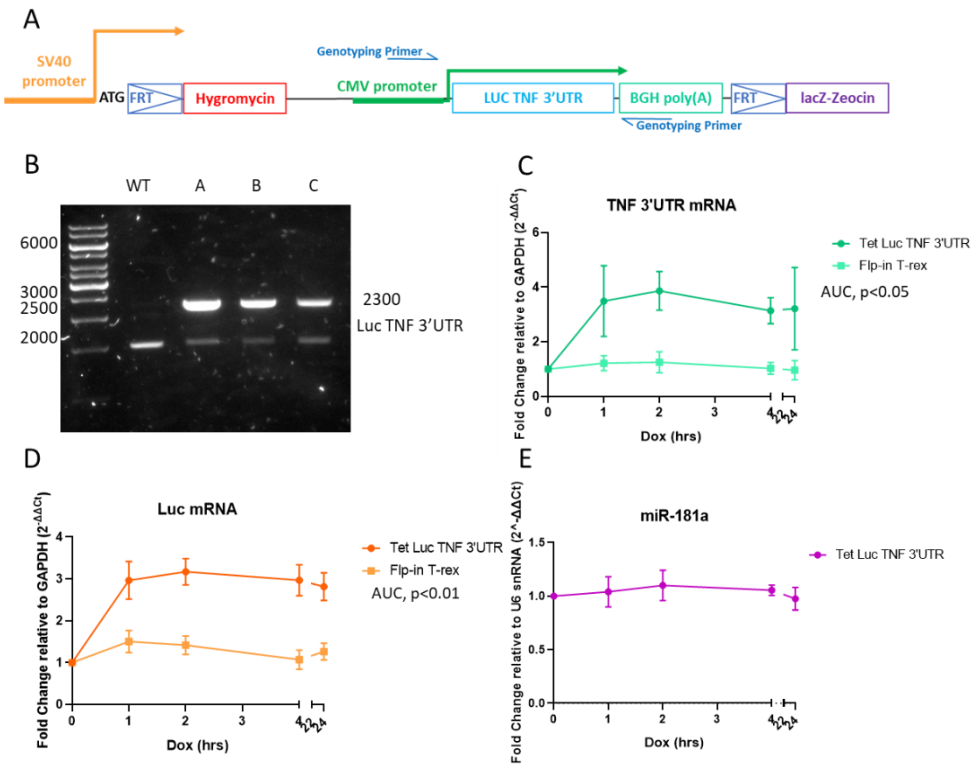

Figure 45. Validation of dox inducible Luc TNF 3'UTR HEK293 cell line. A) Schematic of inserted gene of interest, displaying where the genotyping primers are amplifying. **B)** PCR amplification of Luc TNF 3'UTR gene of interest. Products run on a 1% agarose gel via gel electrophoresis. WT – wild-type flp-in t-rex Hek 293 cells. A- transgenic Tet Luc TNF 3'UTR Hek 293 population A, B – transgenic Tet Luc TNF 3'UTR

Hek 293 population B, C - transgenic Tet Luc TNF 3'UTR Hek 293 population C. **C)** Induction of Luc TNF 3'UTR mRNA over a 24 hour dox (2µg/ml) time course in transgenic Tet Luc TNF 3'UTR and wild-type flp-in t-rex Hek293 cells. Data measured by RT-qPCR and analysed by $2^{-\Delta\Delta Ct}$, relative to zero-hour time point. Primers amplify TNF 3'UTR section of mRNA. Significant induction of Luc TNF 3'UTR mRNA in transgenic cells compared to wild-type cells ($p<0.05$, AUC). N=3. Error represents SD **D)** Same as C but primers amplify luciferase section of mRNA. Significant induction of Luc TNF 3'UTR mRNA in transgenic cells compared to wild-type cells ($p<0.01$, AUC). N=3. Error represents SD. **E)** Same as C but looking at miR-181a expression levels. N=3. Error represents SD.

5.5 Overexpression, but not inhibition, of miR-181a affects Luc TNF 3'UTR mRNA levels

After it was established that dox was able to induce the expression of the Luc TNF 3'UTR mRNA, miR-181a regulation of the mRNA over a time course of transcriptional induction could then be investigated in further detail.

To investigate how miR-181a regulation via the TNF 3'UTR affects mRNA levels in the context of transcriptional induction within the Tet Luc TNF 3'UTR HEK 293 cell line, miR-181a inhibition and overexpression experiments were performed.

The Tet Luc TNF 3'UTR transgenic cells were transfected with either a miR-181a inhibitor or negative control oligo for 24 hours before a four-hour dox time course was performed. RNA was then extracted and Luc TNF 3'UTR mRNA levels were examined via RT-qPCR with two different sets of primers. When looking at the expression of Luc TNF 3'UTR mRNA relative to the zero-hour time point, there is no difference in Luc TNF 3'UTR mRNA induction with miR-181a inhibition compared to the negative control for both sets of primers (Figures 46A and 46B). Similarly, when looking at the effect of miR-181a inhibition relative to the negative control at each time point, there is also no significant difference in Luc TNF 3'UTR mRNA expression with miR-181a inhibition (Figures 46C and 46D). This contrasts with what was observed in RAW264.7 cells treated with LPS to induce an inflammatory response, where miR-181a inhibition resulted in an increase in TNF mRNA levels (Figure 24).

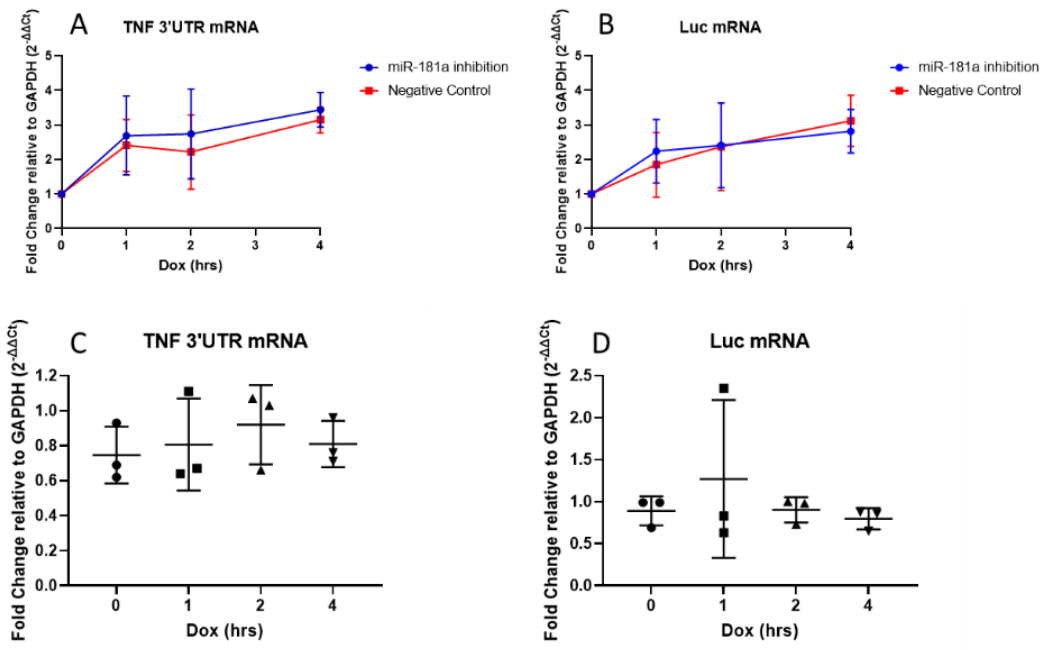

Figure 46. Inhibition of miR-181a has no effect on Luc TNF 3'UTR mRNA levels over a dox time course. **A)** Effect of miR-181a-5p inhibition on Luc TNF 3'UTR mRNA over a four-hour dox (2µg/ml) time course. Measured by RT-qPCR and analysed by $2^{-\Delta\Delta Ct,}$ normalised to GAPDH and plotted relative to the zero-hour time point. Primers amplify the TNF 3'UTR section of the mRNA. N=3. Error represents SD. **B)** Same as A but primers amplify the luciferase section of the mRNA. **C)** Same as A but data is relative to the negative control for each time point. **D)** Same as B but the data is relative to the negative control for each time point. N=3. Error represents SD.

Similar to the inhibition experiment, the Tet Luc TNF 3'UTR cells were transfected with either a miR-181a mimic or a negative control oligo before a four-hour dox time course was performed. RNA was then extracted and Luc TNF 3'UTR mRNA levels were examined via RT-qPCR with two different sets of primers. When looking at the Luc TNF 3'UTR mRNA levels relative to the zero-hour time point, there is a reduction in Luc TNF 3'UTR mRNA with miR-181a overexpression compared to the negative control with both sets of primers (Figures 47A and 47B). Furthermore, when looking at Luc TNF 3'UTR expression relative to the negative control at each time point, there is a significant reduction in Luc TNF mRNA expression between the zero and four-hour time points for both sets of primers with a threefold decrease in expression (Figure 47C). Additionally, with the set of primers amplifying the luciferase section of the gene, there is a significant reduction in Luc TNF 3'UTR mRNA at all time points compared to the zero hour time point (Figure 47D). Relative to the zero-hour time point there is a two to threefold decrease in Luc-TNF mRNA suggesting that the miR-

181a mimic represses Luc-TNF more strongly later on in the dox transcriptional induction time course.

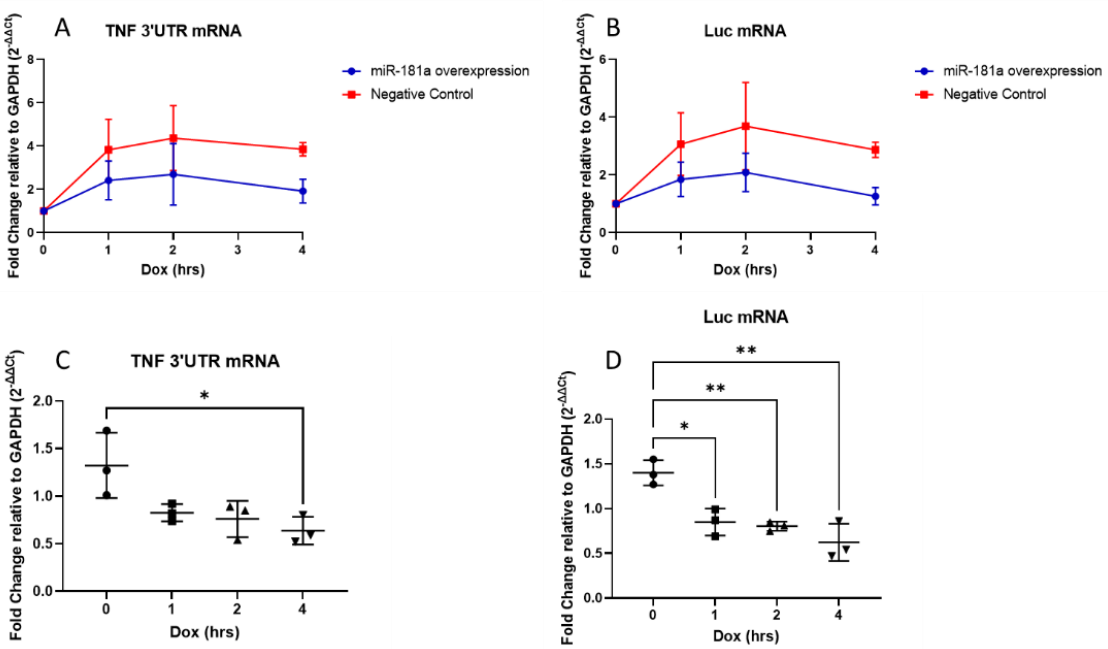

Figure 47. Overexpression of miR-181a reduces Luc TNF 3'UTR mRNA levels over a dox time course. A) Effect of miR-181a-5p overexpression on Luc TNF 3'UTR mRNA over a four-hour dox (2µg/ml) time course. Measured by RT-qPCR and analysed by $2^{-\Delta\Delta Ct,}$ normalised to GAPDH and plotted relative to the zero-hour time point. Primers amplify the TNF 3'UTR section of the mRNA. N=3. Error bars indicate SD **B)** Same as A but primers amplify the luciferase section of the mRNA. N=3 Error bars indicate SD. **C)** Same as A but data is relative to the negative control for each time point. N=3. Error bars indicate SD. **D)** Same as B but the data is relative to the negative control for each time point. N=3. Error bars indicate SD.

5.6 Association of miR-181a with Ago2 does not change with doxycycline induction.

The results in Figure 47 suggest that a miR-181a mimic has a stronger repressive effect on Luc-TNF at later time points with dox transcriptional induction. As such, Ago2 IP was used to directly investigate whether miRNA recruitment to the TNF 3'UTR changes over the course of transcriptional induction in this system.

Tet Luc TNF 3'UTR cells were seeded 24-hours before a four-hour dox time course was performed. Cell lysates were harvested, and an Ago2 IP was performed overnight utilising the same Ago2 antibody as in Figures 35 and 36, which is specific for both mouse and human. RNA was extracted and quantified using RT-qPCR relative to an input control.

When miR-181a levels are shown relative to the input, miR-181a is enriched within the Ago2 immunoprecipitants but not within the IgG isotype control immunoprecipitants, indicating the Ago2 IP specifically isolates associated endogenous miRNAs in HEK 293 cells. When looking at miR-181a enrichment within the Ago2 fractions, it remains very constant over the course of dox induction (Figure 48A).

Luc-TNF 3'UTR mRNA is also enriched within the Ago2 immunoprecipitants relative to input compared the IgG isotype control, indicating that Luc-TNF 3'UTR is specifically associated with Ago2.

On the other hand, Luc TNF 3'UTR mRNA enrichment within the Ago2 immunoprecipitants decreases with dox treatment (Figure 48B). The proportion of Luc-TNF mRNA associated with Ago2 decreased approximately threefold following dox induction.

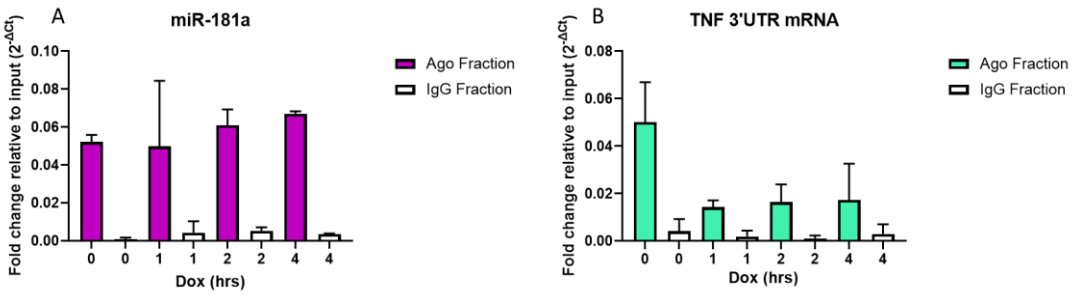

Figure 48. miR-181a and Luc TNF 3'UTR association with Ago2 during dox treatment. A) miR-181a isolated with Ago2 and IgG fractions over a four-hour dox (2µg/ml) time course in luc TNF 3'UTR Hek 293 cells. Data normalised relative to 20% input fraction. N=2. Error represents SD. **B)** Same as A but displaying Luc TNF 3'UTR mRNA levels. N=2. Error represents SD.

5.7 Poly(A) tail lengths of Luc TNF 3'UTR do not change over a doxycycline time course

It was also investigated whether the inducible Luc-TNF reporter system reproduces the poly(A) tail length changes observed over the course of transcriptional induction of TNF in RAW 264.7 cells in response to LPS. This would indicate whether transcriptional induction in combination with elements in the 3'UTR is sufficient to modulate these poly(A) tail length changes or whether other aspects of the inflammatory response are required.

Tet Luc TNF 3'UTR cells were seeded before being treated with dox 24 hours later. RNA was extracted at different time points and a PAT assay performed. The RPL28 experimental control confirms that the PAT assay was successful. The poly(A) tail lengths within the HEK 293 cells were similar to what was seen within RAW 264.7 cells (Figures 33, 34 (chapter 4)) with a modal size of 41nt once the 249nt section of the RPL28 3'UTR has been deducted (Figure 49) Furthermore, the excess primer bands are also present, with the larger excess primer band being the strongest.

Looking at the poly(A) tail lengths for Luc TNF 3'UTR mRNA, there appears to be no change in poly(A) tail length with dox treatment over a 24 hour dox time course (Figure 49). The predominant band is indicative of the portion of 3'UTR amplified by the primers suggesting most of the Luc-TNF mRNA has a very short poly(A) tail or is fully deadenylated.

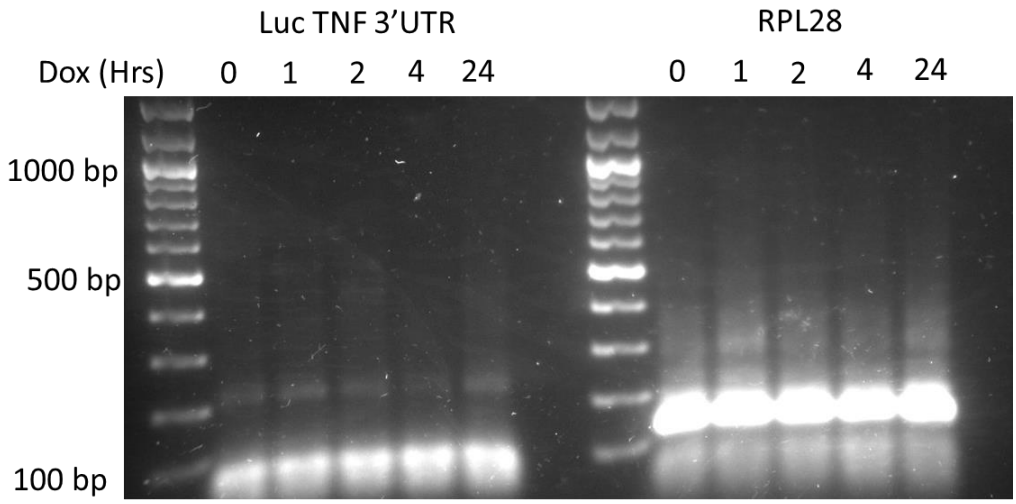

Figure 49. Poly(A) tail lengths of Luc TNF 3'UTR and RPL28 over a 24 hour dox (2µg/ml) time course. Transgenic Tet Luc TNF 3'UTR Hek293 cells were seeded, treated with dox 24 hours later. RNA extracted and a PAT assay performed. Products run on a 1.2% agarose gel via electrophoresis. N=1.

5.8 HuR is needed for stabilisation of TNF mRNA transcripts.

As the 3'UTRs of mRNAs can contain other regulatory elements, how these elements may be affecting TNF regulation and the interplay with miR-181a regulation was investigated. HuR was investigated first, due to its known role in TNF stabilisation during the inflammatory response (Dean *et al.,* 2001, McMullen *et al.,* 2003). To determine whether HuR regulation interacts with miRNA regulation, HuR regulation of TNF mRNA was first investigated within the RAW 264.7 inflammatory

system. To do this, HuR siRNA double knockdown experiments were performed to confirm HuR regulation of TNF mRNA was occurring as expected with the RAW 264.7 model of inflammation.

RAW264.7 cells were transfected with HuR siRNA or a non-targeting siRNA control for 24 hours before transfection with more HuR siRNA or non-targeting siRNA control for a further 24 hours, followed by treatment with LPS over a four-hour time course. RNA was extracted and measured by RT-qPCR and shown as $2^{-\Delta\Delta Ct}$ relative to a RPL28 housekeeping control mRNA.

Confirmation of successful HuR KD was obtained at the RNA level. RT-qPCR shows a consistent 2-4 fold reduction in HuR mRNA at all LPS time points following HuR siRNA transfection (Figure 50A).

When looking at TNF mRNA expression relative to the zero time point with siRNA control treatment, TNF mRNA expression increases over the four hours of inflammation as expected, increasing from a fold change of 30 at one hour to 35 at two hours and 40 at four hours LPS treatment (Figure 50B). Under conditions of HuR knockdown, TNF mRNA induction at one-hour LPS treatment was identical to the control siRNA condition. However, later in the time course, TNF mRNA levels were reduced in HuR knockdown cells while remaining elevated in control siRNA treated cells. The reduction in TNF mRNA expression is particularly clear at the four-hour time point where there is a threefold decrease in TNF mRNA expression within the HuR knockdown conditions verses the siRNA control conditions. This difference in TNF mRNA expression between the siRNA control and HuR siRNA treatments is significant ($p<0.01$, AUC) (Figure 50B).

The same qPCR data was also analysed by direct comparison of the siRNA control TNF mRNA levels versus the HuR siRNA-treated cells at each time point. Overall, there is a downwards trend following HuR KD at later time points, but no statistically significant difference was observed. TNF mRNA expression at 2 hours decreased with a fold change of 0.6 and further decreased at 4 hours with a fold change of 0.5 (Figure 50C). This supports previous evidence that HuR is required for TNF mRNA stability during the inflammatory response.

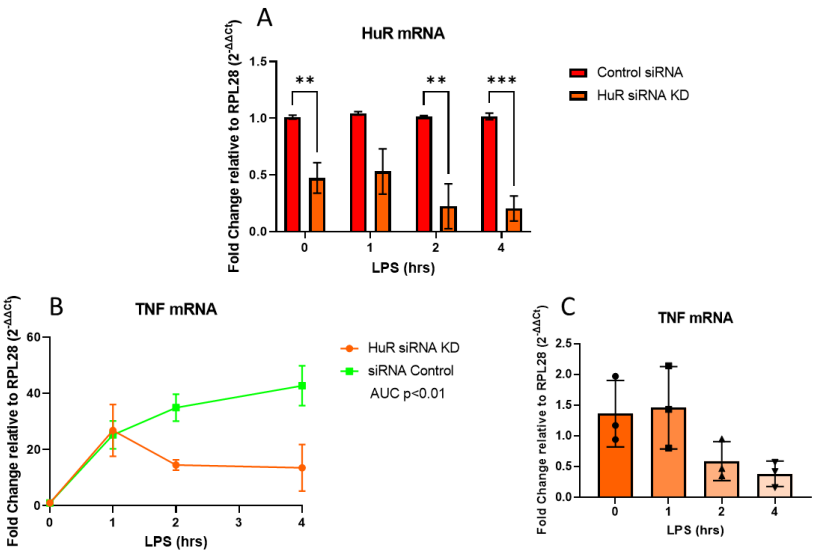

Figure 50. HuR is required for TNF mRNA stability during inflammation. A) HuR mRNA levels with or without HuR siRNA double KD over a four-hour LPS (1µg/ml) time course in RAW 264.7 cells. HuR siRNA (20nmol final) or siRNA control (20nmol final) were transfected over 48 hours. Data measured by RT-qPCR and analysed by $2^{-\Delta\Delta Ct,}$ normalised to RPL28 and plotted relative to the siRNA control. Significant decrease in HuR mRNA with HuR KD (0hr $p<0.05$, 2hr $p<0.01$, 4hr $p<0.0001$, t-tests with Bonferroni correction) N=3. Error represents SD. **B)** Same samples as A but TNF mRNA levels were measured and normalised to RPL28 and plotted relative to the zero-hour time point. Significant decrease in TNF mRNA induction with HuR KD ($p<0.01$, AUC). N=3. Error represents SD **C)** Same as B but data is shown for HuR siRNA relative to the siRNA control at each time point. N=3. Error represents SD.

5.9 TENT4A and TENT4B are needed for stabilisation of TNF mRNA transcripts.

Mixed tailing by TENT4A and TENT4B has recently been identified as particularly affecting ER-localised mRNAs and protecting from deadenylation by CCR4-NOT (Lim *et al.,* 2018). As TNF is translated at the ER and has been shown to be subject to cytoplasmic polyadenylation (Crawford *et al.,* 1997, Kwak *et al.,* 2021), it can be hypothesised that TENT4A/B might add mixed tails to TNF and affect the rate of deadenylation. As miR-181a did not significantly affect TNF poly(A) tail length, it was investigated whether mixed tailing might be involved.

RAW264.7 cells were transfected with TENT 4A and TENT 4B siRNA or a non-targeting siRNA control for 24 hours before transfection with more TENT 4A and TENT 4B siRNA or non-targeting siRNA control for a further 24 hours, followed by treatment with LPS over a four-hour time course. RNA was extracted and measured by RT-qPCR and shown as $2^{-\Delta\Delta Ct}$ relative to a RPL28 housekeeping control mRNA.

Confirmation of successful siRNA KD was obtained at the RNA level. RT-qPCR looking at TENT4A and TENT4B mRNA levels with siRNA control transfection and TENT4A and TENT4B siRNA transfection confirm there is a consistent two-fourfold reduction in TENT4A and TENT4B mRNA at all tested timepoints (Figure 51A).

The siRNA control used within the TENT4A/4B KD experiments is the same as the siRNA control within the HuR KD experiments (Figure 50) as the experiments were performed at the same time. As previously shown, the pattern of TNF induction was similar to earlier experiments without siRNA transfection (Figures 24 and 25 (Chapter 3)).

While TNF induction by LPS was similar at one hour in control and TENT4A and TENT4B siRNA conditions, TENT4A/B knockdown led to a subsequent decrease in TNF mRNA such that at four hours there was a threefold decrease in TNF induction compared to the siRNA control conditions (Figure 51B).

When plotting the same data relative to the siRNA control at each time point to determine whether TENT4A/4B depletion affected TNF mRNA levels at any individual time point, there is a significant decrease at two and four hours with fold changes of 0.5 and 0.4 respectively. However, there was no effect at earlier time points confirming that TENT4A/4B are required for maintenance of high TNF mRNA levels later in the inflammatory response, but not at the early stages (Figure 51C).

The observation that TENT4A/B are required for maintenance of high levels of TNF during the inflammatory response is novel and could be the result of different mechanisms. Either through cytoplasmic polyadenylation or mixed tailing but could also be due to an indirect effect of TENT4A/B, and further investigation would be required to elucidate the exact mechanism.

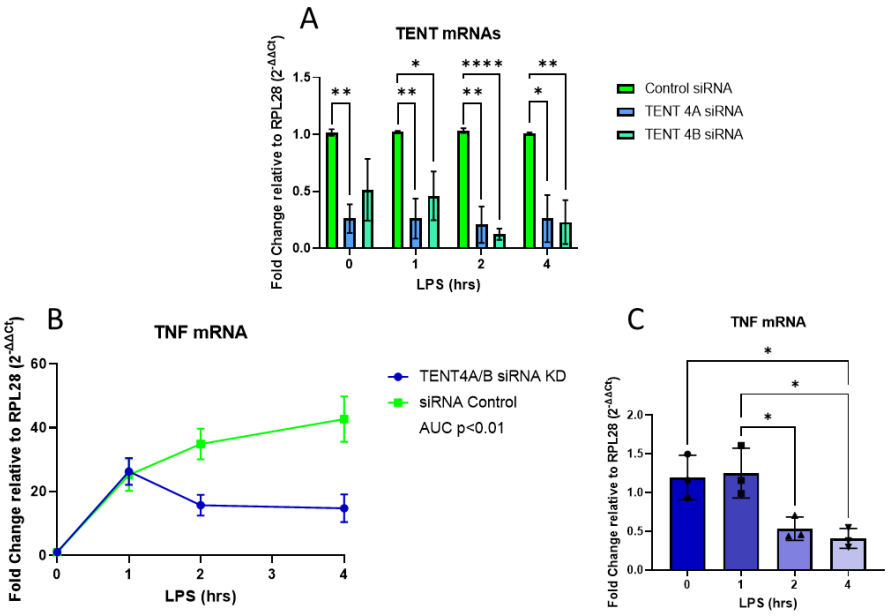

Figure 51. TENT 4A/B are required for TNF mRNA stability during inflammation. A) TENT4A and TENT4B mRNA levels with or without TENT4A and TENT4B siRNA double KD over a four-hour LPS (1µg/ml) time course in RAW 264.7 cells. TENT4A siRNA (20nmol final) and TENT4B (20nmol final) or siRNA control (20nmol final) were transfected over 48 hours. Data measured by RT-qPCR and analysed by $2^{-\Delta\Delta Ct,}$ normalised to RPL28 and plotted relative to the siRNA control. Significant decrease in TENT4A and TENT4B mRNA with TENT4A and TENT4B KD (TENT 4A: 0hr $p<0.01$, 1hr $p<0.01$, 2hr $p<0.01$, 4hr $p<0.05$. TENT 4B: 1hr $p<0.05$, 2hr $p<0.001$, 4hr $p<0.01$, t-tests with Bonferroni correction) N=3. Error represents SD. **B)** Same samples as A but TNF mRNA levels were measured and plotted relative to the zero-hour time point. Significant decrease in TNF mRNA induction with TENT4A and TENT4B KD ($p<0.01$, AUC). N=3. Error represents SD. **C)** Same as B but data is relative to the siRNA control at each time point. Significant reduction in TNF mRNA at later time points compared to zero and one hour time points (0vs4hr $p<0.05$, 1vs4hr $p<0.05$, 1vs2hr $p<0.05$, t-tests with Bonferroni correction). N=3. Error represents SD.

5.10 Discussion

5.10.1 HuR is required for the stabilisation of TNF mRNA transcripts.

HuR is predominantly localised in the nucleus and upon initiation of the inflammatory response, HuR is translocated to the cytoplasm where it can act to stabilise mRNA transcripts (Brennan & Steitz, 2001). HuR has previously been established to be required for stabilisation of TNF mRNA during the inflammatory response (Dean *et al.,* 2001), Figure 50 further supports this. However, there was not enough time to investigate the interplay with miR-181a, although it has been previously suggested that HuR competes with miR-181 for binding of the TNF 3'UTR (Dan *et al.,* 2015)

HuR is known to have roles in regulating the actions of miRNAs, such as facilitating their decoupling from their mRNA targets, and aiding their export via exosomes (Mukherjee *et al.,* 2016, Goswami *et al.,* 2020). HuR has also been found to act as a sponge for miRNAs sequestering them away (Kundu *et al.,* 2012, Poria *et al.,* 2016). It has been suggested that HuR directed decoupling of miRNAs from their mRNA targets is mediated through direct interaction of HuR with the miRNA or via the association of HuR with AREs within close proximity to the miRNA target site (Poria *et al.,* 2016).

This is similar to the miR-181a target site within the TNF mRNA transcript where the AREs are just upstream of the miR-181a target site. As such it may be that a similar mechanism is occurring within the RAW 264.7 cells. HuR may be preventing the action of miR-181a early in inflammation, but as HuR expression decreases miR-181a has a greater effect on TNF mRNA expression levels. However, this would need further investigation.

It may be that HuR is acting in a dual manner to stabilise TNF mRNA transcripts by binding to AREs within the TNF 3'UTR alongside the dislodging of miR-181a from TNF mRNA targets.

In the future, Ago Ips could be performed looking at miR-181a and TNF mRNA enrichment within Ago2 isolates with and without HuR siRNA knockdown to see if HuR is influencing miR-181a association with TNF mRNA transcripts.

5.10.2 TENT4A and TENT4B are involved in stabilising TNF mRNA transcripts.

Unexpectedly, TENT4A and TENT4B appear to be required for the maintenance of high levels of TNF mRNA later in the inflammatory response. This has not been previously shown within inflammation.

While little is known about TENT4A/B, they are known to be non-canonical polymerases that can add adenosine residues to the ends of mRNA within the cytoplasm. TENT4B is known to mediate polyadenylation of a wide range of RNAs including small non-coding RNAs as well as mRNAs (Sinturel *et al.,* 2017, Berndt *et al.,* 2012, Burroughs *et al.,* 2010, Boele *et al.,* 2014, Shin *et al.,* 2017). On the other hand, TENT4A has only been found to adenylate mRNAs and has been reported to be involved in miRNP-mediated translational activation of non-adenylated mRNAs in a cell free system (Wakiyama *et al.,* 2018)

More recently, TENT4A and TENT4B have been found to incorporate intermittent non-adenine residues into the poly(A) tail, with a preference for guanine (Lim *et al.,* 2018). By performing Tail-seq Lim *et al.,* (2018) discovered that guanosine residues were often located at the end or penultimate position within poly(A) tails, particularly long poly(A) tails. The guanylation events performed by TENT4A/B were found to preferentially occur on poly(A) tails for mRNA transcripts that are processed at the ER. The incorporation of non-A residues into the poly(A) tail has been found to stall deadenylation machinery, serving to stabilise the mRNA transcript (Lim *et al.,* 2018).

As such, the loss of high levels of TNF mRNA with TENT4A/B siRNA knockdown may be due to the loss of guanylation of the TNF poly(A) tail. Without guanylation, the transcripts may be less stable making them more susceptible to deadenylation, potentially miRNA mediated deadenylation via CCR4-NOT. The guanylation of TNF mRNA may also contribute to the lack of changes in the poly(A) tail length of TNF mRNA with miR-181a inhibition or overexpression.

However, it is not confirmed as to whether TNF mRNA is indeed being guanylated by TENT4A and TENT4B and direct sequencing of the TNF poly(A) tail using nanopore technology at multiple LPS timepoints would be needed to determine whether guanylation is occurring. It could just be that TENT4A/B polyadenylating TNF in order to stabilise TNF as opposed to performing any mixed tailing. Whether there are any

changes in the poly(A) tail length of TNF mRNA over the course of inflammation with and without TENT4A/B knockdown could be investigated to see if TENT4A/B are influencing the changes in TNF poly(A) tail length.

Furthermore, Lim *et al.,* (2018) suggest that the action of TENT4A/B is mediated through the 3'UTR, as transcripts that undergo guanylation tend to have longer 3'UTRs. Additionally, the pattern of TNF mRNA induction with TENT4A/B knockdown is very similar to that of TNF mRNA induction with HuR knockdown.

Additionally, a study looking at widespread changes in poly(A) tail length in macrophages with LPS stimulation, found that transcripts undergoing poly(A) tail length increases were enriched for HuR binding sites (Kwak *et al.,* 2021). Kwak *et al.,* (2021) also speculate whether TENT proteins are interacting with HuR to mediate the widespread readenylation of transcripts during LPS macrophage activation. As such there may be mechanisms by which either HuR is recruiting the TENT4A/B proteins to the 3'UTR to facilitate their activity, or conversely, TENT4A/B may be aiding the recruitment of HuR to the AREs within the 3'UTR of TNF mRNA.

It would be interesting to look at knocking down other TENT proteins to see whether these are also acting to promote high levels of TNF. TENT5A and TENT5C have been implicated in regulating the innate immune response within bone marrow derived macrophages (BMDMs). BMDMs that do not express TENT5A and TENT5C display defects in polyadenylation of mRNAs that encoded secreted proteins including lysozyme (*Lyz2*) and lysosomal proteases cathepsins (*Ctsd* and *Ctsb*) (Liudkovska *et al.,* 2022). While Liudkovska *et al* (2022) did not identify TNF transcripts in having altered poly(A) tail lengths with TENT5A/C knockout, there is still potential that TENT5A/C may also be contributing the TNF mRNA stability which could be interesting to investigate.

TENT4A/B immunoprecipitations could be performed to look at whether TNF mRNA is associating with the TENT4A/B proteins to confirm whether the effect of knocking down TENT4A/B on TNF mRNA induction is direct or not. The TENT4A/B immunoprecipitations could also be used to look at whether there is a potential interaction of HuR with TENT4A/B to see if HuR is involved in the recruitment of TENT4A/B to TNF mRNA if their action is direct. Sequencing of the TENT4A/B immunoprecipitants at different LPS timepoints could also be used to globally identify any mRNAs that are interacting with the TENT4A/B proteins in response to LPS treatment. This would facilitate the determination of whether the TENT4A/B

proteins are involved in the global changes in poly(A) tail length seen by Kwak *et al.,* 2021.

5.10.4 Transcriptional induction of an mRNA bearing the TNF 3'UTR is not sufficient to replicate the effects of the inflammatory response on endogenous TNF mRNA

Direct regulation by both endogenous and overexpressed miR-181a of a reporter bearing the TNF 3'UTR has been demonstrated, as such a similar approach was used to generate an inducible cell line.

Unexpectedly, while it is possible to transcriptionally induce Luc-TNF 3'UTR mRNA expression within the transgenic cell line, production of protein was unable to be detected via luciferase assay despite the genomic sequence being correct. With more time, western blots for the luciferase protein could be performed as an additional measure to identify whether the luciferase protein is being produced. It may be that luciferase protein is unable to be detected due to translational repression by miR-181a.

There was a change in Luc TNF 3'UTR mRNA levels with miR-181a overexpression but not inhibition. As such miR-181a may be acting more at the level of translation as opposed to mRNA stability, particularly as there was an increase in luciferase protein expression with miR-181a inhibition within the HEK 293 transient transfection experiments within Figure 43A. Furthermore, the change in Luc TNF 3'UTR expression with miR-181a overexpression but not with inhibition may be due to miR-181a being expressed at lower levels within the HEK 293 cells compared to the RAW 264.7 cells. As such it may be that endogenous miR-181a levels are too low to affect the mRNA levels. Performing qPCR on the luciferase mRNA generated in the transient transfections (Figure 43), could allow for a comparison of the effects of miR-181a inhibition on luciferase protein production.

In the future, western blots could be performed alongside luciferase assays to try and detect protein levels with and without miR-181a inhibition. If miR-181a is responsible for the lack of protein expression, protein production should be able to be detected with miR-181a inhibition. Additionally, polysome analysis could be performed to assess whether the Luc TNF 3'UTR mRNA is being translated with and without miR-181a inhibition.

The apparent lack of detectable protein levels could also be attributed to other factors such as HuR. HuR is predominantly localised to the nucleus in resting cellular conditions (Fan *et al.,* 1998) and can act as an adaptor protein for nuclear export of mRNAs containing AREs (Brennan & Steitz, 2001). As HuR is known to bind to the AREs within the 3'UTR of TNF (Dean *et al.,* 2001), it may be binding to the Luc-TNF 3'UTR mRNA and sequestering the mRNA transcript within the nucleus. However, the expression and localisation of HuR within the transgenic cell would need to be assessed for this to be investigated.

5.10.5 Effects of transcriptional induction on poly(A) tail length of LUC TNF 3'UTR mRNA

PAT assays looking at the poly(A) tail length of Luc-TNF 3'UTR mRNA within the HEK 293 cells showed that the mRNA was predominantly deadenylated and that the poly(A) tail length does not change over the course of transcriptional induction.

The trigger for rapid polyadenylation of TNF mRNA seen with LPS stimulation of RAW 264.7 cells may not be encoded within the TNF 3'UTR but may be determined by other factors within the inflammatory response. However, the poly(A) tail length for Luc TNF 3'UTR mRNA was only examined after one hour of dox treatment. All the changes seen in poly(A) tail length for TNF mRNA within the RAW 264.7 cells occur within the first hour of LPS stimulation. As such it could also be that any changes in poly(A) tail length for the Luc TNF 3'UTR mRNA may be occurring very shortly after dox treatment before returning to baseline after one hour of dox treatment.

On the other hand, the poly(A) tails for Luc TNF 3'UTR appear to be deadenylated at all the time point examined. This deadenylated state is often associated with transcripts that are translationally silent. For example, at early stages of oogenesis, maternal mRNAs are deposited in a deadenylated form and then undergo rapid polyadenylation to become translationally active (Richter, 1999). Furthermore, TNF mRNA has also been proposed to be translationally silent within unstimulated macrophages (Crawford *et al.,* 1997, Carpenter *et al.,* 2014). As such the lack of poly(A) tail length changes seen within the inducible HEK 293s may indicate that the Luc-TNF 3'UTR mRNA is translationally silent, and activation of translation is not stimulated by transcriptional induction. Although, the mechanism by which the translational repression of TNF mRNA is maintained in resting macrophages is not clear.

5.10.6 Effects of transcriptional induction on miR-181a regulation via the TNF 3'UTR

When looking at miR-181a enrichment within Ago2 immunoprecipitants over a dox time course, miR-181a enrichment remains constant. This suggests that transcriptional induction is not driving the recruitment of miR-181a to Ago2 and that the increase in miR-181a enrichment within Ago2 immunoprecipitants seen within the RAW264.7 cells is unique to that inflammatory system.

Furthermore, the decrease in Luc TNF 3'UTR enrichment within the Ago2 immunoprecipitants with transcriptional induction is likely due to the increased abundance of mRNA with dox treatment. As there is relatively more mRNA present within the cell, when the samples are normalised to input, there is relatively less miRNA regulation occurring after transcriptional induction.

The differences in miR-181a association with Ago2 seen between the HEK 293s and the RAW 264.7 cells could be due to multiple different reasons. It may be that Ago2 phosphorylation within the RAW 264.7 cells that causes the dissociation of the miRNAs with LPS induction (Mazumder *et al.,* 2013) is not occurring with transcriptional induction within the HEK 293s. It could be that the increase in miR-181a enrichment within Ago isolates in the RAW 264.7 cells could be due to changes in Ago2 expression that may not be occurring within the HEK 293 cells.

LPS triggers a global transcriptional induction event (Janeway & Medzhitov, 2002), inducing the increased expression of many different genes, which may contribute to changes in regulation, whereas dox treatment of the HEK 293 cells is only causing the transcriptional induction of the Luc TNF 3'UTR transgene.

To conclude, both HuR and the TENT4A/B proteins are required for maintenance of high TNF mRNA levels after one hour of LPS treatment. The role of TENT4A/B in maintaining high TNF mRNA is novel and appears parallel to that of HuR. However, the exact mechanism of action of TENT4A/B is unknown and will require further investigation to elucidate exactly what is happening.

Additionally, transcriptional induction of Luc TNF 3'UTR mRNA was successful within doxycycline inducible HEK 293s. As such, this is potentially a useful model system that could be further adapted to more closely study the interaction between transcriptional induction an miR-181a regulation via the TNF 3'UTR. For example, the AREs within the TNF 3'UTR could be removed to look more closely at how AREs may

be affecting miRNA regulation. However, the inability to detect luciferase activity has limited the experiments that could be performed.

Finally, the interaction of miR-181a with Ago with the transgenic HEK 293 cell line differs from miR-181a interaction with Ago within the RAW 264.7 cell line. However, exactly why the two systems differ is not known, and could be due to multiple different reasons.

Chapter 6 – Discussion

6.1 Summary

As miRNAs are important regulators of the inflammatory response, mis-regulation of miRNAs within inflammation can lead to chronic disease. Therefore, investigating how various factors can influence miRNA regulation is important to provide a better understanding of the intricate mechanisms that ensure the inflammatory response proceeds correctly. Certain key inflammatory mediators have been shown to have poly(A) tails that change in length during inflammation (Gandhi, 2016, Kwak *et al.,* 2022). As such, this project aimed to elucidate whether these changing poly(A) tail lengths are impacting on miRNA regulation and how this regulation is changing over the course of inflammation This research contributes towards the fundamental understanding of miRNA function in a physiological system where target mRNA undergoes rapid transcriptional induction as well as changes in poly(A) tail length.

Through the use of databases and cross referencing with the literature, miRNAs were identified that were expected to target the inflammatory mRNAs that were shown to experiences changes in poly(A) tail length during the inflammatory response. MiRNA regulation of these mRNAs was then examined within a RAW 264.7 mouse macrophage model of inflammation. Through inhibition and overexpression experiments alongside the generation of luciferase reporters, miR-181a was confirmed to be directly regulating TNF at both the mRNA and protein levels. Furthermore, changes in miRNA target binding and regulation over the course of the inflammatory response was observed.

In conjunction, changes in miRNA regulation of TNF were examined using an Ago2 IP technique. Ago2 IPs facilitated the investigation of how miRNA binding of TNF mRNA was changing over the course of inflammation as well as establishing how miR-181a association with Ago2 was changing during inflammation. An increase in TNF mRNA and miR-181a enrichment within Ago2 immunoprecipitants was observed over the course of LPS induction. However, further work is needed to elucidate what is driving the increased association of miR-181a with Ago2 as the inflammatory response progresses.

PAT assays were utilised to examine changes in poly(A) tail length, and while the changes in TNF poly(A) tail length previously establish were observed, the pattern of TNF mRNA poly(A) tail length across the LPS time course was unaffected by miR-181a regulation.

Additionally, this study identified a novel role for TENT4A/B, discovering that TENT4A/B are required for maintenance of high TNF mRNA levels later in the inflammatory response.

Additionally, an inducible system to study miR-181a regulation of the TNF 3'UTR was generated. This enabled the investigation of how the TNF 3'UTR is regulated by miR-181a under transcriptional induction, without other confounding processes that are occurring within inflammation. Generation of this stable cell line was successful and provides a useful tool to further examine aspects of the TNF 3'UTR and how they interact with miRNA regulation under transcriptional induction. Overexpression but not inhibition of miR-181a had an effect on Luc TNF 3'UTR mRNA levels. However, luciferase protein was unable to be detected to elucidate whether miR-181a inhibition was having an effect on protein levels.

6.2 Regulation of TNF mRNA by miR-181a changes over time

When the effects of miR-181 inhibition and overexpression on endogenous TNF mRNA and proteins levels were examined over the course of the inflammatory response, regulation of both mRNA and protein was strongest at eight hours. However, there was no effect of miR-181a inhibition on the Luc TNF 3'UTR mRNA within the inducible system. Conversely, there was an effect when miR-181a was overexpressed but the inhibition experiments are more physiologically relevant as overexpression is not representative of what would be occurring endogenously.

Furthermore, when looking at the effect of miR-181a inhibition and overexpression over time, the fold changes are calculated relative to the zero hour time point. As such, different levels of TNF mRNA/ Luc TNF 3'UTR mRNA at the zero hour time point for each treatment results in a much larger difference at later time points, potentially contributing to the large differences between treatments. On the other hand, TNF mRNA enrichment within Ago2 IPs does increase over time suggesting TNF mRNA is subject to greater regulation later in the inflammatory response. Furthermore, as the same data has been plotted relative to the negative control oligo at each time point and the same effects of inhibition and overexpression are seen in both cell lines, it is

likely that the changes seen relative to the zero hour time are true. Additionally, Corsetti *et al.,* (2018) observed a clear effect of miR-181a inhibition and overexpression on TNF mRNA levels with *Brucella abortus* infection. In contrast to this study, Corsetti et al., (2018) saw a much greater change in TNF mRNA levels with miR-181a inhibition and overexpression, however, they did not look at TNF protein levels. This difference in effect with miR-181a inhibition and overexpression could be attributed to different models. The model of inflammation Corsetti *et al.,* (2018) were using was BMDMs which do have different characteristics to RAW 264.7 cells (Barbour *et al.,* 1998). Furthermore, Corsetti *et al.,* (2018) stimulated BMDMs with *Brucella abortus* as opposed to just LPS which may result in more PRRs being activated triggering more inflammatory pathways, generating greater levels of TNF.

Interestingly, within this study, for both the miR-181a inhibition and overexpression experiments, there was a much greater effect on TNF protein expression as opposed to TNF mRNA expression, suggesting that miR-181a may be having more of an effect at the level of translation as opposed to facilitating TNF mRNA degradation.

Additionally, Ago2 IPs also show that miRNA regulation of TNF mRNA is increasing over the course of inflammation and that miR-181a association with Ago2 is increasing over inflammation. Conversely, this increase in TNF mRNA and miR-181 enrichment within Ago2 fractions was not observed within the inducible Tet Luc TNF 3'UTR HEK 293 cell line. This suggests that the changes in Ago2 association with miR-181a and TNF that were observed during LPS-induced inflammation in RAW 264.7 cells are unlikely to be related solely to transcriptional induction of TNF, and may instead be related to cell-specific factors.

Additionally, within the RAW 264.7 cells, miR-181a expression remains constant over inflammation, as such there are other factors that are driving the recruitment of miR-181a to Ago2. It could be that Ago2 expression is changing over the course of inflammation, and this may be driving the increase in miR-181a association. Performing qPCRs and Western blots looking at Ago2 over an inflammatory time course would determine whether Ago2 expression is changing. On the other hand, it could be that miR-181a is associating with other Ago proteins during inflammation. To determine whether this is occurring, IPs for the other Ago proteins could be performed.

Furthermore, Mazumder *et al.,* (2013) found that Ago2 is phosphorylated upon LPS induction of inflammation in RAW 264.7 mouse macrophages. This phosphorylation of Ago2 results in let-7a, miR-155, miR-21, miR-146a and miR-16 dissociating from Ago2, before it is suggested that Ago2 is then dephosphorylated allowing the reassociation of miRNAs. Mazumder *et al.,* (2013) propose this dissociation of miRNAs at the onset of inflammation facilitates the increase in expression of key inflammatory mediators allowing inflammation to progress. However, how long the RAW 264.7 cells were treated with LPS before the reduction of these miRNAs within the Ago2 IP was seen is not indicated. Furthermore, the reassociation of miRNAs with Ago2 is also not shown. Observations of IL-6 and TNF mRNA levels within the Ago2 IP were conducted at a four hour LPS time point and show a decrease in IL6 and TNF mRNA isolated at four hours compared to zero hours. This is in contrast to findings within this study where there is no drop in TNF mRNA within Ago2 immunoprecipitants at four hours of LPS treatment compared to zero hours. Furthermore, when looking at miR-181a association with Ago2, there is no decrease in miR-181a levels at any LPS time point compared to the zero hour time point for either the one hour or six hour time courses. It could be that within this study the phosphorylation and dephosphorylation of Ago2 is occurring very rapidly within the first 15 mins of inflammation. As such, what is observed within the Ago2 IPs of this study may be the gradual reassociation of miR-181a after the phosphorylation and dephosphorylation events. Ago2 phosphorylation could be examined using western blots looking at the phosphorylation states of Ago2 over the course of inflammation, with a particular focus on very early time points. Furthermore, expression of a mutant Ago2 with the phosphorylation sites changed along with IPs looking at miR-181a and TNF mRNA association would facilitate the investigation of how Ago2 phosphorylation may be affecting miR-181a and TNF mRNA association.

To further examine how miRNA regulation is changing during inflammation RNA seq for miRNA and mRNA on Ago2 immunoprecipitants from several LPS time points could be performed. This could generate a global picture of how miRNA regulation of many mRNAs is changing over the course of inflammation within this model, alongside generating a global picture of how miRNA associations within Ago2 are changing during inflammation. In particular, a HITS-CLIP approach could be taken to globally identify miRNA targets more stringently.

Currently, there is variability in the Ago2 IP data. Pull down efficiency can vary between experiments, as can the quality of the RNA isolation due to the tendency of the RNA pellets to float. The addition of a cross linking step for future experiments could help reduce some of the variability. Furthermore, each time point is only normalised to a 20% input sample, with no housekeeping control. Therefore, changing levels of TNF mRNA over the course of inflammation may be affecting relative enrichment of TNF within the Ago2 immunoprecipitants.

6.3 Changing poly(A) tail lengths of TNF mRNA are not affected by miR-181a regulation.

The technique used to investigate poly(A) tail changes for TNF mRNA was the PAT assay. The PAT assay is good for determining general poly(A) tail changes over time, however, there are some consistent limitations of the PAT assay. One limitation is the formation of multimer bands. Multimer bands form during the repeat melting and annealing steps. Loops of unpaired A or T nucleosides within different fragments pair with each other generating the multimer bands. These multimer bands have a chance of obscuring longer poly(A) tail lengths. However, these multimer bands do tend to track the general changes in poly(A) tail length, meaning the PAT assay is still a reliable indicator of general changes in poly(A) tail lengths.

Another limitation is that the PAT technique is end point PCR. This is particularly relevant to the experiments where PAT assays were performed following Ago2 IP. The Ago2 IP is not perfectly specific and as such there is likely to be some contaminating TNF mRNA that is unbound by miRNAs that will also be amplified. These contaminating TNF transcripts may then be obscuring the poly(A) tail lengths of TNF transcripts that are bound by miRNAs.

In the future, an alternative to the PAT assay could be to use Oxford nanopore sequencing to directly measure the poly(A) tail lengths of TNF mRNA over the course of inflammation. As the rate of movement through the pore is constant (Krause *et al.,* 2019), it can be used to determine how many adenosine residues are within a given poly(A) tail. Utilising this direct sequencing method would provide a quantitative measure of poly(A) tail length as well as allow for the identification of any longer poly(A) tail lengths within a sample that were originally obscured by multimer bands. Furthermore, Oxford nanopore sequence may allow for the

identification of any effect of miRNA mediated deadenylation at different time points during inflammation as it would be possible to look individual transcripts giving a more precise range of poly(A) tail lengths at each time point.

Additionally, direct sequencing of poly(A) tails within Ago2 immunoprecipitants using Oxford nanopore over different LPS time points could also be used to identify differences in poly(A) tail length for transcripts that are actively regulated by miRNAs over the inflammatory response. These tail lengths can then be compared to the general pool of mRNA as an indicator of which mRNAs are undergoing greater miRNA mediated deadenylation.

The lack of change seen for the poly(A) tail length of TNF mRNA with miR-181a inhibition and overexpression could be due to miR-181a acting more at the level of translation, particularly as a greater effect of miR-181a regulation on TNF protein levels was observed. As such, miR-181a may not be mediating deadenylation of TNF mRNA, leading to the lack of effect of miR-181a regulation on TNF poly(A) tail length. Rissland *et al.,* (2017) found that miRNAs can alter the association of PABPC and eIF4G with the mRNA and poly(A) tail without impacting on poly(A) tail length. The disruption of PABPC and eIF4G interaction prevents the formation of a closed loop reducing translational efficiency of a transcript. In the future, it would be interesting to look at PABPC association with the poly(A) tail of TNF transcripts using PABPC IPs in combination with miR-181a inhibition and overexpression. This would provide insight as to whether miR-181a is affecting PABPC association with the poly(A) tail of TNF during inflammation.

Interestingly, within this study it has been found that TENT4A and TENT4B are required for the maintenance of high TNF mRNA levels later in the inflammatory response. Kwak *et al.,* (2022), found that there were global changes in cytoplasmic polyadenylation leading to widespread changes in poly(A) tail length of mRNAs induced during inflammation. However, Kwak *et al.,* (2022) were not able to identify the PAP responsible. As TENT4A and B are non-canonical polymerases, it could be that TENT4A/B are contributing to these widespread poly(A) tail changes during inflammation. PAT assays in combination with TENT4A/B KD could be performed to look at whether TENT4A/B are directly affecting the poly(A) tails of TNF. Furthermore, RNA seq on TENT4A/B siRNA knockdown over the course of

inflammation could be used to look at whether the expression and poly(A) tail lengths of these genes are affected by TENT4A/B action.

Furthermore, TENT4A and TENT4B have been found to have mixed tailing capabilities with a preference for adding guanosine residues to the end of poly(A) tails (Lim *et al.,* 2018). Lim *et al.,* (2018) found that these non-adenosine residues can block deadenylation mediated by the CCR4-NOT complex. Additionally, mixed tailing by TENT4A/B was found to occur more frequently in ER-associated mRNAs, as TNF mRNA encodes a secreted protein, TNF mRNA is also enriched at the ER. Direct sequencing of the poly(A) tails of TNF mRNA at different LPS time points would allow for the identification of whether TENT4A/B are performing their mixed tailing capabilities within inflammation or whether their mode of action for maintaining high TNF mRNA levels is different. TENT4A/B knockdowns in combination with miR-181a inhibition over an inflammatory time course could also be performed to look at the interaction of miR-181a regulation with the effects of TENT4A/B. Additionally, the action of TENT4A/B within inflammation could be looked at at a more global level by comparing RNA seq data sets for TENT4A/B siRNA knockdown versus a negative control. This would determine whether TENT4A/B are required for the maintenance of high levels of other excreted cytokines during inflammation.

6.4 Investigation of miR-181a regulation via the TNF 3'UTR under transcriptional induction

To look specifically at miR-181a regulation of the TNF 3'UTR under transcriptional induction, a tetracycline/doxycycline inducible cell line was created. This allows for the investigation of the effects of transcriptional induction on miR-181a regulation via the TNF 3'UTR without the other confounding processes that are occurring during inflammation. As miR-181a repression of protein production from a luciferase reporter containing the TNF 3'UTR within HEK 293 cells has been established, this system was selected to be inserted into a tetracycline/doxycycline inducible promoter within a Flp-in T-rex HEK 293 cell line.

Generation of the Tet Luc TNF 3'UTR HEK 293 cell line was successful, and transcriptional induction of the Luc TNF 3'UTR mRNA can be observed. However, no luciferase protein was detectable under any condition tested. The exact reason as to why protein expression is not observed is unknown. To establish whether there was a mutation in the sequence responsible for the lack of protein expression, the pcDNA

Luc TNF 3'UTR plasmid was re-sequenced using a series of primers to establish the sequence of the entire plasmid and no mistakes were found. Additionally, the PCR fragment generated from amplifying genomic DNA used for genotyping was also sequenced and reveal to also have the correct sequence. There is still a possibility that part of the sequence is incorrect and there could be the formation of a truncated protein that is not functional for detection in luciferase assays. In the future, western blotting for the firefly luciferase protein could be performed as a secondary measure to check for the induction of protein expression, as a truncated protein would be detected. It could also be that there was a problem with the luminometer. While luciferase assays using exogenous reporters were successful, luciferases assays with the Tet Luc TNF 3'UTR HEK 293 cell line were performed much later and no check was performed to confirm that the luminometer was working correctly.

It could also be that miR-181a is translationally repressing the Luc TNF 3'UTR mRNA, preventing the production of protein. As such miR-181a inhibition experiments alongside luciferase assays and western blots could be used to establish whether it is translational repression that is occurring. Expression of the Luc TNF 3'UTR gene from an endogenous locus may also be much lower than that of exogenous reporters, meaning there is generally much less mRNA and protein being produced that is able to be detected. In the future, luciferases assays could be performed with a greater input, to see if this improves detection.

Despite the limitations of the Tet Luc TNF 3'UTR HEK 293 inducible cell line, it is still a useful tool to study miR-181a regulation via the TNF 3'UTR under transcriptional induction at the mRNA level. In the future, the AREs within the TNF 3'UTR could be removed allowing for the investigation of how regulation via the AREs is interacting with miR-181a regulation during transcriptional induction outside of the context of the inflammatory response. HuR and TTP are known to bind to the AREs within the TNF 3'UTR (Dean *et al.,* 2001, Fabian *et al.,* 2013). Furthermore, HuR has already been implicated in affecting miRNA regulation within other systems (Mukherjee *et al.,* 2016, Goswami *et al.,* 2020, Kundu *et al.,* 2012, Poria *et al.,* 2016). Furthermore, the role of TENT4A/B could also be examined within this system to see if the AREs, ARE binding proteins or other 3'UTR features are potentially responsible for the recruitment and therefore action of TENT4A/B or whether the effects of TENT4A/B are indirect.

6.5 Conclusions

Overall the studies within this thesis have confirmed that TNF mRNA undergoes poly(A) tail length elongation early into the inflammatory response (Crawford, 1997, Gandhi, 2016) (Figure 52A). However, the poly(A) polymerase responsible for these tail elongations has not been identified. There is a possibility that the TENT4A/B non-canonical polymerases may be facilitating these tail elongations. However, further investigation is needed to establish the exact role TENT4A/B are playing.

Furthermore, TENT4A/B alongside HuR are required for maintenance of high TNF mRNA levels (Figure 52B). It may be instead or alongside facilitating TNF mRNA poly(A) tail elongations, TENT4A/B may also be performing mixed tailing, adding guanosine residues to the end of the poly(A) tail. This addition of guanosine residues may be contributing to the ability of TENT4A/B to maintain high TNF mRNA levels within inflammation by preventing the action of the CCR4-NOT complex. The guanosine residues cause the CCR4-NOT complex to stall, slowing down deadenylation and therefore degradation of mRNA transcripts (Lim *et al.,* 2018). However, more investigation looking at the composition of the poly(A) tail length of TNF would be required to determine whether TENT4A/B are facilitating mixed tailing within this system.

There is also the possibility that TENT4A/B are interacting with HuR to facilitate either the recruitment of HuR to the TNF mRNA or vice versa, HuR may be facilitating the recruitment of TENT4A/B to the TNF mRNA transcript. But this also requires further investigation.

Another key finding of this thesis is that miR-181a is facilitating the translational repression of TNF mRNA transcript as opposed to facilitating their degradation (Figure 52C). It would be interesting to see if this is the case for other miRNAs that regulate cytokine expression during inflammation.

Finally, miR-181a regulation of TNF mRNA has been found to increase as the inflammatory response progresses. However, the exact mechanism facilitating this increased association with Ago2 and therefore increased regulation is not known. It could be that Ago2 expression is increasing over the course of inflammation facilitating greater miRNA regulation. Alternatively, it could also be that the

phosphorylation state of Ago2 is changing over the course of the response affecting how miRNAs interact with the Ago2 complex as inflammation progresses. Another alternative is that miR-181a may be sequestered away by a sponge at early stages in the inflammatory response and is released as inflammation progresses facilitatin greater regulation of TNF mRNA (Figure 52D). However, further investigation is needed to determine exactly what is occurring.

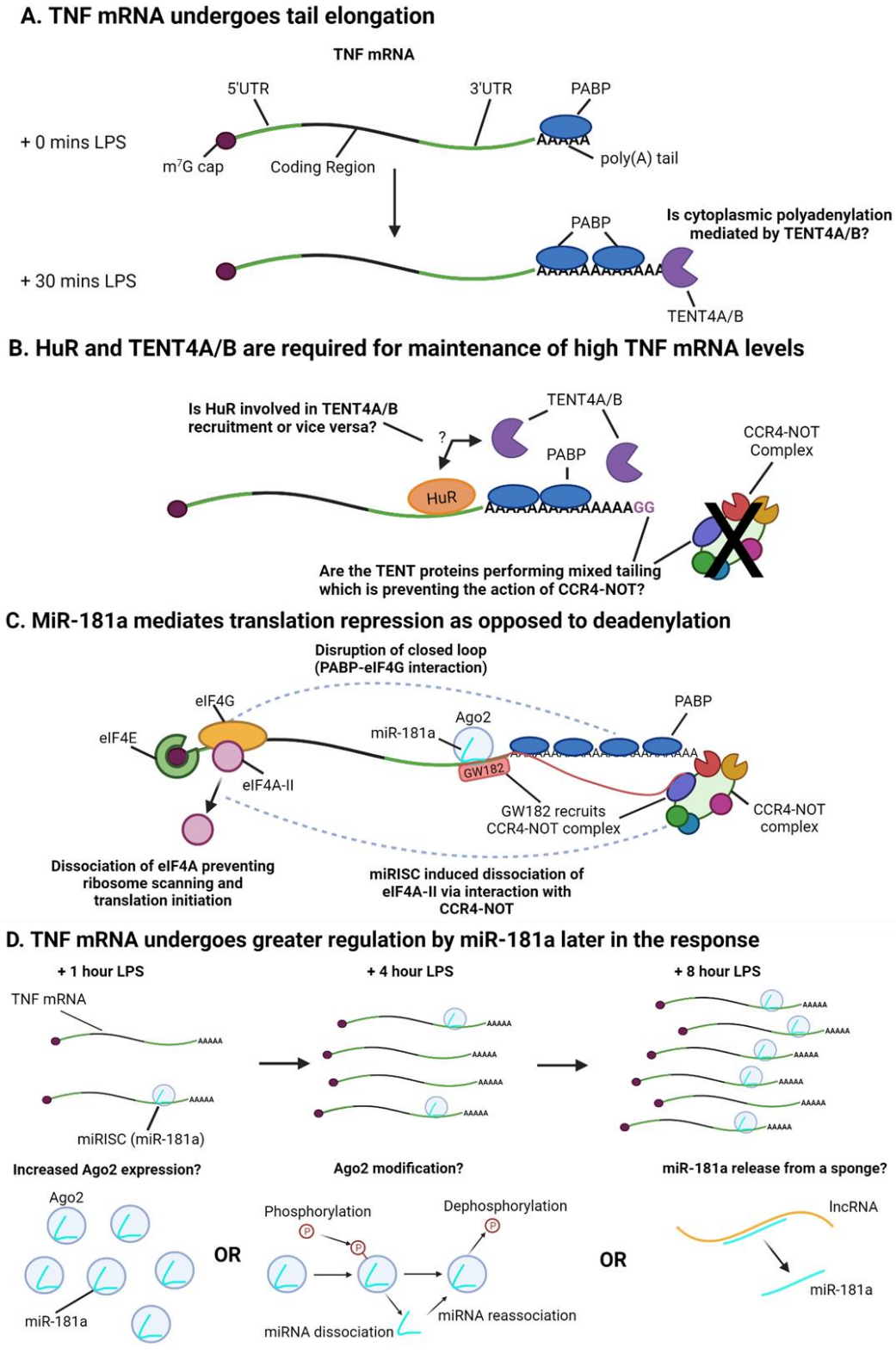

Figure 52. Graphical representation of thesis findings and conclusions. A. TNF mRNA undergoes tail elongation after 30 mins of stimulation with LPS. **B.** Both HuR and TENT4A/B expression are required for maintenance of high TNF mRNA levels after 1 hour of inflammation. **C.** MiR-181a is mediating translational repression of TNF mRNA as opposed to deadenylation. **D.** TNF mRNA undergoes greater regulation by miR-181a later in the inflammatory response.

Chapter 7 - References

Adam. SA, Nakagawa. T, Swanson. MS, Woodruff. TK, Dreyfuss. G. mRNA polyadenylate-binding protein: gene isolation and sequencing and identification of a ribonucleoprotein consensus sequence. (1986) *Mol Cell Biol* **6** 2932–2943.

Ahrenstedt. O, Hällgren. R, Knutson. L, Jejunal release of prostaglandin E2 in Crohn's disease: Relation to disease activity and first-degree relatives. (1994). *J. Gastroenterol. Hepatol.* **9**, 539–543

Akira. S., Uematsu. S., and Takeuchi. O. (2006). Pathogen recognition and innate immunity. *Cell.* **124,** 783–801.

Akman. H.B., and Erson-Bensan. A.E. (2014) Alternative polyadenylation and its impact on cellular processes. *MicroRNA.* **3**.

Alhusaini, N. & Coller, J. The deadenylase components Not2p, Not3p, and Not5p promote mRNA decapping. (2016) *RNA* **22** 709–721

Alivernini S, Gremese E, McSharry C, Tolusso B, Ferraccioli G, McInnes IB, Kurowska-Stolarska M. MicroRNA-155-at the Critical Interface of Innate and Adaptive Immunity in Arthritis. (2018) *Front Immunol.* **8** 1932.

Altmann, M., et al., The Saccharomyces cerevisiae translation initiation factor Tif3 and its mamalian homologue, eIF-4B, have RNA annealing activity (1995). *EMBO J*. **14**(15) 3820-3827.

Ameres. S. L., Horwich. M.D., Hung. J.H., Xu. J., Ghidiyal. M., Weng. Z., and Zamore. P.D. Target RNA-directed trimming and tailing of small silencing RNAs. (2010). *Science* **328**, 1534–1539.

An J, Zhu X, Wang H, Jin X. A dynamic interplay between alternative polyadenylation and microRNA regulation: implications for cancer. (2013) *Int J Oncol*. **43**(4) 995-1001.

Andreassi. C. & Riccio. A. To localize or not to localize: mRNA fate is in 3'UTR ends. (2009). *Trends in Cell Biology.* **19**, 465–474.

Apponi. L.H., Leung. S.W., Williams. K.R., Valentini. S.R., Corbett. A.H., and Pavlath. G.K. Loss of nuclear poly(A)-binding protein 1 causes defects in myogenesis and mRNA biogenesis. (2010) *Hum Mol Genet.* **19**(6) 1058-65.

ATCC (2023) *RAW 264.7* accessed 14th June 2023, < https://www.atcc.org/products/tib-71#required-products>

Auyeung. V.C., Ulitsky. I., McGeary. S.E., and Bartel. D.P. Beyond secondary structure: primary-sequence determinants license pri-miRNA hairpins for processing. (2013) *Cell* **152**, 844–858.

Baer, B. W. & Kornberg, R. D. The protein responsible for the repeating structure of cytoplasmic poly(A)-ribonucleoprotein. (1983) *J. Cell Biol.* **96** 717–721.

Baillat D, Shiekhattar R. Functional dissection of the human TNRC6 (GW182-related) family of proteins. (2009) *Mol Cell Biol.* **29**(15) 4144-55.

Baley. J., and Li. J. MicroRNAs and ovarian function. (2012) *Journal of Ovarian Research.* **5,** 8.

Barkoff, A., Ballantyne, S. & Wickens, M. Meiotic maturation in Xenopus requires polyadenylation of multiple mRNAs. (1998) *EMBO J.* **17** 3168–3175.

Barnard DC, Ryan K, Manley JL, Richter JD. Symplekin and xGLD-2 are required for CPEB-mediated cytoplasmic polyadenylation. (2004) *Cell.* **119**(5) 641-51.

Barnett. R.E., Conklin. D.J., Ryan. L., Keskey. R.C., Ramjee. V., Sepulveda. E.R., Srivastava.S., Bhatnagar. A., and Cheadle. W.G. Antiinflammatory effects of miR-21 in the macrophage response to peritonitis. (2016) *Journal of Leukocyte Biology.* **99**, 361-371.

Barral. P.M., Sarkar. D., Su. Z.Z., Barber. G.N., DeSalle. R., Racaniello. V.R., Fisher. P.B. Functions of the cytoplasmic RNA sensors RIG-I and MDA-5: key regulators of innate immunity. (2009) *Pharmacol Ther*. **124**(2) 219-34.

Barreau. C, Paillard. L, Osborne. H.B. AU-rich elements and associated factors: are there unifying principles? (2005) *Nucleic Acids Res.* **33**(22) 7138-50.

Bartel, D. P. MicroRNAs: target recognition and regulatory functions. (2009). *Cell.* **136**, 215–233.

Behm-Ansmant I, Rehwinkel J, Doerks T, Stark A, Bork P, Izaurralde E. mRNA degradation by miRNAs and GW182 requires both CCR4-NOT deadenylase and DCP1:DCP2 decapping complexes. *Genes Dev.* (2006) **20** 1885–98.

Berndt H, Harnisch C, Rammelt C, Stöhr N, Zirkel A, Dohm JC, Himmelbauer H, Tavanez JP, Hüttelmaier S, Wahle E. Maturation of mammalian H/ACA box snoRNAs: PAPD5-dependent adenylation and PARN-dependent trimming. (2012) *RNA* **18**(5) 958-72.

Bernstein, P., Peltz, S. W. & Ross, J. The poly(A)-poly(A)-binding protein complex is a major determinant of mRNA stability in vitro. (1989) *Mol. Cell. Biol.* **9** 659–670.

Bhattacharyya, S.N, Habermacher. R, Martine. U, Closs. E.I, Filipowicz. W. Relief of microRNA-mediated translational repression in human cells subjected to stress. (2006) *Cell 125* 111-1124

Bi, X. & Goss, D. J. Wheat germ poly(A)-binding protein increases the ATPase and the RNA helicase activity of translation initiation factors eIF4A, eIF4B, and eIF-iso4F. (2000) *J. Biol. Chem.* **275**, 17740–17746.

Boele. J., Persson. H., Shin. J.W., et al. PAPD5-mediated 3’ adenylation and subsequent degradation of miR-21 is disrupted in proliferative disease. (2014). *Proceedings of the National Academy of Sciences USA* **111**, 11467–11472.

Boldin. M. P., Taganov. K. D., Rao. D. S., *et al*. miR-146a is a significant brake on autoimmunity, myeloproliferation, and cancer in mice. (2011) *The Journal of experimental medicine*, **208**, 1189–1201.

Borman, A. M., Michel, Y. M. & Kean, K. M. Biochemical characterisation of cap-poly(A) synergy in rabbit reticulocyte lysates: the eIF4G-PABP interaction increases the functional affinity of eIF4E for the capped mRNA 5’-end. (2000) *Nucleic Acids Res.* **28** 4068–4075.

Bradley, J.R. TNF-Mediated inflammatory disease. (2008) *J. Pathol.* **214** 149–160

Braun JE, Huntzinger E, Fauser M, Izaurralde E. GW182 proteins directly recruit cytoplasmic deadenylase complexes to miRNA targets. (2011) *Mol Cell.* **44**(1) 120-33.

Braun. J.E., Truffault. V., Boland. A., Huntsinger. E., Chang. C.T., Haas. G., Weichernrieder. O., Coles. M., and Izaurralde. E. A direct interaction between DCP1 and XRN1 couples mRNA decapping to 5' exonucleolytic degradation. (2012) *Nature Structural and Molecular Biology.* **19**, 1324–1331.

Braun JE, Huntzinger E, Izaurralde E. The role of GW182 proteins in miRNA-mediated gene silencing. (2013) *Adv Exp Med Biol.* **768** 147–163

M. Brengues, D. Teixeira, R. Parker. Movement of eukaryotic mRNAs between polysomes and cytoplasmic processing bodies. (2005) *Science,* **310** 486-489

Brennan CM, Steitz JA. HuR and mRNA stability. (2001) *Cell Mol Life Sci*. **58**(2) 266-77.

Brenner, D. Blaser, H.; Mak, T.W. Regulation of tumour necrosis factor signalling: Live or let die. (2015) *Nat. Rev. Immunol.* **15** 362–374.

Brennan, J. J. & Gilmore, T. D. Evolutionary origins of Toll-like receptor signaling. (2018) *Mol. Biol. Evol.* **35** 1576–1587

Brikos C, O'Neill LA. Signalling of toll-like receptors. (2008) *Handb Exp Pharmacol*. **183** 21-50.

Broderick, J. A. & Zamore, P. D. Competitive endogenous RNAs cannot alter microRNA function *in vivo*. (2014) *Mol. Cell* **54**, 711–713

Brooks, S. A. & Blackshear, P. J. Tristetraprolin (TTP): interactions with mRNA and proteins, and current thoughts on mechanisms of action. (2013) *Biochim. Biophys. Acta* **1829** 666–679

Brown, K.M. and G.M. Gilmartin, A mechanism for the regulation of pre-mRNA 3' processing by human cleavage factor Im. (2003) *Mol Cell*. **12**(6) 1467-76.

Buccitelli C, Selbach M. mRNAs, proteins and the emerging principles of gene expression control. (2020) *Nat Rev Genet.* **21**(10) 630-644.

Burdon PC, Martin C, Rankin SM. The CXC chemokine MIP-2 stimulates neutrophil mobilization from the rat bone marrow in a CD49d-dependent manner. (2005) *Blood.* **105**(6) 2543-8.

Burke SJ, Lu D, Sparer TE, Masi T, Goff MR, Karlstad MD, Collier JJ. NF-κB and STAT1 control CXCL1 and CXCL2 gene transcription. (2014) *Am J Physiol Endocrinol Metab*. **306**(2) E131-49.

Burns, D. M., D'Ambrogio, A., Nottrott, S. & Richter, J. D. CPEB and two poly(A) polymerases control miR-122 stability and p53 mRNA translation. (2011) *Nature* **473** 105–108.

Burroughs AM, Ando Y, de Hoon MJ, Tomaru Y, Nishibu T, Ukekawa R, Funakoshi T, Kurokawa T, Suzuki H, Hayashizaki Y, Daub CO. A comprehensive survey of 3' animal miRNA modification events and a possible role for 3' adenylation in modulating miRNA targeting effectiveness. (2010) *Genome Res*. **20**(10) 1398-410.

Caput D, Beutler B, Hartog K, Thayer R, Brown-Shimer S, Cerami A. Identification of a common nucleotide sequence in the 3'-untranslated region of mRNA molecules specifying inflammatory mediators. (1986) *Proc Natl Acad Sci U S A.* **83**(6) 1670-4.

Carballo, E., Lai, W. S. & Blackshear, P. J. Feedback inhibition of macrophage tumour necrosis factor-alpha production by tristetraprolin. (1998) *Science* **281** 1001–1005.

Carmody, S.R. and S.R. Wente, mRNA nuclear export at a glance. (2009) *J Cell Sci.* **122**(12) 1933-7.

Carpenter S, Ricci EP, Mercier BC, Moore MJ, Fitzgerald KA. Post-transcriptional regulation of gene expression in innate immunity. (2014) *Nat Rev Immunol.* **14**(6) 361-76.

Cekic C, Casella CR, Sag D, Antignano F, Kolb J, Suttles J, Hughes MR, Krystal G, Mitchell TC. MyD88-dependent SHIP1 regulates proinflammatory signaling pathways in dendritic cells after monophosphoryl lipid A stimulation of TLR4. (2011) *J Immunol.* **186**(7) 3858-65.

Chamaillard M, Hashimoto M, Horie Y, Masumoto J, Qiu S, Saab L, Ogura Y, Kawasaki A, Fukase K, Kusumoto S, Valvano MA, Foster SJ, Mak TW, Nuñez G, Inohara N. An essential role for NOD1 in host recognition of bacterial peptidoglycan containing diaminopimelic acid. (2003) *Nat Immunol*. **4**(7) 702-7.

Chang, H. et al. Terminal uridylyltransferases execute programmed clearance of maternal transcriptome in vertebrate embryos. (2018) *Mol. Cell* **70** 72–82

Chatterjee, S., Fasler, M., Büssing, I., & Großhans, H. Target-mediated protection of endogenous MicroRNAs in *C. elegans* . (2011). *Developmental Cell*, **20**(3), 388–396.

Cheloufi, S., Dos Santos, C. O., Chong, M. M. & Hannon, G. J. A Dicer-independent miRNA biogenesis pathway that requires AGO catalysis. (2010) *Nature* **465**, 584–589.

Chen CY, Shyu AB. AU-rich elements: characterization and importance in mRNA degradation. (1995) *Trends Biochem Sci.* **20**(11) 465-70.

Chen. Y., Boland. A., Kuzuoglu-Ozturk. D., Bawankar. P., Loh. B., Chang. C.T., Weichenrieder. O., and Izaurralde. E. A DDX6-CNOT1 complex and W-binding pockets in CNOT9 reveal direct links between miRNA target recognition and silencing. (2014) *Molecular Cell.* **54**, 737–750.

Chiurchiù V, Leuti A, Maccarrone M. Bioactive Lipids and Chronic Inflammation: Managing the Fire Within. (2018) *Front Immunol.* **9** 38.

Chorghade,S., Seimetz,J., Emmons,R., Yang,J., Bresson,S.M., De Lisio,M., Parise,G., Conrad,N.K. and Kalsotra,A. Poly(A) tail length regulates PABPC1 expression to tune translation in the heart. (2017) *Elife*, 10.7554/eLife.24139.001.

Chow KT, Gale M Jr, Loo YM. RIG-I and Other RNA Sensors in Antiviral Immunity. (2018) *Annu Rev Immunol.* **36** 667-694.

Chuenchor W, Jin T, Ravilious G, Xiao TS. Structures of pattern recognition receptors reveal molecular mechanisms of autoinhibition, ligand recognition and oligomerization. (2104) *Curr Opin Immunol*. **26** 14-20.

Cichocki, F., Grzywacz, B., & Miller, J. S. Human NK Cell Development: One Road or Many? (2019) *Frontiers in immunology*, **10** 2078.

Cifuentes, D. et al. A novel miRNA processing pathway independent of Dicer requires Argonaute2 catalytic activity. (2010) *Science* **328**, 1694–1698.

Córdova-Rivas S, Fraire-Soto I, Mercado-Casas Torres A, Servín-González LS, Granados-López AJ, López-Hernández Y, Reyes-Estrada CA, Gutiérrez-Hernández R, Castañeda-Delgado JE, Ramírez-Hernández L, Varela-Silva JA, López JA. 5p and 3p Strands of miR-34 Family Members Have Differential Effects in Cell Proliferation, Migration, and Invasion in Cervical Cancer Cells. (2019) *Int J Mol Sci.* **20**(3) 545.

Cornett AL, Lutz CS. Regulation of COX-2 expression by miR-146a in lung cancer cells. (2014) *RNA.* **20**(9) 1419-30.

Corsetti. P.P., de Almeida. L.A., Goncalves. A.N.A., Gomes. M.T.R., Guimaraes. E.S., Marques. J.T., and Oliveira. S.C.. miR-181a-5p regulates TNF-a and miR-21a-5p influences gualynate-binding protein 5 and IL-10 expression in macrophages affecting host control of *Brucella* abortus infection. (2018) *Frontiers in Immunology.* **9** 1331.

Crawford EK, Ensor JE, Kalvakolanu I, Hasday JD. The role of 3' poly(A) tail metabolism in tumor necrosis factor-alpha regulation. (1997) *J Biol Chem*. **272**(34) 21120-7.

Cuchet-Lourenço D, Eletto D, Wu C, Plagnol V, Papapietro O, Curtis J, Ceron-Gutierrez L, Bacon CM, Hackett S, Alsaleem B, Maes M, Gaspar M, Alisaac A, Goss E, Alldrissi E, Siegmund D, Wajant H, Kumararatne D, AlZahrani MS, Arkwright PD, Abinun M, Doffinger R, Nejentsev S. Biallelic *RIPK1* mutations in humans cause severe immunodeficiency, arthritis, and intestinal inflammation. (2018) *Science*. **361**(6404) 810-813.

Curtale. G., Mirolo. M., Renzi. T.A., Rossato. M., Bazzoni. F., and Locati. M. Negative regulation of toll-like receptor 4 signalling by IL-10-dependent microRNA-146b. (2013) *Proceedings of the National Academy of Sciences USA*. **110**, 11499-11504.

Curtale. G., Rubino. M., and Locati. M. MicroRNAs as molecular switches in macrophage activation. (2019) *Frontiers in Immunology.* **10**, 799.

Dambuza IM, Brown GD. C-type lectins in immunity: recent developments. (2015) *Curr Opin Immunol.* **32** 21-7.

Dan C, Jinjun B, Zi-Chun H, Lin M, Wei C, Xu Z, Ri Z, Shun C, Wen-Zhu S, Qing-Cai J, Wu Y. Modulation of TNF-α mRNA stability by human antigen R and miR181s in sepsis-induced immunoparalysis. (2015) *EMBO Mol Med.* **7**(2) 140-57.

Dean JL, Wait R, Mahtani KR, Sully G, Clark AR, Saklatvala J . The 3' untranslated region of tumor necrosis factor alpha mRNA is a target of the mRNA-stabilizing factor HuR. (2001) *Mol Cell Biol* **21** 721 – 730

Daub, J. et al. The RNA WikiProject: community annotation of RNA families. (2008) *RNA* **14** 2462–2464.

Davis-Dusenbery, B. N. & Hata, A. Mechanisms of control of microRNA biogenesis. (2010) *J. Biochem.* **148** 381–392.

Decker CJ, Parker R. A turnover pathway for both stable and unstable mRNAs in yeast: evidence for a requirement for deadenylation. (1993) *Genes Dev*. **7**(8) 1632-43.

De Filippo, K, Henderson RB, Laschinger M, Hogg N. Neutrophil chemokines KC and macrophage-inflammatory protein-2 are newly synthesized by tissue macrophages using distinct TLR signaling pathways. (2008) *J Immunol*. **180** 4308-4315.

Deo, R.C., et al., Recognition of polyadenulate RNA by the poly(A)-binding protein. (1999) *Cell*. **98** 835-845.

Derti A, Garrett-Engele P, Macisaac KD, Stevens RC, Sriram S, Chen R, et al. A quantitative atlas of polyadenylation in five mammals. (2012) *Genome Res*. **22**(6) 1173–83

Dever, T.E. and R. Green, The Elongation, Termination and Recycling Phases of Translation in Eukaryotes. (2012*) Cold Spring Harbor perspectives in biology*. **4**(7) a013706-a013706.

Dey I, Lejeune M, Chadee K. Prostaglandin E2 receptor distribution and function in the gastrointestinal tract. (2006) *Br J Pharmacol*. **149**(6) 611-23.

Diebold SS, Kaisho T, Hemmi H, Akira S, Reis e Sousa C. Innate antiviral responses by means of TLR7-mediated recognition of single-stranded RNA. (2004) *Science*. **303**(5663) 1529-31.

Diederichs. S., and Haber. D.A. Dual role for argonautes in MicroRNA processing and posttranscriptional regulation of microRNA expression. (2007) *Cell.* **131**, 1097–1108.

Dubois RN, Abramson SB, Crofford L, Gupta RA, Simon LS, Van De Putte LB, Lipsky PE. Cyclooxygenase in biology and disease. (1998) *FASEB J.* **12** 1063–1073.

Ebert, M. S., Neilson, J. R. & Sharp, P. A. MicroRNA sponges: competitive inhibitors of small RNAs in mammalian cells. (2007) *Nat. Methods* **4**, 721–726.

Ebner S, Sharon N, Ben-Tal N. Evolutionary analysis reveals collective properties and specificity in the C-type lectin and lectin-like domain superfamily. (2003) *Proteins.* **53**(1) 44-55.

Eckmann. C.R., Rammelt. C., and Wahle. E. Control of poly(A) tail length. (2010) *WIREs RNA.* ***2.***

Edmonds M, Vaughan MH Jr, Nakazato H. Polyadenylic acid sequences in the heterogeneous nuclear RNA and rapidly labelled polyribosomal RNA of HeLa cells: possible evidence for a precursor relationship. (1971) *Proc Natl Acad Sci U S A.* **68**(6) 1336-40.

Eisen. T.J., Eichhorn. S.W., Subtelny. A.O., and Bartel. D.P. MicroRNAs cause accelerated decay of short-tailed target mRNAs. (2020) *Molecular Cell.* **77** 775-785.

Elkayam,E., Faehnle,C.R., Morales,M., Sun,J., Li,H. and Joshua-Tor,L. Multivalent recruitment of human Argonaute by GW182. (2017) *Mol. Cell*. **67** 646–658.

Elkon. R., Ugalde. A.P., and Agami. R. Alternative cleavage and polyadenylation: extent, regulation and function. (2013) *Nature Genetics.* **14** 496- 506.

Fabian MR, Mathonnet G, Sundermeier T, Mathys H, Zipprich JT, Svitkin YV, Rivas F, Jinek M, Wohlschlegel J, Doudna JA, Chen CY, Shyu AB, Yates JR 3rd, Hannon GJ, Filipowicz W, Duchaine TF, Sonenberg N. Mammalian miRNA RISC recruits CAF1 and PABP to affect PABP-dependent deadenylation. (2009) *Mol Cell.* **35**(6) 868-80.

Fabian MR, Frank F, Rouya C, Siddiqui N, Lai WS, Karetnikov A, Blackshear PJ, Nagar B, Sonenberg N. Structural basis for the recruitment of the human CCR4-NOT deadenylase complex by tristetraprolin. (2013) *Nat Struct Mol Biol*. **20**(6) 735-9.

Fan XC, Steitz JA. Overexpression of HuR, a nuclear-cytoplasmic shuttling protein, increases the in vivo stability of ARE-containing mRNAs. (1998) *EMBO J.* **17**(12) 3448-60.

Farhat K, Riekenberg S, Heine H, Debarry J, Lang R, Mages J, Buwitt-Beckmann U, Röschmann K, Jung G, Wiesmüller KH, Ulmer AJ. Heterodimerization of TLR2 with TLR1 or TLR6 expands the ligand spectrum but does not lead to differential signaling. (2008) *J Leukoc Biol*. **83**(3) 692-701.

Faust C, Beil C, Dittrich W, Rao E, Langer T. Impact of lipopolysaccharides on cultivation and recombinant protein expression in human embryonal kidney (HEK-293) cells. (2021) *Eng Life Sci*. **21**(11) 778-785.

Faustman D, Davis M. TNF receptor 2 pathway: drug target for autoimmune diseases. (2010) *Nat Rev Drug Discov***.** **9**(6) 482-93.

Fernandez-Miranda. G., and Mendez. R. The CPEB-family of proteins, translational control in senescence and cancer. (2014) *Aging Research Reviews.* **11** 460-472.

Ferrante CJ, Leibovich SJ. Regulation of Macrophage Polarization and Wound Healing. (2012) *Adv Wound Care (New Rochelle).* **1**(1) 10-16.

Ferrer RA, Saalbach A, Grünwedel M, Lohmann N, Forstreuter I, Saupe S, Wandel E, Simon JC, Franz S. Dermal Fibroblasts Promote Alternative Macrophage Activation Improving Impaired Wound Healing. (2017) *J Invest Dermatol.* **137**(4) 941-950.

Filipowicz, W., et al., A protein binding the methylated 5'-terminal sequence, m7GpppN, of eukaryotic messenger RNA. (1976) *Proc Natl Acad Sci U S A.* **73**(5) 1559-63.

Flaherty, S.M., et al., Participation of the nuclear cap binding complex in pre-mRNA 3' processing. (1997) *Proc Natl Acad Sci U S A.* **94**(22) 11893-8.

Font-Nieves M., Sans-Fons M. G., Gorina R., Bonfill-Teixidor E., Salas-Perdomo A., Marquez-Kisinousky L., et al. Induction of COX-2 enzyme and down-regulation of COX-1 expression by lipopolysaccharide (LPS) control prostaglandin E2 production in astrocytes. (2012) *J. Biol. Chem.* **287** 6454–6468.

Forman, J. J., Legesse-Miller, A. & Coller, H. A. A search for conserved sequences in coding regions reveals that the let-7 microRNA targets Dicer within its coding sequence. (2008) *Proc. Natl Acad. Sci. USA* **105** 14879–14884.

Fox. C.A., Sheets. M.D., and Wickens. M.P. Poly(A) addition during maturation of frog oocytes: distinct nuclear and cytoplasmic activities and regulation by the sequence UUUUUAU. (1989) *Genes and Development.* **3** 2151-2162.

Franca. G.S., Vibranovski. M.D., and Galtate. P.A. Host gene constraints and genomic context impact the expression and evolution of human microRNAs. (2016) *Nature communications.* **25** 11438.

Franken L, Schiwon M, Kurts C. Macrophages: sentinels and regulators of the immune system. (2016) *Cell Microbiol*. **18**(4) 475-87.

Freeman SA, Grinstein S. Phagocytosis: receptors, signal integration, and the cytoskeleton. (2014) *Immunol Rev.* **262**(1) 193-215.

Fujihara M, Muroi M, Tanamoto K, Suzuki T, Azuma H, Ikeda H . Molecular mechanisms of macrophage activation and deactivation by lipopolysaccharide: roles of the receptor complex. (2003) *Pharmacol Ther* **100** 171–194.

Fukaya. T., Iwakawa. H.O. and Tomari. Y. MicroRNAs block assembly of eIF4F translation initiation complex in Drosophila. (2014) *Molecular Cell.* **56** 67–78.

Fuke. H., and Ohno. M. Role of poly(A) tail as an identity element for mRNA nuclear export. (2008) *Nucleic Acids Research.* **36** 1037-1049.

Fukunaga, R. et al. Dicer partner proteins tune the length of mature miRNAs in flies and mammals. (2012) *Cell* **151** 533–546.

Funk CD. Prostaglandins and leukotrienes: advances in eicosanoid biology. *Science.* 2001;294:1871–1875.

Gandhi. R. (2016). The role of polyadenylation in the induction of inflammatory genes (unpublished doctoral dissertation) University of Nottingham, Nottingham, UK.

Gandhi J, Khera L, Gaur N, Paul C, Kaul R. Role of Modulator of Inflammation Cyclooxygenase-2 in Gamma herpes virus Mediated Tumorigenesis. (2017) *Front Microbiol.* **28**(8) 538.

Garneau NL, Wilusz J, Wilusz CJ. The highways and byways of mRNA decay. (2007) *Nat Rev Mol Cell Biol.* **8**(2) 113-26.

Gebert, L.F.R., MacRae, I.J. Regulation of microRNA function in animals. (2019) *Nat Rev Mol Cell Biol* **20**, 21–37.

Ginhoux, F. & Jung, S. Monocytes and macrophages: developmental pathways and tissue homeostasis. *Nat. Rev. Immunol.* (2014) **14** 392–404

Girardin SE, Boneca IG, Viala J, Chamaillard M, Labigne A, Thomas G, Philpott DJ, Sansonetti PJ. Nod2 is a general sensor of peptidoglycan through muramyl dipeptide (MDP) detection. (2003) *J Biol Chem.* **278**(11) 8869-72.

Golden. R.J, Chen.B, Li. T., Braun. J., Manjunath. H, Chen. X *et al.,* An Argonaute phosphorylation cycle promotes microRNA-mediated silencing. (2017) *Nature.* **542**(7640).

Gordon S, Taylor PR. Monocyte and macrophage heterogeneity. (2005) *Nat Rev Immunol.* **5**(12) 953-64.

Gorgoni B, Gray, N.K. The roles of cytoplasmic poly(A)-binding proteins in regulating gene expression: a developmental perspective (2004) *Brief. Fucnt. Genomics Proteomics.* **3** 125-141.

Goswami A, Mukherjee K, Mazumder A, Ganguly S, Mukherjee I, Chakrabarti S, Roy S, Sundar S, Chattopadhyay K, Bhattacharyya SN. MicroRNA exporter HuR clears the internalized pathogens by promoting pro-inflammatory response in infected macrophages. (2020) *EMBO Mol Med*. **12**(3) e11011.

Grell, M.; Douni, E.;Wajant, H.; Lohden, M.; Clauss, M.; Maxeiner, B.; Georgopoulos, S.; Lesslauer,W.; Kollias, G.; Pfizenmaier, K.; et al. The transmembrane form of tumor necrosis factor is the prime activating ligand of the 80 kDa tumor necrosis factor receptor. (1995) *Cell* **83** 793–802

Griffiths-Jones S, Hui JH, Marco A, Ronshaugen M. MicroRNA evolution by arm switching. (2011) *EMBO Rep.* **12**(2) 172-7.

Grimson. A., Farh. K.K., Johnston. W.K., Garrett-Engele. P., Lim. L.P., and Bartel. D.P. MicroRNA targeting specificity in mammals: determinants beyond seed pairing. (2007) *Molecular Cell*. **27** 91–105.

Grunberg, S. and S. Hahn, Structural insights into transcription initiation by RNA polymerase II. (2013) *Trends Biochem Sci.* **38**(12) 603-11.

Guilliams M, De Kleer I, Henri S, Post S, Vanhoutte L, De Prijck S, Deswarte K, Malissen B, Hammad H, Lambrecht BN. Alveolar macrophages develop from fetal monocytes that differentiate into long-lived cells in the first week of life via GM-CSF. (2013) *J Exp Med.* **210**(10) 1977-92.

Gutiérrez-Vázquez. C., Enright. A.J., Rodriguez-Galan. A., Perez-Garcia. A., Collier. P., Jones. M.R., Benes. V., Mizgerd. J.P., Mittelbrunn. M., Ramiro. A.R., and Sanchez-Madreid. F. 3' Uridylation controls mature microRNA turnover during CD4 T cell activation. (2017) *RNA* **23** 882–891.

Hake. L. E., and Richter. J.D. CPEB is a specificity factor that mediates cytoplasmic polyadenylation during Xenopus oocyte maturation. (1994) *Cell.* **79** 317-627.

Han J, Brown T, Beutler B. Endotoxin-responsive sequences control cachectin/tumor necrosis factor biosynthesis at the translational level. (1990) *J Exp Med.* **171** 465–475. (Erratum, **171** 971–972.

Hashimoto Y, Akiyama Y, Yuasa Y. Multiple-to-multiple relationships between microRNAs and target genes in gastric cancer. (2013) *PLoS One*. **8**(5) e62589

He. Y., Sun. X., Huang. C., Long. X.R., Lin. X., Zhang. L., Lv. X.W., and Li. J. MiR-146a regulates IL-6 production in lipopolysaccharide-induced RAW264.7 macrophage cells by inhibiting Notch1. (2014) *Inflammation*. **37** 71–82.

Heo I, Joo C, Cho J, Ha M, Han J, Kim VN. Lin28 mediates the terminal uridylation of let-7 precursor MicroRNA. (2008) *Mol Cell.* **32**(2) 276-84.

Heil F, Hemmi H, Hochrein H, Ampenberger F, Kirschning C, Akira S, Lipford G, Wagner H, Bauer S. Species-specific recognition of single-stranded RNA via toll-like receptor 7 and 8. (2004) *Science.* **303**(5663) 1526-9.

Hemmi H, Takeuchi O, Kawai T, Kaisho T, Sato S, Sanjo H, Matsumoto M, Hoshino K, Wagner H, Takeda K, Akira S. A Toll-like receptor recognizes bacterial DNA. (2000) *Nature.* **408**(6813) 740-5.

Heo, I. et al. TUT4 in concert with Lin28 suppresses microRNA biogenesis through pre-microRNA uridylation. (2009) *Cell* **138** 696–708

Herbert, K. M., Pimienta, G., DeGregorio, S. J., Alexandrov, A. & Steitz, J. A. Phosphorylation of DGCR8 increases its intracellular stability and induces a progrowth miRNA profile. (2013) *Cell Rep.* **5** 1070–1081.

Herzel, L., et al., Splicing and transcription touch base: co-transcriptional spliceosome assembly and function. (2017) *Nat Rev Mol Cell Biol*, **18**(10) 637-650.

Hopkinson-Woolley, J., Hughes, D., Gordon, S. & Martin, P. Macrophage recruitment during limb development and wound healing in the embryonic and foetal mouse. (1994) *J. Cell Sci.* **107** 1159–1167

Hoque. M. Ji. Z., Zheng. D., Luo. W., Li. W., You. B., Park. J.Y., Yehia. G., and Tian. B. Analysis of alternative cleavage and polyadenylation by 3‘ region extraction and deep sequencing. (2013) *Nature Methods* **10** 133–139.

Horiuchi, T.; Mitoma, H.; Harashima, S.; Tsukamoto, H.; Shimoda, T. Transmembrane TNF-alpha: Structure, function and interaction with anti-TNF agents. (2010) *Rheumatology*. **49** 1215–1228.

Hu, Q. et al. DICER- and AGO3-dependent generation of retinoic acid-induced DR2 *Alu* RNAs regulates human stem cell proliferation. (2012) *Nature Struct. Mol. Biol.* **19** 1168–1175.

Huang, H., et al., GTP hydrolysis controls stringent selection of the AUG start codon during translation initiation in Saccharomyces cerevisiae. (1997) *Genes Dev*. **11** 2396-2413.

Huntzinger. E., and Izaurralde, E. Gene silencing by microRNAs: contributions of translational repression and mRNA decay. (2011) *Nature Reviews Genetics.* **12** 99–110.

Hutchison ER, Kawamoto EM, Taub DD, Lal A, Abdelmohsen K, Zhang Y, et al. Evidence for miR-181 involvement in neuroinflammatory responses of astrocytes. (2013) *Glia* **61** 1018–28.

Hsu H, Xiong J, Goeddel DV . The TNF receptor 1-associated protein TRADD signals cell death and NF-kappa B activation. (1995) *Cell* **81** 495–504.

Icli B, Dorbala P, Feinberg MW. An emerging role for the miR-26 family in cardiovascular disease. (2014) *Trends Cardiovasc Med.* **24**(6) 241-8.

Indrieri A, Carrella S, Carotenuto P, Banfi S, Franco B. The Pervasive Role of the miR-181 Family in Development, Neurodegeneration, and Cancer. (2020) *Int J Mol Sci.* **21**(6) 2092.

Ivanov A, Mikhailova T, Eliseev B, Yeramala L, Sokolova E, Susorov D, Shuvalov A, Schaffitzel C, Alkalaeva E. PABP enhances release factor recruitment and stop codon recognition during translation termination. (2016) *Nucleic Acids Res*. **44**(16) 7766-76.

Ivshina. M., Lasko. P., and Richter. J.D. Cytoplasmic polyadenylation element binding proteins in development, health, and disease. (2014) *Annual Review of Cell and Developmental Biology.* **30** 393-415.

Izaurralde, E., et al., A cap binding protein that may mediate nuclear export of RNA polymerase II-transcribed RNAs. (1992) *J Cell Biol.* **118**(6) 1287-95.

Izaurralde, E., et al., A nuclear cap binding protein complex involved in pre-mRNA splicing. (1994) *Cell.* **78**(4) 657-68.

Jackson. R.J., Hellen. C.U., and Pestova. T.V. The mechanism of eukaryotic translation initiation and principles of its regulation. (2010) *Nature Reviews, Molecular Cell Biology.* **11** 113–127.

Jakubzick, C., Randolph, G. & Henson, P. Monocyte differentiation and antigen-presenting functions. (2017) *Nat Rev Immunol* **17**, 349–362

Jakymiw, A. et al. Disruption of GW bodies impairs mammalian RNA interference. (2005) *Nature Cell Biol.* **7** 1267–1274.

Janeway CA Jr, Travers P, Walport M, et al. Immunobiology: The Immune System in Health and Disease. 5th edition. New York: Garland Science; 2001. The components of the immune system.

Janeway CA Jr, Medzhitov R. Innate immune recognition. (2002) *Annu Rev Immunol.* **20** 197-216.

Jang, D.-i.; Lee, A-H.; Shin, H.-Y.; Song, H.-R.; Park, J.-H.; Kang, T.-B.; Lee, S.-R.; Yang, S.-H. The Role of Tumor Necrosis Factor Alpha (TNF-α) in Autoimmune Disease and Current TNF-αInhibitors in Therapeutics. (2021) *Int. J. Mol. Sci.* **22** 2719.

Jiang, H., Wolgast, M., Beebe, L. M. & Reese, J. C. Ccr4-Not maintains genomic integrity by controlling the ubiquitylation and degradation of arrested RNAPII. (2019) *Genes. Dev.* **33** 705–717

Jiang M, Dai J, Yin M, Jiang C, Ren M, Tian L. LncRNA MEG8 sponging miR-181a-5p contributes to M1 macrophage polarization by regulating SHP2 expression in Henoch-Schonlein purpura rats. (2021) *Ann Med.* **53**(1).

Jonas. S., and Izaurralde. E.. Towards a molecular understanding of microRNA-mediated gene silencing. (2015) *Nature Reviews Genetics.* **16,** 421–433.

Kahvejian,A., Svitkin,Y. V, Sukarieh,R., M'Boutchou,M.-N. and Sonenberg,N. Mammalian poly(A)-binding protein is a eukaryotic translation initiation factor, which acts via multiple mechanisms. (2005) *Genes Dev.*, **19**, 104–13.

Kamenska. A., Lu. W.T., Kubacka. D., Broomhead. H., Minshall. N., Bushell. M., and Standart. N.. Human 4E-T represses translation of bound mRNAs and enhances microRNA-mediated silencing. (2014) *Nucleic Acids Research***. 42,** 3298–3313.

Kang YC, Zhang L, Su Y, Li Y, Ren WL, Wei WS. MicroRNA-26b Regulates the Microglial Inflammatory Response in Hypoxia/Ischemia and Affects the Development of Vascular Cognitive Impairment. (2018) *Front Cell Neurosci*. **12** 154.

Kartha, R. V. & Subramanian, S. Competing endogenous RNAs (ceRNAs): new entrants to the intricacies of gene regulation. (2014) *Front. Genet.* **5**, 8.

Katoh. T., Sakaguchi. Y., Miyauchi. K., Suzuki. T., Kashiwabara. S., Baba. T., and Suzuki. T Selective stabilization of mammalian microRNAs by 3' adenylation mediated by the cytoplasmic poly(A) polymerase GLD-2. (2009) *Genes and Development.* **23**, 433–438.

Katsanou V, Papadaki O, Milatos S, Blackshear PJ, Anderson P, Kollias G, Kontoyiannis DL. HuR as a negative posttranscriptional modulator in inflammation. (2005) *Mol Cell*. **19**(6) 777-89.

Kawai, T. & Akira, S. The role of pattern-recognition receptors in innate immunity: update on Toll-like receptors. (2010) *Nat. Immunol.* **11** 373–384

Keller. W., Bienroth. S., Lang. K.M., and Christofori. G. Cleavage and polyadenylation factor CPF specifically interacts with the pre-mRNA 3' processing signal AAUAAA. (1991) *The EMBO Journal.* **10**, 4241– 4249.

Kerwitz,Y., Kühn,U., Lilie,H., Knoth,A., Scheuermann,T., Friedrich,H., Schwarz,E. and Wahle,E. Stimulation of poly(A) polymerase through a direct interaction with the nuclear poly(A) binding protein allosterically regulated by RNA. (2003) EMBO J., 22, 3705–14.

Khalaj K, Ahn SH, Bidarimath M, Nasirzadeh Y, Singh SS, Fazleabas AT, Young SL, Lessey BA, Koti M, Tayade C. A balancing act: RNA binding protein HuR/TTP axis in endometriosis patients. (2017) *Sci Rep.* **7**(1) 5883.

Khvorova, A., Reynolds, A. & Jayasena, S. D. Functional siRNAs and miRNAs exhibit strand bias. (2003) *Cell* **115** 209–216.

Kim J.H & Richter J.D. Opposing polymerase-deadenylase activities regulate cytoplasmic polyadenylation. (2006) *Mo. Cell.* **24** 173-183.

Kim, H.H. et al. HuR recruits let-7/RISC to repress c-Myc expression. (2009) *Genes Dev.* **23**, 1743–1748.

Kim. Y.K., Heo. I., and Kim. V.N.. Modifications of small RNAs and their associated proteins. (2010) *Cell.* **143,** 703–709.

Kim, B. et al. TUT7 controls the fate of precursor microRNAs by using three different uridylation mechanisms. (2015) *EMBO J.* **34**, 1801–1815

Kim H, Kim J, Yu S, Lee YY, Park J, Choi RJ, Yoon SJ, Kang SG, Kim VN. A Mechanism for microRNA Arm Switching Regulated by Uridylation. (2020) *Mol Cell.* **78**(6) 1224-1236.

Kondrashov. A., Meijer. H., Barthet-Barateig. A., Parker. H., Khurshid. A., Tessier. S., Sicard. M., Knox. A., Pang. L., and De Moor. C.H. Inhibition of polyadenylation reduces inflammatory gene induction. (2012) *RNA.* **18,** 2236-2250.

Kornberg RD, Thomas JO. Chromatin structure; oligomers of the histones. (1974) *Science.* **184**(4139) 865-8.

Krause M, Niazi AM, Labun K, Torres Cleuren YN, Müller FS, Valen E. *tailfindr*: alignment-free poly(A) length measurement for Oxford Nanopore RNA and DNA sequencing. (2019) *RNA.* **25**(10) 1229-1241.

Krol, J., Loedige, I. & Filipowicz, W. The widespread regulation of microRNA biogenesis, function and decay. (2010) *Nature Rev. Genet.* **11** 597–610.

Kuhn U, Nemeth A, Meyer S, Wahle E. The RNA binding domains of the nuclear poly(A)-binding protein. (2003) *J Biol Chem* **278** 16916–16925

Kuhn. U., Gundel. M., Knoth. A., Kerwitz. Y., Rudel. S., and Wahle. E. Poly(A) tail length is controlled by the nuclear poly(A)-binding protein regulating the interaction between poly(A) polymerase and the cleavage and polyadenylation specificity factor. (2009) *Journal of Biological Chemistry*. **284,** 22803–22814.

Kundu P, Fabian MR, Sonenberg N, Bhattacharyya SN, Filipowicz W. HuR protein attenuates miRNA-mediated repression by promoting miRISC dissociation from the target RNA. (2012) *Nucleic Acids Res.* **40**(11) 5088-100.

Kwak. P.B. and Tomari. Y. The N domain of Argonaute drives duplex unwinding during RISC assembly. (2012) *Nature Structural and Molecular Biology.* **19**, 145–151.

Kwak Y, Daly CWP, Fogarty EA, Grimson A, Kwak H. Dynamic and widespread control of poly(A) tail length during macrophage activation. (2022) *RNA.* **28**(7) 947-971.

Kwon. Y., Kim. Y., Eom. S., Kim. M., Park. D., kim. H., Noh. K., Lee. H., Lee. Y.S., Choe. J., Kim. Y.M., and Jeoung. D. MicroRNA-26a/-26b-COX2-MIP2 loop regulates allergic inflammation and allergic inflammation-promoted enhanced tumorigenic and metastatic potential of cancer cells. (2015) *The Journal of Biochemistry.* **290,** 14245-14266.

Lagos-Quintana. M., Rauhut. R., Lendeckel. W., and Tuschl. T. Identification of novel genes coding for small expressed RNAs. (2001) *Science.* **294,** 853-858.

Lagos-Quintana. M., Rauhut. R., Yalcin. A., Meyer. J., Lendeckel. W., and Tuschl. T. Identification of tissue-specific microRNAs from mouse. (2002) *Current Biology.* **12,** 735-9.

Lai, W. S. *et al*. Evidence that tristetraprolin binds to AU-rich elements and promotes the deadenylation and destabilization of tumor necrosis factor alpha mRNA. (1999) *Mol. Cell. Biol.* **19**, 4311–4323.

Lau. N.C., Lim. L.P., Weinstein. E.G., and Bartel. D.P. An abundant class of tiny RNAs with probable regulatory roles in Caenorhabditis elegans. (2001) *Science.* **294**, 858-62.

Lee. H. Y., and Doudna. J. A. TRBP alters human precursor microRNA processing in vitro. (2012) *RNA.* **18,** 2012–2019.

Lee. R.C., Feinbaum. R.L., and Ambros. V. The C.elegans heterochronic gene lin-4 encodes small RNAs with antisense complementarity to lin-14. (1993) *Cell.* **75**, 843-854.

Lee. R.C, and Ambros. V. An extensive class of small RNAs in Caenorhabditis elegans. (2001) *Science.* **294,** 862-4.

Lee.Y., Kim. M., Han. J., Yeom. K.H., Lee. S., and Kim. V.N. MicroRNA genes are transcribed by RNA polymerase II. (2004) *The EMBO Journal.* **23**, 4051-4060.

Leuti A, Fazio D, Fava M, Piccoli A, Oddi S, Maccarrone M. Bioactive lipids, inflammation and chronic diseases. (2020) *Adv Drug Deliv Rev*. **159** 133-169.

Li D, Wu M. Pattern recognition receptors in health and diseases. (2021) *Signal Transduct Target Ther.* **6**(1) 291.

Lim,J., Lee,M., Son,A., Chang,H. and Kim,V.N. mTAIL-seq reveals dynamic poly(A) tail regulation in oocyte-to-embryo development. (2016) *Genes Dev.*, **30**, 1671–82.

Liu,J., Carmell,M.A., Rivas,F.V., Marsden,C.G., Thomson,J.M., Song,J.J., Hammond,S.M., Joshua-Tor,L. and Hannon,G.J. Argonaute2 is the catalytic engine of mammalian RNAi. (2004) *Science*, **305**, 1437–1441.

Liu J, Rivas FV, Wohlschlegel J, Yates JR 3rd, Parker R, Hannon GJ. A role for the P-body component GW182 in microRNA function. (2005) *Nat Cell Biol.* **7**(12) 1261-6.

Liu, W., et al., Structural basis for nematode eIF4E binding an m(2,2,7)G-Cap and its implications for translation initiation. (2011) *Nucleic Acids Res*, **39**(20) 8820-32.

Liu. G., and Abraham. E. MicroRNAs in immune response and macrophage polarisation. *Arteriosclerosis, thrombosis and vascular biology.* (2013) **33,** 170-177.

Liu ZG, Han J . Cellular responses to Tumor Necrosis Factor (TNF). (2001) *Current Issues in Molecular Biology* **3** 79–90.

Liu, Y. et al. C3PO, an endoribonuclease that promotes RNAi by facilitating RISC activation. (2009) *Science* **325** 750–753 .

Loo. Y.M., and Gale. M. Jr. Immune signalling by RIG-I-like receptors. (2011) *Immunity.* **34** 680–92.

Lotze MT, Zeh HJ, Rubartelli A, Sparvero LJ, Amoscato AA, Washburn NR, Devera ME, Liang X, Tör M, Billiar T. The grateful dead: damage-associated molecular pattern molecules and reduction/oxidation regulate immunity. (2007) *Immunol Rev.* **220** 60-81.

Liudkovska V, Krawczyk PS, Brouze A, Gumińska N, Wegierski T, Cysewski D, Mackiewicz Z, Ewbank JJ, Drabikowski K, Mroczek S, Dziembowski A. TENT5 cytoplasmic noncanonical poly(A) polymerases regulate the innate immune response in animals. (2022) *Sci Adv.* **8**(46) eadd9468.

Maekawa. T., Kufer. T.A., and Schulze-Lefert. P. NLR functions in plant and animal immune systems. So far and yet so close. (2011) *Nature Immunology.* **12**, 817–26.

Mahesh G, Biswas R. MicroRNA-155: A Master Regulator of Inflammation. (2019) *J Interferon Cytokine Res.***39**(6) 321-330.

Mandel, C.R., Y. Bai, and L. Tong, Protein factors in pre-mRNA 3'-end processing. (2008) *Cell Mol Life Sci.* **65**(7-8) 1099-122.

Mangus DA, Evans MC, Jacobson A. Poly(A)-binding proteins: multifunctional scaffolds for the post-transcriptional control of gene expression. (2003) *Genome Biol*. **4**(7) 223.

Mangus DA, Evans MC, Agrin NS, Smith M, Gongidi P, Jacobson A. Positive and negative regulation of poly(A) nuclease. (2004) *Mol Cell Biol*. **24**(12) 5521-33.

Mantovani A, Sica A, Sozzani S, Allavena P, Vecchi A, Locati M. The chemokine system in diverse forms of macrophage activation and polarization. (2004) *Trends Immunol.* **25**(12) 677-86.

Marcotrigiano, J., et al., A conserved HEAT domain within eIF4G directs assembly of the translation initiation machinery. (2001) *Molecular Cell*. **7** 193-203.

Martin KC, Ephrussi A. mRNA localization: gene expression in the spatial dimension. (2009) *Cell.* **136**(4) 719-30.

Mathonnet G., et al., MicroRNA inhibition of translation initiation in vitro by targeting the cap-binding complex eIF4F. (2007) *Science **317*** 1764.

Mathys. H., Basquin. J., Ozgur. S., Czarnocki-Cieciura. M., Bonneau. F., Aartse. A., Dziembowski. A., Nowotny. M., Conti. E., and Filipowicz. W. Structural and biochemical insights to the role of the CCR4-NOT complex and DDX6 ATPase in microRNA repression. (2014) *Molecular Cell.* **54**, 751–765.

Matricon J, Barnich N, Ardid D. Immunopathogenesis of inflammatory bowel disease. (2010) *Self Nonself.* **1**(4) 299-309.

Mayr, C., and Bartel. D.P. Widespread shortening of 3'UTRs by alternative cleavage and polyadenylation activates oncogenes in cancer cells. (2009) *Cell,* **138,** 673–684.

Mayr C. Regulation by 3'-Untranslated Regions. (2017) *Annu Rev Genet***. 51** 171-194.

Mayr C. What Are 3' UTRs Doing? (2019) *Cold Spring Harb Perspect Biol*. **11**(10) a034728.

Mazumder A, Bose M, Chakraborty A, Chakrabarti S, Bhattacharyya SN. A transient reversal of miRNA-mediated repression controls macrophage activation. (2013) *EMBO Rep.* **14**(11) 1008-16.

McGrew, L. L. & Richter, J. D. Translational control by cytoplasmic polyadenylation during Xenopus oocyte maturation: characterization of cis and trans elements and regulation by cyclin/MPF. (1990) *EMBO J.* **9** 3743–3751

McMullen MR, Cocuzzi E, Hatzoglou M, Nagy LE . Chronic ethanol exposure increases the binding of HuR to the TNFalpha 3'-untranslated region in macrophages. (2003) *J Biol Chem.* **278** 38333 – 38341.

Medzhitov R, Janeway CA Jr. Innate immunity: the virtues of a nonclonal system of recognition. (1997) *Cell.* **91**(3) 295-8.

Medzhitov. R. Recognition of microorganisms and activation of the immune response. (2007) *Nature.* **449,** 819-826

Medzhitov R. Origin and physiological roles of inflammation. (2008) *Nature.* **454**(7203) 428-35.

Meijer. H.A., Kong. Y.W., Lu. W.T., Wilczynska. A., Spriggs. R.V., Robinson. S.W., Godfrey. J.D., Willis. A. E., and Bushell. M. Translational repression and eIF4A2 activity are critical for microRNA-mediated gene regulation. (2013) *Science.* **340,** 82–85.

Meijer HA, Schmidt T, Gillen SL, Langlais C, Jukes-Jones R, de Moor CH, Cain K, Wilczynska A, Bushell M. DEAD-box helicase eIF4A2 inhibits CNOT7 deadenylation activity. (2019) *Nucleic Acids Res*. **47**(15) 8224-8238.

Meister G, Landthaler M, Peters L, Chen PY, Urlaub H, Lührmann R, Tuschl T. Identification of novel argonaute-associated proteins. (2005) *Curr Biol*. **15**(23) 2149-55.

Mehta. A., and Baltimore. D. MicroRNAs as regulatory elements in immune system logic. (2016) *Nature Reviews Immunology.* **16,** 279-294.

Mendez. R., Hake. L.E., Andresson. T., Littlepage. L.E., Ruderman. J.V., and Richter. J.D. Phosphorylation of CPE binding factor by Eg2 regulates translation of c-mos mRNA. (2000) *Nature.* **16,** 302-307.

Medeiros R., Figueiredo C. P., Pandolfo P., Duarte F. S., Prediger R. D., Passos G. F., et al. The role of TNF-alpha signaling pathway on COX-2 upregulation and cognitive decline induced by beta-amyloid peptide. (2010) *Behav. Brain Res.* 209 165–173.

Meng F, Lowell CA. Lipopolysaccharide (LPS)-induced macrophage activation and signal transduction in the absence of Src-family kinases Hck, Fgr, and Lyn. (1997) *J Exp Med.* **185**(9) 1661-70.

Merrick, W.C., Cap-dependent and cap-independent translation in eukaryotic systems. (2004) *Gene*, **332** 1-11

Mignone F, Gissi C, Liuni S, Pesole G. Untranslated regions of mRNAs. (2002) *Genome Biol.* **3**(3).

Mills CD, Kincaid K, Alt JM, Heilman MJ, Hill AM. M-1/M-2 macrophages and the Th1/Th2 paradigm. (2000) *J Immunol.* **164**(12) 6166-73.

Min, K.-W. et al. AUF1 facilitates microRNA-mediated gene silencing. (2017) *Nucleic Acids Res.* **45**, 6064–6073.

Miyake K . Innate recognition of lipopolysaccharide by CD14 and toll-like receptor 4-MD-2: unique roles for MD-2. (2003) *Int Immunopharmacol* **3** 119–128.

Modzelewski, A. J., Holmes, R. J., Hilz, S., Grimson, A. & Cohen, P. E. AGO4 regulates entry into meiosis and influences silencing of sex chromosomes in the male mouse germline. (2012) *Dev. Cell* **23**, 251–264.

Monteys, A. M. et al. Structure and activity of putative intronic miRNA promoters. (2010) *RNA* **16** 495–505.

Morgan, M. et al. mRNA 3’ uridylation and poly(A) tail length sculpt the mammalian maternal transcriptome. (2017) *Nature* **548** 347–351

Moretti F, Kaiser C, Zdanowicz-Specht A, Hentze MW. PABP and the poly(A) tail augment microRNA repression by facilitated miRISC binding. (2012) *Nat Struct Mol Biol.* **19**(6) 603-8.

Mroczek, S. et al. The non-canonical poly(A) polymerase FAM46C acts as an onco-suppressor in multiple myeloma. (2017) *Nat. Commun.* **8** 619.

Muhlrad D, Decker CJ, Parker R. Deadenylation of the unstable mRNA encoded by the yeast MFA2 gene leads to decapping followed by 5'-->3' digestion of the transcript. (1994) *Genes Dev.* **8**(7) 855-66

Mukherjee K, Ghoshal B, Ghosh S, Chakrabarty Y, Shwetha S, Das S, Bhattacharyya SN. Reversible HuR-microRNA binding controls extracellular export of miR-122 and augments stress response. (2016) *EMBO Rep.* **17**(8) 1184-203.

Mullen, T. E. & Marzluff, W. F. Degradation of histone mRNA requires oligouridylation followed by decapping and simultaneous degradation of the mRNA both 5′ to 3′ and 3′ to 5′. (2008) *Genes. Dev.* **22** 50–65.

Murao A, Aziz M, Wang H, Brenner M, Wang P. Release mechanisms of major DAMPs. (2021) *Apoptosis.* **26**(3-4) 152-162

Murray PJ, Wynn TA. Protective and pathogenic functions of macrophage subsets. (2011) *Nat Rev Immunol.* **11**(11) 723-37.

Nagaike, T., Suzuki, T., Katoh, T. & Ueda, T. Human mitochondrial mRNAs are stabilized with polyadenylation regulated by mitochondria-specific poly(A) polymerase and polynucleotide phosphorylase. (2005) *J. Biol. Chem.* **280** 19721–19727

Nagata S. Apoptosis by death factor. (1997) *Cell*. **88** 355–65.

Nahid. M.A., Pauley. K.M., Satoh. M., and Chan. E.K. miR-146a is critical for endotoxin-induced tolerance: implication in innate immunity. (2009) *Journal of Biological Chemistry.* **284,** 34590–34599.

Naito M, Hasegawa G, Takahashi K. Development, differentiation, and maturation of Kupffer cells. (1997) *Microsc Res Tech.* **39**(4) 350-64.

Nam. J.W., Rissland. O.S., Koppstein. D., Abreu-Goodger. C., Jan. C.H., Agarwal. V., Yildirim. M.A., Rodriguez. A., and Bartel. D.P. Global analyses of the effect of different cellular contexts on microRNA targeting. (2014) *Molecular Cell.* **53**, 1031–1043.

Neilsen. C.T., Goodall. G.J. and Bracken. C.P. IsomiRs – the overlooked repertoire in the dynamic microRNAome. (2012) *Trends in Genetics.* **28,** 544–549.

Nguyen. T.A., Jo. M.H., Choi. Y.G., Park. J., Kwon. S.C., Hohng. S., Kim. V.N., and Woo. J.S. Functional anatomy of the human microprocessor. (2015) *Cell.* **161**, 1374–1387.

Nguyen. T.A., Park. J., Dang. T.L., C. Y., and Kim. V.N. Microprocessor depends on hemin to recognise the apical loop of primary microRNA. (2018) *Nucleic Acids Research.* **46,** 5726-5736.

Nicholson AL, Pasquinelli AE. Tales of Detailed Poly(A) Tails. (2019) *Trends Cell Biol.* **29**(3) 191-200.

Nilsen TW, Graveley BR. Expansion of the eukaryotic proteome by alternative splicing. (2010) *Nature.* **463**(7280) 457-63.

Nishikura, K. A-To-I editing of coding and non-coding RNAs by ADARs. (2016) *Nature Reviews Molecular Cell Biology.* **17,** 83–96.

Nishimura. T., Padamsi. Z., Fakim. H., Milette. S., Dunham. W.H., Gingras. A.C., and Fabian, M.R. The eIF4E-binding protein 4E-T is a component of the mRNA decay machinery that bridges the 50 and 30 termini of target mRNAs. (2015) *Cell Reports.* **11,** 1425–1436.

O'Connell. R.M., Taganov. K.D., Boldin. M.P., Cheng. G., and Baltimore. D. MicroRNA-155 is induced during the macrophage inflammatory response. (2007) *Proceedings of the National Academy of Sciences USA.* **104**, 1604–1609.

O'Connell RM, Chaudhuri AA, Rao DS, Baltimore D. Inositol phosphatase SHIP1 is a primary target of miR-155. (2009) *Proc Natl Acad Sci U S A.* **106**(17) 7113-8.

O'Neill LA, Bowie AG. The family of five: TIR-domain-containing adaptors in Toll-like receptor signalling. (2007) *Nat Rev Immunol.* **7**(5) 353-64.

O'Neill. L.A., Sheedy. F.J., and McCoy. C.E. MicroRNAs: the fine-tuners of toll-like receptor signalling. (2011) *Nature Reviews Immunology.* **11,** 136-175.

O'Neill. L.A., Golenbock. D., and Bowie. A.G. The history of toll-like receptors – redefining innate immunity. (2013) *Nature Reviews Immunology*. **13**,453–60.

Ozgur. S., Basquin. J., Kamenska. A., Filipowicz. W., Standart. N., and Conti. E. Structure of a human 4E- T/DDX6/CNOT1 complex reveals the different interplay of DDX6-binding proteins with the CCR4-NOT complex. (2015) *Cell Reports.* **13**, 703–711.

Panasenko, O. O. The role of the E3 ligase Not4 in cotranslational quality control. (2014) *Front. Genet.* **5** 141

Park, B., Song, D., Kim, H. *et al.* The structural basis of lipopolysaccharide recognition by the TLR4–MD-2 complex. (2009) *Nature* **458** 1191–1195.

Park, J.H, Shin C. MicroRNA-directed cleavage of targets: mechanism and experimental approaches. (2014) *BMB Rep.* **47**(8) 417-23.

Park, J.-E., Yi, H., Kim, Y., Chang, H. and Kim, V.N. Regulation of Poly(A) Tail and Translation during the Somatic Cell Cycle. (2016) *Mol. Cell*, **62**, 462–471.

Park, M.S., Sim, G., Kehling, A.C. and Nakanishi ,K. Human Argonaute2 and Argonaute3 are catalytically activated by different lengths of guide RNA. (2020) *Proc. Natl. Acad. Sci. U.S.A.*, **117**, 28576–28578.

Parker. G "Cells of the Immune System". In: Parker G.(eds).
(2017) *Immunopathology in Toxicology and Drug* Humana Press, Cham. 95-201.

Passmore LA, Coller J. Roles of mRNA poly(A) tails in regulation of eukaryotic gene expression. (2022) *Nat Rev Mol Cell Biol.* **23**(2) 93-106.

Patel JR, Jain A, Chou YY, Baum A, Ha T, García-Sastre A. ATPase-driven oligomerization of RIG-I on RNA allows optimal activation of type-I interferon. (2013) *EMBO Rep*. **14**(9) 780-7.

Pathak S, Grillo AR, Scarpa M, Brun P, D'Incà R, Nai L, Banerjee A, Cavallo D, Barzon L, Palù G, Sturniolo GC, Buda A, Castagliuolo I. MiR-155 modulates the inflammatory phenotype of intestinal myofibroblasts by targeting SOCS1 in ulcerative colitis. (2015) *Exp Mol Med.* **4**7(5) e164.

Pelus LM, Fukuda S. Peripheral blood stem cell mobilization: the CXCR2 ligand GRObeta rapidly mobilizes hematopoietic stem cells with enhanced engraftment properties. (2006) *Exp Hematol.* **34**(8) 1010-20.

Peng. Y., and Croce. C.M. The role of microRNAs in human cancer. (2016) *Signal Transduction and Targeted Therapy.* **1,** 15004.

Petri, S. et al. Increased siRNA duplex stability correlates with reduced off-target and elevated on-target effects. (2011) *RNA* **17** 737–749.

Pillai R. S., et al., Inhibition of translational initiation by Let-7 MicroRNA in human cells. (2005) *Science **309*** 1573.

Poliseno, L. et al. A coding-independent function of gene and pseudogene mRNAs regulates tumour biology. (2010) *Nature* **465**, 1033–1038

Pope SD, Medzhitov R. Emerging Principles of Gene Expression Programs and Their Regulation. (2018) *Mol Cell.* **71**(3) 389-397.

Poria DK, Guha A, Nandi I, Ray PS. RNA-binding protein HuR sequesters microRNA-21 to prevent translation repression of proinflammatory tumour suppressor gene programmed cell death 4. (2016) *Oncogene.* **35**(13) 1703-15.

Probert, L. Tnf and Its Receptors in the Cns: The Essential, the Desirable and the Deleterious Effects. (2015) *Neuroscience.* **302** 2–22.

Qi, H. H. et al. Prolyl 4-hydroxylation regulates Argonaute 2 stability. (2008) *Nature* **455**, 421–424.

Radford, H. E., Meijer, H. A. & de Moor, C. H. Translational control by cytoplasmic polyadenylation in Xenopus oocytes. (2008) *Biochim. Biophys. Acta* **1779** 217–229.

Raisch, T. et al. Reconstitution of recombinant human CCR4-NOT reveals molecular insights into regulated deadenylation. (2019) *Nat. Commun.* **10** 3173

Ren, F., Zhang, N., Zhang, L. *et al.* Alternative Polyadenylation: a new frontier in post transcriptional regulation. (2020) *Biomark Res* **8** 67

Rehwinkel, J., Behm-Ansmant, I., Gatfield, D. & Izaurralde, E. A crucial role for GW182 and the DCP1:DCP2 decapping complex in miRNA-mediated gene silencing. (2005) *RNA* **11**, 1640–1647.

Rehwinkel J, Gack MU. RIG-I-like receptors: their regulation and roles in RNA sensing. (2020) *Nat Rev Immunol.* **20**(9) 537-551.

Richter JD. Cytoplasmic polyadenylation in development and beyond. (1999) *Microbiol Mol Biol Rev*. **63**(2) 446-56.

Ricklin D, Hajishengallis G, Yang K, Lambris JD. Complement: a key system for immune surveillance and homeostasis. (2010) *Nat Immunol.* **11**(9) 785-97.

Rissland OS, Subtelny AO, Wang M, Lugowski A, Nicholson B, Laver JD, Sidhu SS, Smibert CA, Lipshitz HD, Bartel DP. The influence of microRNAs and poly(A) tail length on endogenous mRNA-protein complexes. (2017) *Genome Biol.* **18**(1) 211.

Ro, S. Park, C. Young, D. Sanders, K. M., Yan, W.. Tissue-dependent paired expression of miRNAs. (2007) *Nucleic Acids Research*, **35**(17), 5944–5953.

Roeder, R.G., The role of general initiation factors in transcription by RNA polymerase II. *(1996) Trends Biochem Sci.* **21**(9) 327-35.

Rothe J, Gehr G, Loetscher H, Lesslauer W. Tumor necrosis factor receptors: structure and function. (1992) *Immunol Res.* **11** 81–90.

Rouhana L, Wickens M. Autoregulation of GLD-2 cytoplasmic poly(A) polymerase. (2007) *RNA*. **13**(2) 188-99.

Rubartelli A, Lotze MT. Inside, outside, upside down: damage-associated molecular-pattern molecules (DAMPs) and redox. (2007) *Trends Immunol.* **28**(10) 429-36.

Ruby. J.G., Jan. C.H., and Bartel. D.P. Intronic microRNA precursors that bypass Drosha processing. (2007) *Nature.* **448,** 83–86.

Rudel, S. et al. Phosphorylation of human Argonaute proteins affects small RNA binding. (2011) *Nucleic Acids Res.* **39**, 2330–2343.

Ruegger. S., and Grosshans. H. microRNA turnover: when, how, and why. (2012) *Trends in Biochemical Science.* **37**, 436–446.

Ruggiero T, Trabucchi M, De Santa F, Zupo S, Harfe BD, Mcmanus MT, Rosenfeld MG, Briata P, Gherzi R. LPS induces KH-type splicing regulatory protein-dependent processing of microRNA-155 precursors in macrophages (2009). *FASEB J.* **23**, 2898-2908.

Sachs AB, Bond MW, Kornberg RD. A single gene from yeast for both nuclear and cytoplasmic polyadenylate-binding proteins: Domain structure and expression. (1986) *Cell* **45** 827–835.

Sachs. A. (2000). Physical and functional interactions between the mRNA cap structure and the poly(A) tail. in Translational control of gene expression (ed. M.B. Mathews), pp. 447–466. Cold Spring Harbor Laboratory Press, Cold Spring Harbor, NY.

Sarkissian M, Mendez R, Richter JD. Progesterone and insulin stimulation of CPEB-dependent polyadenylation is regulated by Aurora A and glycogen synthase kinase-3. (2004) *Genes Dev.* **18**(1) 48-61.

Sato H, Maquat LE. Remodeling of the pioneer translation initiation complex involves translation and the karyopherin importin beta. (2009) *Genes Dev*. **23**(21) 2537-50.

Satoh H., Amagase K., Ebara S., Akiba Y., Takeuchi K. Cyclooxygenase (COX)-1 and COX-2 both play an important role in the protection of the duodenal mucosa in cats. (2012) *J. Pharmacol. Exp. Ther.* 344 189–195.

Scaffidi P, Misteli T, Bianchi ME. Release of chromatin protein HMGB1 by necrotic cells triggers inflammation. (2002) *Nature.* **418**(6894) 191-5.

Schirle, N. T., Sheu-Gruttadauria, J., Chandradoss, S. D., Joo, C. & MacRae, I. J. Water-mediated recognition of t1-adenosine anchors Argonaute2 to microRNA targets. (2015) *eLife* **4**, e07646

Schmitt, E., B. S., and Y. Mechulam, The large subunit of initiation factor aiF2 is a close structural homologue of elongation factors. (2002) *EMBO* **21**(7) 1821-1832.

Schmidt, M. J., West, S. & Norbury, C. J. The human cytoplasmic RNA terminal U-transferase ZCCHC11 targets histone mRNAs for degradation. (2011) *RNA* **17** 39–44

Schneider-Poetsch, T., et al., Garbled messages and corrupted translations. (2010) *Nat Chem Biol.* **6**(3) 189-198.

Schwarz, D. S. et al. Asymmetry in the assembly of the RNAi enzyme complex. (2003) *Cell* **115** 199–208.

Schumann U, Zhang HN, Sibbritt T, Pan A, Horvath A, Gross S, Clark SJ, Yang L, Preiss T Multiple links between 5-methylcytosine content of mRNA and translation. (2020). *BMC Biol* **18**(1):40

Sen GL, Blau HM. Argonaute 2/RISC resides in sites of mammalian mRNA decay known as cytoplasmic bodies. (2005) *Nat Cell Biol*. **7**(6) 633-6.

Sgromo, A. et al. Drosophila Bag-of-marbles directly interacts with the CAF40 subunit of the CCR4-NOT complex to elicit repression of mRNA targets. (2018) *RNA* **24** 381–395

Shatkin, A.J., Capping of eucaryotic mRNAs. (1976) *Cell.* **9**(4) 645-53.

Sheedy. F.J., Palsson-McDermott. E., Hennessy. E.J., Martin. C., O'Leary. J.J., Ruan. Q., Johnson. D.S., Chen. Y., and O'Neill. L.A. Negative regulation of TLR4 via targeting of the proinflammatory tumor suppressor PDCD4 by the microRNA miR-21. (2010) *Nature Immunology.* **11,** 141– 147.

Shen, J. et al. EGFR modulates microRNA maturation in response to hypoxia through phosphorylation of AGO2. (2013) *Nature* **497** 383–387.

Sheu- Gruttadauria. J., and MacRae. I.J. Structural foundations of RNA silencing by Argonaute. (2017) *Journal of Molecular Biology.* **429**, 2619–2639.

Shin J, Paek KY, Ivshina M, Stackpole EE, Richter JD. Essential role for non-canonical poly(A) polymerase GLD4 in cytoplasmic polyadenylation and carbohydrate metabolism. (2017) *Nucleic Acids Res.* **45**(11) 6793-6804.

Simón, E. & Séraphin, B. A specific role for the C-terminal region of the poly(A)-binding protein in mRNA decay. (2007) *Nucleic Acids Res.* **35** 6017–6028.

Simmonds RE..Transient up-regulation of miR-155-3p by lipopolysaccharide in primary human monocyte-derived macrophages results in RISC incorporation but does not alter TNF expression. (2019) *Wellcome Open Res.* **4**, 43.

Sinturel F, Gerber A, Mauvoisin D, Wang J, Gatfield D, Stubblefield JJ, Green CB, Gachon F, Schibler U. Diurnal Oscillations in Liver Mass and Cell Size Accompany Ribosome Assembly Cycles. (2017) *Cell.* **169**(4) 651-663.e14.

Slezak-Prochazka. I., Kluiver. J., de Jong. D., Kortman. G., Halsema. N., Poppema. S., Kroesen. B., and van den Berg. A. Cellular localization and processing of primary transcripts of exonic microRNAs. (2013) *PLoS One*. **8,** 76647.

Slobodin,B., Bahat,A., Sehrawat,U., Becker-Herman,S., Zuckerman,B., Weiss,A.N., Han,R., Elkon,R., Agami,R., Ulitsky,I., *et al.* Transcription Dynamics Regulate Poly(A) Tails and Expression of the RNA Degradation Machinery to Balance mRNA Levels. (2020) *Mol. Cell*, **78**, 434-444.e5.

Smith. W.L and Murphy, R.C. The eicosanoid: cyclooxygenase, lipoxygenase, and epoxygenase pathways Biochemistry of Lipids, Lipoproteins and Membranes (4th ed.), Elsevier Science (2002), pp. 341-371

Sonenberg, N., et al., Eukaryotic mRNA cap binding protein: purification by affinity chromatography on sepharose-coupled m7GDP. (1979) *Proc. Natl. Acad. Sci. USA*, **76**(9) 4345-4349

Srikantan S, Gorospe M. HuR function in disease. (2012) *Front Biosci* **17**(1) 189-205.

Subtelny,A.O., Eichhorn,S.W., Chen,G.R., Sive,H. and Bartel,D.P. Poly(A)-tail profiling reveals an embryonic switch in translational control. (2014) *Nature*, **508**, 66.

Sun X, Sit A, Feinberg MW. Role of miR-181 family in regulating vascular inflammation and immunity. (2014) *Trends Cardiovasc Med*. **24**(3) 105-12.

Takeuchi O, Akira S. Pattern recognition receptors and inflammation. (2010) *Cell*. **140**(6) 805-20.

Tam W.. Identification and characterization of human BIC, a gene on chromosome 21 that encodes a noncoding RNA. (2001) *Gene* **274**(1–2) 157–167

Tang D, Kang R, Coyne CB, Zeh HJ, Lotze MT. PAMPs and DAMPs: signal 0s that spur autophagy and immunity. (2012) *Immunol Rev*. **249**(1) 158-75.

Tang, X., Zhang, Y., Tucker, L. & Ramratnam, B. Phosphorylation of the RNase III enzyme Drosha at Serine300 or Serine302 is required for its nuclear localization. (2010) *Nucleic Acids Res.* **38** 6610–6619.

Terns, M.P. and S.T. Jacob, Role of poly(A) polymerase in the cleavage and polyadenylation of mRNA precursor. (1989) *Mol Cell Biol.* **9**(4) 1435-44.

Thomson, D., Dinger, M. Endogenous microRNA sponges: evidence and controversy. (2016) *Nat Rev Genet* **17**, 272–283

Tian. J., An. X., and Niu. L.. Role of microRNAs in cardiac development and disease. (2017) *Experimental and Therapeutic Medicine.* **13,** 3-8.

Tokumaru, S., Suzuki, M., Yamada, H., Nagino, M. & Takahashi, T. *let-7* regulates Dicer expression and constitutes a negative feedback loop. (2008) *Carcinogenesis* **29** 2073–2077.

Trabucchi, M. et al. The RNA-binding protein KSRP promotes the biogenesis of a subset of microRNAs. (2009) *Nature* **459** 1010–1014.

Tracey KJ, Cerami A . Tumor necrosis factor, other cytokines and disease. (1993) *Annu Rev Cell Biol.* **9** 317–43.

Trebino CE, Stock JL, Gibbons CP, Naiman BM, Wachtmann TS, Umland JP, Pandher K, Lapointe JM, Saha S, Roach ML, Carter D, Thomas NA, Durtschi BA, McNeish JD, Hambor JE, Jakobsson PJ, Carty TJ, Perez JR, Audoly LP. Impaired inflammatory and pain responses in mice lacking an inducible prostaglandin E synthase. (2003) *Proc Natl Acad Sci U S A.* **100** 9044–9049

Treiber. T., Treiber. N., and Meister. G. Regulation of microRNA biogenesis and its crosstalk with other cellular pathways. (2019) *Nature Reviews Molecular Cell Biology.* **19,** 808.

Trippe, R. et al. Identification, cloning, and functional analysis of the human U6 snRNA-specific terminal uridylyl transferase. (2006) *RNA* **12** 1494–1504

Tsai KW, Leung CM, Lo YH, Chen TW, Chan WC, Yu SY, Tu YT, Lam HC, Li SC, Ger LP, Liu WS, Chang HT. Arm Selection Preference of MicroRNA-193a Varies in Breast Cancer. (2016). *Sci Rep*. **16**

Uchida N, Hoshino S, Katada T. Identification of a human cytoplasmic poly(A) nuclease complex stimulated by poly(A)-binding protein. (2004) *J Biol Chem*. **279**(2) 1383-91.

Udagawa N, Takahashi N, Akatsu T, Tanaka H, Sasaki T, Nishihara T, Koga T, Martin TJ, Suda T. Origin of osteoclasts: mature monocytes and macrophages are capable of differentiating into osteoclasts under a suitable microenvironment prepared by bone marrow-derived stromal cells. (1990) *Proc Natl Acad Sci U S A.* **87**(18) 7260-4.

Udagawa T, Swanger SA, Takeuchi K, Kim JH, Nalavadi V, Shin J, Lorenz LJ, Zukin RS, Bassell GJ, Richter JD. Bidirectional control of mRNA translation and synaptic plasticity by the cytoplasmic polyadenylation complex. (2012) *Mol Cell*. **47**(2) 253-66.

Uribe-Querol E, Rosales C. Phagocytosis: Our Current Understanding of a Universal Biological Process. (2020) *Front Immunol.* **11** 1066.

Wada, T., Kikuchi, J. & Furukawa, Y. Histone deacetylase 1 enhances microRNA processing via deacetylation of DGCR8. (2012) *EMBO Rep.* **13** 142–149.

Wahle,E. A Novel Poly(A)-Binding Protein Acts As a Specificity Factor in the Second Phase of Messenger RNA Polyadenylation. (1991) *Cell*, **66,** 759–768.

Wakiyama M, Ogami K, Iwaoka R, Aoki K, Hoshino SI. MicroRNP-mediated translational activation of nonadenylated mRNAs in a mammalian cell-free system. (2018) *Genes Cells*. **23**(5) 332-344.

Wahle. E., and Winkler, G.S.. RNA decay machines: deadenylation by the Ccr4–Not and Pan2–Pan3 complexes. (2013) *Biochimica et Biophysica Acta.* **1829,** 561–570.

Wang J, Mukaida N, Zhang Y, Ito T, Nakao S, Matsushima K. Enhanced mobilization of hematopoietic progenitor cells by mouse MIP-2 and granulocyte colony-stimulating factor in mice. (1997*) J Leukoc Biol.* **62**(4) 503-9.

Warkocki, Z., Liudkovska, V., Gewartowska, O., Mroczek, S. & Dziembowski, A. Terminal nucleotidyl transferases (TENTs) in mammalian RNA metabolism. (2018) *Philos. Trans. R. Soc. Lond. B Biol. Sci.* **373** 20180162.

Watters TM, Kenny EF, O'Neill LA . Structure, function and regulation of the Toll/IL-1 receptor adaptor proteins. (2007) *Immunol Cell Biol* **85** 411–419

Webster MW, Chen YH, Stowell JAW, Alhusaini N, Sweet T, Graveley BR, Coller J, Passmore LA. mRNA Deadenylation Is Coupled to Translation Rates by the Differential Activities of Ccr4-Not Nucleases. (2018) *Mol Cell***. 70**(6) 1089-1100.e8.

Weiss G, Schaible UE. Macrophage defense mechanisms against intracellular bacteria. (2015) *Immunol Rev.* **264**(1) 182-203.

Wigington CP, Williams KR, Meers MP, Bassell GJ, Corbett AH. Poly(A) RNA-binding proteins and polyadenosine RNA: new members and novel functions. (2014) *Wiley Interdiscip Rev RNA*. **5**(5) 601-22.

Wilczynska. A., Git. A., Argasinska. J., Belloc. E., and Standart. N. CPEB and miR-15/16 co-regulate translation of cyclin E1 mRNA during Xenopus Oocyte maturation. (2016) *PLoS One.* **11,** e0146792.

Wilczynska A, Gillen SL, Schmidt T, Meijer HA, Jukes-Jones R, Langlais C, Kopra K, Lu WT, Godfrey JD, Hawley BR, Hodge K, Zanivan S, Cain K, Le Quesne J, Bushell M. eIF4A2 drives repression of translation at initiation by Ccr4-Not through purine-rich motifs in the 5'UTR. (2019*) Genome Biol.* **20**(1) 262.

Will, S., Reiche, K., Hofacker, I. L., Stadler, P. F. & Backofen, R. Inferring noncoding RNA families and classes by means of genome-scale structure-based clustering. (2007) *PLoS Comput Biol* **3**, 1–12.

Williams. K. (2021). Tying the CNOT: CNOT1 regulates poly(A) tail length at the end and the beginning (unpublished doctoral dissertation) University of Nottingham, Nottingham, UK).

Wilson, W. C. et al. A human mitochondrial poly(A) polymerase mutation reveals the complexities of post-transcriptional mitochondrial gene expression. (2014) *Hum. Mol. Genet.* **23** 6345–6355

Wynn TA, Vannella KM. Macrophages in Tissue Repair, Regeneration, and Fibrosis. (2016) *Immunity.* **44**(3) 450-462.

Xiang . K and Bartel. D.P The molecular basis of coupling between poly(A)-tail length and translational efficiency. (2021) *eLife* **10** e66493.

Xie. M., Li. M., Vilborg. A., Lee. N., Shu. M.D. Yartseva. V., Sestan. N., and Steitz. J.A. Mammalian 5' - capped microRNA precursors that generate a single microRNA. (2013) *Cell.* **155,** 1568–1580.

Xie W, Li M, Xu N, Lv Q, Huang N, He J, et al. miR-181a regulates inflammation responses in monocytes and macrophages. (2013*) PLoS One* **8** e58639

Yamamoto M, Sato S, Hemmi H, Hoshino K, Kaisho T, Sanjo H, Takeuchi O, Sugiyama M, Okabe M, Takeda K, Akira S. Role of adaptor TRIF in the MyD88-independent toll-like receptor signaling pathway. (2003) *Science.* **301**(5633) 640-3.

Yamashita A, Chang TC, Yamashita Y, Zhu W, Zhong Z, Chen CY, Shyu AB. Concerted action of poly(A) nucleases and decapping enzyme in mammalian mRNA turnover. (2005) *Nat Struct Mol Biol*. **12**(12) 1054-63.

Yang. J.S., Maurin. T., Robine. N., Rasmussen. K.D., Jeffrey. K.L., Chandwani. R., Papapetrou. E.P., Sadelain. M., O'Carroll. D and Lai. E.C. Conserved vertebrate mir-451 provides a platform for Dicer-independent, Ago2-mediated microRNA biogenesis. (2010) *Proceedings of the National Academy of Sciences USA.* **107,** 15163-15168.

Yao. C, Narumiya. S, Prostaglandin-cytokine crosstalk in chronic inflammation. (2019) *Br. J. Pharmacol.* **176**, 337–354.

Ye, X. et al. Structure of C3PO and mechanism of human RISC activation. (2011) *Nature Struct. Mol. Biol.* **18**, 650–657.

Yi. R., Qin. Y., Macara. I.G., and Cullen. B.R.. Exportin-5 mediates the nuclear export of pre-microRNAs and short hairpin RNAs. (2003) *Genes and Development.* **17**, 3011-3016.

Yi H, Park J, Ha M, Lim J, Chang H, Kim VN. PABP Cooperates with the CCR4-NOT Complex to Promote mRNA Deadenylation and Block Precocious Decay. (2018) *Mol Cell*. **70**(6) 1081-1088.e5.

Yoon JH, Jo MH, White EJ, De S, Hafner M, Zucconi BE, Abdelmohsen K, Martindale JL, Yang X, Wood WH 3rd, Shin YM, Song JJ, Tuschl T, Becker KG, Wilson GM, Hohng S, Gorospe M. AUF1 promotes let-7b loading on Argonaute 2. (2015) *Genes Dev*. **29**(15) 1599-604.

Yoneyama M, Onomoto K, Jogi M, Akaboshi T, Fujita T. Viral RNA detection by RIG-I-like receptors. (2015) *Curr Opin Immunol***. 32** 48-53.

Young LE, Sanduja S, Bemis-Standoli K, et al. The mRNA binding proteins HuR and tristetraprolin regulate cyclooxygenase 2 expression during colon carcinogenesis. (2009) *Gastroenterology* **136** 1669–1679.

Yu, S., Kim, V.N. A tale of non-canonical tails: gene regulation by post-transcriptional RNA tailing. (2020) *Nat Rev Mol Cell Biol* **21** 542–556.

Yucel-Lindberg T., Ahola H., Carlstedt-Duke J., Modeer T. Involvement of tyrosine kinases on cyclooxygenase expression and prostaglandin E2 production in human gingival fibroblasts stimulated with interleukin-1beta and epidermal growth factor. (1999) *Biochem. Biophys. Res. Commun.* **257** 528–532.

Zeng, Y., Sankala, H., Zhang, X. & Graves, P. R. Phosphorylation of Argonaute 2 at serine-387 facilitates its localization to processing bodies. (2008) *Biochem. J.* **413**, 429–436.

Zekri, L., Huntzinger, E., Heimstadt, S. & Izaurralde, E. The silencing domain of GW182 interacts with PABPC1 to promote translational repression and degradation of microRNA targets and is required for target release. (2009) *Mol. Cell. Biol.* **29**, 6220–6231.

Zhou, H., Huang, X., Cui, H., Luo, X., Tang, Y., Chen, S., Wu, L., and Shen, N. miR-155andi ts star-formpartnermiR-155*cooperatively regulate type I interferon production by human plasmacytoid dendritic cells. (2010) *Blood* **116** 5885–5894

Zhu J, Wang FL, Wang HB, Dong N, Zhu XM, Wu Y, Wang YT, Yao YM. TNF-α mRNA is negatively regulated by microRNA-181a-5p in maturation of dendritic cells induced by high mobility group box-1 protein. (2017) *Sci Rep.* **7**(1) 12239

Zou. C.D., Zhao. W.M., Wang. X.N., Li. Q., Huang. H., Cheng. W.P., Jin. J.F., Zhang. H., Wu. M.J., Tai. S., Zou. C.X., and Gao. X. MicroRNA-107: a novel promoter of tumor progression that targets the CPEB3/EGFR axis in human hepatocellular carcinoma. (2016) *Oncotarget.* **7,** 266-278.

Zuk, D. and A. Jacobson, A single amino acid substitution in yeast eIF-5A results in mRNA stabilization. (1998) *EMBO J*. **17**(10) 2914-2925.

Chapter 8 - Supplementary Information

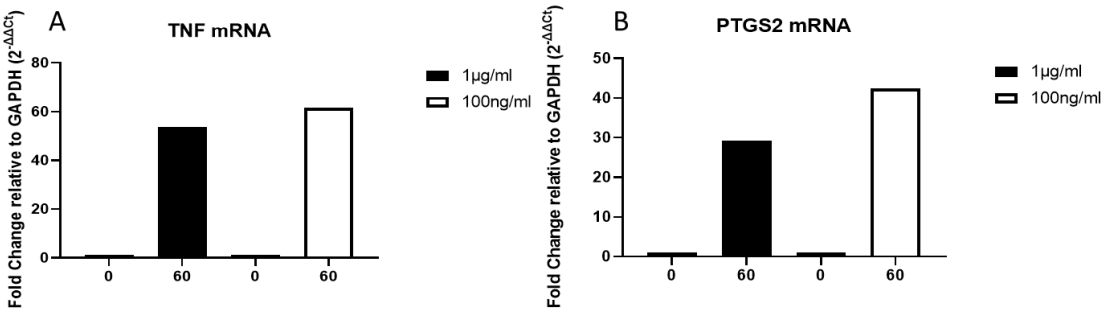

Supplementary Figure 1. Testing Sigma LPS concentrations. A) TNF mRNA induction in response to LPS induction with either 1µg/ml or 100ng/ml LPS. Data measured by RT-qPCR and analysed by $2^{-\Delta\Delta Ct}$, data normalised to GAPDH and plotted relative to the zero hour time point. N=1. **B).** Same as A but looking at PTGS2 induction.

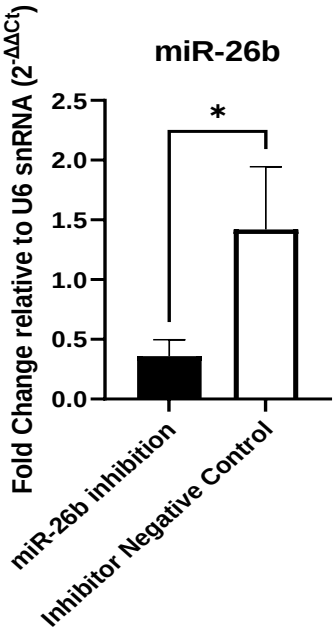

Supplementary Figure 2. Transfection efficiency of miR-26b inhibitor. Effect of transfection miR-26b inhibitor on miR-26b expression levels. Data measured by RT-qPCR and analysed by $2^{-\Delta\Delta Ct}$, data normalised to U6 and plotted relative to no transfection control.

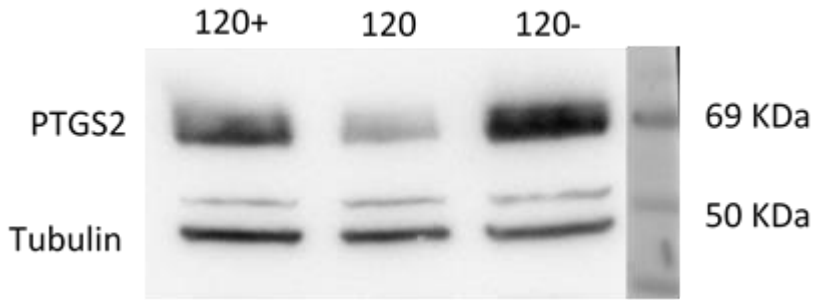

Supplementary Figure 3. Western blot showing effect of miR-26b-5p inhibition on PTGS2 protein levels 120 minutes after LPS treatment (1ug/ml). miR-26b inhibitor (10nmol) or negative control oligo (10nmol) were transfected over 24 hours. 0+, 120+ denotes miR-26b-5p inhibition, 0 120 denotes no transfection control, 0-, 120-, denotes Negative Control A. Tubulin used as a loading control. N=2

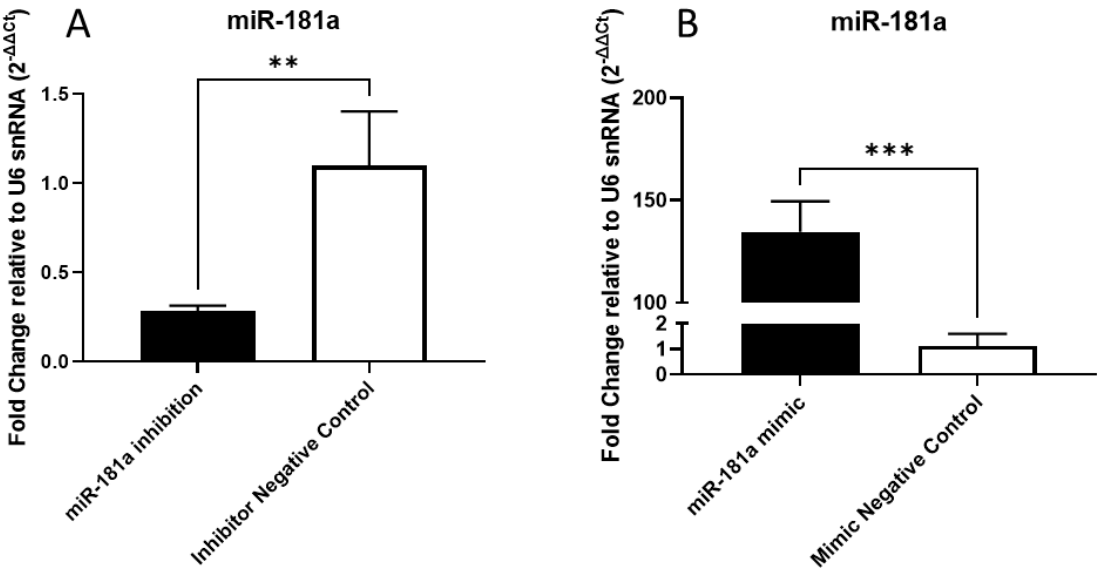

Supplementary Figure 4. Transfection efficiency of miR-181a inhibitor and mimic. A) Effect of transfecting miR-181a inhibitor on miR-181a expression levels. Data measured by RT-qpCR and analysed by $2^{-\Delta\Delta Ct}$, data normalised to U6 and plotted relative to no transfection control. **B)** Same as B but looking at the effect of transfecting the miR-181a mimic on miR-181a levels

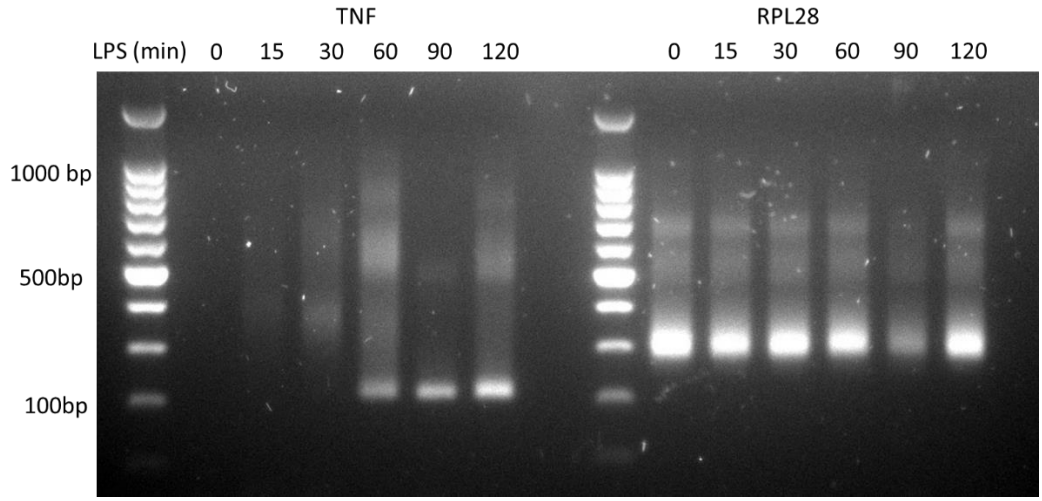

Supplementary Figure 5. Poly(A) tail lengths of TNF and RPL28 over a 120 minute LPS (1µg/ml) time course. Agarose gel electrophoresis following PAT assay on total RNA from RAW 264.7 cells treated with LPS. Primers used were specific to TNF or RP

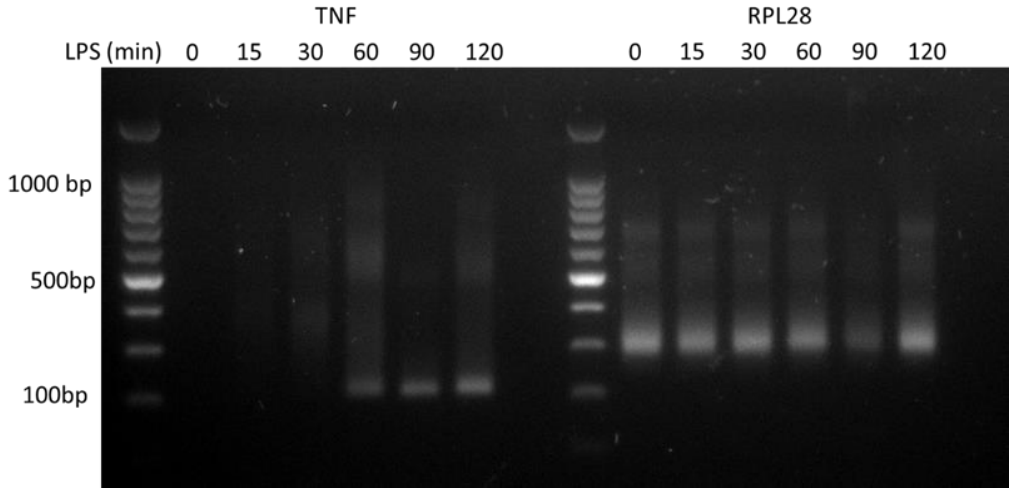

Supplementary Figure 6. Poly(A) tail lengths of TNF and RPL28 over a 120 minute LPS (1µg/ml) time course. Agarose gel electrophoresis following PAT assay on total RNA from RAW 264.7 cells treated with LPS. Primers used were specific to TNF or RPL28.

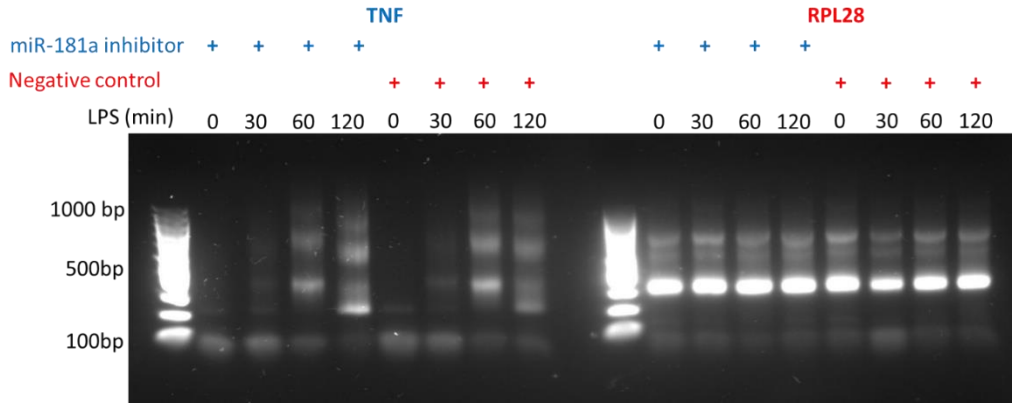

Supplementary Figure 7. TNF and RPL28 poly(A) tail lengths with miR-181a inhibition over a 120 minute LPS (1µg/ml) time course. Time course showing, miR-181a inhibitor or negative control (10nm final concentration) conditions. Poly(A) tail lengths were analysed by PAT assay and agarose gel electrophoresis

.

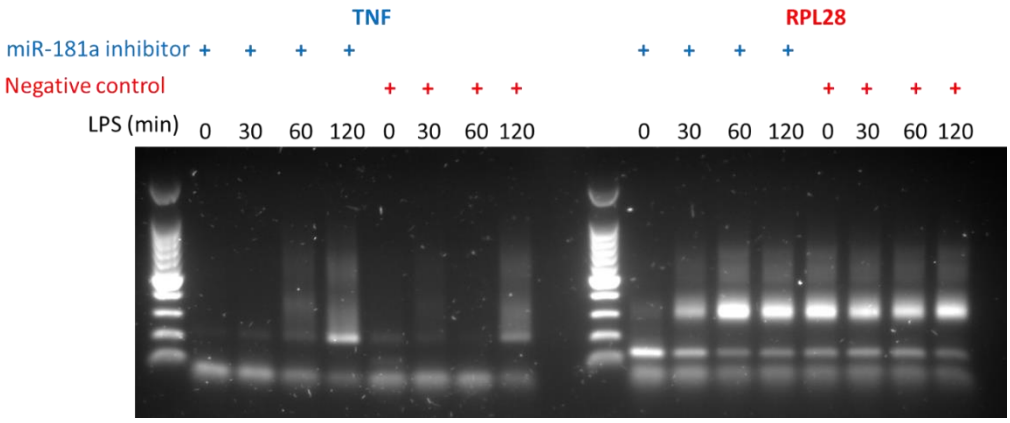

Supplementary Figure 8. TNF and RPL28 poly(A) tail lengths with miR-181a inhibition over a 120 minute LPS (1µg/ml) time course. Time course showing, miR-181a inhibitor or negative control (10nm final concentration) conditions. Poly(A) tail lengths were analysed by PAT assay and agarose gel electrophoresis

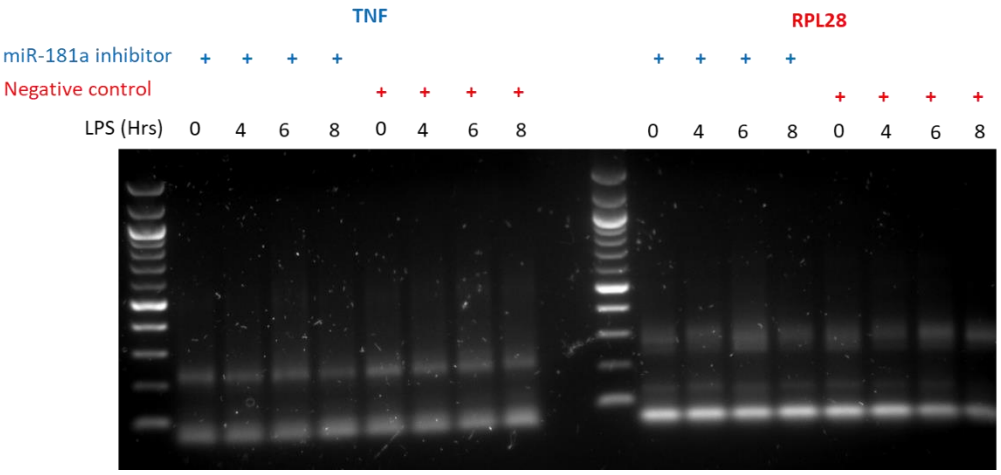

Supplementary Figure 9. TNF and RPL28 poly(A) tail lengths with miR-181a inhibition over an eight hour LPS (1µg/ml) time course. Time course showing, miR-181a inhibitor or negative control (10nm final concentration) conditions. Poly(A) tail lengths were analysed by PAT assay and agarose gel electrophoresis

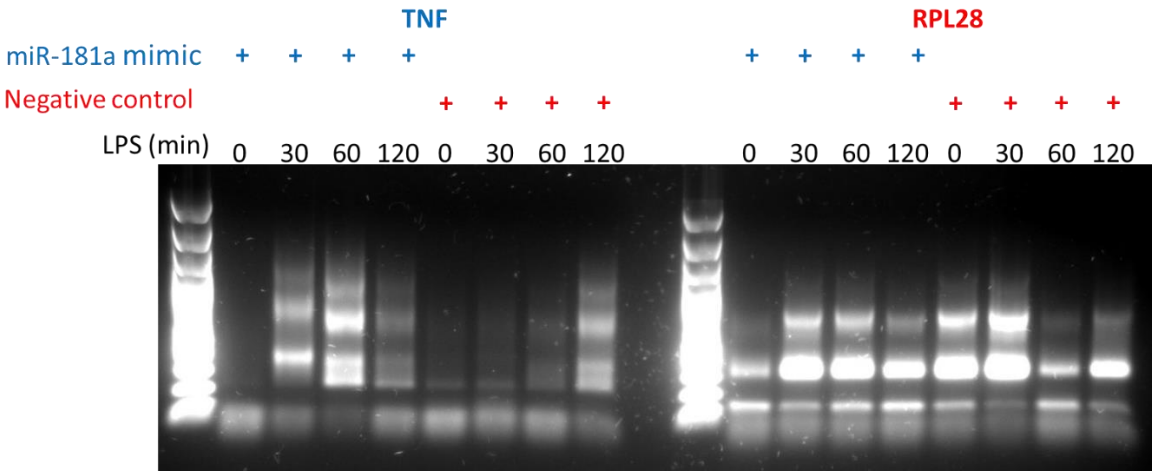

Supplementary Figure 10. TNF and RPL28 poly(A) tail lengths with miR-181a overexpression over a 120 minute LPS (1µg/ml) time course. Time course showing, miR-181a mimic or negative control (10nm final concentration) conditions. Poly(A) tail lengths were analysed by PAT assay and agarose gel electrophoresis

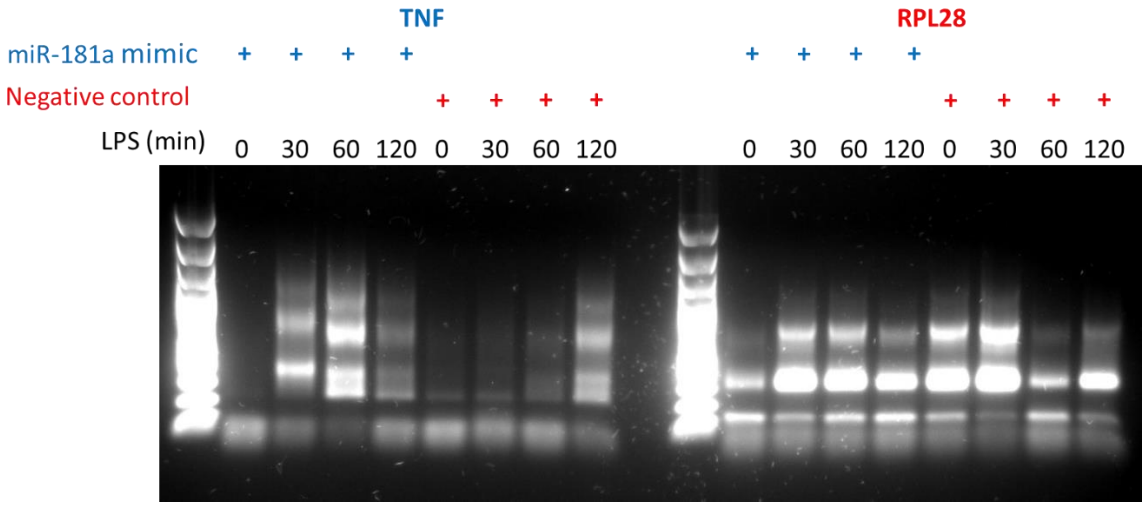

Supplementary Figure 11. TNF and RPL28 poly(A) tail lengths with miR-181a overexpression over a 120 minute LPS (1µg/ml) time course. Time course showing, miR-181a mimic or negative control (10nm final concentration) conditions. Poly(A) tail lengths were analysed by PAT assay and agarose gel electrophoresis

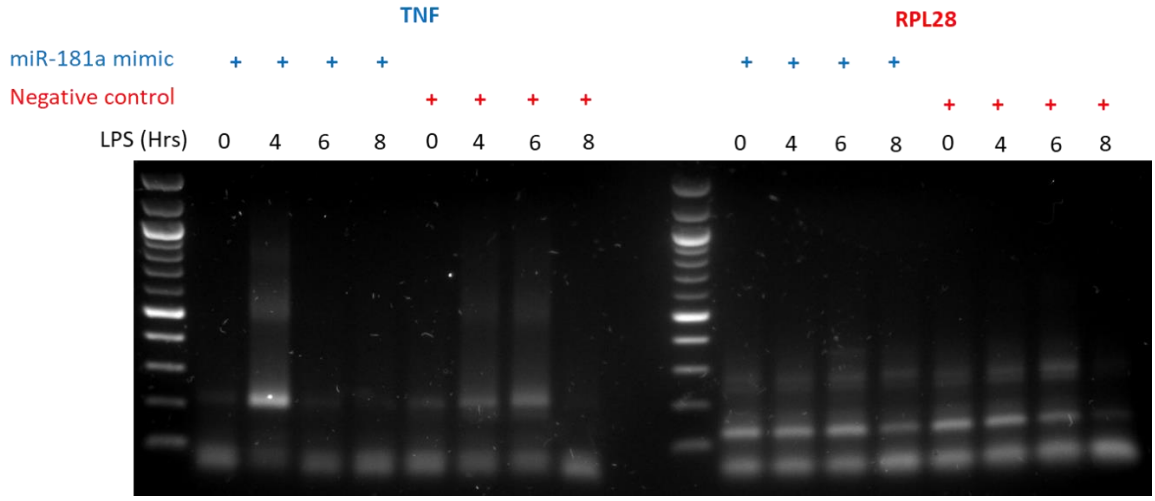

Supplementary Figure 12. TNF and RPL28 poly(A) tail lengths with miR-181a overexpression over an eight hour LPS (1µg/ml) time course. Time course showing, miR-181a mimic or negative control (10nm final concentration) conditions. Poly(A) tail lengths were analysed by PAT assay and agarose gel electrophoresis

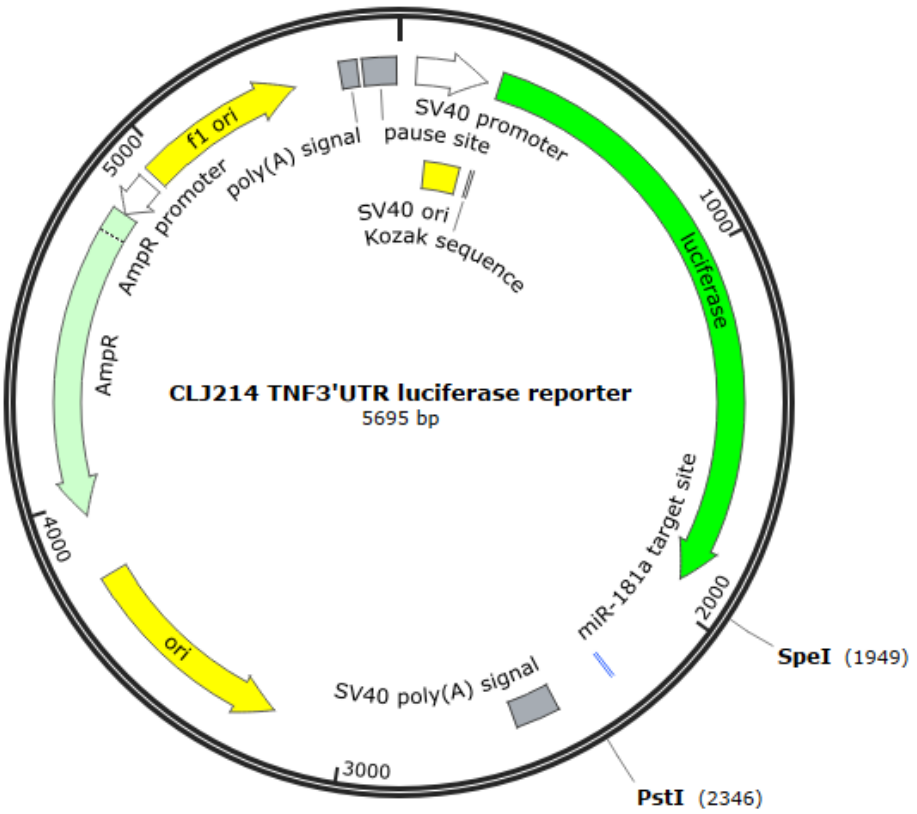

Supplementary Figure 13. Plasmid map of the Luciferase reporter containing the TNF 3'UTR. Referred to in the text as the WT Luciferase reporter. Shows the location of the firefly luciferase coding region (Green), miR-181a target site (blue), SV40 promoter (White) and restriction sites SpeI and PstI

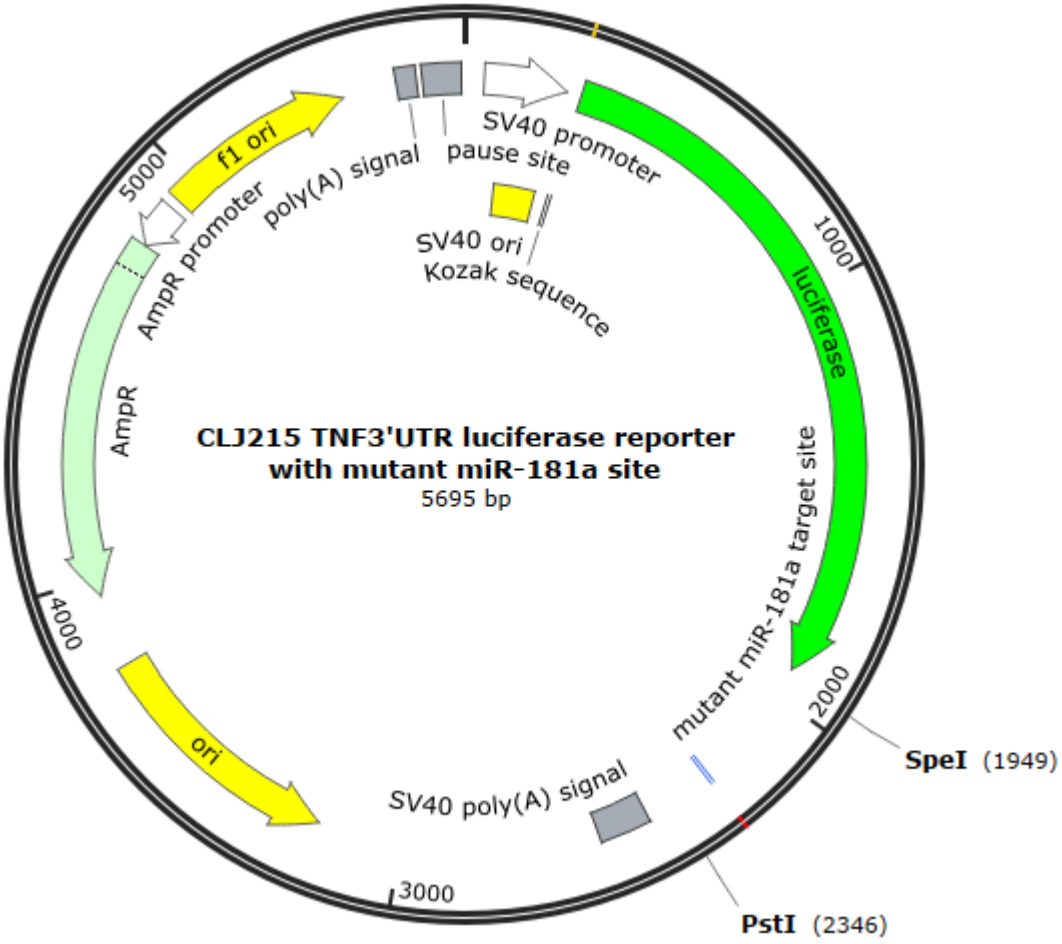

Supplementary Figure 14. Plasmid map of the luciferase reporter containing the TNF 3'UTR with mutant miR-181a target site. Referred to in the main text as mutant luciferase reporter. Shows the location of the firefly luciferase coding region (Green), mutant miR-181a target site (Blue), SV40 promoter (White) and the restriction sites SpeI and PstI.

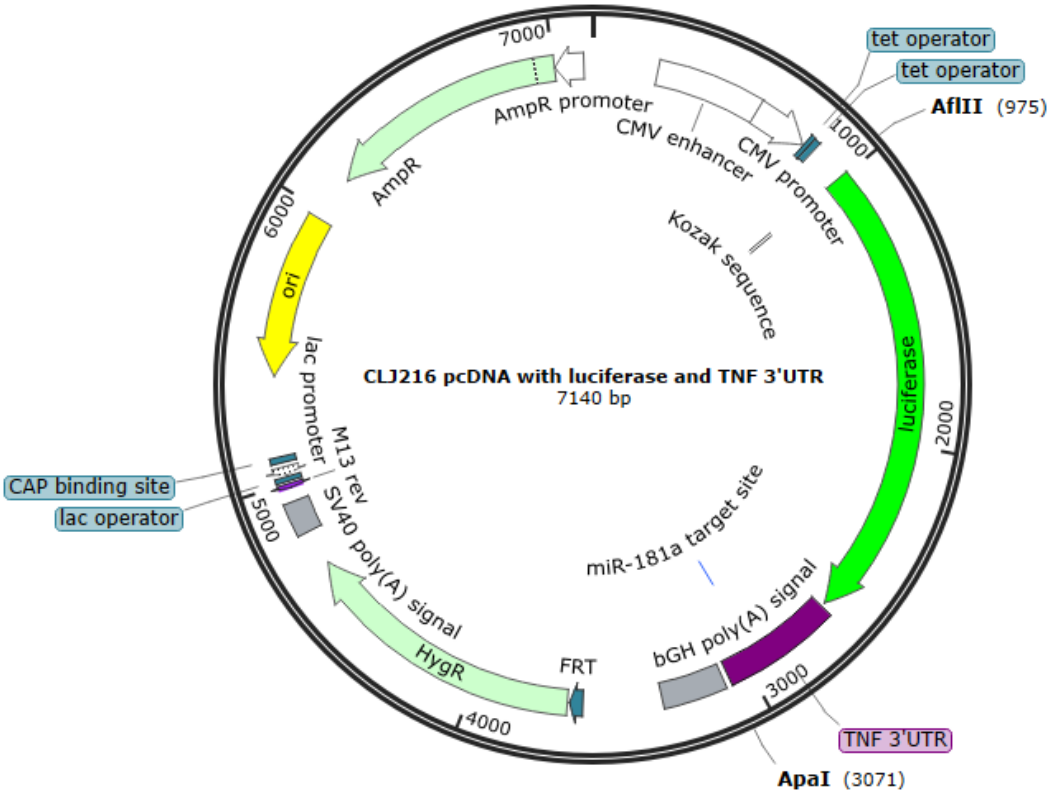

Supplementary Figure 15. Plasmid map of the expression vector containing firefly luciferase and the TNF 3'UTR. Referred to in the main text as Luc TNF 3'UTR. Shows the location of the firefly luciferase coding region (Green), TNF 3'UTR (Purple), miR-181a target site (Blue), CMV promoter (White), Hygromycing resistance gene (Pale green), and the Flip-recombinase target site (FRT, blue arrow) and the restriction sites AflII and ApaI.

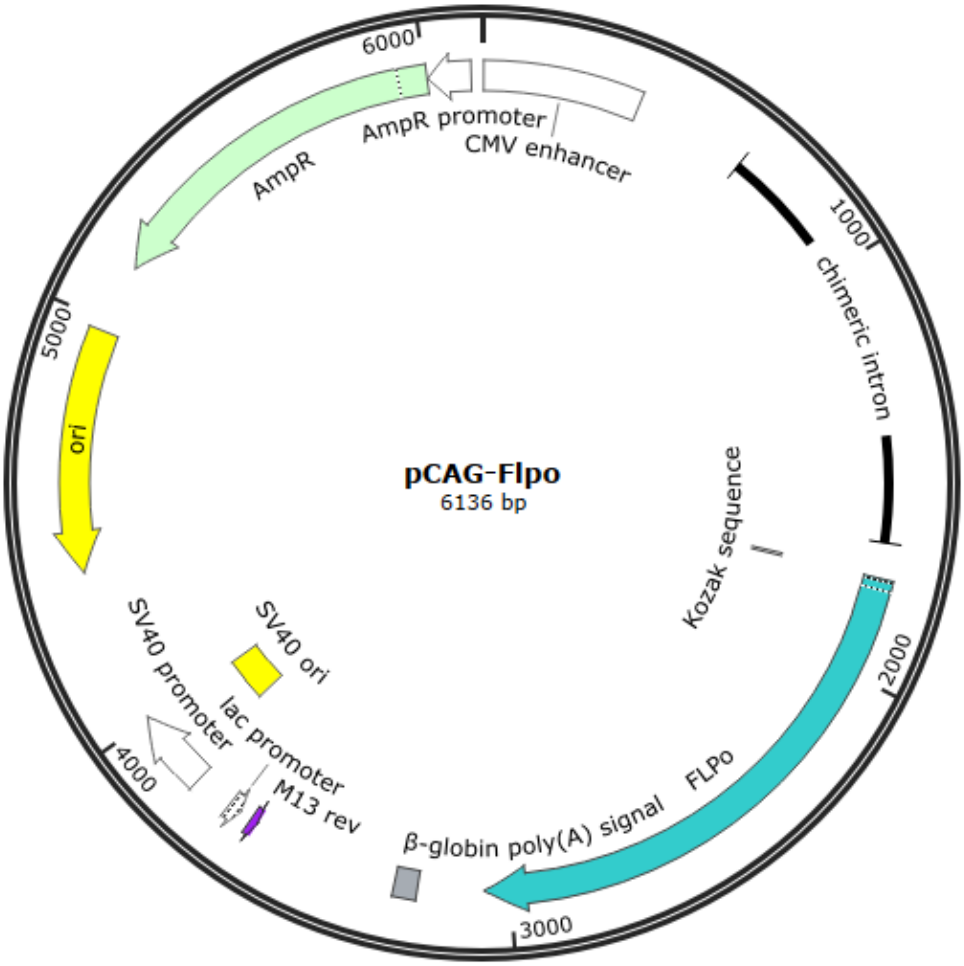

Supplementary Figure 16. Plasmid map of the vector containing the Flip-in recombinase. Shows the location of the Flip-in recombinase region (Turquoise) and Ampicillin resistance gene (Pale green).

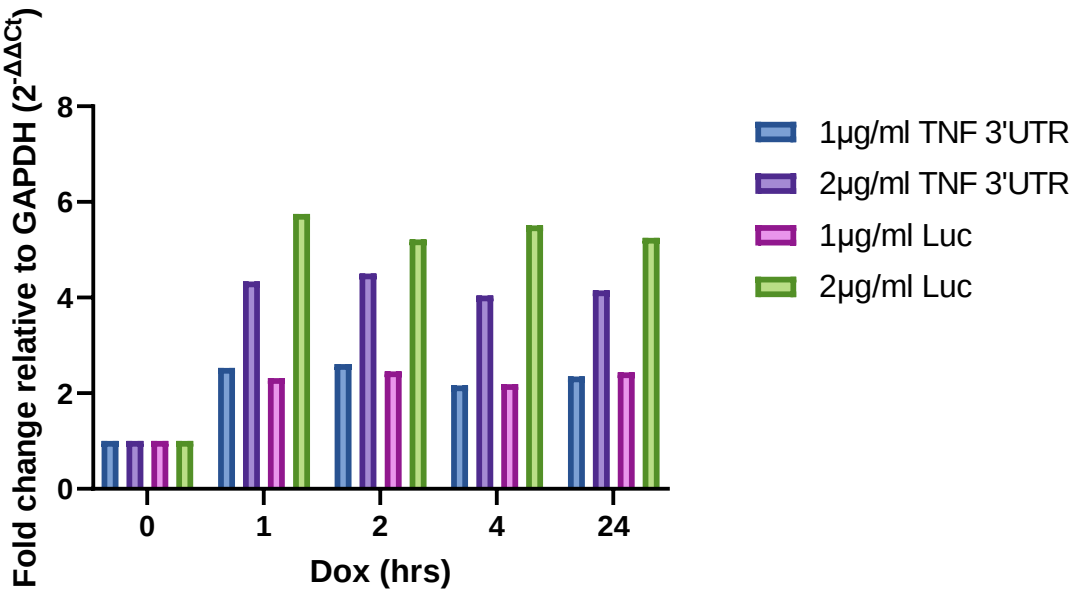

Supplementary Figure 17. Testing doxycycline concentrations on inducible cell line for induction of Luc TNF 3'UTR mRNA. Data measured by RT qPCR and analysed by $2^{-\Delta\Delta Ct}$, normalised to GAPDH and plotted relative to the zero-time point. TNF 3'UTR and Luc refer to the different sets of primers used. TNF 3'UTR primers amplify the TNF 3'UTR region of the gene. Luc primers amplify the firefly luciferase region of the gene. N=1.

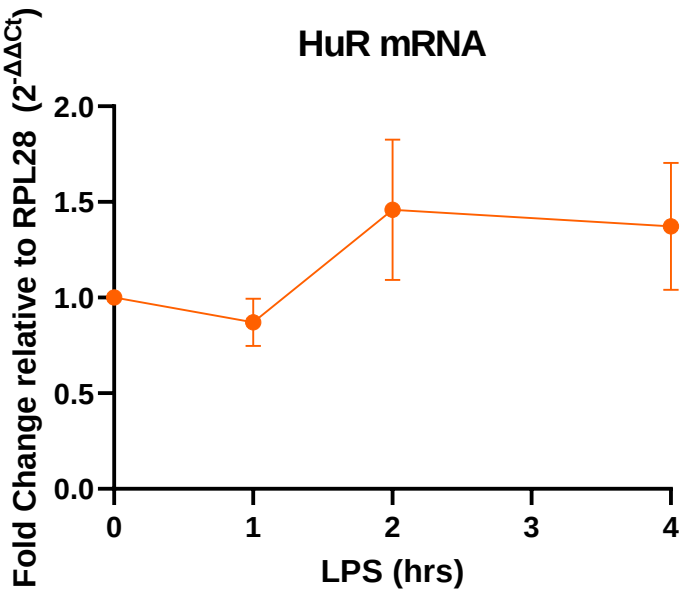

Supplementary Figure 18. HuR mRNA expression levels over a four hour LPS time course. Data measured by RT-qPCR and analysed by $2^{-\Delta\Delta Ct}$, normalised to RPL28 and plotted relative to the zero hour time point. 1µg/ml LPS. N=3.

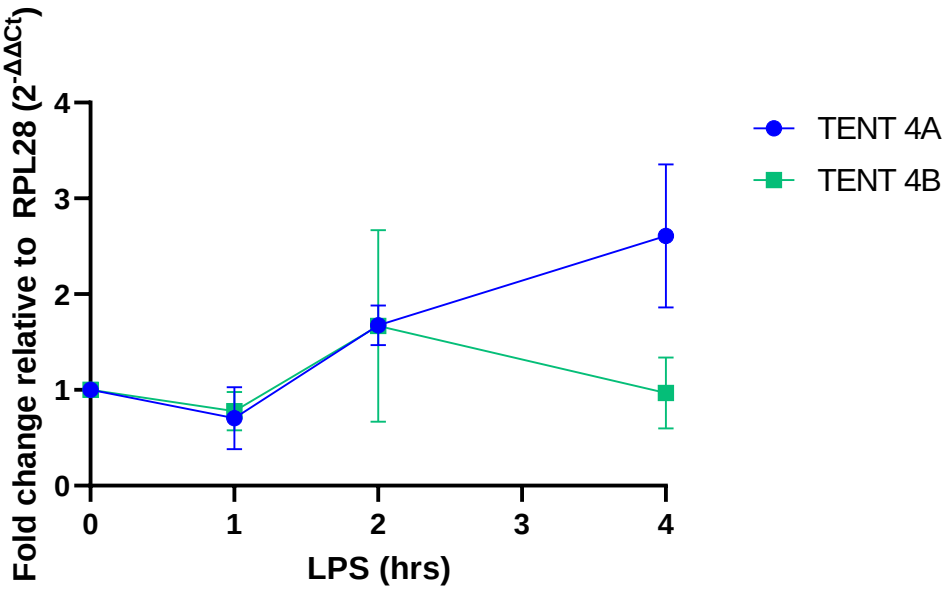

Supplementary Figure 19. TENT4A and TENT4B mRNA expression levels over a four-hour LPS time course. Data measured by RT-qPCR and analysed by $2^{-\Delta\Delta Ct}$, normalised to RPL28 and plotted relative to the zero-hour time point. 1µg/ml LPS. N=3.

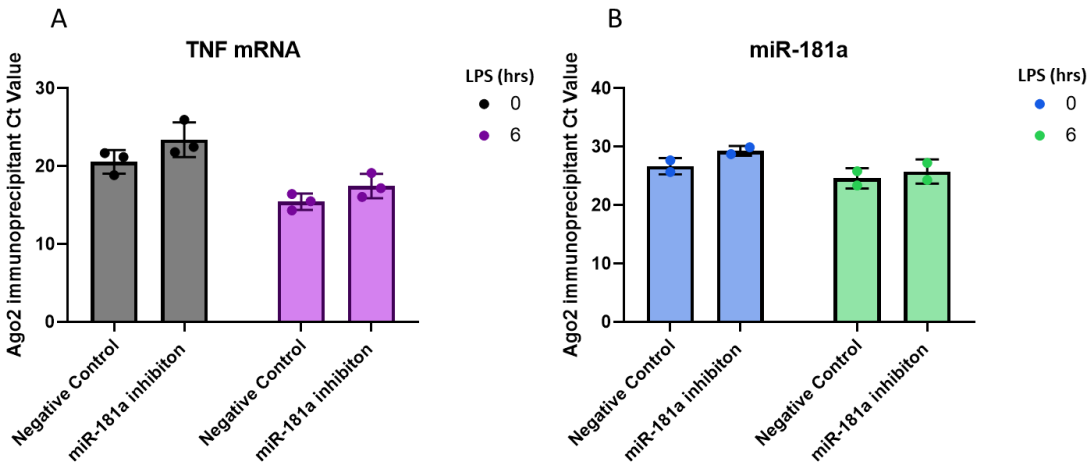

Supplementary Figure 20. Ct values for RNA analysed in Ago2 Ips with miR-181a inhibition A) Ct values for the TNF mRNA isolated within the Ago2 immunoprecipitants with and without miR-181a inhibition from Figure 37. miR-181a isolated within Ago2 and IgG immunoprecipitants with miR-181a inhibitor or Negative Control oligo (10nm final concentration) over a six-hour LPS (1µg/ml) time course. N=3. Error represents SD. **B)** Same as A but showing the Ct values for miR-181a . N=2. Error represents SD.

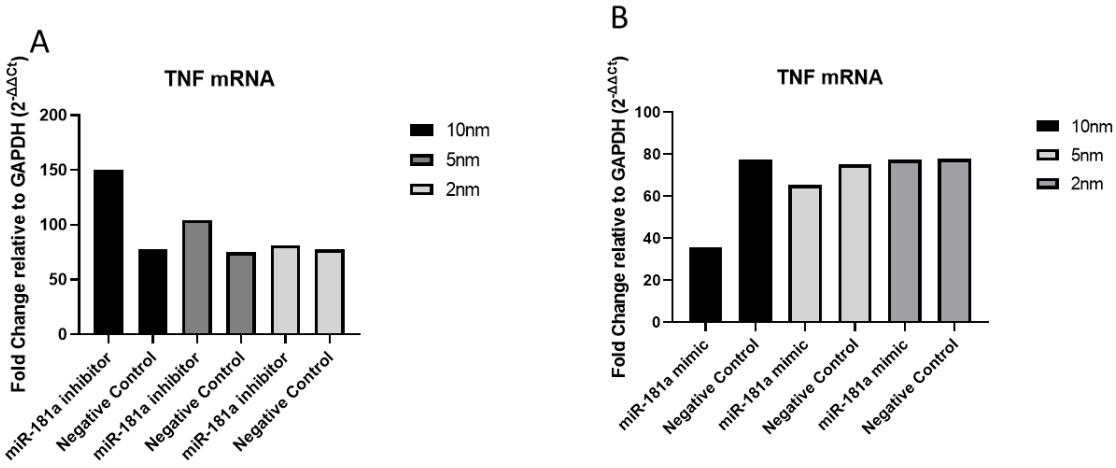

Supplementary Figure 21. Testing miR-181a inhibitor and mimic concentrations in RAW 264.7 cells. A) RAW 264.7 cells transfected with 10nm, 5nm and 2nm miR-181a inhibitor and treated with Sigma LPS (1µg/ml) for 120 minutes. Data was analysed by RT-qPCR and plotted relative to GAPDH. N=1. **B)** Same as A but testing miR-181a mimic concentrations of 10nm, 5nm and 2nm. N=1

Supplementary Table 1 Ct values for housekeeping genes for normalisation of qPCR data in RAW 264.7 cells. RAW 264.7 cells were treated with 1µg/ml LPS over an eight hour time course. Values show are triplicate values for each sample. N=1. ACTB was ruled out for use as a housekeeping normalisation control

LPS (hrs)	GAPDH			ACTB			HPRT			RPL28		
0	13.31	13.14	13.43	16.43	16.33	16.76	20.57	20.41	20.53	17.58	17.21	17.18
1	13.31	13.33	13.97	12.75	12.31	12.48	20.85	21.04	21.09	17.22	17.37	17.44
4	13.46	13.49	13.93	12.22	12.87	12.56	20.55	20.32	20.59	17.41	17.85	17.6
8	13.09	12.99	13.61	14.23	14.05	14.17	20.8	20.8	20.81	17.93	17.82	17.73